INSTITUTO POLITÉCNICO DE BRAGANÇA

Synthesis and Characterization of Smart Hydrogels for Controlled Drug Release considering RAFT Polymerization and SEC Tetra-Detection

Carla Alexandra Lopes Machado

Dissertation submitted to

Escola Superior de Tecnologia e de Gestão

Instituto Politécnico de Bragança

To obtain the Master Degree in

Chemical Engineering

July 2014

Synthesis and Characterization of Smart Hydrogels for Controlled Drug Release considering RAFT Polymerization and SEC Tetra-Detection

Carla Alexandra Lopes Machado

Dissertation submitted to

Escola Superior de Tecnologia e de Gestão

Instituto Politécnico de Bragança

To obtain the Master Degree in

Chemical Engineering

Advisor:

Professor Doutor Rolando Carlos Pereira Simões Dias

July 2014

To my Sisters,

Acknowledgements

I gratefully acknowledge Professor Doctor Rolando Dias who provided scientific support and guidance during my master studies. His knowledge on this field and enthusiasm for research is unmatched.

I want to thank Doctor Porkodi Kadhirvel for all the help and support during this time.

I want to truly thank the support by FCT and FEDER under Programme COMPETE (Project PEst-C/EQB/LA0020/2013), QREN, ON2 and FEDER (Project NORTE-07-0162-FEDER-000050) and QREN, ON2 and FEDER (Project NORTE-07-0124-FEDER- 0000014 - Polymer Reaction Engineering).

The department of chemistry at ESTiG, its facilities and all the materials waived for the preparation of this work.

To my friends, the best in the world, Sofia, Paulo, Daniela, Hugo, Filipa, Tânia and Patricia for always being there, no matter what.

To my amazing family, that always believed in me.

To my parents, Dulce and Rui, and my sisters, Marta and Ana, for all the love and strength that they always gave me… I love you!

And last, but not least, to Rodrigo, my one in a million, that stand by me through good times and bad times, with his love, kindness and friendship.

Nothing of this would be possible without you all.

Abstract

Smart hydrogels find important applications in biotechnology, biomedicine, pharmaceutics or environmental industries. Drug or gene delivery, bio-separations, bio-sensing and tissue engineering are some examples of processes where this class of advanced materials show an increasing importance along the time. This work is devoted to the synthesis, characterization and assessment of the performance of smart hydrogels for drug adsorption and release (desorption) applications. This research aims contribute for the development of designing tools linking the synthesis conditions with the structure and final performance of such kinds of advanced materials.

Classical Free Radical Polymerization (FRP) and Reversible Addition-Fragmentation Chain-Transfer (RAFT) polymerization are both considered in the experimental program performed. Effect of the polymerization technique (FRP/RAFT) on the structure and properties of smart hydrogels is thus assessed. A continuous flow micro-reactor allowing the production of smart hydrogel particles was built up in this research plan. Comparison of the structure and properties of smart materials synthetized in batch reactor and continuous flow micro-reactor was thus also tried. Molecular imprinting was considered as a third research vector to obtain advanced hydrogels with tailored properties. Molecularly Imprinted Polymers (MIPs) were produced in batch and continuous flow micro-reactor and considering alternatively the RAFT/FRP polymerization techniques. An innovative combination of different designing tools (synthesis technique/kind of reactor/molecular imprinting) was thus tried in this research.

Some information concerning the molecular architecture of the synthetized materials, especially the structure of the soluble linear analogues of the hydrogels, was obtained using a Size Exclusion Chromatography (SEC) instrument with tetra-detection, namely Refractive Index (RI), Ultraviolet (UV), Light – Scattering (LS) and Intrinsic Viscosity (IV). These analyses were performed using directly water as eluent (trying to avoid organic solvents to analyse water compatible materials). High differences between the structure of FRP and RAFT products were identified using this characterization

technique, which confirms the usefulness of RAFT polymerization to modify polymer properties.

End use properties of the synthetized smart hydrogels, namely concerning drug adsorption and release were tested using different experimental approaches. Different model drugs used in medicine were considered, namely 5-fluorouracil (used in cancer treatment), ibuprofen (anti-inflammatory/analgesic), isonicotinic acid (used in tuberculosis treatment) and caffeine (stimulant of the central nervous system). At a first stage, considering batch adsorption (incubation) of these drugs in stimuli-responsive hydrogels, the subsequent dynamics of release of the drugs were experimentally measured, also in a batch process, using ultraviolet spectroscopy. Temperature and pH changes were considered as stimuli to trigger these release processes. Materials based on acrylic acid (introducing in the networks sensibility to pH) and N-isopropylacrylamide (introducing in the networks sensibility to the temperature) were used within this purpose. Studies concerning the batch adsorption of drugs (especially caffeine) on the smart hydrogels produced in this work were additionally explored by trying the measurement of adsorption isotherms. Solid Phase Extraction (SPE) was also considered in order to assess the amount of drug adsorbed in the smart hydrogels when the surrounding conditions (pH of the aqueous solution and therefore the swelling ratio of the networks) are changed.

Frontal analysis (FA), a high precision technique for adsorption studies, was considered in a last stage to evaluate the performance of the synthetized smart hydrogels. The same GPC system considered in polymer structure analysis was used and *in-line* UV monitoring was especially useful to quantify the dynamics of adsorption and desorption of the drugs in the hydrogels, considering the FA continuous process. These studies were performed through the packing of produced materials (bulk hydrogels obtained in batch reactor or particles synthetized in micro-reactor) in empty GPC columns (different sizes were available). High swelling of these materials was taken as advantage to induce the self-packing of the smart hydrogels in the GPC columns. Molecularly imprinted and non-imprinted smart hydrogels were considered in these affinity studies. Effect of drug structure on the affinity and selectivity of the materials was also studied by frontal analysis by comparing compounds with different chemical structures, namely caffeine and 4-aminopyridine.

Research here presented shows the feasibility of the production of particles of smart hydrogels combining operation in continuous micro-reactor with RAFT polymerization and molecular imprinting.

Key Words: RAFT polymerization, Micro-reactor, Molecular imprinting

Resumo

Os hidrogéis inteligentes têm importantes aplicações nas áreas da biotecnologia, biomedicina, farmácia e ambiente. A libertação de fármacos ou de genes, bio separações, bio sensores e engenharia dos tecidos são alguns exemplos de processos onde esta classe de materiais avançados mostram um aumento da sua importância ao longo do tempo. Este trabalho é dedicado à síntese, caracterização e avaliação do desempenho de hidrogéis inteligentes para aplicações de adsorção e libertação (dessorção) de fármacos. Esta pesquisa pretende contribuir para o desenvolvimento de ferramentas de projeto relacionando as condições de síntese com a estrutura e a performance final neste tipo de materiais.

A Polimerização Radicalar Clássica (FRP) e a Polimerização via Transferência de Cadeia Reversível por Adição-Fragmentação (RAFT) são ambas consideradas no programa experimental efetuado. O efeito da técnica de polimerização (FRP/RAFT) na estrutura e propriedades dos hidrogéis inteligentes é assim avaliada. Neste trabalho foi construído um micro reator de fluxo contínuo que permitiu a produção de partículas destes hidrogéis. A comparação da estrutura e propriedades destes materiais sintetizados em reator fechado e num micro reator de fluxo contínuo foi também feita. A impressão molecular foi considerada como o terceiro vetor de pesquisa para obter hidrogéis avançados com propriedades adaptadas. Polímeros Molecularmente Impressos (MIP) foram produzidos em reator fechado e em micro reator de fluxo continuo considerando, alternativamente, as técnicas de polimerização FRP/RAFT. Uma combinação inovadora de diferentes ferramentas de projeto (técnica de síntese/tipo de reator/impressão molecular) foi assim tentada nesta pesquisa.

Informação relativa à arquitetura molecular dos materiais sintetizados, especialmente a estrutura dos polímeros lineares solúveis análogos aos hidrogéis, foi obtida usando Cromatografia de Exclusão de Tamanho (SEC) com tetra-deteção, nomeadamente Índice de Refração (IR), Ultravioleta (UV), Dispersão de Luz (LS) e Viscosidade Intrínseca (VI). Estas análises foram efetuadas utilizando diretamente a água como eluente (tentando assim evitar o uso de solventes orgânicos na análise de materiais compatíveis com a água). Foram identificadas grandes diferenças entre a estrutura de

produtos FRP e RAFT utilizando esta técnica de caracterização, que confirma a utilidade da polimerização RAFT na modificação das propriedades dos polímeros.

As propriedades finais dos hidrogéis sintetizados, nomeadamente a adsorção e libertação de fármacos, foram testadas usando diferentes abordagens experimentais. Foram consideradas diferentes fármacos utilizados na medicina como o 5-Fluoruracilo (usado no tratamento do cancro), o ibuprofeno (anti-inflamatório/analgésico), a isoniazida (utilizada no tratamento da tuberculose) e a cafeina (estimulante do sistema nervoso central).

Numa primeira fase, considerando adsorção em modo fechado (incubação) destes fármacos em hidrogéis inteligentes, as posteriores dinâmicas de libertação dos fármacos foram medidas experimentalmente, também em modo fechado, utilizando espectroscopia UV. As mudanças de temperatura e pH foram consideradas como estímulos para provocar estes processos de libertação. Materiais baseados em ácido acrílico (introduzindo nas redes sensibilidade ao pH) e N-isopropilacrilamida (introduzindo nas redes sensibilidade à temperatura) foram usadas com este objetivo. Estudos relativos à adsorção de fármacos (especialmente a cafeína) em modo fechado em hidrogéis inteligentes produzidos neste trabalho foram explorados com o intuito de medir isotérmicas de adsorção. Extração em Fase Sólida (SPE) foi também considerada com intenção de avaliar a quantidade de fármaco adsorvida nos hidrogéis quando as condições do meio envolvente (pH das soluções e portanto a razão de inchamento das redes) são alteradas.

A Análise Frontal, uma técnica de alta precisão para testes de adsorção, foi considerada numa última etapa para avaliar a performance dos hidrogéis inteligentes sintetizados. O mesmo sistema de GPC utilizado para analisar a estrutura dos polímeros foi aqui considerado, tendo sido a monitorização UV *in-line* especialmente útil para a quantificação de dinâmicas de adsorção e dessorção de fármacos nos hidrogéis através análise frontal (processo contínuo). Estes estudos foram efetuados através do empacotamento dos materiais produzidos (hidrogéis bulk obtidos em reator fechado ou partículas sintetizadas em micro reator) em colunas de GPC vazias (com diferentes tamanhos disponíveis). O elevado inchamento dos materiais foi usado como vantagem para induzir o auto empacotamento dos hidrogéis nas colunas de GPC. Polímeros

moleculamente impressos e não impressos foram considerados nestes estudos de afinidade. O efeito da estrutura molecular do fármaco na afinidade e seletividade dos materiais foi também estudado através de análise frontal comparando compostos com diferentes estruturas químicas, nomeadamente a cafeína e a 4-aminopiridina.

A investigação aqui apresentada mostra a viabilidade da produção de partículas de hidrogéis inteligentes combinando operação contínua em micro reator com polimerização RAFT e impressão molecular.

Palavras-chave: Polimerização RAFT, Micro reator, Impressão molecular.

INDEX

List of Figures

List of tables

List of Annexes

List of Abbreviations

AA	*Acrylic acid*
AIBN	*2,2'-Azobis(2-methylpropionitrile)*
APS	*Ammonium Peroxidisulphate*
CAF	*Caffeine*
CAT	*Catalyst*
C_{MAX}	*Maximum concentration of drug that is expected to measure by UV in consequence of the incubation process*
CL	*Crosslinker*
C_{UV}	*Drug concentration in the remaining solution, measured by UV, after incubation.*
C_0	*Estimation of drug concentration on the hydrogel (mg/g) using method 2.*
C_1	*Estimation of drug concentration on the hydrogel (mg/g) using method 1 and based on their swelling ratio.*
C_2	*Estimation of drug concentration on the hydrogel (mg/g) using method 1 and based on the UV analysis of the remaining solution.*
DDMAT	*2-(Dodecylthiocarbonothioylthio)-2-methylpropionic acid*
DMAEMA	*N,N-Dimethylaminoethyl Methacrylate*
FRP	*Free Radical Polymerization*
GPC	*Gel Permeation Chromatography*
HG	*Hydrogel*
I	*Initiator*
IBU	*Ibuprofen*
INH	*Isonicotinylhdrazine*
MBA_m	*N-N'-Methylene-bisacrylamide*
MIP	*Molecularly Imprinted Polymer*
m_{SH}	*Mass of swelled hydrogel*
m_{WAI}	*Mass of remaining water recovered after incubation*
M1	*Monomer 1*
M2	*Monomer 2*
m_1	*Mass of hydrogel used in the incubation process*
m_2	*Mass of water used in the incubation process*
m_3	*Mass of drug used in the incubation process*
NIP	*Non-Imprinted Polymer*
NIPA	*N-isopropylacrylamide*

PAA	*Poly (acrylic acid).*
PDMAEMA	*Poly (N,N-Dimethylaminoethyl Methacrylate)*
PNIPA	*Poly (N-isopropylacrylamide)*
RAFT	*Reversible Addition-Fragmentation chain Transfer Polymerization*
SEC	*Size Exclusion Chromatography*
SEM	*Scanning Electron Microscope*
SR	*Swelling ratio*
T	*Temperature*
TEMED	*N,N,N,N-Tetramethylenediamine*
UV	*Ultra Violet*
W_{DI}	*Desionized water*
5-FU	*5-Fluoruracil*

CHAPTER 1 – Introduction

Research on Smart Hydrogels and Molecularly Imprinted Polymers (MIPs) is nowadays a hot subject in polymer science and engineering. The interest in these advanced materials is driven by their new applications as biomaterials for controlled delivery, tissue engineering, nanotechnologies and micro-fabrication. In fact, these advanced materials also have a growing importance in several technological domains and medicine. Superabsorbent materials useful in sanitary industries and agriculture, polymer networks responsive to temperature/pH changes for drug delivery and MIPs for molecular recognition in environment or biotechnology are significant examples of these materials. Intelligent hydrogels and MIPs have also been explored in the last few years in order to try mimicking biological delivery through feedback-controlled release. Combination between swelling induced delivery and molecular imprinting is pointed out as a solution to obtain released products with longer therapeutic lifespan [1]. Recognition of biological molecules such as peptides/proteins [2] and cell delivery [3] are other application examples that were recently investigated in this field.

New chemical tools revolutionizing the radical polymerization of vinyl monomers were discovered in the last two decades. In fact, with the advent of the Controlled Radical Polymerization (CRP) techniques, huge improvements on the molecular architectures of vinyl polymers become possible (see reviews [1-3] and references therein). Comparatively to classical free radical polymerization (FRP), CRP allows the synthesis of polymeric materials with controlled topology (e.g. linear, stars, graft/comb, hyperbranched polymers), with controlled composition (e.g. gradient/block copolymers) and with controlled functionality (e.g. chains with side functional groups, multifunctional stars). With linear polymerization, CRP allows the production of materials with narrow molecular weight distributions and copolymers with tailored sequence length distribution [4-7]. Termination reactions are almost suppressed using CRP and radical average life time is in the range of hours rather than seconds that is characteristic of FRP. The heterogeneous chain born time distribution inherent to FRP is replaced by the almost simultaneous formation/growth of polymer chains in CRP. These

abilities to control the molecular architecture with CRP are achieved with the same mild reaction conditions of FRP (tolerance to impurities, compatibility with water, and versatility with functional monomers) which is a distinctive key feature comparatively to live ionic polymerization. Three main CRP techniques were especially studied in the last years: NMRP (nitroxide-mediated radical polymerization), atom transfer radical polymerization (ATRP) and reversible addition-fragmentation chain transfer radical polymerization (RAFT). Macromolecular design by interchange of xanthates (MADIX) is often considered a RAFT-like process and other less used CRP techniques exist (e.g. iodine-transfer polymerization, organotellurium mediated polymerization, etc) [1-3].

Current research efforts in hydrogels and MIPs are also driven by the emergence of controlled radical polymerization. Properties of such advanced materials, usually obtained through classical free radical polymerization, can be substantially improved using CRP. The question arises because FRP gels have a heterogeneous structure (due to slow initiation, fast propagation and termination reactions, as above mentioned) with deleterious effect on their end use properties. This effect can be minimized using CRP mechanisms which are able to generate products with well-defined structures. Among CRP techniques, Reversible Addition-Fragmentation Chain Transfer can be applied to the synthesis of water compatible polymers both directly in aqueous media as well as in the presence of organic solvents [4-8].

Continuous reactors are fundamental devices in chemical engineering and industrial processes. On other hand, high surface area/volume enhancing heat transfer, constant product quality at high through-put and small set-up volume are some advantages of continuous flow micro-reactors which have been exploited lately for several purposes, namely process intensification. Moreover, microfluidics devices such as micro-reactors allow the production and manipulation of individual particles and droplets which is an important issue in many technological applications [7, 8].

Molecularly imprinted polymers are a special kind of polymer networks that in general are synthesized using a functional monomer exhibiting interaction with the template molecule (e.g. a drug molecule) and a crosslinker to provide structural support to the polymer network. These monomers are dissolved with the template in an appropriated

solvent and a complex is formed between the functional monomer and the template. A free radical non-linear crosslinking polymerization is then promoted and a network including the template molecule is built. Removal of the template leaves a polymer network with three-dimensional binding cavities with stereo-specificity to the template molecule [2-4].

As schematically depicted in Figure 1, this work combines these three lines of research: droplet polymerization in microfluidic reactors with controlled radical polymerization (RAFT polymerization is used aiming the improvement of the molecular architecture of networks) and molecular imprinting is here reported.

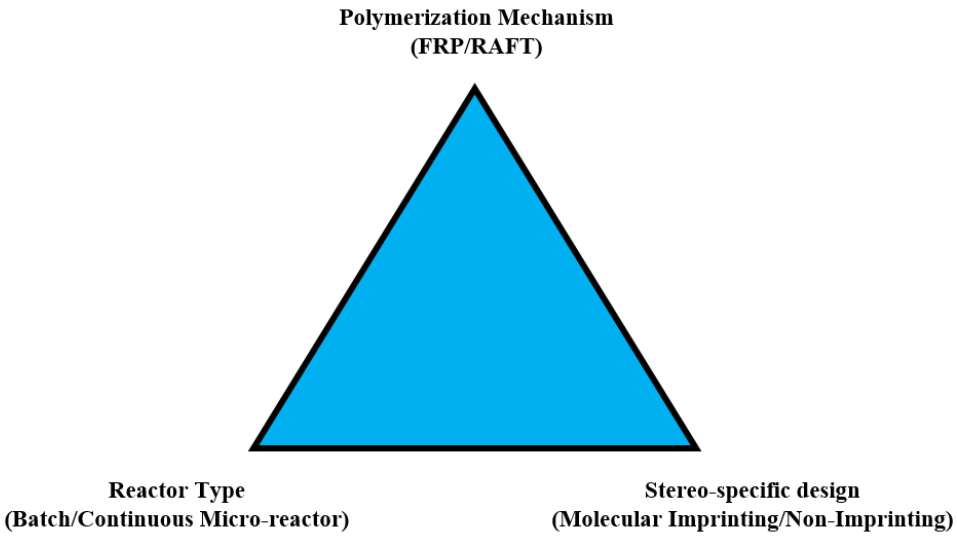

Figure 1. The three vector approach used in this work to synthesize smart hydrogels. Different polymerization mechanisms (FRP/RAFT), reactor types (batch/continuous micro-reactor) and stereo-specific designs (molecular imprinting/non-imprinting) are combined in order to aid the production of materials with tailored properties.

A contribution for the development of designing tools aiding the synthesis of advanced materials with important applications in many technological/biotechnological fields is thus intended.

CHAPTER 2 - Batch Drug Release from Smart Hydrogels Triggered by Temperature and pH

2.1. Introduction

Hydrogels have received significant attention because of their ability to retain high water contents and related potential for many biomedical applications.
They can be defined as a two- or multicomponent systems consisting on a three-dimensional high molecular weight network composed of a polymer backbone, water – that fills the space between the macromolecules – and a crosslinking agent.

"*Stimuli-responsive*" hydrogels have been investigated for the development of "smart" materials in various fields because of their capability of changing their volume and properties in response to environmental stimuli [9]. In aqueous media, stimuli-sensitive systems have the objective of changing the hydrophilic character of functional groups into a hydrophobic one, or vice versa.

The stimuli applied for that purpose can be chemical or physical. Acid-base or electrochemical reactions are examples of chemical stimuli as change of pH value, of ionic strength, of temperature or pressure, are examples of physical ones. This work will be focused in thermo-sensitive hydrogels, as PNIPA, and pH-sensitive hydrogels, as poly (acrylic acid).

All the pH-sensitive polymers contain pendant acidic or basic groups that either accept or release protons in response to changes in environmental pH [10, 11]. Swelling of the hydrogel increases as the external pH increases in the case of weakly acidic (anionic) groups, but decreases if the polymer contains weakly basic (cationic) groups [10, 11].

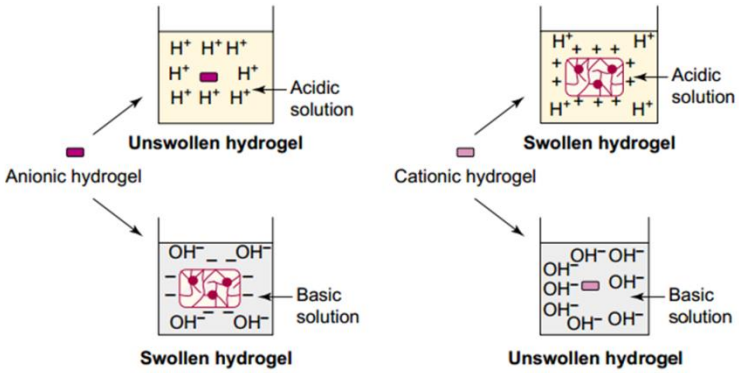

Figure 2. The pH-responsive swelling of anionic and cationic hydrogels [12].

Temperature-sensitive hydrogels are, probably, the most common studied class of environment-sensitive polymer systems in drug-delivery research. These hydrogels are able to swell or shrink as a result of changing the temperature of the surrounding fluid [10, 11]. Giving PNIPA as an example, if the temperature of the aqueous solution is near 25 ºC the polymer swells, if it is near 37 ºC the hydrogel collapses.

Polymers that can respond to external stimuli are of great interest in medicine, especially as controlled drug release vehicles. Highly specialized hydrogels have been developed for the delivery and release of drugs into specific tissues. For example, poly (acrylic acid) can be incubated with a drug to be release in the stomach where the pH is acidic or in the intestines where the pH is basic. On the other hand, an incubated NIPA polymer can be used to release the drug in tumor cells where the temperature is higher than the rest of the body.

Incubated drugs such as isonicotinylhdrazine (INH) (used in tuberculosis treatment), ibuprofen (analgesic/anti-inflammatory), 5-fluoruracil (used in cancer treatment) and caffeine (stimulant of the central nervous system), have been used in order to study the behavior of different types of polymers obtained with different types of polymerization, in controlled drug release. The molecular structures of the drugs are shown in Figures 3, 4, 5 and 6.

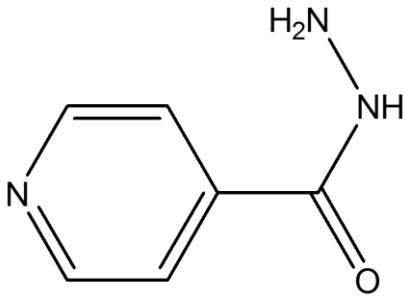

Figure 3. Molecular structure of INH.

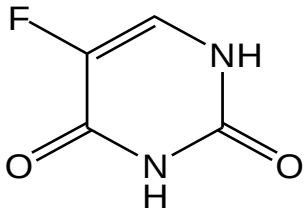

Figure 4. Molecular structure of 5-Fluoruracil.

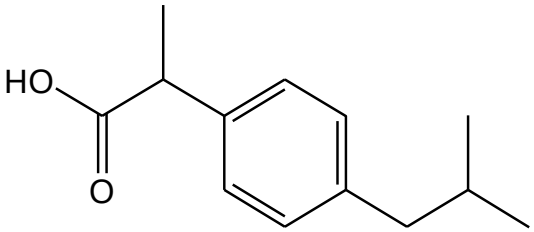

Figure 5. Molecular structure of Ibuprofen.

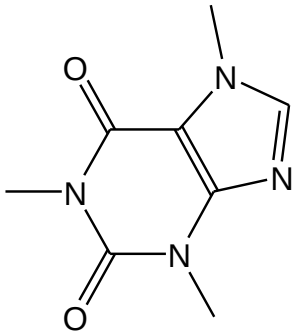

Figure 6. Molecular structure of Caffeine.

2.2. Controlled Drug Release

The term "drug delivery" may be defined as techniques that are used to get the therapeutic agents inside the human body [10, 11]. Controlled drug release systems offer numerous advantages when compared to conventional dosage forms including improved efficacy and reduced toxicity [13]. As so, it is easy to understand the importance of knowing and trying to improve this type of systems. With this purpose, it is studied how the drug is released depending on the external *stimuli*, the type of monomer and the polymerization used to synthetize the smart hydrogel. The polymer networks used in this work were synthetized using methods previously described in papers of this research group [14, 15].

2.3. Experimental Procedure

2.3.1. Incubation

In this study it is important to estimate the quantities of drugs that are going to be incubated in the hydrogel in order to have a reference of the maximum concentrations expected in controlled drug release tests [16]. These estimations may be complex and they are dependent on the incubation method that is going to be used. Figure 7 shows the microscopic images of PAA hydrogels incubated with four drugs. Here it is shown the differences in the morphology of the hydrogel when incubated with different drugs.

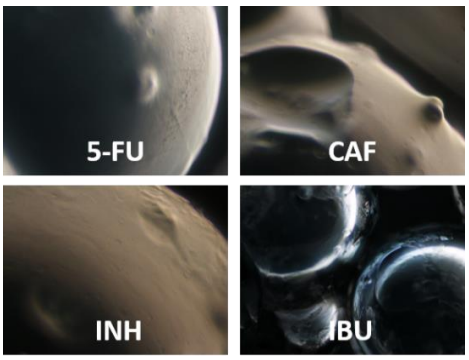

Figure 7. Microscopic images of PAA hydrogels incubated with the four drugs.

The data with the quantities used in this process is presented in Erro! A origem da referência não foi encontrada.. There is exposed the amount of hydrogel (m_1), water (m_2) and drugs (m_3) utilized in these procedures and the mass of swollen hydrogel (m_{SH}).

2.3.1.1. Method 1 – Drying after filtering;

To start the controlled drug release tests it is necessary to incubate the polymer with a drug. It was carried out by incubating the fixed quantity of hydrogel in a specified drug concentration, for 48 h. In this method the polymer was incubated with an excess of water, i.e. not all the water is going to be retained in the hydrogel and, consequently, not all the drug penetrates in the polymer, as showed in Figure 8.

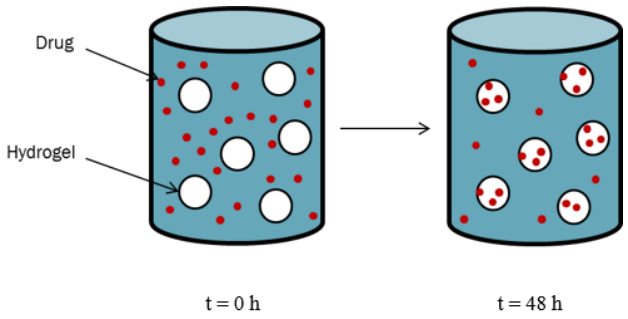

Figure 8. Incubation process using Method 1.

After 48 hours, the hydrogel has to be filtrated in order to remove the remaining solution. Then the concentration of this solution is measured, by UV, with the objective of knowing its drug concentration, i.e. the amount of drug that didn't penetrate into the polymer.

The estimations for Method 1 were obtained in two different ways. Considering a homogeneous distribution of the drug between the solid and the liquid phases and regarding the swelling ratio (SR) of the hydrogel, C_1 is obtained using the following equation:

$$C_1 = \frac{(m_{SH} - m_1) \times \frac{m_3}{m_2}}{m_1} = \frac{m_3}{m_2}(SR - 1) \tag{2.1}$$

Where C_1 can be defined as the estimation of the drug concentration on the hydrogel (mg/g) using Method 1 based on its swelling rate.

Another way of estimating of the drug concentration is based on the UV analyses of the drug concentration in the remaining solution. This can be calculated using the following equation by subtracting the drug concentration in solution from total.

$$C_2 = \frac{m_3 - m_{WAI} \times C_{UV}}{m_1} \tag{2.2}$$

Where m_{WAI} is the mass of water of the remaining solution; C_{UV} is the drug concentration in the remaining solution measured by UV after incubation (expressed in mg of drug/g of hydrogel) and C_2 is the estimation of the drug concentration on the hydrogel (expressed in mg of drug/g of hydrogel) using Method 1 and based in the drug concentration in the remaining solution.

2.3.1.2. Method 2 – Direct drying of the incubated hydrogel.

In this second method the polymer is incubated with exact amount of water that is necessary for its maximum swelling, assuming that all the water and the drug go inside the hydrogel, as showed in Figure 9.

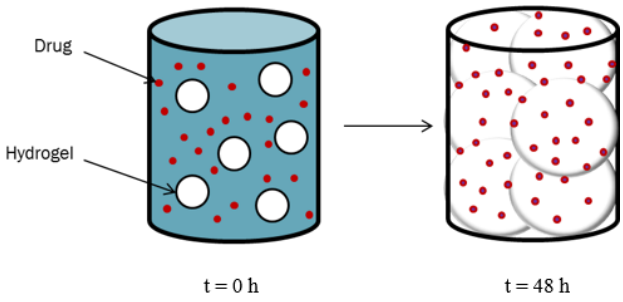

Figure 9. Incubation process using Method 2.

One of the critical drawbacks about this method is the fact that it is supposed that the entire drug doesn't get inside the gel and the possibility exists that some amount stays on its surface. Thus when starting the controlled drug release tests, the results of the

initial samples could be not as expected, because of the fast release of drugs from the surface to the aqueous solution.

In this method the concentration of the drug in the hydrogel is directly calculated by the following equation:

$$C_0 = \frac{m_3}{m_1} \tag{2.3}$$

Where C_0 is the estimation of the drug concentration on the hydrogel (expressed in mg of drug/g of hydrogel) using Method 2.

2.3.2. Controlled Drug Release Tests

The main purpose of this process is to study how the drug is released over time. To accomplish that, it is necessary to put the hydrogel in suitable experimental conditions such as pH, initial drug concentration, temperature, etc. The hydrogels used for this purpose are PNIPA and PAA obtained by FRP and PAA obtained by RAFT polymerization. The experimental conditions used in their syntheses are exhibited in Table 2. The only difference, in this procedure, between using a thermo-sensitive or a pH-sensitive hydrogel, is the aqueous solution where the polymer is going to be immersed in. If it is a thermo-sensitive one, the aqueous solution is deionized water and it is going to be heated until 25 ºC or 37 ºC, in a water bath. On the other hand, if it is going to be used a pH-sensitive hydrogel the aqueous solution has to be acidic or basic. To start the controlled release tests the incubated hydrogel is immersed in the aqueous solution as demonstrated in Figure 10 and Figure 11**.**

Figure 10. Illustrative image of the controlled drug release tests with PNIPA (thermo-sensitive hydrogel) at 37 ºC.

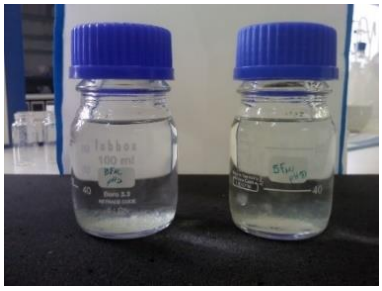

Figure 11. Illustrative image of the controlled drug release testes with PAA (pH-sensitive hydrogel) at pH 2 and 10 at room temperature.

The quantities used in the drug release tests performed are presented in Table 3**.** Sampling of the system was done by taking ≈ 3 mL of solution at prescribed at time instants, namely 0.5, 1, 5, 10, 30, 60, 120, 180, 360 and 1440 minutes. Samples were subsequently analyzed by UV for drug concentration estimation. The results thus obtained are presented in section 2.4. of this chapter.

Table 1. Data for estimation of the amount of drugs loaded in the hydrogels used in the releasing tests.

HG	Drug	m_1 (g)	m_2 (g)	m_3 (mg)	m_{SH} (g)	m_{WAI} (g)	C_{UV} (mg/g)	C_0 (mg/g)	C_1 (mg/g)	C_2 (mg/g)
HG1 (Method1)	**5-FU**	0.8005	160.4101	200.5	11.3317	149.8789	0.0131	-	16.4437	5.1816
	CAF	0.8022	160.1758	200.4	8.3605	152.6175	0.0114	-	11.7881	31.9899
	IBU	0.8081	160.0660	200	10.9906	149.8835	0.0124	-	15.7442	29.7825
	INH	0.8117	160.0918	200.3	10.1170	150.7865	0.0145	-	14.3432	-9.5297
HG2 (Method2)	**5-FU**	0.7407	14.8122	37.1	15.5900	-	-	50.0878	-	-
	CAF	0.7406	14.8151	37.1	15.5928	-	-	50.0945	-	-
	IBU	0.7398	14.8060	37.4	15.5832	-	-	50.5542	-	-
	INH	0.7397	14.8074	37	15.5841	-	-	50.0203	-	-
HG3 (Method2)	**5-FU**	0.7502	15.0573	37.6	15.8451	-	-	50.1200	-	-
	CAF	0.7503	15.0186	37.5	15.8064	-	-	49.9800	-	-
	IBU	0.7510	15.0211	37.6	15.8097	-	-	50.0666	-	-
	INH	0.7512	15.0436	37.5	15.8323	-	-	49.9201	-	-
HG1 (Method2)	**5-FU**	0.2005	4.0130	9.7	4.2232	-	-	48.3791	-	-
	CAF	0.1995	4.0115	9.8	4.2208	-	-	49.1228	-	-
	IBU	0.2010	4.0019	9.8	4.2127	-	-	48.7562	-	-
	INH	0.2015	4.0086	9.7	4.2198	-	-	48.1389	-	-

Table 2. Experimental conditions used in the synthesis of smart hydrogels. These materials were synthetized in previous research work of this group [14, 15].

Hydrogel / ***Synthesis Parameters***	**HG1**	**HG2**	**HG3**
Monomer 1	NIPA	AA	AA
Monomer 2	-	-	-
Crosslinker (CL)	MBA_m	MBA_m	MBA_m
Initiator (I)	APS	AIBN	APS
Catalyst (CAT)	TEMED	-	TEMED
RAFT Agent	-	DDMAT	-
Solvent	Water	DMF	Water
Monomer concentration	17.8 %	37.9 %	42.6 %
Ratio M1/(M2+M1)	100 %	100 %	100 %
Ratio CL/(M1+M2)	1.0 %	1.0 %	1.0 %
Ratio I/(M1+M2)	0.5 %	0.04 %	0.5 %
Synthesis temp.	20 ºC	70 ºC	20 ºC
Ratio I/CAT	1	-	1
Ratio RAFT/I	-	8.5	-
Neutralization	0 %	0 %	60 %

Table 3. Description of the release tests performed combining different drugs with different smart hydrogels.

Hydrogel	Drug	*m* HG incubated [g]	*m* Aqueous Solution [g]	pH	T [ºC]
HG1 (Method 1)	**5-FU**	0.3083	80.3634	≈7	25
		0.3138	80.2329	≈7	37
	CAF	0.1797	47.9206	≈7	25
		0.3000	80.0305	≈7	37
	IBU	0.3039	80.0022	≈7	25
		0.3003	80.0354	≈7	37
	INH	0.3008	80.0062	≈7	25
		0.3023	80.0178	≈7	37
HG2 (Method 2)	**5-FU**	0.3936	100.0025	≈2	20
		0.3769	100.0275	≈10	20
	CAF	0.3921	100.0277	≈2	20
		0.3916	100.0257	≈10	20
	IBU	0.3853	100.0022	≈2	20
		0.3852	100.0305	≈10	20
	INH	0.3815	100.0228	≈2	20
		0.3835	100.0050	≈10	20
HG3 (Method 2)	**5-FU**	0.3778	100.0029	≈1	20
		0.3784	100.0117	≈8	20
	CAF	0.3732	100.0011	≈1	20
		0.3741	100.0112	≈8	20
	IBU	0.3714	100.0190	≈1	20
		0.3715	100.0156	≈8	20
	INH	0.3912	100.0197	≈1	20
		0.3902	100.0097	≈8	20
HG1 (Method 2)	**5-FU**	0.0896	100.0157	≈7	25
		0.0909	100.0122	≈7	37
	CAF	0.0929	100.0136	≈7	25
		0.0928	100.0219	≈7	37
	IBU	0.0978	100.0267	≈7	25
		0.0966	100.0108	≈7	37
	INH	0.0904	100.0192	≈7	25
		0.0900	100.0108	≈7	37

2.4. Results and Discussion

In Figure 12 to Figure 15 are presented the results for molecules release from a PNIPA hydrogel, including the four drugs studied here and using Method 1 in the incubation process. All the results concern the release tests at 25 ºC. Figure 15 shows the amount of drugs *viz* INH, 5-FU, CAF and IBU, released per gram of hydrogel, being INH the drug with the highest amount.

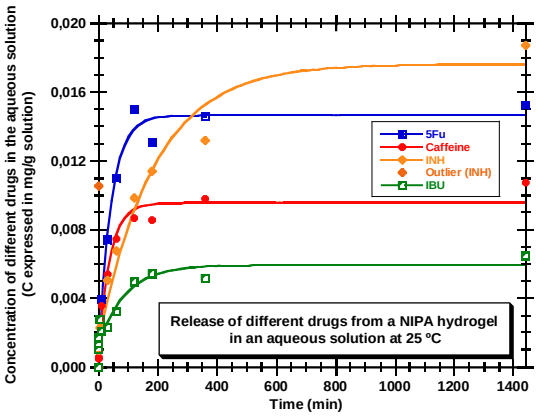

Figure 12. Comparison of the results of the release tests performed at 25 ºC with NIPA hydrogel (HG1) incubated with four drugs. Dynamics of drug concentration are shown here.

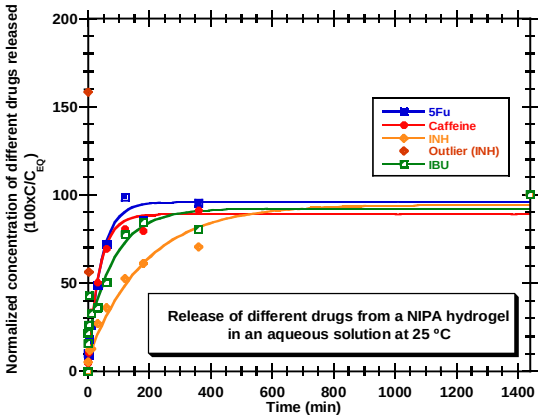

Figure 13. Comparison of the results of the release tests performed at 25 ºC with NIPA hydrogel (HG1) incubated with four drugs. Dynamics of normalized drug concentration are shown here.

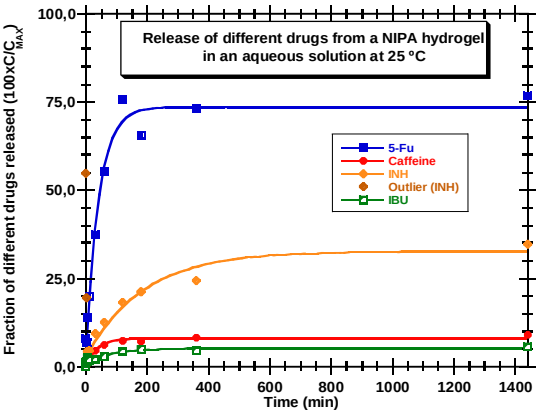

Figure 14. Comparison of the results of the release tests performed at 25 ºC with NIPA hydrogel (HG1) incubated with four drugs. Dynamics of drug fraction are shown here.

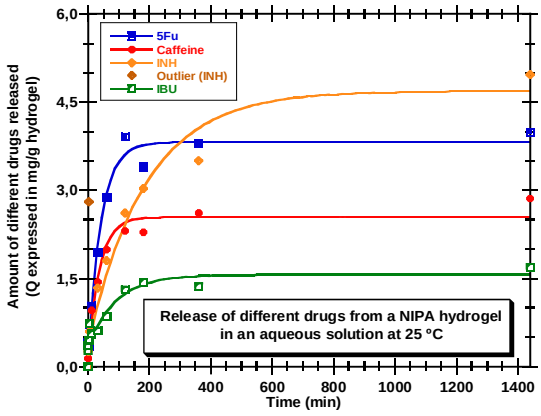

Figure 15. Comparison of the results of the release tests performed at 25 ºC with NIPA hydrogel (HG1) incubated with four drugs. Dynamics of drug amount are shown here.

This drug shows a peculiar behavior on the release profile when compared to the other three drugs. An INH incubated PNIPA releases the drug slower than the others but it does not mean that they are not useful as well. For example, if the objective is to release the drug fast and in small quantities, ibuprofen could be the chosen one.

In Figure 16 to Figure 19 the results of the controlled release tests can be seen for a PNIPA hydrogel incubated with the four drugs aforementioned, at 37 ºC.

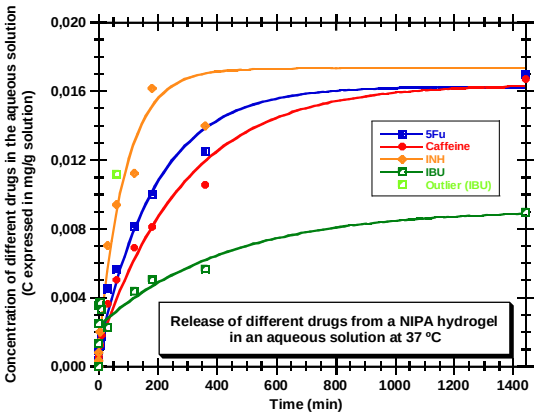

Figure 16. Comparison of the results of the release tests performed at 37 ºC with NIPA hydrogel (HG1) incubated with four drugs. Dynamics of drug concentration are shown here.

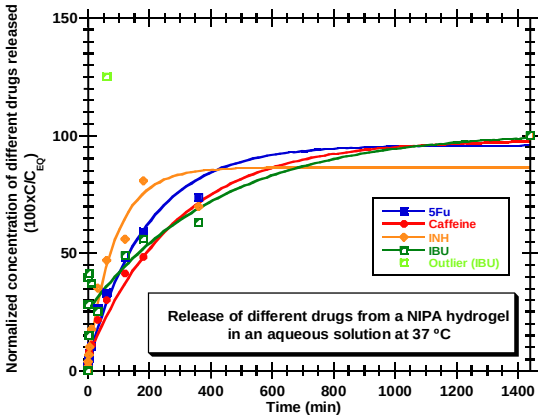

Figure 17. Comparison of the results of the release tests performed at 37 ºC with NIPA hydrogel (HG1) incubated with four drugs. Dynamics of normalized drug concentration are shown here.

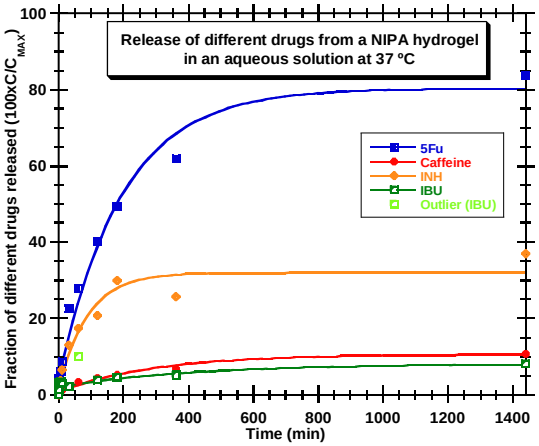

Figure 18. Comparison of the results of the release tests performed at 37 ºC with NIPA hydrogel (HG1) incubated with four drugs. Dynamics of drug fraction are shown here.

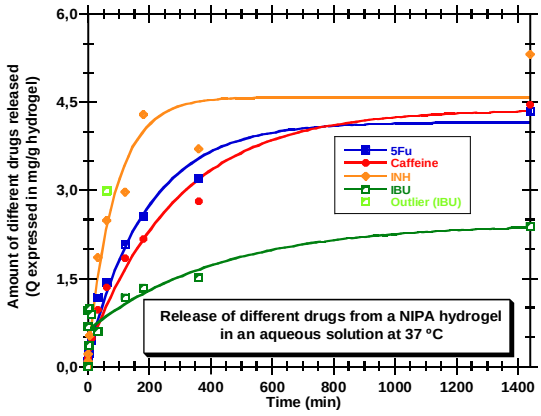

Figure 19. Comparison of the results of the release tests performed at 37 ºC with NIPA hydrogel (HG1) incubated with four drugs. Dynamics of drug amount are shown here.

The INH incubated NIPA is, comparing to the results for 25 ºC, still the one with the highest amount of drug released but now the release occurs slower than in the other drugs (in mg of drug/g of hydrogel). In terms of fraction of drug release, 5-FU incubated PNIPA presents the highest value among the other drugs. This fraction is calculated with reference to C_{MAX} and C_{MAX} can be defined as the maximum concentration obtained by UV for every drug.

In Figure 20 to Figure 23 are shown the results of PAA (HG2) at pH 2.

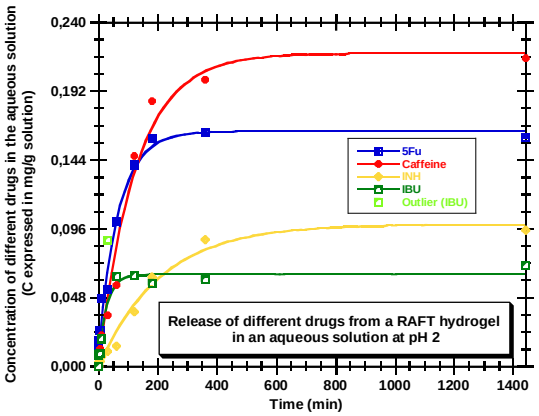

Figure 20. Comparison of the results of the release tests performed at pH 2 with PAA hydrogel (HG2) incubated with four drugs. Dynamics of drug concentration are shown here.

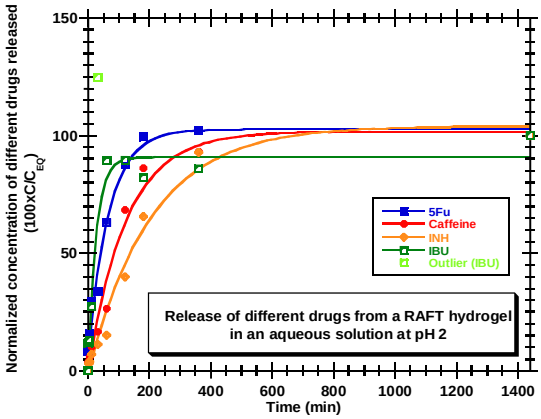

Figure 21. Comparison of the results of the release tests performed at pH 2 with PAA hydrogel (HG2) incubated with four drugs. Dynamics of normalized drug concentration are shown here.

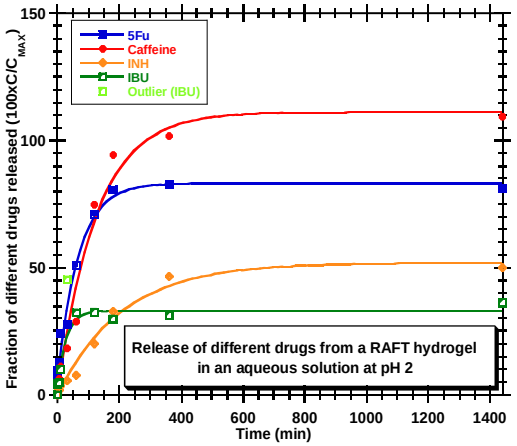

Figure 22. Comparison of the results of the release tests performed at pH 2 with PAA hydrogel (HG2) incubated with four drugs. Dynamics of drug fraction are shown here.

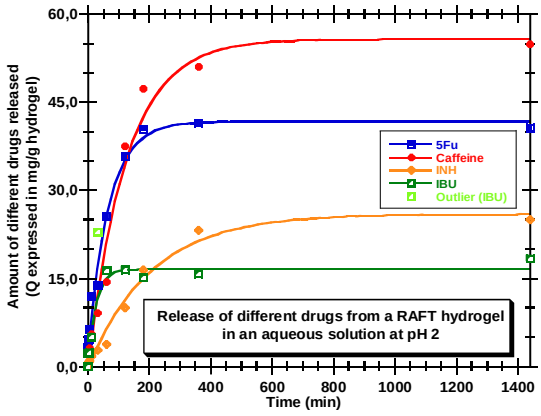

Figure 23. Comparison of the results of the release tests performed at pH 2 with PAA hydrogel (HG2) incubated with four drugs. Dynamics of drug amount are shown here.

In this case, using Method 2 in the incubation process, caffeine has a better release than the other three drugs. With its release profile, in Figure 22, can be seen that caffeine incubated PAA does not release the drug too fast when compared, for example, with ibuprofen that is the fastest one with a lower fraction of drug release.

In Figure 24 to Figure 27 are presented the results of a PAA hydrogel (HG2) at pH 10, in controlled drug release tests.

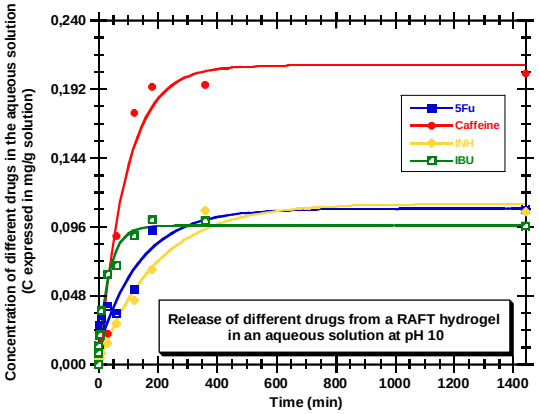

Figure 24. Comparison of the results of the release tests performed at pH 10 with PAA hydrogel (HG2) incubated with four drugs. Dynamics of drug concentration are shown here.

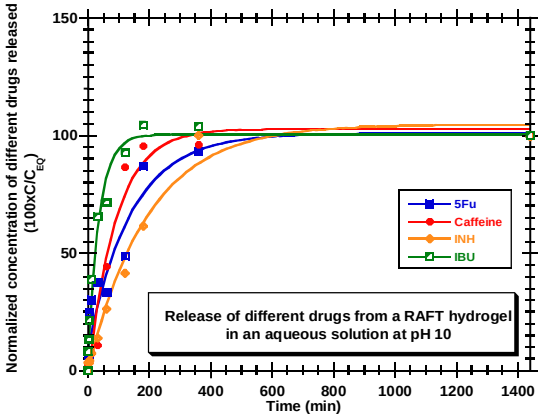

Figure 25. Comparison of the results of the release tests performed at pH 10 with PAA hydrogel (HG2) incubated with four drugs. Dynamics of normalized drug concentration are shown here.

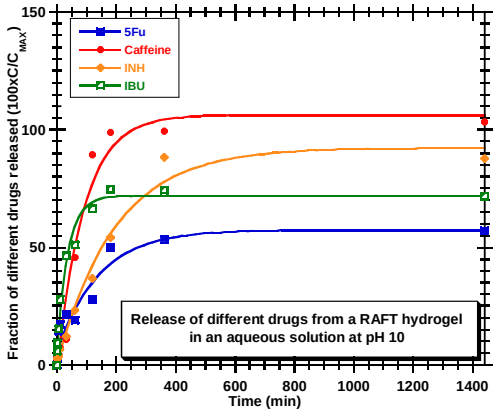

Figure 26. Comparison of the results of the release tests performed at pH 10 with PAA hydrogel (HG2) incubated with four drugs. Dynamics of drug fraction are shown here.

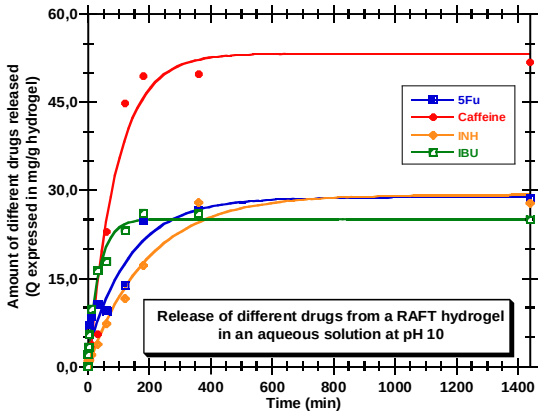

Figure 27. Comparison of the results of the release tests performed at pH 10 with PAA hydrogel (HG2) incubated with four drugs. Dynamics of drug amount are shown here.

Comparing to the results of the tests performed with the same hydrogel at pH 2, it can be seen that caffeine incubated PAA is still the one with a higher amount of drug release. On the other hand, IBU it's not the drug with the lowest amount released as it was at pH 2. This happens because IBU has a higher solubility in aqueous alkaline solutions than in acidic ones and so it is easy to understand that it would be a higher trend to release at pH 10.

From Figure 28 to Figure 31 are shown the results for PAA hydrogel (HG3) at pH 1.

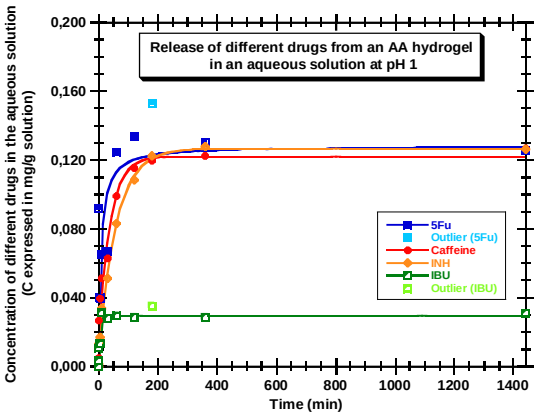

Figure 28. Comparison of the results of the release tests performed at pH 1 with PAA hydrogel (HG3) incubated with four drugs. Dynamics of drug concentration are shown here.

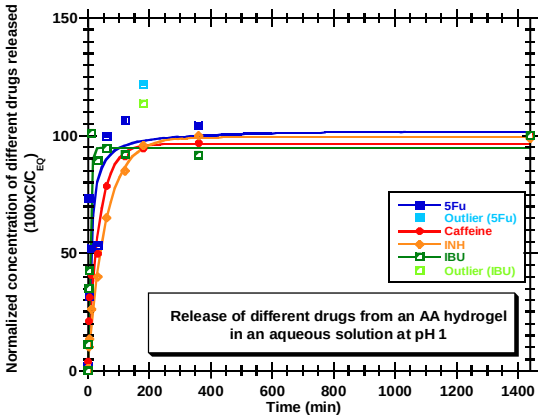

Figure 29. Comparison of the results of the release tests performed at pH 1 with PAA hydrogel (HG3) incubated with four drugs. Dynamics of normalized drug concentration are shown here.

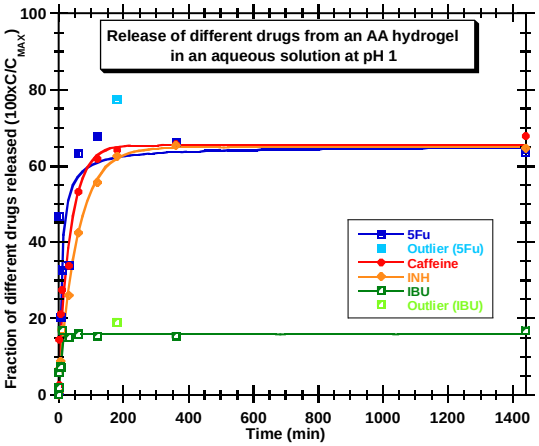

Figure 30. Comparison of the results of the release tests performed at pH 1 with PAA hydrogel (HG3) incubated with four drugs. Dynamics of drug fraction are shown here.

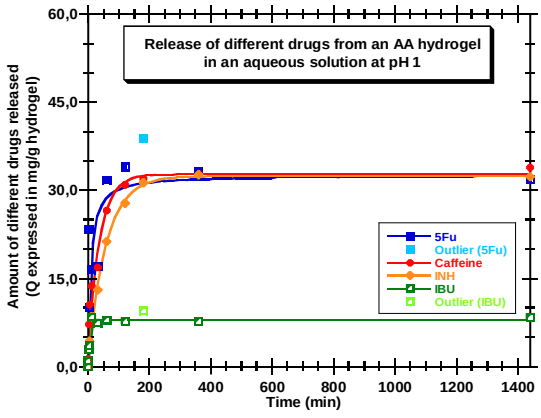

Figure 31. Comparison of the results of the release tests performed at pH 1 with PAA hydrogel (HG3) incubated with four drugs. Dynamics of drug amount are shown here.

The differences between 5-FU, INH and CAF, concerning to their release, are not too evident. The amount of drug release from those three drugs is almost the same when t=1440 min. IBU incubated PAA, on the other hand, has the lowest fraction of drug released due to IBU solubility, as it was explained before.

In Figure 32 to Figure 35 are shown the results for an incubated PAA (HG3) at pH 8.

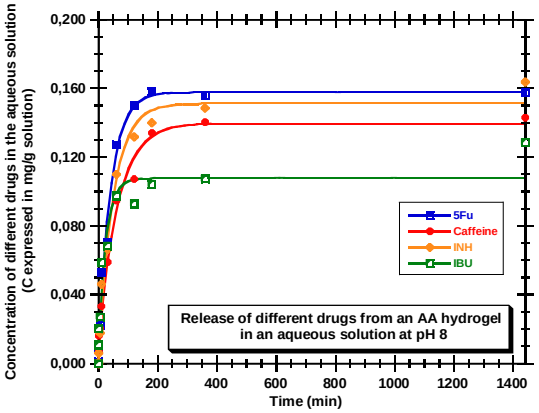

Figure 32. Comparison of the results of the release tests performed at pH 8 with PAA hydrogel (HG3) incubated with four drugs. Dynamics of drug concentration are shown here.

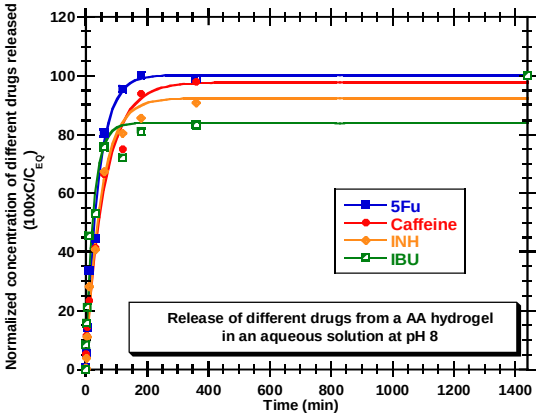

Figure 33. Comparison of the results of the release tests performed at pH 8 with PAA hydrogel (HG3) incubated with four drugs. Dynamics of normalized drug concentration are shown here.

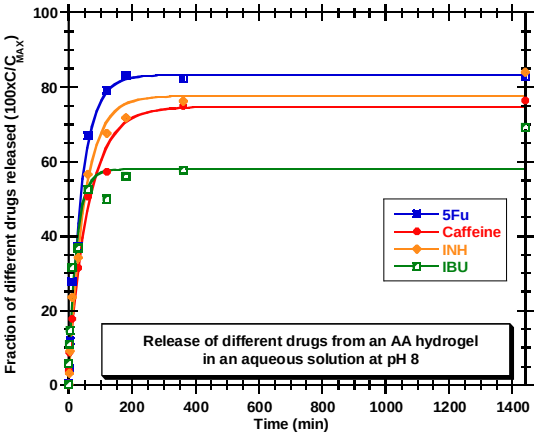

Figure 34. Comparison of the results of the release tests performed at pH 8 with PAA hydrogel (HG3) incubated with four drugs. Dynamics of drug fraction are shown here.

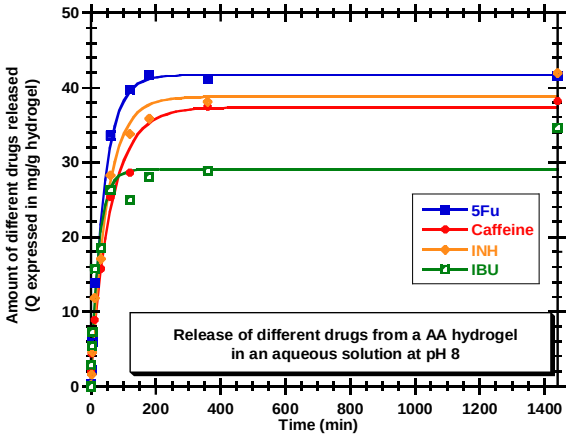

Figure 35. Comparison of the results of the release tests performed at pH 8 with PAA hydrogel (HG3) incubated with four drugs. Dynamics of drug amount are shown here.

Comparatively to tests performed at pH 1 these results show that, although the values of fraction released are still near to each other, now it is possible to observe that 5-FU is the drug with the higher quantity of drug release. IBU incubated PAA continues to be the one with the lowest amount of drug release in this conditions but, comparing to the results at pH 1, it now releases the double.

In Figure 36 to Figure 39 are shown the results for an incubated PNIPA using method 2 at 25 ºC.

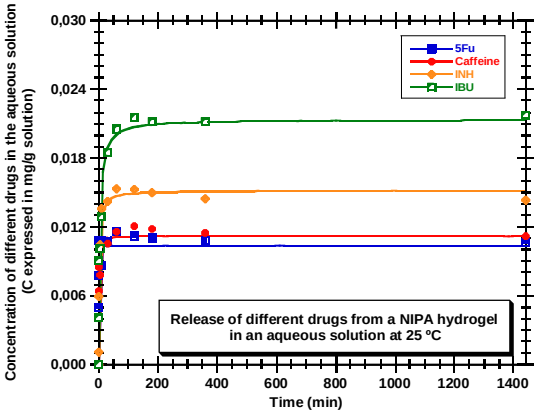

Figure 36. Comparison of the results of the release tests performed at 25 ºC with NIPA hydrogel (HG1) incubated with four drugs. Dynamics of drug concentration are shown here

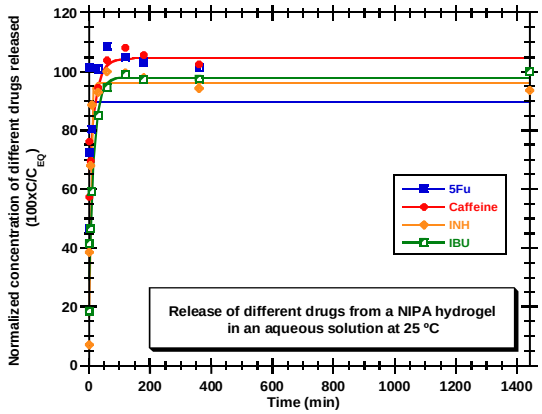

Figure 37. Comparison of the results of the release tests performed at 25 ºC with NIPA hydrogel (HG1) incubated with four drugs. Dynamics of normalized drug concentration are shown here

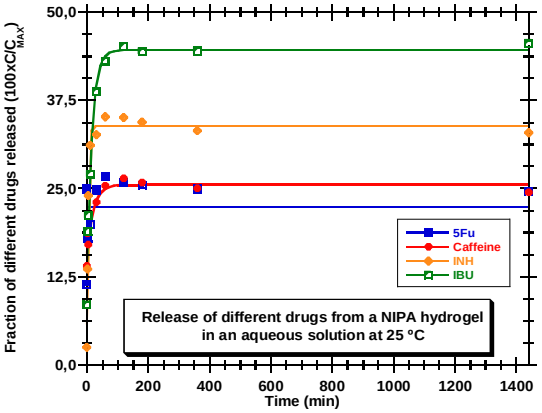

Figure 38. Comparison of the results of the release tests performed at 25 ºC with NIPA hydrogel (HG1) incubated with four drugs. Dynamics of drug fraction are shown here

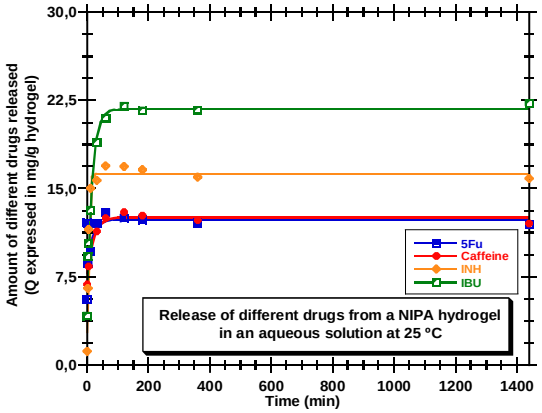

Figure 39. Comparison of the results of the release tests performed at 25 ºC with NIPA hydrogel (HG1) incubated with four drugs. Dynamics of drug amount are shown here

In this conditions IBU is the drug with a higher amount of drug release. Comparing with the results in page 14 where it was used method one in the incubation process, IBU has the lowest amount.

In Figure 40 to Figure 43 are presented the results for an incubated PNIPA using method 2, at 37 ºC. It can be seen that INH deviates a lot from the other drugs.

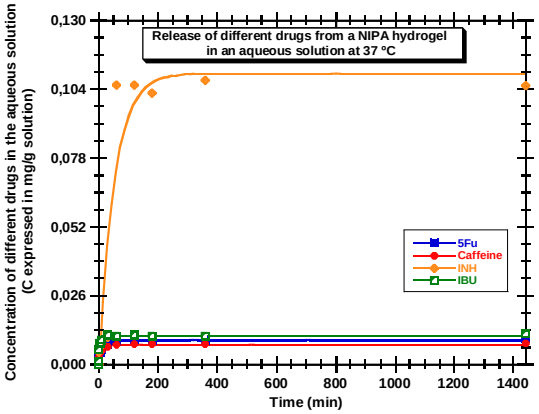

Figure 40. Comparison of the results of the release tests performed at 37 ºC with NIPA hydrogel (HG1) incubated with four drugs. Dynamics of drug concentration are shown here

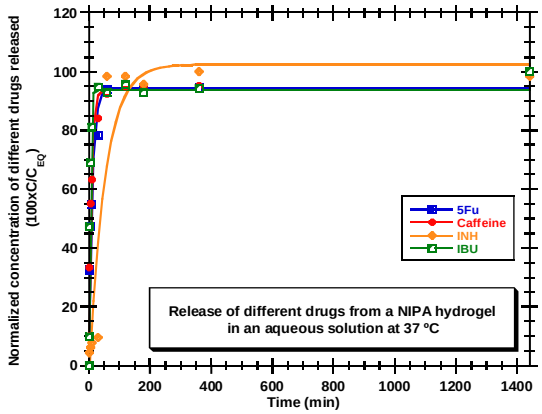

Figure 41. Comparison of the results of the release tests performed at 37 ºC with NIPA hydrogel (HG1) incubated with four drugs. Dynamics of normalized drug concentration are shown here

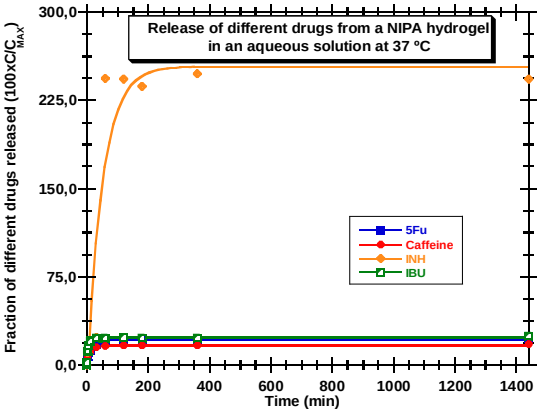

Figure 42. Comparison of the results of the release tests performed at 37 ºC with NIPA hydrogel (HG1) incubated with four drugs. Dynamics of drug fraction are shown here

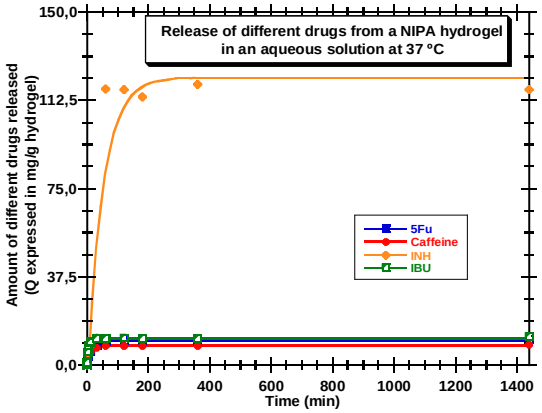

Figure 43. Comparison of the results of the release tests performed at 37 ºC with NIPA hydrogel (HG1) incubated with four drugs. Dynamics of drug amount are shown here

Detailed additional information concerning the drug release tests performed in this work can be found in the annexes of this work.

Results above described are an overview of the work performed during the batch controlled release testing in smart hydrogels considering four different drugs used in medicine (isonicotinylhdrazine, ibuprofen, 5-fluoruracil and caffeine). Within this purpose, temperature-sensitive and pH-sensitive hydrogels were used. N-isopropylacrylamide (NIPA) was considered to generate polymer networks with sensitivity to changes in the temperature of the environmental conditions and Acrylic Acid (AA) was used to obtain pH-sensitive materials. FRP and RAFT materials were alternatively used in these studies in order to study the impact of the synthesis conditions on the performance of these kinds of advanced materials. Results obtained in the context of controlled release can be found in the annexes of this work in their expanded form

In conclusion, hydrogels were loaded with the four targeted drugs through the exploitation of the swelling behavior of these materials in aqueous solutions. Two different batch incubation methods were tested, namely with and without the filtration of the remaining aqueous solution. In the first case (big excess of aqueous media followed by filtration), smaller amounts of drug are incubated in the hydrogel while with the second approach (all the initial aqueous media is taken by the hydrogel) some of the drug is eventually located in the surface of the material.

After loading, the different samples correspondent to different combinations of hydrogels/drugs were submitted to batch drug release tests triggered by different conditions of the surrounding aqueous media. Release studies at T=25 ºC and T=37 ºC were performed with the T-sensitive hydrogels and acid/alkaline conditions were considered with the pH-sensitive materials. In each case, dynamics of drug release was experimentally measured through UV detection in aqueous media of samples collected at different times (*t=0* is correspondent to the beginning of the drug release process). Results obtained showed the importance of selection of the right combination between hydrogel/drug/surrounding conditions in order to achieve some control on the release

process. In fact, physical and chemical interactions between hydrogels, drugs and aqueous solution play a fundamental role in these release mechanisms. For instance, results here obtained showed a huge difference in the release of ibuprofen in acidic or alkaline conditions due to the higher solubility of this molecule in the latter conditions (see the annexes of this work for an overview of all the results thus obtained).

The results above described with batch controlled release also highlight the need to look for routes with potential improvement of the affinity between drugs and hydrogels. The use of the molecular imprinting technique was selected within this purpose because, in principle, is the best way to increase the affinity and selectivity of a template molecule (e.g. a drug) with a polymer network. These ideas will be explored in the forthcoming chapters of this thesis.

CHAPTER 3 - Synthesis of RAFT Smart Hydrogels in Batch and Micro-Reactors

3.1. Introduction

Hydrogels are among the best materials for a number of biomedical applications because of their certain unique biophysical properties such as ease of fabrication to various geometrical forms, soft and rubbery texture, living tissue like resemblance, unusual stability to biofluids, minimum mechanical irritation to surrounding tissue, etc [17].

Different types of polymerization provide different properties to the hydrogels. For this reason, in this chapter it will be presented in addition to the types of polymerization, the different monomers and drugs used.

3.2. Free Radical Polymerization

This type of polymerization usually consists in three well defined stages: Initiation, propagation and termination. Note that the number and type of kinetic mechanisms involved in radical polymerization may be substantially higher, being here only presented a simple illustration of these reaction processes [16].

The polymerization starts with the decomposition of the initiator in two free radicals capable of breaking the carbon-carbon double bond of the monomer.

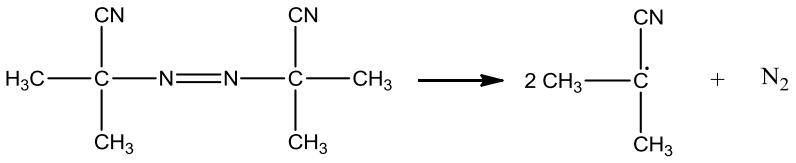

Figure 44. Decomposition of the initiator (using AIBN as example).

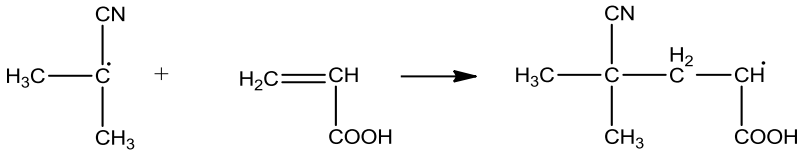

Figure 45. Initiation of the monomer (using acrylic acid as example).

In the propagation step the radical formed in the initiation process is able to add successive monomer units causing the growing of the chain.

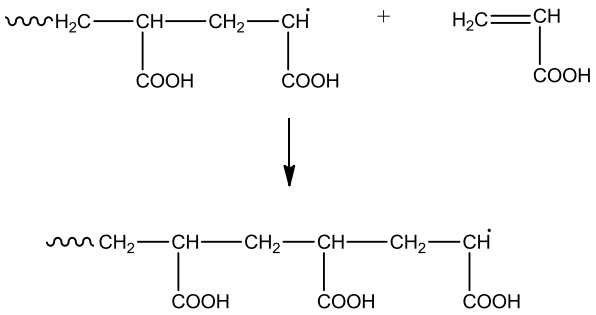

Figure 46. Propagation of the monomer.

The step of crosslinking of the dangling bonds of the crosslinker down the big difference between a linear radical polymerization (usually with formation of soluble products) and a non-linear radical polymerization (potentially leading to the formation of insoluble hydrogels).

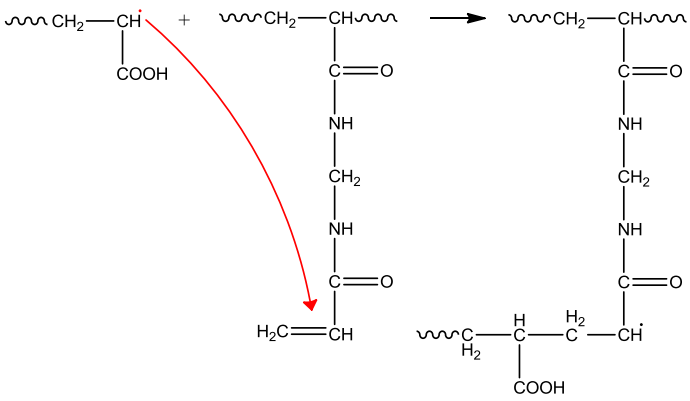

Figure 47. Crosslinking with double pendant of the Crosslinker (using MBAm as example).

In the latter case it is formed a three dimensional network polymer which is not fusible or can't be solubilized in any solvent. In Figure 48 is presented an example of linear and non-linear polymers synthetized in this work.

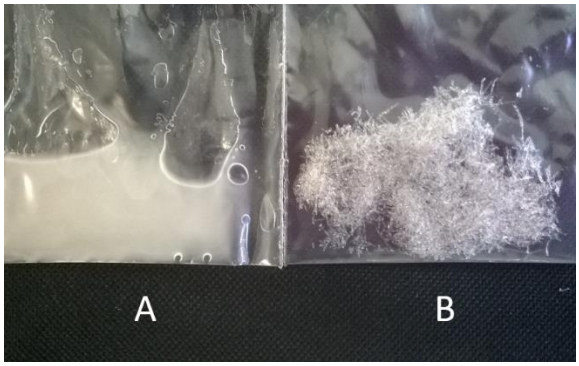

Figure 48. A - Linear polymer (CM06); B - Non-linear polymer (CM03).

In theory, the propagation reaction could continue until the supply of monomers reach exhaustion. However, this outcome is highly unlikely. Frequently the growth of a polymer chain is stopped by the termination stage. This stage typically occurs in two modes: combination and dismutation. The chain growth is stopped by the mutual "death" of the two radicals. Termination by combination occurs when the polymer growth is stopped by formation of a covalent bond between the electrons unpaired of the two growing chains, forming a single chain [18, 19].

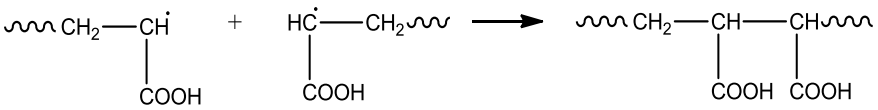

Figure 49. Termination by combination.

The dismutation holds a propagating reaction when a radical removes a hydrogen from an active chain. A carbon-carbon bond takes the place of the missing hydrogen [18, 19].

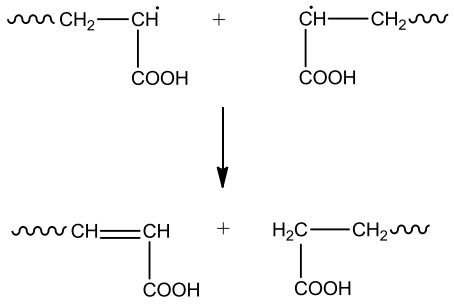

Figure 50. Termination by dismutation.

3.3. Controlled Radical Polymerization

Free radical polymerization presents a few limitations as regards the final product. The polydispersity is always high and the production of copolymers is very limited.The high polydispersity happens due to the initiation, propagation and termination steps occur in seconds although the polymerization is usually completed in minutes, even hours.

Copolymers are produced when, in the reaction mixture, there is more than one type of monomers. The incorporation of each monomer in the grown chain depends on its instantaneous concentration and its relative reactivity. So, the copolymers produced by FRP have always chains with an high proportion of one of the monomers (when the conditions are better for its incorporation in the chain) and of the other monomer (when there is a lack of the first one due to its consumption) [20].

At the end of the XX century the Controlled Radical Polymerizations appeared. These came to address the deficits identified on Free Radical Polymerizations, since the CRP are capable of generating polymeric products with low polydispersity and different morphologies.

One of the several types of CRP is the Reversible Addition-Fragmentation chain Transfer Polymerization (RAFT). Like the FRP, RAFT polymerization occurs by free radicals. The main difference is that in the last one the activity of these radicals can be

controlled with the addition of a RAFT agent providing different characteristics to the final product.

The mechanism of RAFT polymerization is used in various kinds of monomers and can be conducted in different solvents and under different reaction conditions. In this mechanism, one transfer agent chain, of the type of trithiocarbonates (for example), reacts with a primary radical from the decomposition of an initiator or a macroradical yielding a new transfer agent chain and a radical, which is able to restart polymerization, as showed in Figure 51 [21, 22].

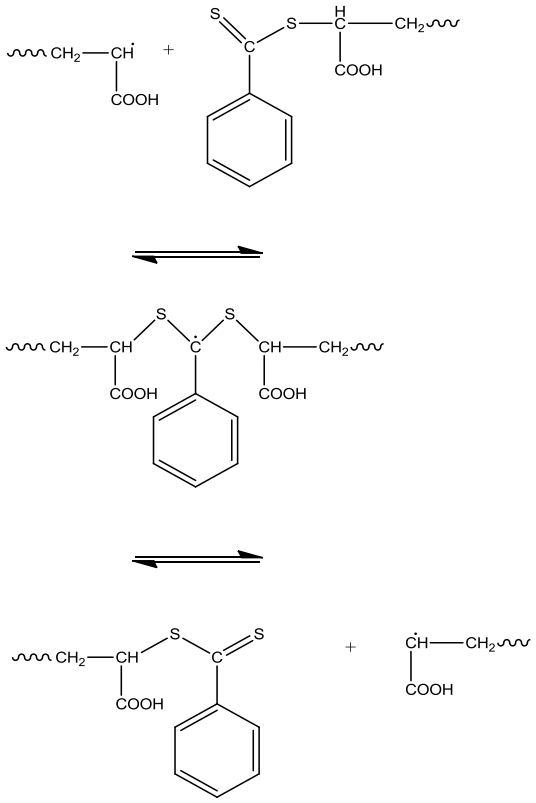

Figure 51. Mechanism of activation/deactivation by RAFT polymerization.

There are three main classes of RAFT agents:

- Dithiobenzoates;
- Trithiocarbonates;
- Dithiocarbamates.

The RAFT agent used in this work is 4-Cyano-4-(phenylcarbonothioylthio)pentanoic acid (CPA) and belongs to dithiobenzoate class. The main advantage of using this RAFT agent is the fact that it is partially soluble in water.

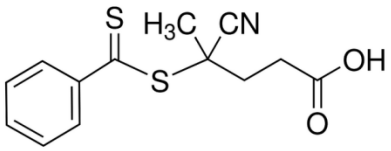

Figure 52. Molecular structure of CPA.

Making use of this type of polymerization it was synthetized molecularly imprinted polymers as well as non-imprinted polymers. The procedures are explained in the next topic.

3.4. Molecularly Imprinted and Non-Imprinted Polymers

The molecular imprinted method is quite simple and easy to perform and it creates selective sites in a polymer matrix. The procedure is based on the fact that the target molecule (template) is present during the polymer synthesis and chemically interacts with the monomer. These monomers contain functional groups and its linkage to the template is made by covalent interactions [23, 24].

By removing the template molecules the polymer stays with cavities whose size, shape and three-dimensional arrangement of binding sites are determined by the structure of the template molecules. If one of the enantiomers of the drug is used as the template, the resulting polymer might be able to discriminate between the two of them [24, 25].

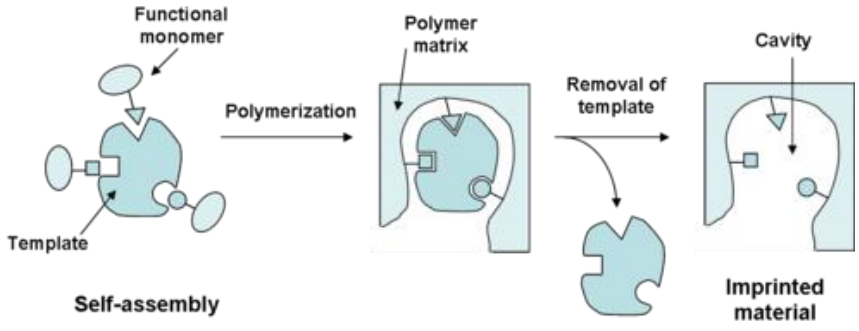

Figure 53. Imprinting procedure.

The efficiency of the imprinting process is tested in parallel on a non-imprinted polymer which does not contain the template molecule during the synthesis [23, 24]. The affinity to the template is studied with adsorption tests, by SPE (Solid Phase Extraction) and Frontal Analysis and the results are presented in Chapter 5 of this work.

The choice of the template was made because caffeine is a *"basic"* molecule and due to the acidic characteristic of acrylic acid, the non-ligand pairs of caffeine tend to create hydrogen bounds with the monomer, leading to a potential strong interaction between monomer and template (as sought with molecular imprinting).

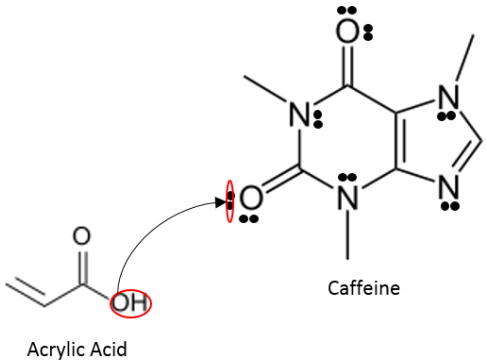

Figure 54. Potential molecular interaction between caffeine and acrylic acid.

3.5. Micro-reactor

Micro-reactors have been gaining, recently, very interest in pharmaceutical industries due to the improved product quality.[26, 27]

In its simple form, MR begins with two streams of different materials. In this case, one stream has the monomer solution (please see the Experimental Procedure topic) and the other one has the oil phase (paraffin) in order to help the flow of the solution even when it is already reacted. They are pumped in a predefined flow rate into a tube where the synthesis happens. The tube is immersed in an oil bath to allow the control of the reaction temperature.

Based on the flow rate and the volume of the tube a specific residence time within the MR is needed to guarantee that all the starting solution is converted to the desired

product which is collected in the outlet of the MR in a flask containing acetone, for example.

3.5.1. Micro-reactor build up

Continuous flow micro-reactor was built up using two Knauer HPLC pumps (model Azura P 4. 1S, titanium head) with maximum delivery pressure of 40 MPa and flow rate in the range 0.001 to 10 ml/min. Valco tee devices were used to connect the two lines coming from the pumps with generation of the fed to the micro-reactor. Different T connectors with internal diameters 0.25, 0.5, 0.75, and 1.0 mm were considered. PTFE tubings with different internal diameters (0.2, 0.5, 0.8, 1.0 and 1.5 mm) were used as continuous flow micro-reactors. The maximum length of all micro-reactors used is 20 m. The micro-reactor tubing was rolled up on a metallic cylinder and immersed in oil bath with controlled temperature. A container was connected to the end of the reactor in order to collect the carrier fluid (often liquid paraffin) and the aqueous-phase polymer particles. In this container, a polymer precipitating solvent (e.g. methanol or acetone) was also often included and mixing by a magnetic stirrer was also promoted. A scheme of this micro-reactor set-up is presented in Figure 55.

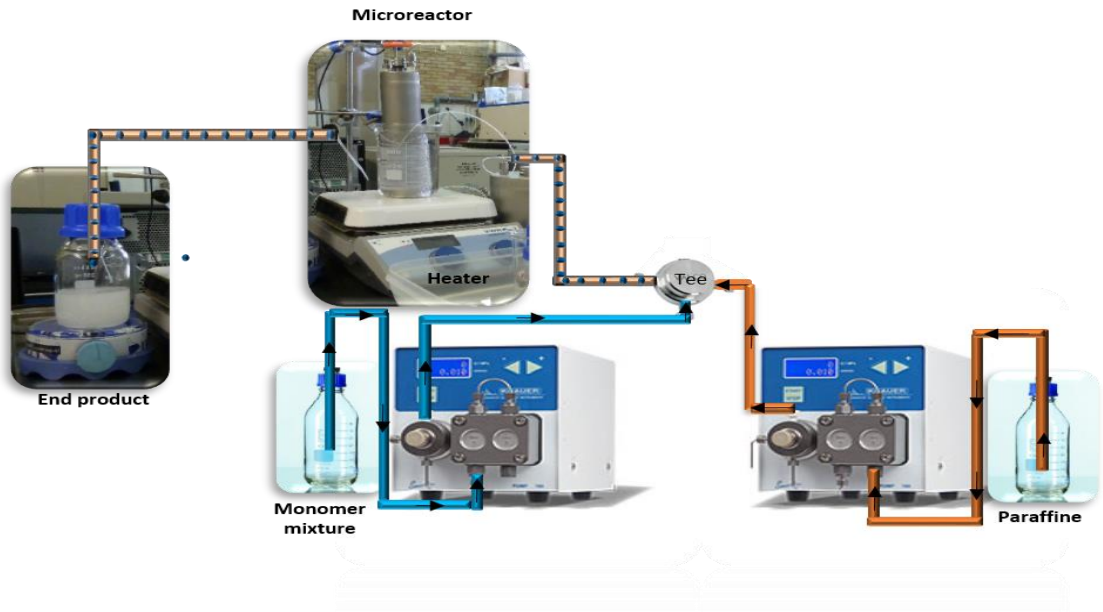

Figure 55. Droplet based microreactor device illustration [26].

3.6. Batch reactor

Batch reactors are stirred tanks sufficiently large to handle the full inventory of a complete batch cycle, being the reagents add all at the same time in controlled conditions. In this work the flasks were placed in an oil bath in order to control the reaction temperature as illustrates Figure 56.

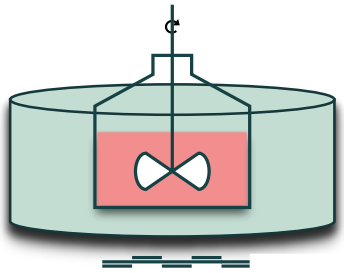

Figure 56. Depiction of the batch polymerization process used in this work.

3.7. Experimental procedure

The polymers were synthetized by CRP – RAFT and FRP. The only difference between the two of them, when preparing the monomer solution, is that the first one uses a RAFT agent in order to improve the molecular architecture of the polymer, as it was explained before.

3.7.1. Preparation of the monomer solution for non-linear polymers

The preparation of the solution is the same apart the reactor that is going to be used. The solution is prepared with acrylic acid (AA) and methylene-bisacrilamide (MBAm) as crosslinker. V50 (2,2'-azobis(2-methylproprionamidine) dihydrochloride) and AIBN (2,2'-Azobis(2-methylpropionitrile)) were selected as water and organic compatible, respectively, thermal initiators. It was used CPA, for controlled radical polymerization, as RAFT agent. For MIP it was used caffeine as the target molecule.

First of all an amount of monomer is mixed with some water and the crosslinker (and, for MIP the target is added too) while the CPA is mixed with the rest of the monomer. When the CPA and the crosslinker are totally dissolved the two solutions are mixed together and are degased with argon in order to take out all the oxygen once it is an inhibitor of the reaction. The water that is still needed is added to the initiator and is then mixed with the degased solution to start the reaction. Note that for FRP the procedure is the same apart adding the RAFT agent.

In Figures 57, 58, 59, 60 and 61 are shown examples of polymers obtained in this work.

Figure 57. A: RAFT non-linear polymer (CM11). **B:** FRP non-linear polymer (CM02). (Both synthesis in a MR).

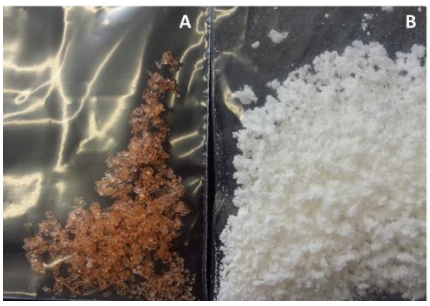

Figure 58. A: Non-linear polymer synthetized on a MR (CM10). **B:** Non-linear polymer synthetized in a batch reactor (CM05). (Both synthesis using RAFT polymerization).

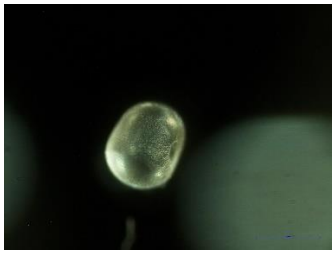

Figure 59. Microscopic images of RAFT imprinted smart hydrogel particles obtained in continuous flow micro-reactor.

3.7.2. Preparation of the solution for linear polymers

The main difference between the linear and non-linear polymers is the use or not of the crosslinker. In the first case the crosslinker isn't a part of the monomer solution. Thus it is necessary to add the monomer to some amount of water and CPA and the remaining water is added to the initiator. Like before, the solution monomer + water + CPA is going to be degased with argon and only after the initiator is added. When polymerizing with FRP the CPA is not part of the solution.

The conditions and quantities used in each synthesis are showed in Table 4.

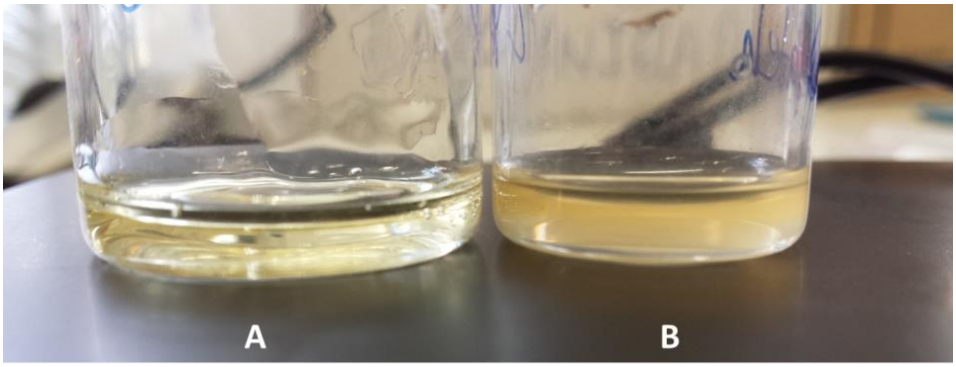

Figure 60. A: FRP linear polymer (CM07). **B:** RAFT linear polymer (CM09). (Both synthesis in a batch reactor).

3.7.3. Cleaning of the polymers with *Soxhlet* Extraction

Molecularly imprinted polymers have their cavities full of the target right after the synthesis and could still have some monomer that did not react or another compound (e.g. solvent or initiator).

.

In order to correctly characterize the material it is necessary to clean it first to remove all the unwanted compounds. With this purpose it was used the *soxhlet* extraction.

Figure 61. Polymers right after polymerization, without cleaning.

The polymer that is going to be cleaned is placed inside a filter paper cylinder which is loaded into the extraction chamber of the *soxhlet*. The extraction solvent, in this case a mixture with methanol and water, is taken into a distillation flask that is placed in a heater and connected to the main chamber. The *soxhlet* is then equipped with the condenser.

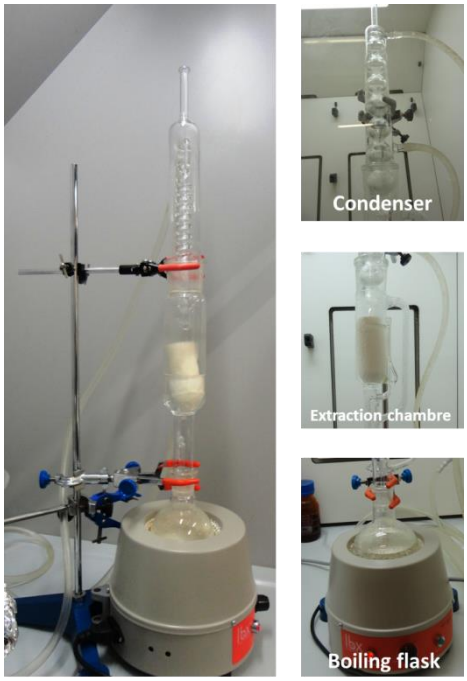

Figure 62. Soxhlet Extraction Equipment used in this work.

The process begins when the solvent reaches its boiling point. Once this happens, the vapor travels up in a distillation arm and when reaching the condenser it ensures that any vapor cools and falls down into the chamber. The chamber containing the solid material is slowly filled with warm solvent. Some of compound that we want to take out

of the polymer will be dissolved in it. When the *Soxhlet* chamber is almost full, the chamber is automatically emptied by a siphon side arm, with the solvent running back down to the distillation flask. This procedure can take hours or even days.

Figure 63. Polymers after cleaning in the Soxhlet.

The parameters showed in Table 4 have the following meaning:

Weight fraction of monomer:

$$Y_M = \frac{monomer\ mass\ (mg)}{monomer\ mass\ (mg) + mass\ of\ water\ (mg)} \times 100 \quad (3.1)$$

Initiator mole ratio:

$$Y_I = \frac{n\ of\ initiator\ (mol)}{n\ of\ monomer\ (mol)} \times 100 \quad (3.2)$$

Crosslinker mole fraction:

$$Y_{CL} = \frac{n\ of\ CL\ (mol)}{n\ of\ CL\ (mol) + n\ of\ monomer\ (mol)} \times 100 \quad (3.3)$$

RAFT agent mole ratio:

$$Y_{RAFT/I} = \frac{n\ of\ RAFT\ agent\ (mol)}{n\ of\ initiator\ (mol)} \quad (3.4)$$

Template/Crosslinker mole ratio:

$$Y_{T/CL} = \frac{n\ of\ template\ (mol)}{n\ of\ crosslinker\ (mol)} \quad (3.5)$$

The results here presented report the work performed with the synthesis of conventional (non-imprinted) and MIP hydrogels in batch reactor using FRP and RAFT techniques. Besides the expected improvement of the affinity between hydrogels and specific drugs considering MIP materials, these synthesis were also a contribution to the assessment of the influence of the kinetic mechanisms involved (FRP/RAFT) on network performance. Moreover, it was also showed the feasibility of a new experimental approach, using a continuous microfluidic reactor, and allowing the synthesis of smart hydrogel micro-particles. Imprinted/non-imprinted and FRP/RAFT products were obtained within this task [26, 27]. Expecting for particular interactions between caffeine and acrylic acid molecules, this combination was selected in the molecular imprinting studies here performed.

Table 4. Experimental conditions used in the synthesis of the polymers**.**

Run	M	I	CL	Template	Y_M	Y_I	Y_{CL}	$Y_{raft/I}$	$Y_{T/CL}$	S.	T (°C)	Reactor
CM01	AA	AIBN	MBAm	-	41.2	1.01	2.01	0.10	-	DMF	75	Micro-reactor
CM02	AA	AIBN	MBAm	-	41.2	1.01	2.01	0.10	-	DMF	75	Micro-reactor
CM03	AA	V50	MBAm	-	40.0	1.01	2.01	0.10	-	water	70	Micro-reactor
CM04	AA	V50	MBAm	-	40.0	1.01	2.01	1.00	-	water	50	Batch
CM05	AA	V50	MBAm	CAF	40.0	1.01	2.01	1.00	1.00	water	50	Batch
CM06	AA	V50	-	-	40.0	1.01	-	-	-	water	50	Micro-reactor
CM07	AA	V50	-	-	40.0	1.01	-	-	-	water	50	Batch
CM08	AA	V50	-	-	40.0	1.01	-	1.0	-	water	70	Micro-reactor
CM09	AA	V50	-	-	40.0	1.01	-	1.0	-	water	70	Batch
CM10	AA	V50	MBAm	CAF	40.0	1.01	2.01	1.0	1.00	water	90	Micro-reactor
CM11	AA	V50	MBAm	-	40.0	1.01	2.01	1.0	-	water	90	Micro-reactor

CHAPTER 4 - Characterization of Products' Molecular Architecture using SEC with Tetra-Detection

4.1. Introduction

Gel Permeation Chromatography (GPC) or Size Exclusion Chromatography (SEC) is an analytical technique used for the determination of molecular weight and molecular weight distribution of natural and synthetic polymers.

The separation process takes place in columns which are packed with porous material such as polystyrene gels, glass beads, silica gel, etc. Because of their size the larger molecules cannot fit and elute faster through the porous packing material than the smaller ones. The columns used were A7Guard, A6000 and A3000 from Viscotek.

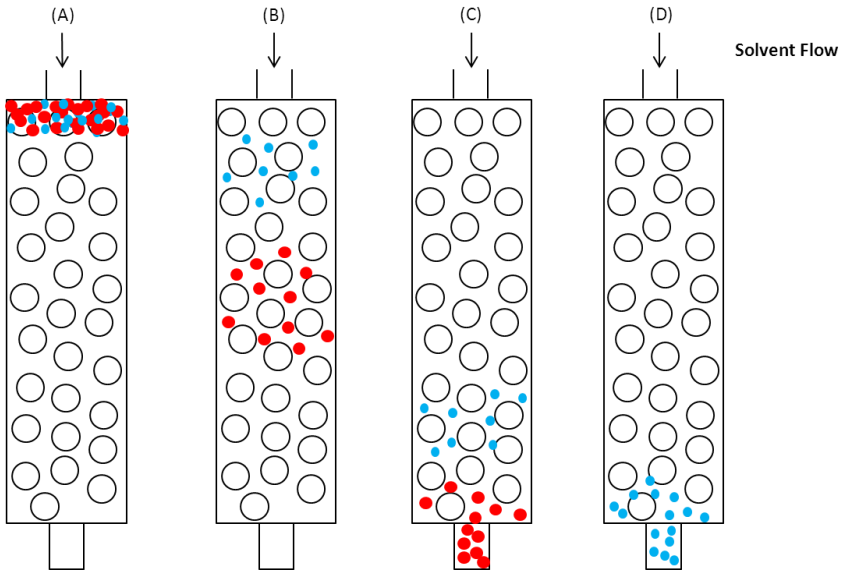

Figure 64. Illustration of SEC separation showing the separation of low (●) and high MW (●) polymers. **A:** Start of separation. **B:** Smaller molecules get trapped in the micropores of the packed bed while bigger molecules elute in the interstitial regions. **C:** The separation is complete and the bigger molecules start to exit the column. **D:** The smaller molecules leave the column [28, 29].

To perform these studies was used a system of size exclusion chromatography (GPC / SEC) including a pumping module solvent and sample injection (Viscotek GPCmax VE 2001 model) that is also equipped with four detection signals, namely refraction index (RI), light scattering (LS) Intrinsic viscosity (IV-DP) and ultraviolet (UV). UV detection is especially useful in the context of the tests conducted here as will be detailed below. In Figure 65 it is presented a simplified schematic representation of the GPC system used in this work.

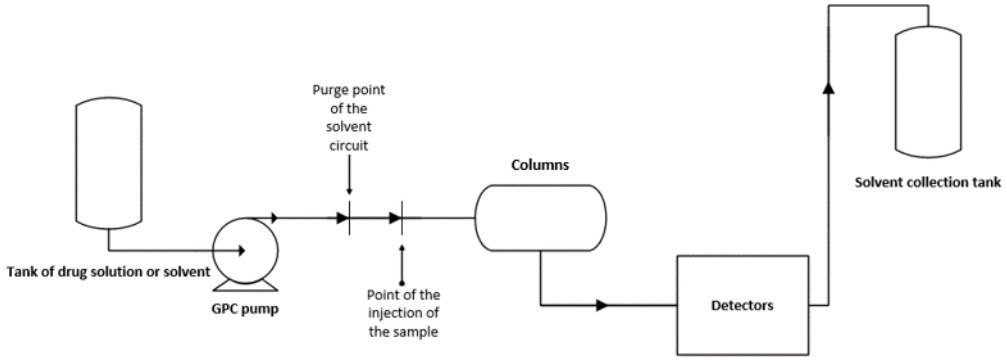

Figure 65. Simplified schematic representation of the GPC system used to study the weight mass distribution of linear polymers synthetized in this work.

The RI and UV detectors measure the concentration and are necessary for the determination of both molecular weight and intrinsic viscosity. The LS detectors provide a direct measurement of molecular weight and eliminate the need for column calibration. Finally, the viscometer detector provides a direct measurement of intrinsic viscosity and allows the determination of molecular size, conformation and structure [29].

4.2. Experimental procedure

To start these tests it was necessary to analyze first three standards with known molecular weight: 5300, 66600 and 920000 g/mol. PEO (PolyEtylene Oxide) standards were used within this purpose.

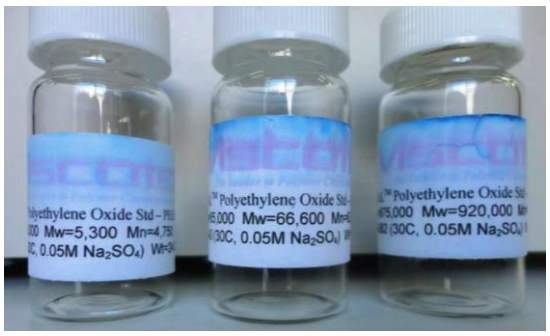

Figure 66. PEO standards for the construction of the calibration curve.

The purpose is to make a calibration line (see Figure 67) where it can be related the retention volume with the molecular weight for the polymers that are going to be studied. The following equation was used with this aim.

$$M = \alpha \times Ve^{\beta} \Leftrightarrow$$
$$\log M = \log \alpha + \beta \times \log Ve \tag{4.1}$$

With:

M – The molecular weight of the polymers (g/mol);
α – The intercept of the calibration curve;
Ve – The retention volume;
β – The slop of the calibration curve.

The polymers used are the linear ones once they are able to dissolve in water.

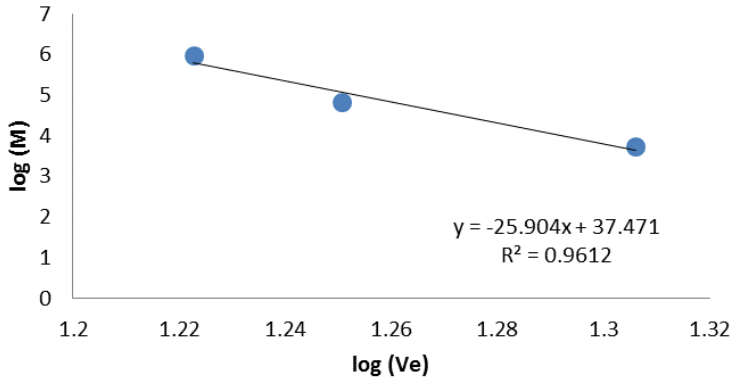

Figure 67. Calibration line using PEO standards.

The quantities used for each polymer are presented in Table 5.

Table 5. Quantities of hydrogel used in these tests.

RUN	Mass of hydrogel (mg)	Volume of water (mL)
CM06	16.70	10.0
CM06	47.70	10.0
CM07	16.50	10.0
CM08	16.80	10.0
CM09	16.30	10.0
CM09	42.10	10.0

When the polymers are totally dissolved in water the experiment can begin. First the vials are filled with all the solutions and placed inside of the instrument.

Figure 68. Vials placed inside the GPC.

Then the injection is made and the solution flows at 0.5 mL/min through the detectors and it is collected in the outlet collection tank.

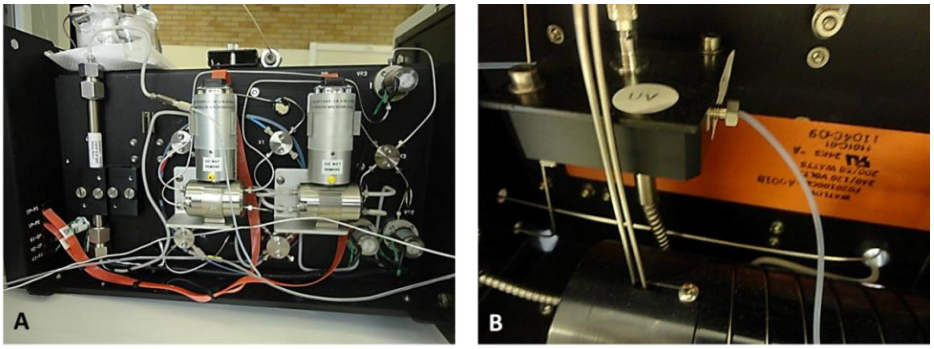

Figure 69. The detectors of the GPC instrument. **A:** RI, LS and IV detectors. **B:** UV detector.

4.3. Results and discussion

In Figure 70 to Figure 73 are presented the chromatograms of the different detectors for a linear polymer synthetized by FRP in a batch reactor. The detector with the best signal is the UV (Figure 71) and there are well visible two peaks. The first peak corresponds to the population with a low MW and so with a bigger retention volume. The second one corresponds to the population with a high MW implying a lower retention volume. It can still be seen that in this polymer exists more population with a higher MW.

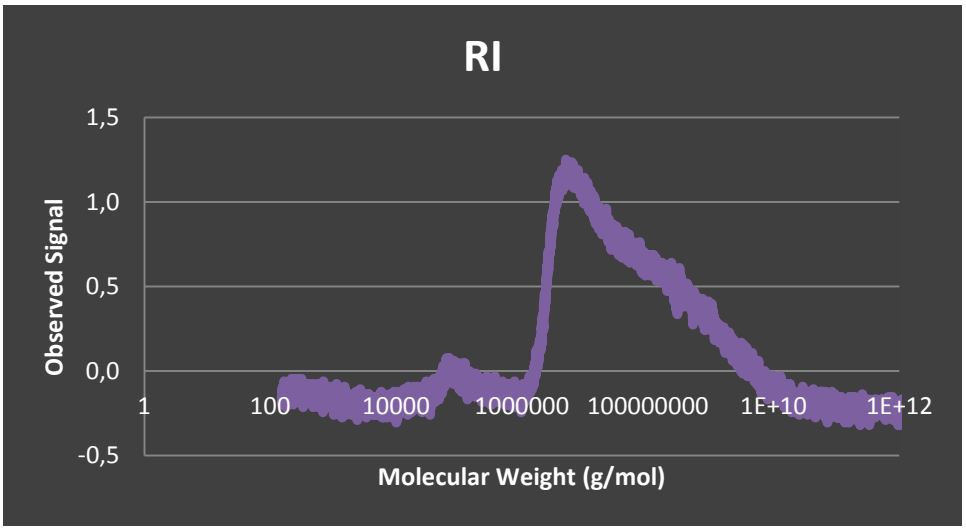

Figure 70. Refraction Index chromatogram of a linear polymer synthetized by FRP in a batch reactor (CM07).

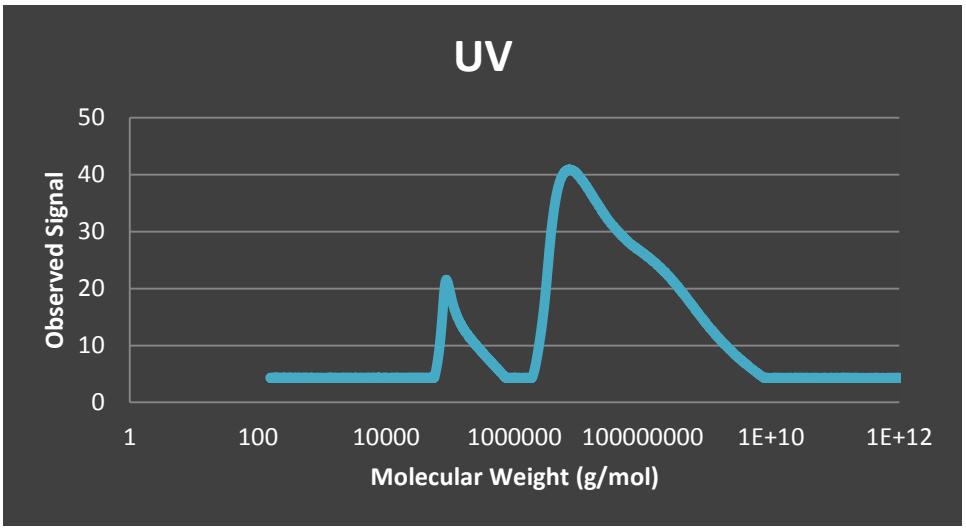

Figure 71. UV chromatogram of a linear polymer synthetized by FRP in a batch reactor (CM07) (Detection at 272 nm).

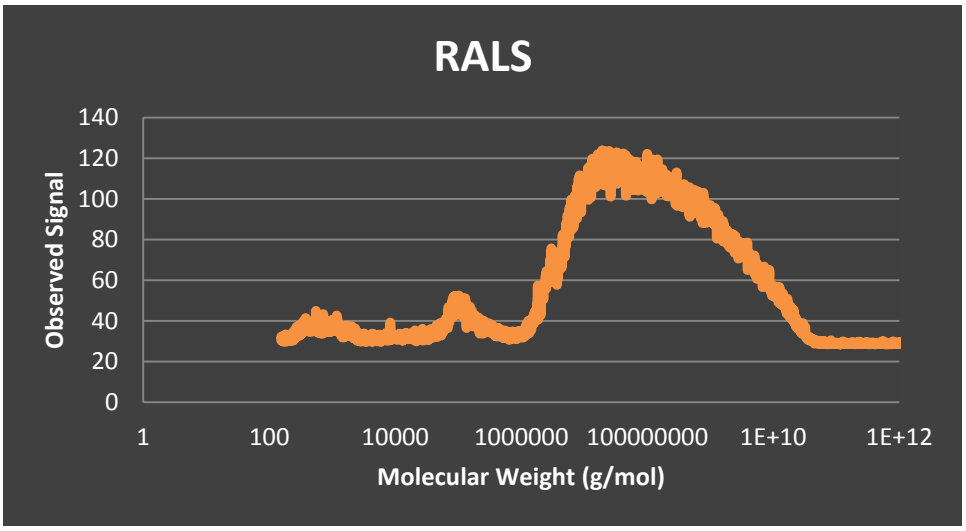

Figure 72. RALS chromatogram of a linear polymer synthetized by FRP in a batch reactor (CM07).

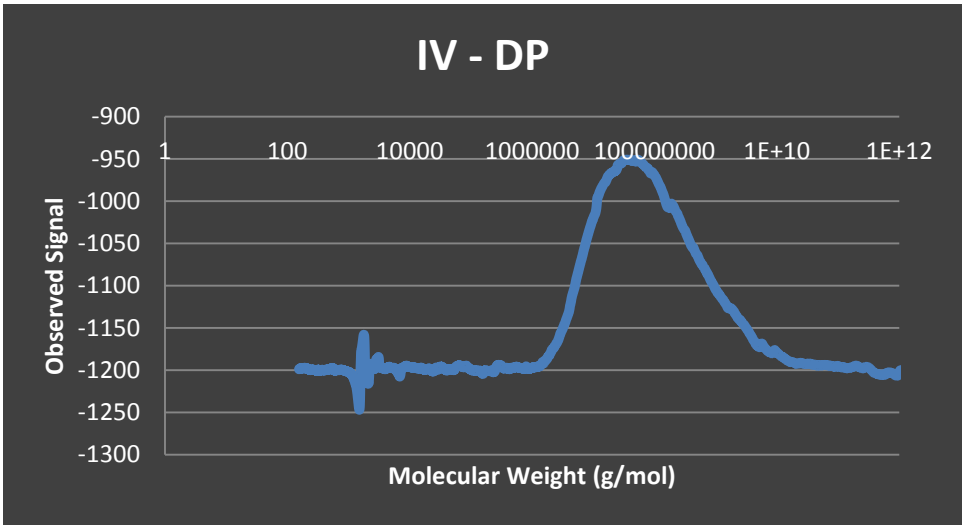

Figure 73. IV chromatogram of a linear polymer synthetized by FRP in a batch reactor (CM07).

In Figure 74 to Figure 76 are presented the chromatograms of the different detectors for a linear polymer synthetized by RAFT in a micro-reactor. In this case, observing Figure 75, the difference between the peaks is sharper than in the previous results. It means that with a RAFT polymerization the population is more homogeneous than using FRP.

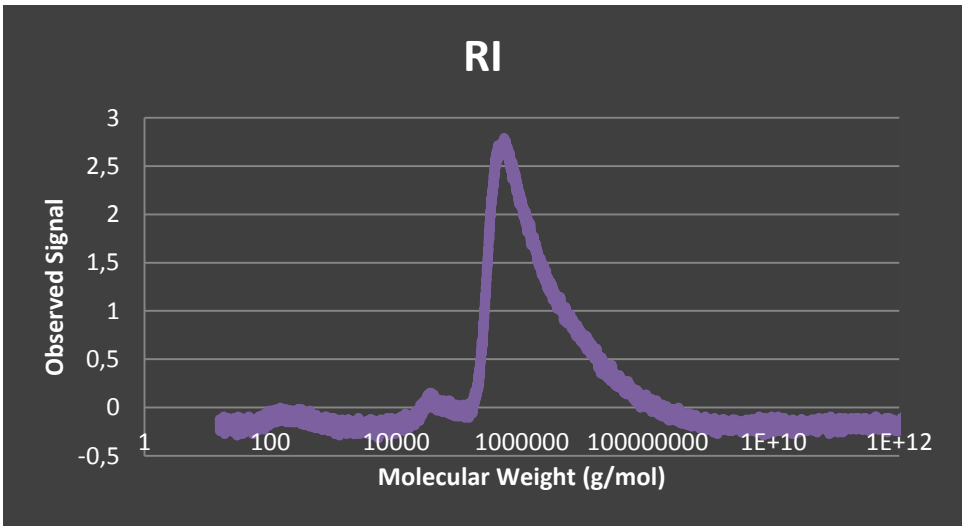

Figure 74. RI chromatogram of a linear polymer synthetized by RAFT in a micro-reactor (CM08).

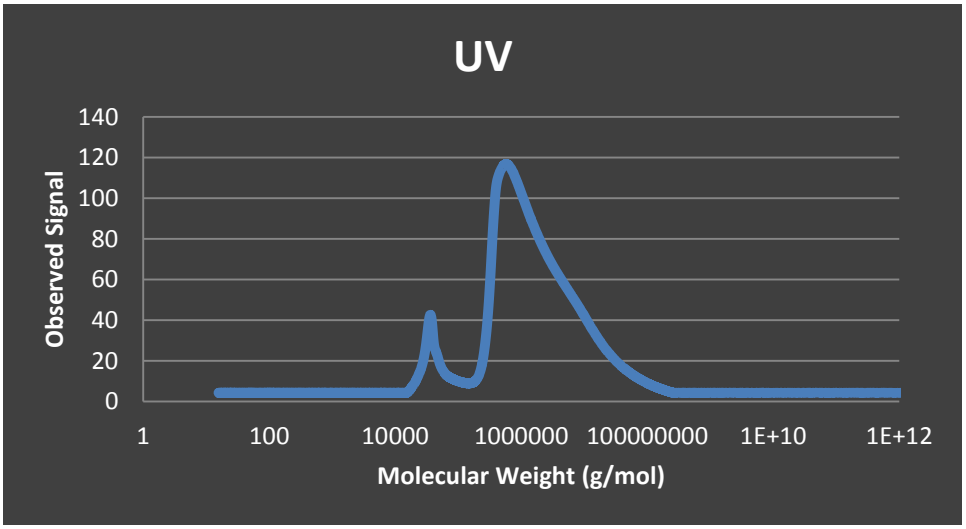

Figure 75. UV chromatogram of a linear polymer synthetized by RAFT in a micro-reactor (CM08) (Detection at 272 nm).

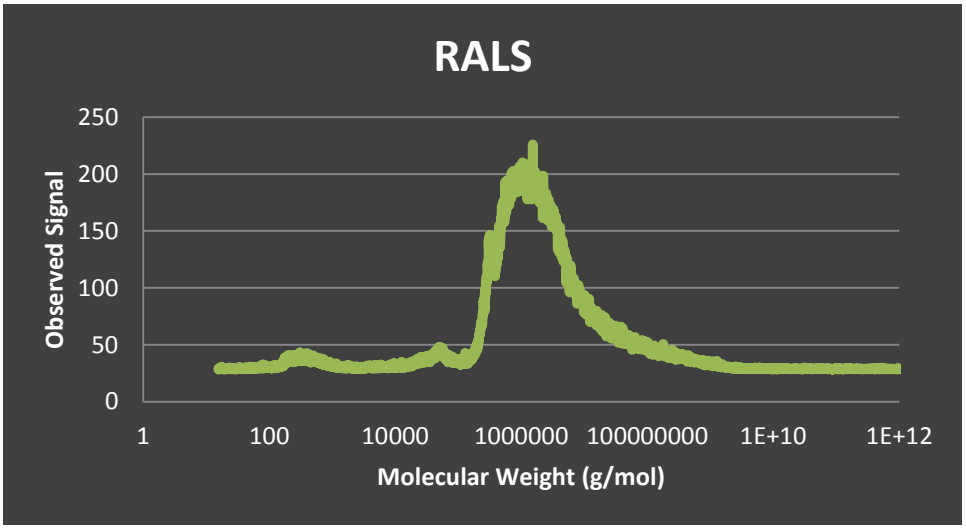

Figure 76. RALS chromatogram of a linear polymer synthetized by RAFT in a micro-reactor (CM08).

In Figure 77 to Figure 79 are presented the chromatograms of the different detectors for a linear polymer synthetized by RAFT in a batch reactor.

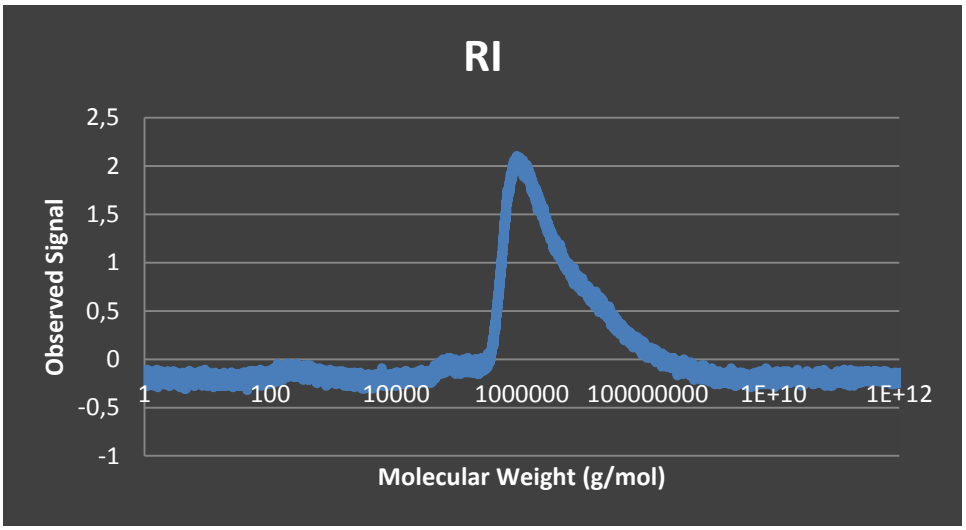

Figure 77. RI chromatogram of a linear polymer synthetized by RAFT in a batch reactor (CM09).

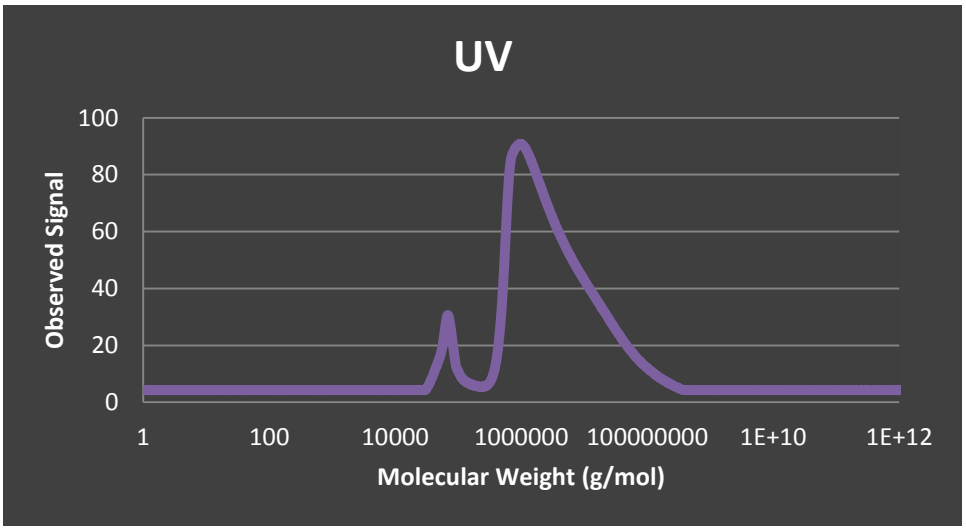

Figure 78. UV chromatogram of a linear polymer synthetized by RAFT in a batch reactor (CM09) (Detection at 272 nm).,

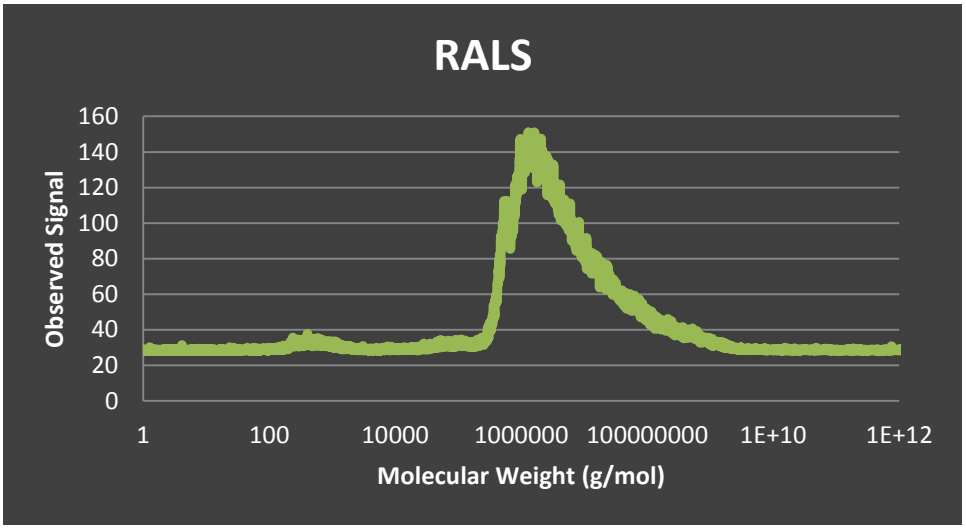

Figure 79. RALS chromatogram of a linear polymer synthetized by RAFT in a batch reactor (CM09).

In order to understand the differences related to the type of reactor used in the hydrogels synthesis and the influence of the type of polymerization in the final product, the following four graphics were made. In Figure 80, where is compared the type of reactors used in a RAFT polymerization, it can be seen that when the hydrogel is synthetized in a micro-reactor it presents a peak corresponding to a lower molecular weight when compared to the batch reactor, even though the difference is not substantial.

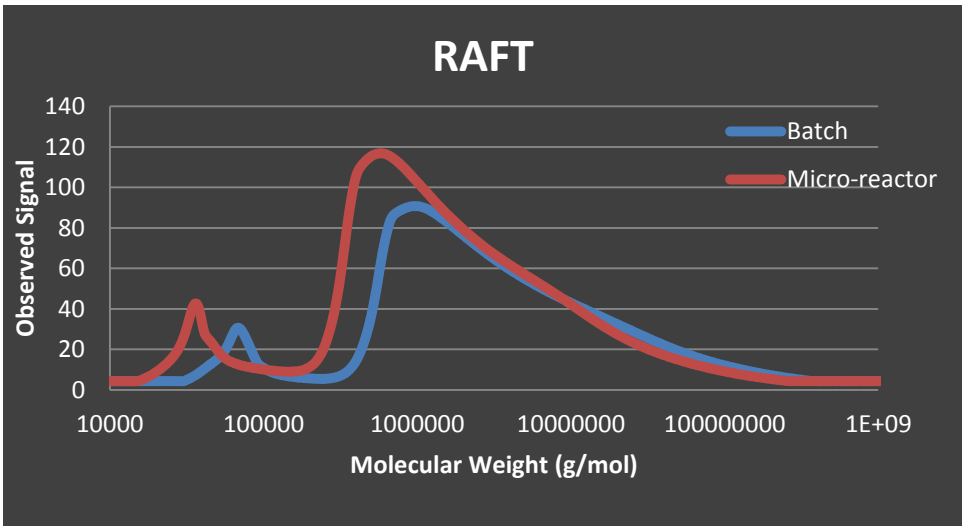

Figure 80. Comparison of UV chromatograms for linear polymers synthetized in a micro-reactor (CM08) and in a batch reactor (CM09) using RAFT polymerization.

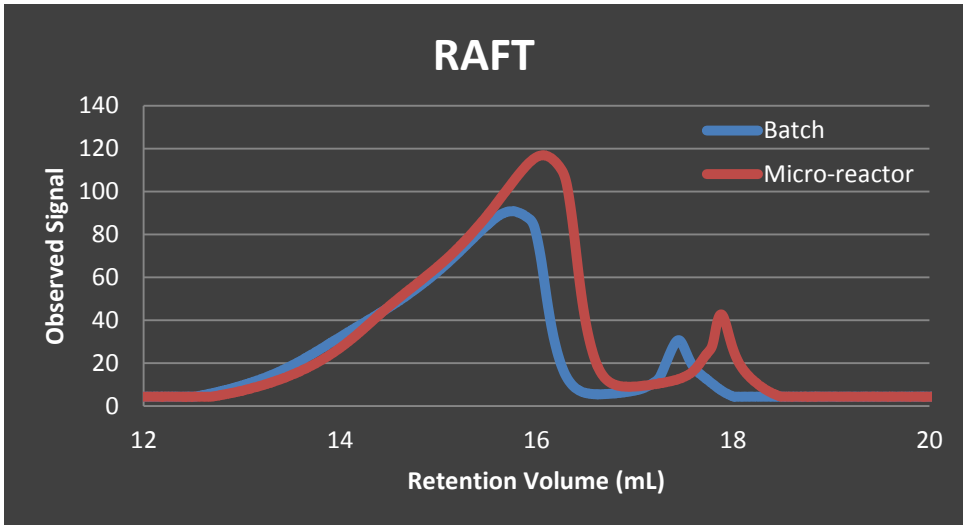

Figure 81. Comparison of UV chromatograms for linear polymers synthetized in a micro-reactor (CM08) and in a batch reactor (CM09) using RAFT polymerization.

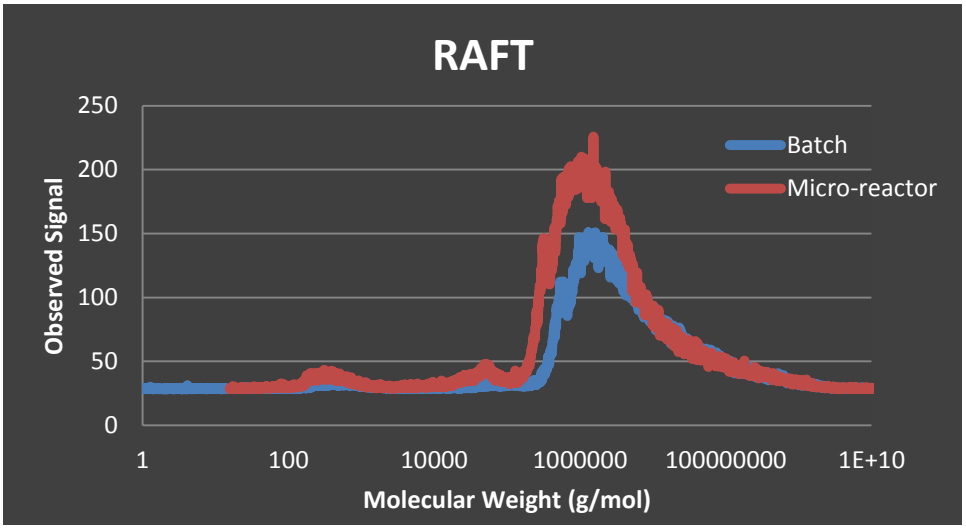

Figure 82. Comparison of RALS chromatograms for linear polymers synthetized in a micro-reactor (CM08) and in a batch reactor (CM09) using RAFT polymerization.

In Figure 83 are presented the UV chromatograms for hydrogels synthetized by RAFT and FRP in a micro-reactor. It shows the difference of the polydispersity of the polymer. The polymers synthetized by FRP in these conditions show a higher polydispersity. It means that the population is more heterogeneous than when synthetized by RAFT. Thus

it can be concluded that the RAFT polymerization can be used in order to manipulate the properties of the polymers.

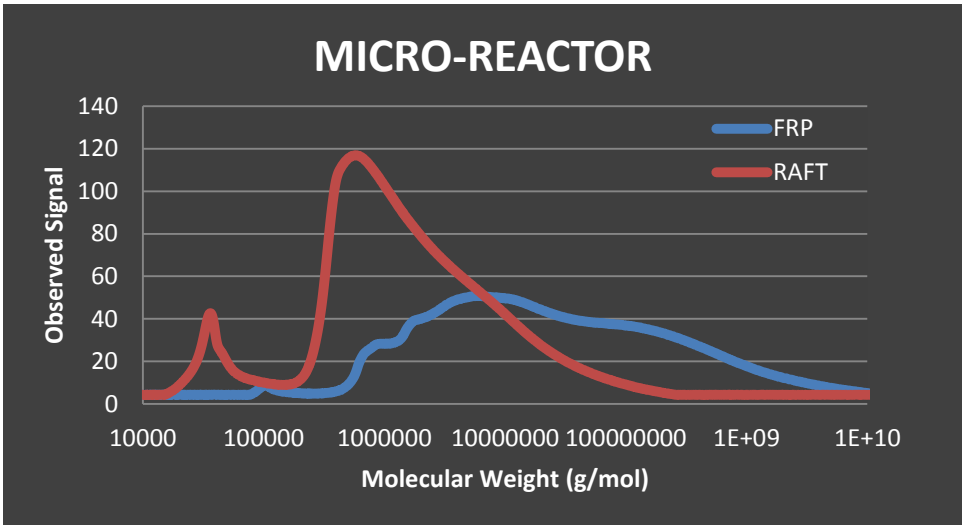

Figure 83. Comparison of UV chromatograms for linear polymers synthetized using FRP (CM06) and RAFT (CM08) polymerization in a micro-reactor.

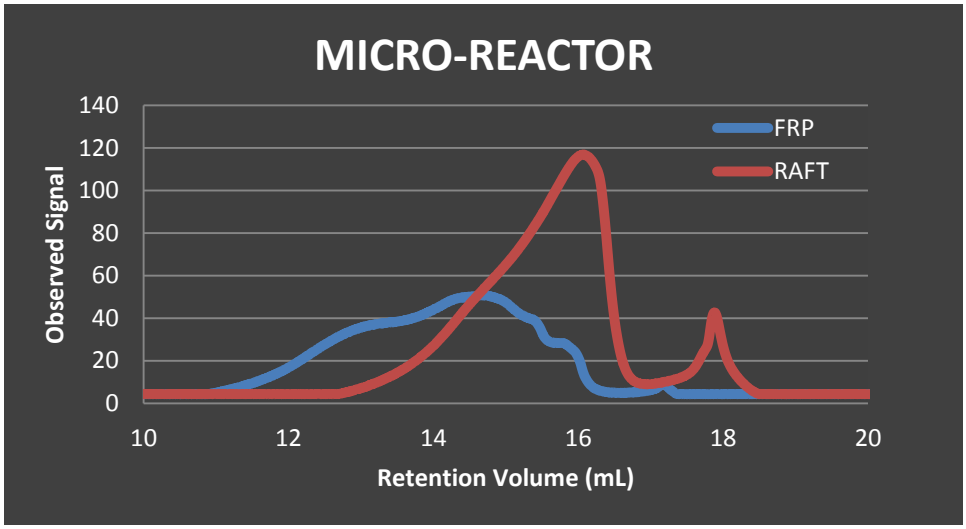

Figure 84. Comparison of UV chromatograms for linear polymers synthetized using FRP (CM06) and RAFT (CM08) polymerization in a micro-reactor.

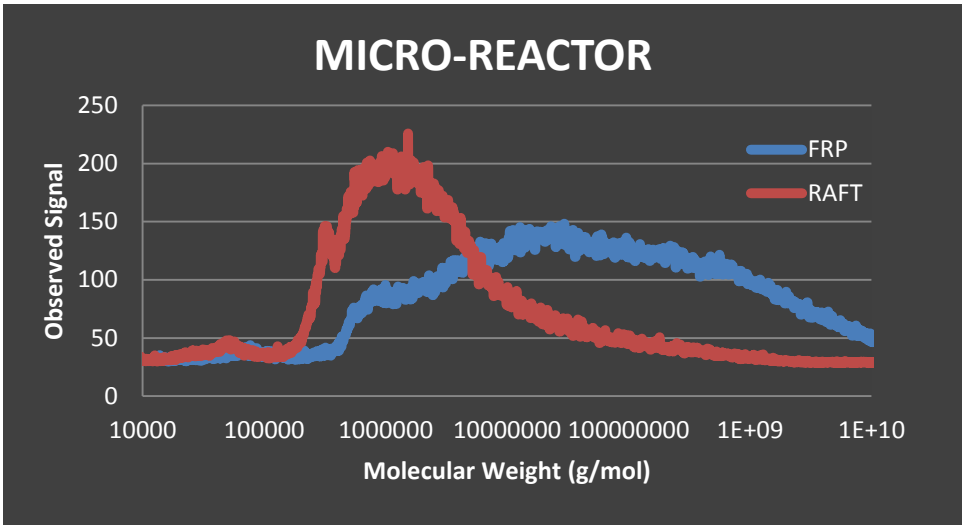

Figure 85. Comparison of RALS chromatograms for linear polymers synthetized using FRP (CM06) and RAFT (CM08) polymerization in a micro-reactor.

Results above described (and expanded in the annexes of this work) show the use of size exclusion chromatography with tetra-detection (refractive index + ultraviolet + light – scattering + intrinsic viscosity) to measure the molecular architecture of the products synthetized, namely the primary structure of the linear (soluble) analogues of the polymer networks obtained. These measurements were performed using directly water as eluent, avoiding the use of organic solvents with water compatible polymers. Nevertheless, working directly with water as eluent is hampered by the low quality of the light – scattering signal that is observed in these conditions. Presence of salts in the water (e.g. sodium azide to prevent the growth of bacteria in the GPC columns) is probably the source of these issues. In spite of these difficulties, SEC measurements lead to important results because the difference between the molecular architecture of FRP and RAFT products was highlighted. In fact, was shown the strong impact of the RAFT mechanism on the size of the primary chains of the polymers which confirms the possibility for using this mechanism to obtain tailored products (increasing the initial ratio RAFT/monomer is possible to decrease the size of the primary chains). Moreover, SEC measurements also showed that, with the synthesis conditions used, the difference between the molecular architecture of batch/micro-reactor products is small when compared with FRP/RAFT materials.

CHAPTER 5 - Measurement of Drug Adsorption and Release in Batch Process and using Frontal Analysis

5.1. Measurement of Drug Adsorption in Batch process

5.1.1. Introduction

The physical adsorption may be defined as a surface phenomenon in which a solute (in this work a drug) is reversibly retained on the surface of a solid (for this purpose were used, in this investigation, hydrogels). This phenomenon is enhanced by the forces of interaction between the solid and the solute (drug/hydrogel) which generate the formation of layers (single or multiple) of the drug on the surface of the hydrogel. This interaction may be due to Van der Waals forces or electrostatic charge effect, for example. The adsorbent (solid) can thus be used to increase the concentration of a solute (adsorbate) on its surface in a reversible manner, i.e., it is also possible (in principle) to subsequently desorbing (releasing) from the same surface. To this effect should be enhanced by breaking the physical bonds between solute/solid. The adsorption process is favored when the adsorbent has a high specific surface area (surface area per unit volume) and/or a large amount of micropores. [30-32]

The equilibrium adsorption mechanism is based on the existence of different affinities between adsorbents and solutes generating specific selectivity solute/sorbent that can be exploited in practice to, for example, separate components present in a solution, purifying a stream (liquid or gaseous) containing a harmful component or concentrating a solute in solid medium (e.g., a drug loading of a polymer matrix). In this work, the adsorption of different biomolecules (e.g. drugs) in different types of hydrogels is explored.

5.1.2. Experimental procedure

5.1.2.1. Part I – Adsorption tests in batch process at neutral pH

To start these tests was necessary to prepare twenty solutions that were used as references when measuring adsorption on UV. Nineteen of them are constituted by a mother solution of caffeine (20 mM) and water, at different concentrations, and the other one only with water.

Other 40 solutions were prepared (20 with MIP (CM05) and 20 with NIP (CM06)). These solutions have the same concentration of caffeine as the references. The only thing that differs is that an amount of NIP or MIP is added to it in order to know the adsorption of each material in different concentrations. The quantities of MIP and NIP used and the concentrations of each solution can be found in Annex 72.

After this, the solution containing the polymer standed for a period of 24 hours with stirring at 20 ºC. When this time is elapsed the solutions were filtered and the concentration of the remaining solution is measured by UV (272 nm).

A calibration line was made with the references in order to be possible to relate the absorbance with the concentration of the solutions. In order to maintain the absorbance values in the linear region it can be necessary to dilute the solutions. It is important that the same dilution is made in each solution.

For the calculation of the amount of drug adsorbed in the hydrogel (expressed in mmol of drug per gram of hydrogel) the following equation was used:

$$q^{molar} = \frac{\frac{[UV_{SOL-}(UV_{ADSOR} - UV_0)]D_F}{\alpha_{CALIB}} \times \frac{V_{ADSOR}}{1000}}{\frac{m_{HG}}{1000}} \quad (5.1)$$

With:

$\boldsymbol{UV_{SOL}}$ – The UV absorption (UV-units) of the aqueous solution used for the specific drug concentration considered.

$\boldsymbol{UV_{ADSOR}}$ – The UV absorption (UV-units) of the aqueous phase after de adsorption process.

$\boldsymbol{UV_0}$ – The UV absorption (UV-units) of the blank solution (without drug) containing the same amount of hydrogel used in the adsorption test.

$\boldsymbol{D_F}$ – The dilution factor considered in the previous UV measurements. All the three UV measurements (UV_{SOL} , UV_{ADSOR} and UV_0) should be performed using the same dilution factor.

$\boldsymbol{\alpha_{CALIB}}$ – The slope of the calibration straight line relating the UV absorption with concentration for the drug considered in that specific wavelength. It is assumed that the units of this slope are UV-units/mM.

$\boldsymbol{V_{ADSOR}}$ – The volume of solution, expressed in mL, used in the adsorption process.

$\boldsymbol{m_{HG}}$ – The mass of hydrogel, expressed in mg, used in the adsorption process.

To calculate the amount of drug adsorbed (expressed in mg of drug per gram of hydrogel (mg/g)) it is necessary to multiply the previous value by the molar mass of the drug:

$$q^{mass} = q^{molar} \times M_w \tag{5.2}$$

With:

$\boldsymbol{M_w}$ – The molar mass of the drug expressed in mg/mmol=g/mol

In order to calculate the concentration of drug in the aqueous phase after the adsorption process, expressed in mM:

$$C^{eq} = \frac{(UV_{ADSOR} - UV_0)D_F}{\alpha_{CALIB}} \tag{5.3}$$

5.1.2.2.Part II – Adsorption tests in batch process at different pH

These tests were made using MIP and NIP synthetized in a batch reactor and also in a micro-reactor in order to compare the influence of the process in its final characteristics. In this case all the solutions have the same concentration of CAF (5 mM) and they only differ in the pH. For each polymer three different solutions were prepared with different pH: 2, 7 and 10. Like before, when the solutions are prepared the adsorption process was performed during 24 hours. After this time the solutions are measured by UV at 272 nm to know their new concentration and so the fraction of caffeine that went inside of the polymer. The calculations are made using the following equations:

$$\alpha = \frac{A_0 - A_1}{A_0} \tag{5.4}$$

With:

α – Fraction of drug that is retained in the polymer;

A_0 – The UV absorption (in UV units) of the mother solution;

A_1 – The UV absorption (in UV units) of the aqueous solution after the adsorption process.

Once different pH values were used, it is interesting to know the swelling ratio of the polymer. With this purpose all the remaining solution is removed from the flask and the polymer is weighted. The SR can then be calculated using the following equation:

$$SR = \frac{mass\ of\ swollen\ polymer}{mass\ of\ dried\ polymer} \tag{5.5}$$

In order to know how the polymers release the drug in these conditions they were poured in 10 mL of water for 5 minutes. After that, the solutions were filtered and measured by UV. The fraction of drug released can be calculated with the following expression:

$$L = \frac{A_2}{A_0 - A_1} \tag{5.6}$$

With:

L – Amount of drug released;

A_0 – The UV absorption (in UV units) of the mother solution;

A_1 – The UV absorption (in UV units) of the aqueous solution after the adsorption process;

A_2 – The UV absorption (in UV units) of the aqueous solution after percolate by the clean water.

The quantities used of each material are presented in Table 6.

Table 6. Amount of hydrogel used in these tests.

	Micro-reactor		**Batch reactor**	
	MIP (mg)	**NIP (mg)**	**MIP (mg)**	**NIP (mg)**
pH 2	50.2	51.3	50.3	51.9
pH 7	52.5	50.6	50.8	51.0
pH 10	52.0	50.5	50.0	50.7

5.1.3. Results and Discussion

5.1.3.1. Part I - Adsorption tests in batch process at neutral pH

In Figure 86 to Figure 89 the results for adsorption tests in batch process at neutral pH with a solution of caffeine of 5 mM are presented. These results are important to show the difficulty in obtaining reliable results with this process. This happens because the amount of drug adsorbed is very low and so it is hard to measure in this conditions. Thus, it was used frontal analysis which is a more precise technique even when the adsorbed quantities are potentially small.

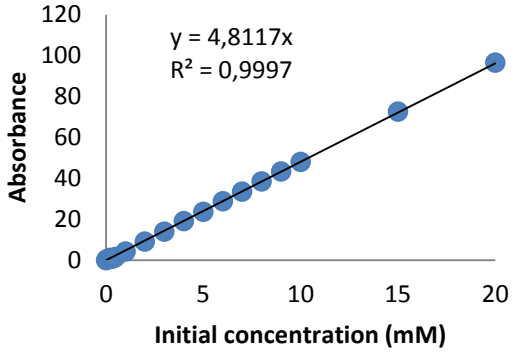

Figure 86. Calibration curve of absorbance vs. concentration for batch tests performed with a molecularly imprinted polymer.

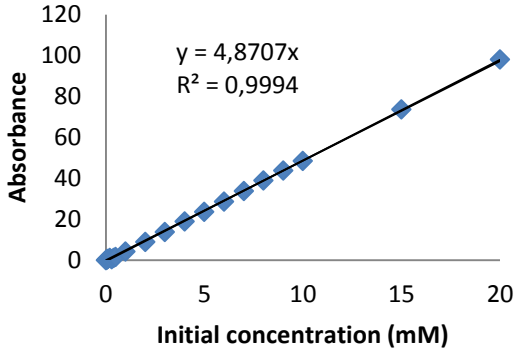

Figure 87. Calibration curve of absorbance vs. concentration for batch tests performed with a non-imprinted polymer.

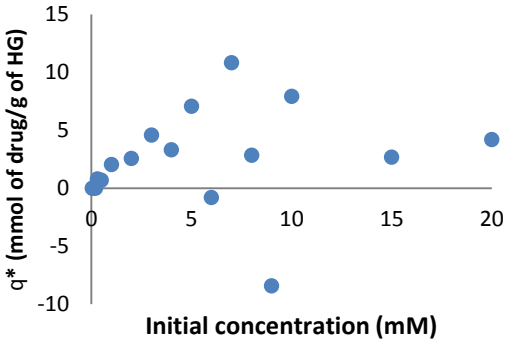

Figure 88. Batch adsorption test of caffeine in a RAFT acrylic acid MIP hydrogel synthetized in micro-reactor (CM10).

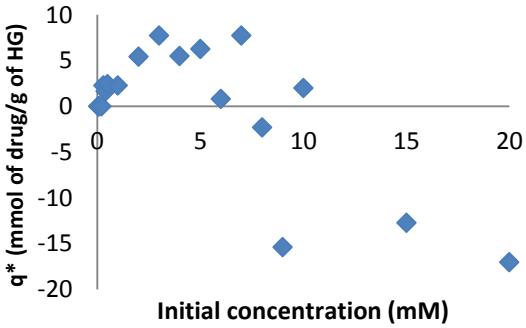

Figure 89. Batch adsorption test of caffeine in a RAFT acrylic acid NIP hydrogel synthetized in micro-reactor (CM11).

5.1.3.2. Part II - Adsorption tests in batch process at different pH

In Figure 90 to Figure 93 the results for adsorption tests in batch process at different pH are presented. As can be seen the polymer which retained more caffeine is the NIP synthetized in a batch reactor when poured in a solution with neutral pH. Once every polymer retained less than expected it either means that the polymer was not completely clean or the affinity of the drug with the polymer is not high. Even using *Soxlet* Extraction for cleaning the material it is possible that a target molecule or some kind of impurities remained inside the polymer influencing the results.

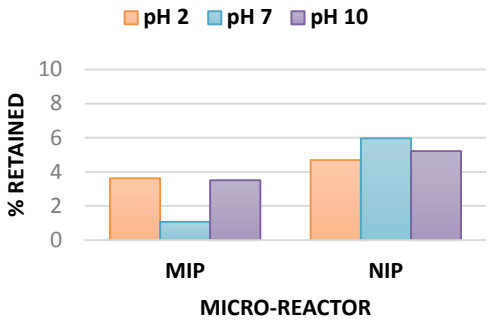

Figure 90. Comparison of the amount of drug retained of MIP (CM10) and NIP (CM11) synthetized in a micro-reactor, at different pH.

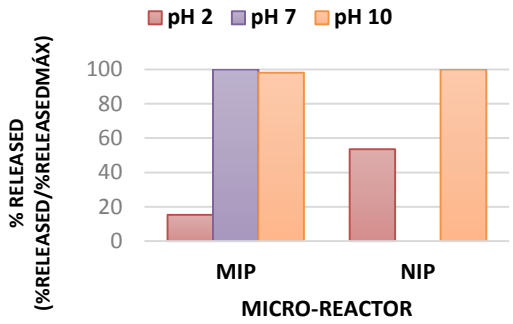

Figure 91. Comparison of the amount of drug released of MIP (CM10) and NIP (CM11) synthetized in a micro-reactor, at different pH.

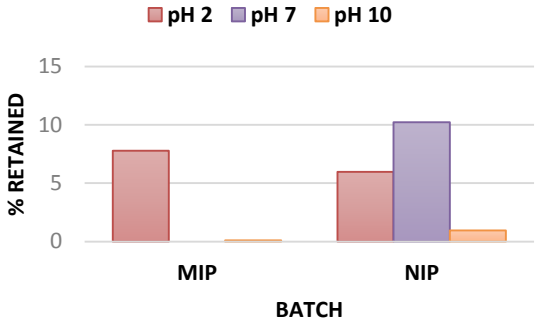

Figure 92. Comparison of the amount of drug retained of MIP (CM05) and NIP (CM04) synthetized in a batch reactor, at different pH.

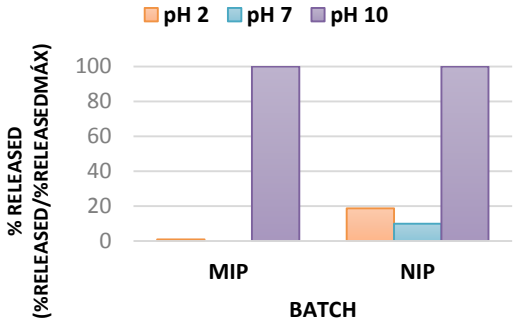

Figure 93. Comparison of the amount of drug released of MIP (CM05) and NIP (CM04) synthetized in a batch reactor, at different pH.

It is also worth mentioning that the release seems to have been complete in some cases.

Figure 94 presents the swelling ratio of the polymers used is these tests. As can be seen, the hydrogels tend to swell more at pH 10 than at pH 2 and 7. This happens because acrylic acid hydrogels are anionic thus they are able to swell more in basic than in acidic solutions. It is important to notice that hydrogels synthetized in a micro-reactor have a lower swelling ratio. This means that the properties of the materials can be controlled using this reactor.

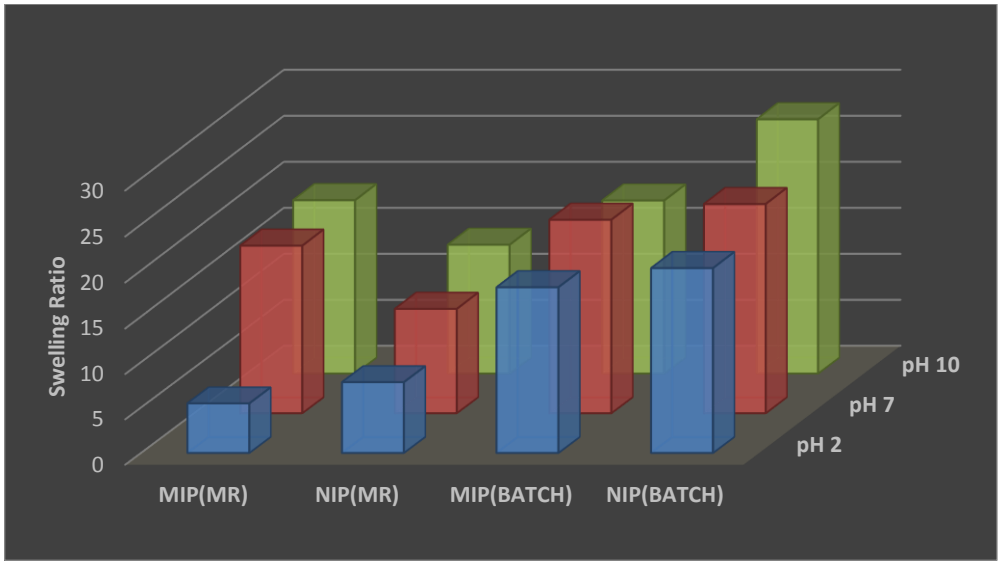

Figure 94. Swelling ratio of different hydrogels in solutions with different pH.

5.2. Adsorption tests in SPE process

Solid phase extraction (SPE) is an extraction method that uses a solid phase and a liquid phase to isolate one, or one type, of solute from a solution. It is usually used to clean up a sample before using a chromatographic or other analytical method to quantify the amount of solute in the sample. The stationary phase is contained in a plastic column (normally has 1-10 mL of capacity). The column might have a filter on its bottom in order to not allow the stationary phase pass through and might also have a stopcock to control the flow of solvent through the column [33].

5.2.1. Experimental Procedure

In this particular case, SPE was used to understand how some materials can adsorb in a continuous process. A 5 mM solution of caffeine and CM04, CM05, CM10 and CM11 polymers were used. The quantities used are shown in Table 7.

In order to have a reference, the concentration of the solution of caffeine is measured by UV before it is placed on the columns with the polymer.

Table 7. Amount of hydrogel and solution containing the drug template used in SPE process.

RUN	Mass of hydrogel (mg)	Volume of 5mM solution of CAF (mL)
CM04	50.8	10.0
CM05	51.0	10.0
CM10	51.3	10.0
CM11	50.3	10.0

To start this experiment the polymers are placed in the columns and then the columns are filled with 10 mL of the caffeine solution.

Figure 95. A: Column only with the polymer. **B:** Column containing the polymer and the CAF solution.

After all the columns are filled, the stopcock is open in each of them in order to let the aqueous solution pass one drop at a time and is collected in flasks that are placed in the bottom of the outlet of the column. This only happens because the instrument is connected to a vacuum pump that pulls the solution out.

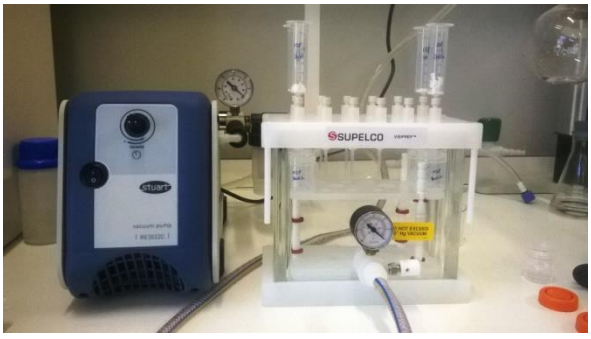

Figure 96. SPE instrument connected to a vacuum pump.

When all the aqueous solution leave the column its absorbance is measured by UV in order to know the amount of drug that got trapped into the polymer.

5.2.2. Results and Discussion

In Figure 97 the comparison of the amount of drug retained in MIP and NIP synthetized in different reactors are presented. As expected the molecularly imprinted polymers retained more drug than the non-imprinted. Once the swelling ratio of MIP synthetized in a batch reactor is higher than the SR of MIP synthetized in a micro-reactor it leads to a bigger amount of drug retained in this polymer.

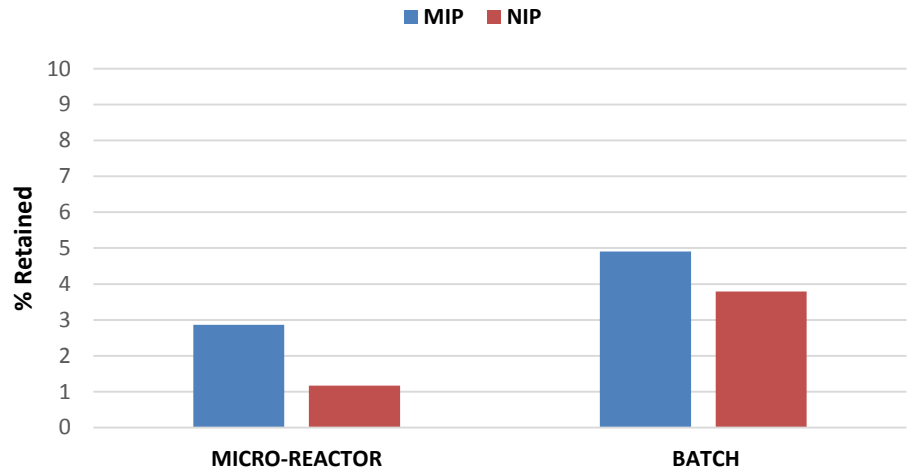

Figure 97. Comparison of the amount of drug retained of MIP and NIP synthetized in a batch reactor and in micro-reactor, at neutral pH.

5.3. Measurement of Drug Adsorption using Frontal Analysis

5.3.1. Introduction

In order to evaluate the adsorption and release of different drugs in different types of hydrogels experimental studies of these processes were carried out in packed columns operating continuously. With this goal, a predefined dry mass of a hydrogel was placed in a selected column (see example in Figure 98). Then the packing (swelling) of the hydrogel was made by pumping water through the column to obtain stable pressure conditions in the system (e.g. 2.5 MPa considering a pumping rate of 0.33 mL / min).

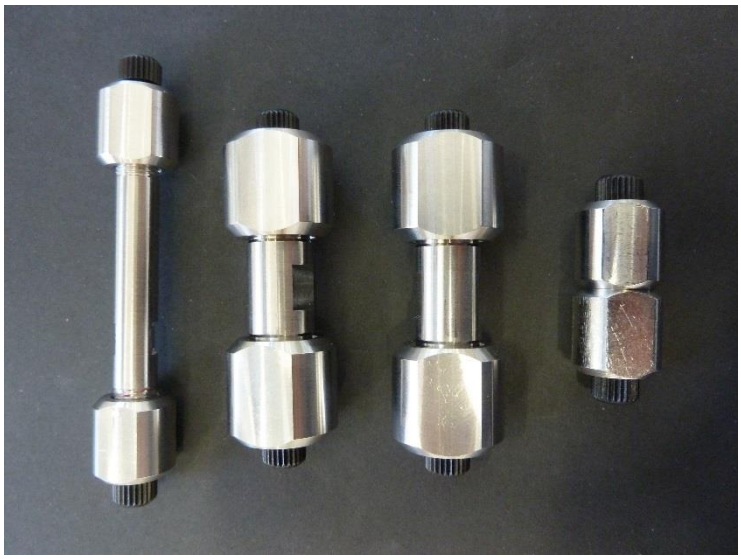

Figure 98. Photo illustration of packing columns used in experimental studies of the adsorption and release of drugs in hydrogels considering continuous operation mode.

To perform these studies a system of size exclusion chromatography (GPC / SEC) was used including a pumping module solvent and sample injection (Viscotek GPCmax VE 2001 model) that is also equipped with four detection signals, namely refractive index (IR), light scattering (LS) Intrinsic viscosity (IV-DP) and ultraviolet (UV). UV detection is especially useful in the context of the tests conducted here as will be detailed below. In Figure 99, a simplified schematic representation of the GPC system used in this work is illustrated.

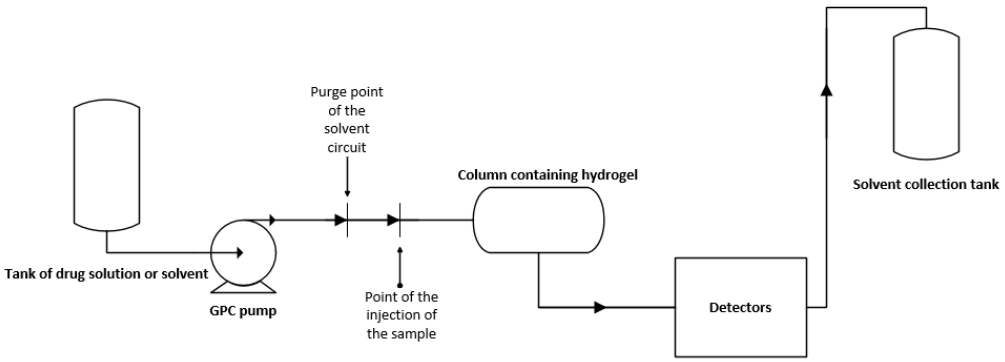

Figure 99. Simplified schematic representation of the GPC system used in this work to experimentally study the adsorption and release of drugs in hydrogels considering continuous operation mode.

5.3.2. Tests with an Anionic Hydrogel based in Acrylic Acid

In order to evaluate the affinity of some drugs considered in this work and anionic hydrogels structure, tests were conducted using the network NIH4 polymer (hydrogel of acrylic acid obtained by FRP synthesis) as filler for the column. For this purpose 15 mg of dried hydrogel were placed in a packed column which was then integrated into the GPC system. During 24 h water was pumped in the GPC system at a flow rate of 0.1 mL/min in order to pack the hydrogel inside the column since it is known its swelling ratio in the presence of this solvent. The amount of dried hydrogel that was packed in the column was estimated based on the swelling ratio of the hydrogel (over 100 times) and the internal volume of the column (0.17 mL).

5.3.3. Injection of aqueous solutions containing drugs

In these tests, injection (impulse concentration) of aqueous solutions of different drugs on the GPC system was performed. For this purpose, the mechanism of the automatic injection device GPC (the volume of the injected solution is 100 mL) was considered.
In order to evaluate the effect of hydrogel retention of different types of molecules, in each case, the injection was performed in the presence and absence of the column containing the hydrogel. These tests were performed considering the GPC system operating at room temperature (T ~ 20 °C). Given the high UV absorption of the drugs considered in this work, the UV signal from the detector was used to monitor the concentration at the column outlet of the molecules considered.

Figure 100 shows the signal recorded on UV absorption detector as a result of the injection into the GPC system of an aqueous solution of the sodium salt of ibuprofen with 0.5 mM concentration. Here the normalized UV signal, which is obtained by dividing the actual signal by the maximum observed value is shown. This test was performed assuming a flow rate of eluent of 0.1 mL/min and monitoring the UV absorption at 223 nm. Comparison of the peaks observed in the presence and absence of the hydrogel column allows concluding that there is an effective affinity between the drug and the material under consideration (note the high retention of the drug in the

system when the hydrogel column is used). Ibuprofen was considered in this particular test just for exploratory purposes.

It should also be noted that the retention time (or elution) of drug molecules in the system (t_e) and the corresponding retention volume (or elution) (V_e) are related by the flow considered in the operation of the system (Q):

$$V_e = Q \times t_e \tag{5.7}$$

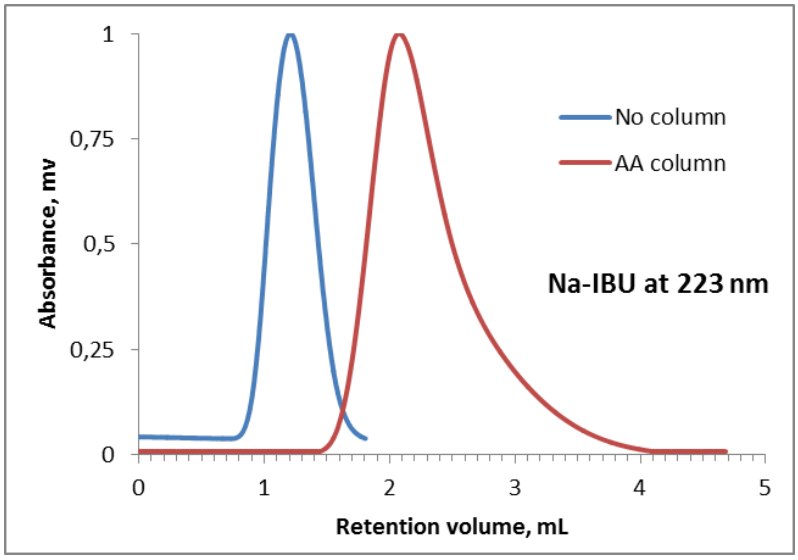

Figure 100. Signal recorded on UV absorption detector as a result of injection into the GPC system of an aqueous solution of the sodium salt of ibuprofen with 0.5 mM concentration.

5.3.4. General Aspects About Experimental Procedure for Adsorption (Saturation) and Desorption (Release) of Drugs in Continuous Operation

In Figures 101 and 102 the schematic representation of the ideal adsorption processes (saturation) and desorption (release) of drugs in hydrogels packed in columns operating

in continuous mode is shown. To achieve the saturation process (adsorption), the GPC system with the hydrogel column is initially supplied with pure water (concentration of drug C = 0) for a sufficiently long period of time until a stable behavior of the detectors (null drug concentration) is achieved. At a given instant (t = 0) the system is fed with an aqueous solution containing the selected drug (initial drug concentration C = C0), thereby causing a step change of drug concentration at the entrance of the column. After some time of operation (in these tests was used UV monitoring) the presence of the drug is detected in the output stream of the column. If this process is carried out for a sufficiently long period of time, this hydrogel will reach saturation of the drug (i.e. becomes incapable of adsorbing additional amounts of this molecule), and the concentration at the column outlet becomes constant [30-32].

For the study of the release (desorption) of the drug, the hydrogel is in t = 0 in a saturation state (given above description), and at a given time, the feed containing the drug (C = C0) is replaced by a stream of pure water (C = 0). In this way it causes a negative step change on the drug concentration at the column inlet. The percolate of pure water in the hydrogel causes desorption (release) of the drug and after a sufficiently long operating time it should release the drug entirely. After the end of drug release, the detectors measured the presence of pure water.

The procedures described above and outlined in Figures 101 and 102 occur in ideal operating conditions. However, in practice, several experimental problems cause deviations from this ideal behavior. One of the aspects to be taken into special consideration in making these tests relates to the early processes of drug supply or water in steps of saturation and release, respectively. In fact, when making the change of the supply reservoirs (see Figure 99), it is necessary to adequately purge the tubing located between the reservoir and the inlet of the column (see Figure 99) to ensure that it does not supply with a mixing the two solutions. Note that the volume of liquid present in these feed pipes is large enough to cause mixing of the two solutions (containing / not containing-drug) and thereby to spoil the steps of feeding shown in Figure 101 and Figure 102. This difficulty is enhanced by using in these tests relatively low feed rates

(to ensure acceptable pressures in the columns) which worsen the effects of possible mixing of these currents.

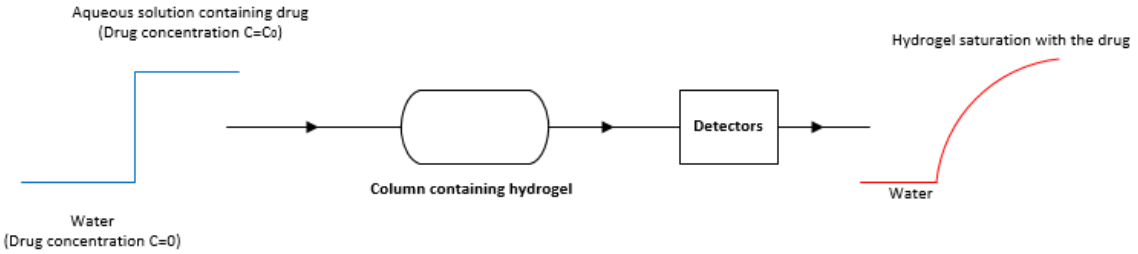

Figure 101. Schematic representation of the experimental procedure associated with the saturation of a hydrogel with a drug considering continuous operation mode. With this purpose, the GPC system with the hydrogel column is supplied with pure water (concentration of drug C = 0) for a sufficiently long period of time until a stable behavior of the detectors (null drug concentration). At a given instant (t = 0) the system is feed with an aqueous solution containing the selected drug (drug concentration C = C0), thereby causing a step change of the drug concentration at the entrance of the column. After some time of operation is detected (e.g. using UV) the presence of the drug in the output stream of the column. If this process is carried out for a sufficiently long period of time, this hydrogel will reach saturation of the drug (i.e. becomes incapable of adsorbing additional amounts of this molecule), and the concentration at the column outlet becomes constant.

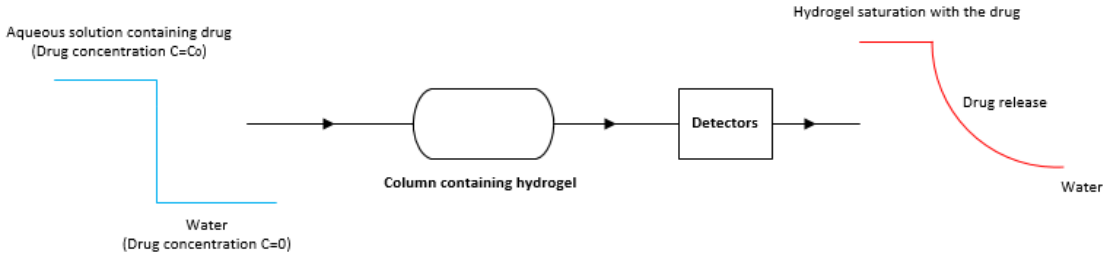

Figure 102. Schematic representation of the experimental procedure associated with the release of a drug from a hydrogel considering continuous operation mode. Starting with the hydrogel in a state of saturation (see Figure 101), at a given instant, the feed containing the drug (C = C0) is replaced with the feed containing pure water (C = 0). In this way it causes a negative step change on the drug concentration at the column inlet. The percolate of pure water in the hydrogel causes desorption (release) of the drug and after a sufficiently long operating time it should release the drug entirely. After the end of drug release, the detectors measured the presence of pure water.

In Figure 103 these aspects are illustrated by comparing the observed responses of saturation in the column with ibuprofen salt, considering two different feed rates and without a prior purge of the feeding tubing of the column.

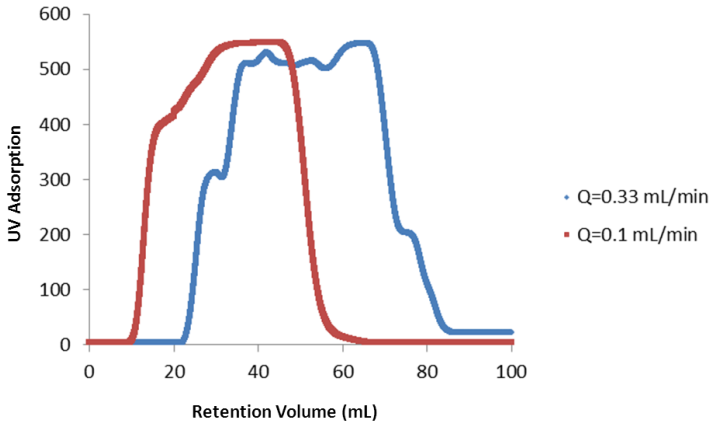

Figure 103. UV responses obtained in the study of the effect of not purging the feeding lines from the GPC system when performing saturation and continuous drug release testing. In this case, the system is considered without the presence of the hydrogel column (direct feeding to the UV detector) in order to isolate the effect of no purging of the feed. It was considered as a case study a solution of 0.5 mM Na-IBU with detection at 223 nm and tests were performed at 0.10 and 0.33 mL/min. The results presented here show the occurrence of saturation/release profiles are strongly non-ideal in the absence of purging of the feed system between saturation/release/saturation steps (due to the mixing of solutions with different compositions). For this reason, the next tests were performed considering a minimum purge of 40 mL between different steps.

5.3.5. Theoretical Foundations of Frontal Analysis

Frontal analysis is considered the more accurate chromatography technique for the determination of adsorption isotherms of a component in stationary phase (e.g. in a solid/liquid process). As described above, this method consists in replacing the current of the mobile phase (e.g. water) by a solution containing the studied component (e.g. a drug) at a known concentration. The "breakthrough" curve (elution curve) of the solute is registered on the outlet of the column (e.g. using a UV detector). A material balance of the solute (mass conservation) between the moment at which the solution begins to flow through the column, and the instant it reaches saturation (concentration step) allows to calculate the amount adsorbed on the stationary phase (q*) that is thus in equilibrium with the mobile phase (where the solute concentration is C0).

In Figure 104 are schematically represented the different stages in an adsorption process for a column operating in continuous mode.

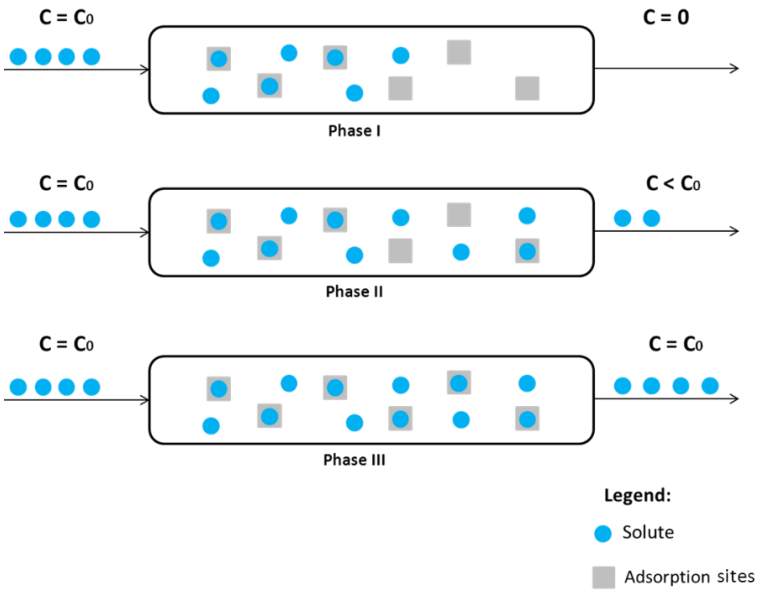

Figure 104. Schematic representation of different liquid/solid adsorption phases in a column operating in a continuous process. In Phase I, the column has not been fully covered by the solute. There are adsorption sites occupied and other ones free with zero solute concentration at the column outlet. In Phase II, the column has been completely percolated by the solute but there are still free adsorption sites. At the outlet of the column is observed a value lower than the input concentration. In Phase III, all the adsorption places were occupied with a concentration observed in the outlet of the column equal to the initial concentration (saturation).

In Figures 105, 106, 107 and 108 the details related to the calculation method of the quantities of solute (e.g. drug) adsorbed onto the stationary phase (adsorbent) in a packed column operating continuously, are given.

Amount of solute adsorbed per unit of volume of stationary phase, V_a:

$$q^* = \frac{C_0(V_{eq} - V_0)}{V_a} \tag{5.8}$$

Amount of solute adsorbed per unit of dry mass of the stationary phase, m_s:

$$q^* = \frac{C_0(V_{eq} - V_0)}{m_S} \tag{5.9}$$

The values of m_s and V_a are known by weighing the amount of dry material that is packed in the column and estimate the volume that the material is going to occupy after the swelling process. One possibility is to consider that the materials can fill all of the geometrical volume of the column (V_G) once they have a high swelling capacity.

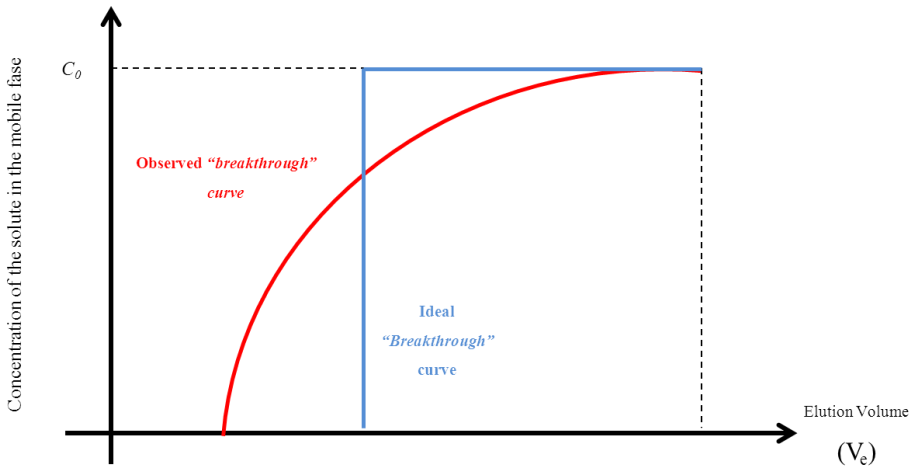

Figure 105. Schematic representation of the ideal "breakthrough" curve (without output of the solute before the saturation) and a real "breakthrough" curve (including Phases I, II and III with exit of solute from the column before adsorbent saturation).

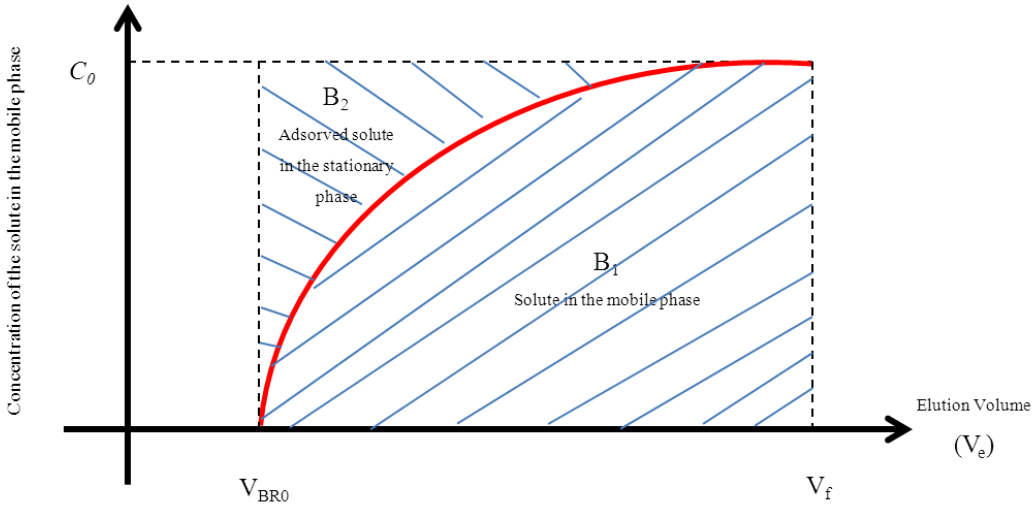

Figure 106. Schematic representation of the adsorption process between the beginning of the "breakthrough" curve (elution volume = VBR0) and the saturation (elution volume=Vf). This period corresponds to Phase II. At this time, the total amount of solute introduced into the system is C0 × (Vf - VBR0) corresponding to the area B1 + B2. The area B1 represents the observed amount of solute in the mobile phase and, by difference, B2 is the amount of solute that was adsorbed in the solid during this period.

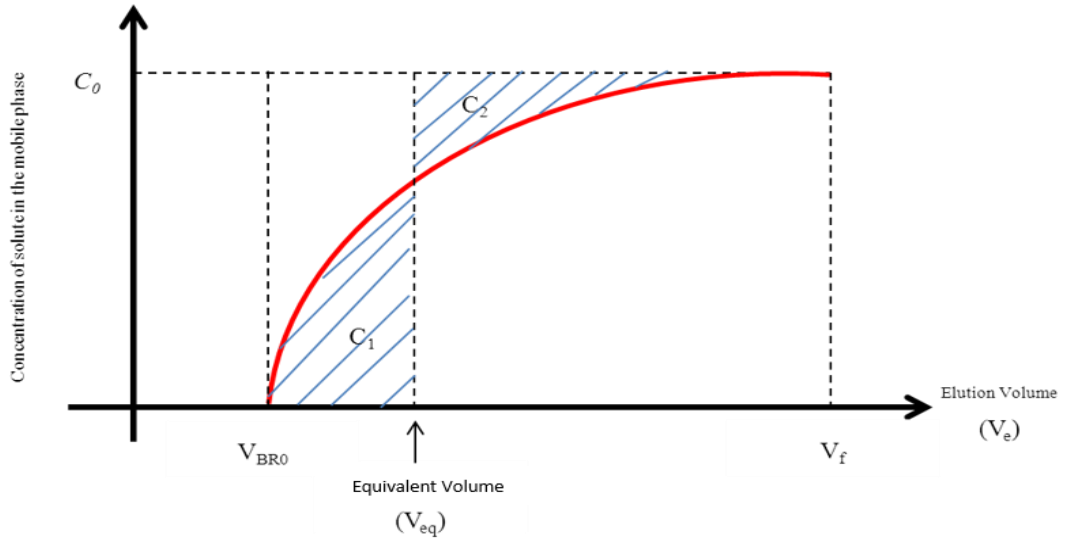

Figure 107. Schematic representation of the calculation of equivalent volume (Veq) to quantify the amount of solute adsorbed. The objective is to calculate the area B2 shown in Figure 106. In fact, comparing Figures 106 and 107, the area B2 may be substituted for the rectangle area C0 × (Veq-VBR0) since it is ensured that the areas C1 and C2 are equal. Calculation of the equivalent volume (Veq) is therefore to find elution volume in which C1 = C2.

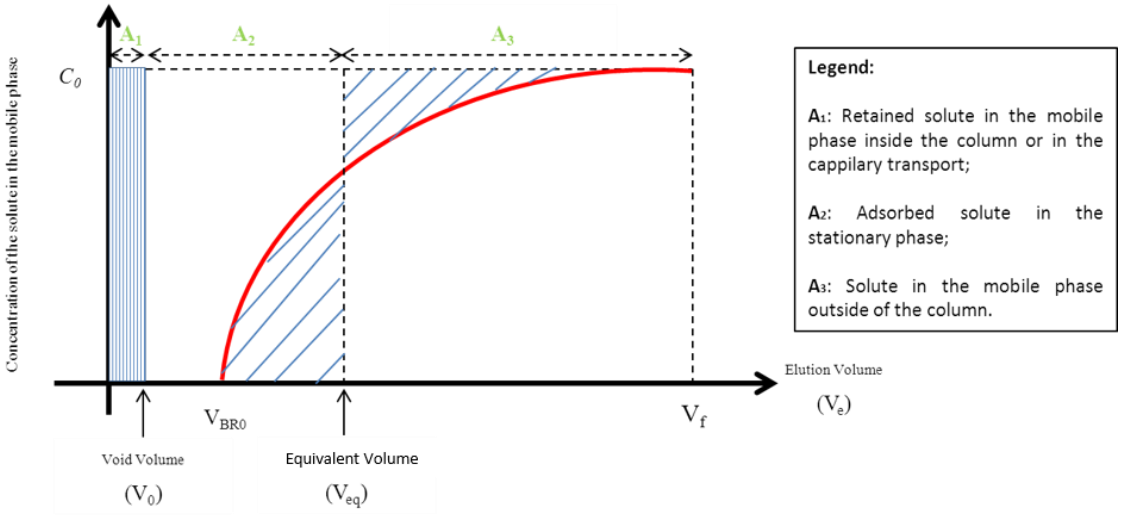

Figure 108. General representation of the quantification of the adsorption process running in column operating in a continuous process including the void volume (quantifies the entrapped solute in the mobile phase inside the column or in the capillary transport), the adsorbed solute in Phase I, which matches the area of the rectangle C0 × (VBR0-V0) and also the amount of solute adsorbed in phase II, which corresponds to the area of the rectangle C0 × (Veq-VBR0). The total amount of solute adsorbed onto the stationary phase is thus: C0 × (VBR0-V0) + C0 × (Veq-VBR0) = C0 × (Veq-V0).

5.3.6. Experimental Procedure

5.3.6.1. Packing of the columns

When starting the tests the column needs to be disassembled to be packed with the hydrogel. In each end of the columns exist one filter and two frits as shows Figure 109.

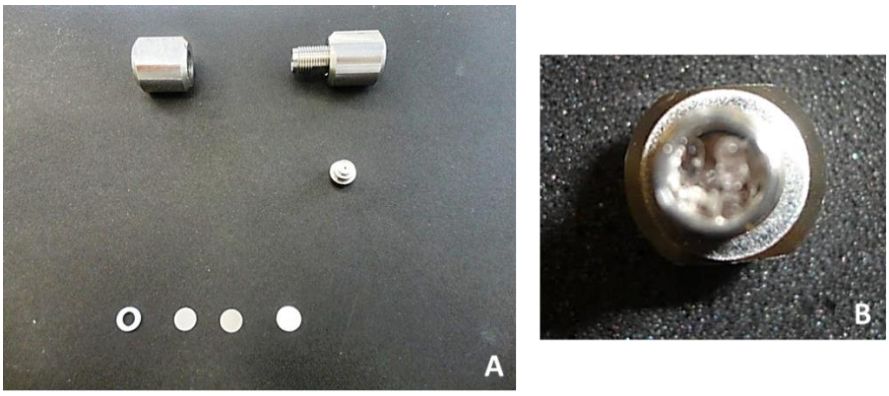

Figure 109. A: Constitution of the packing column; **B:** Column packed of hydrogel.

In order to estimate the amount of hydrogel needed to completely pack the column it is necessary to know its filling volume. It was calculated with the following equation.

$$V = \frac{\pi \times D^2}{4} \times L \tag{5.10}$$

With:

V – The packing volume of the column (mm^3);

D – The internal diameter of the column (mm);

L – The lenght of the column (mm).

Once the swelling ratio of the polymers is known, it is possible to calculate the amount of dried hydrogel needed.

$$V_d = \frac{V}{SR} \tag{5.11}$$

With:

V_d – The volume of dried hydrogel (cm^3);

V – The filling volume of the column (cm^3);

SR – The swelling ratio of the hydrogel.

The mass of hydrogel that is correspondent to this dried volume (V_d) was roughly estimated considering that the density of the hydrogel is 1 g/cm^3.

5.3.6.2.Injection, Adsorption and Desorption of drugs

These tests were made in 3 steps. First it was made an injection of the solution was made containing the selected drug, which percolates through the packed hydrogel, and it is monitored by UV absorption in the correspondent flowing cell. This analysis gives information concerning the retention in the hydrogel of the small amount of drug injected. The analysis of the drug adsorption capability of the hydrogels was assessed through saturation testing. Within this purpose, the dead volume between the solution container and the column inlet was purged by pumping the solution during the time that was estimated to be needed to eliminate this dead volume (~40 mL). After, the column was plugged to the pumping system and the saturation procedure was started at the desired flow-rate (e.g. 0.5 mL/min). Time evolution of the UV adsorption was recorded in the GPC system. The saturation test was performed up to the achievement of a plateau in UV signal. Release of the drug from the saturated hydrogel was performed in the reverse way: pumping system was turned off, feeding container was changed to water, column was disconnected from the pumping system and the dead volume was purged again by removing ~ 40 mL of liquid. Then, the column was plugged again in the system and the pumping was started at the same flow rate used in the saturation procedure. Time evolution of the UV adsorption was also recorded in the GPC system during this release process. The desorption procedure was finished when a steady low plateau of the UV signal was observed.

5.3.7. Results and Discussion

These tests started using a caffeine solution of 5 mM. The next results show that with this solution the values are over the maximum that the instrument can read and so it is not possible to take conclusions in these conditions. Thus, it was necessary to make a solution less concentrated in order to really understand the affinity with caffeine with the different materials.

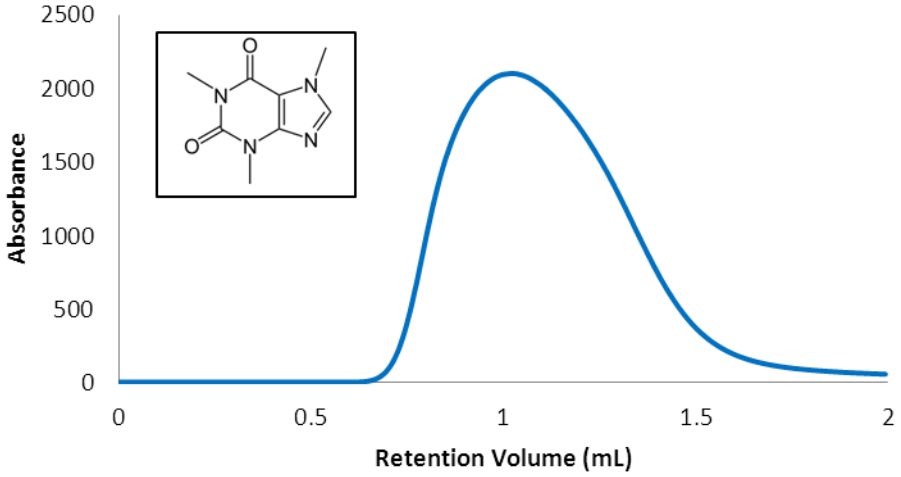

Figure 110. Profile observed for the injection of CAF (5 mM) in a column packed with a molecularly imprinted polymer synthetized in a micro-reactor (CM10).

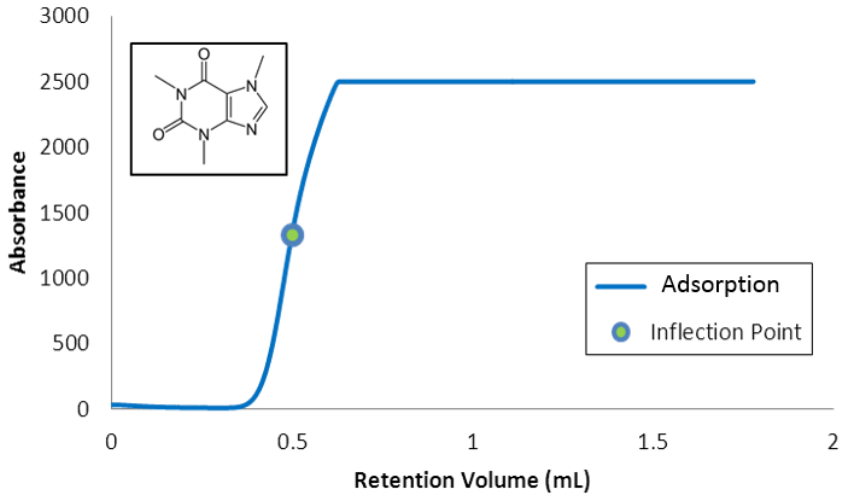

Figure 111. Profile observed for the adsorption of CAF (5 mM) in a column packed with a molecularly imprinted polymer synthetized in a micro-reactor (CM10).

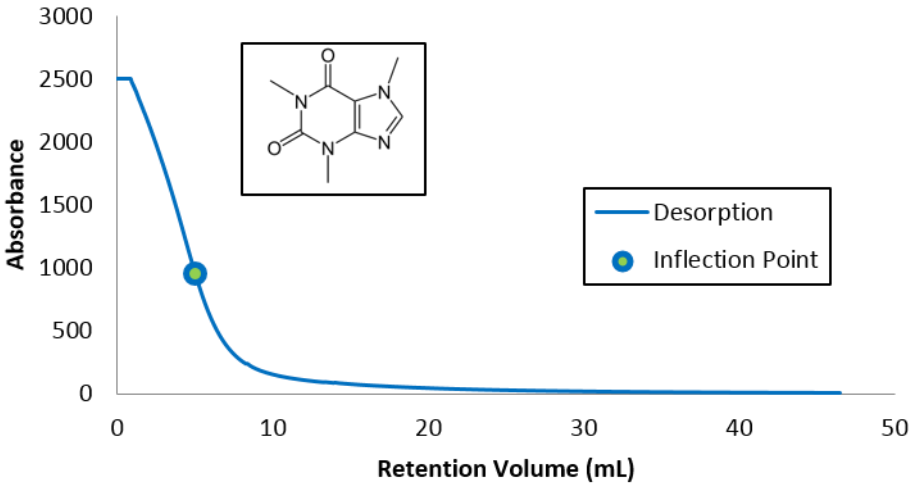

Figure 112. Profile observed for the desorption process of CAF (5 mM) in a column packed with a molecularly imprinted polymer synthetized in a micro-reactor (CM10).

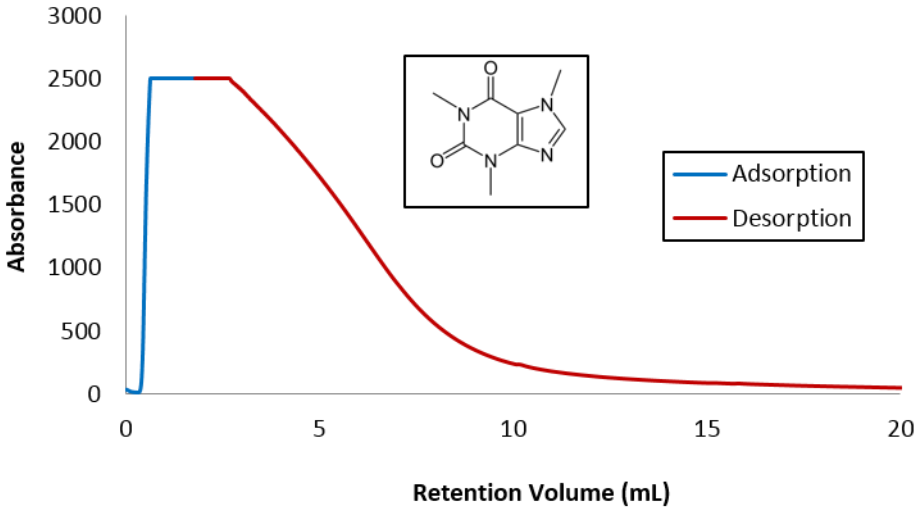

Figure 113. Profile observed for the adsorption and desorption of CAF (5 mM) in a column packed with a molecularly imprinted polymer synthetized in a micro-reactor (CM10).

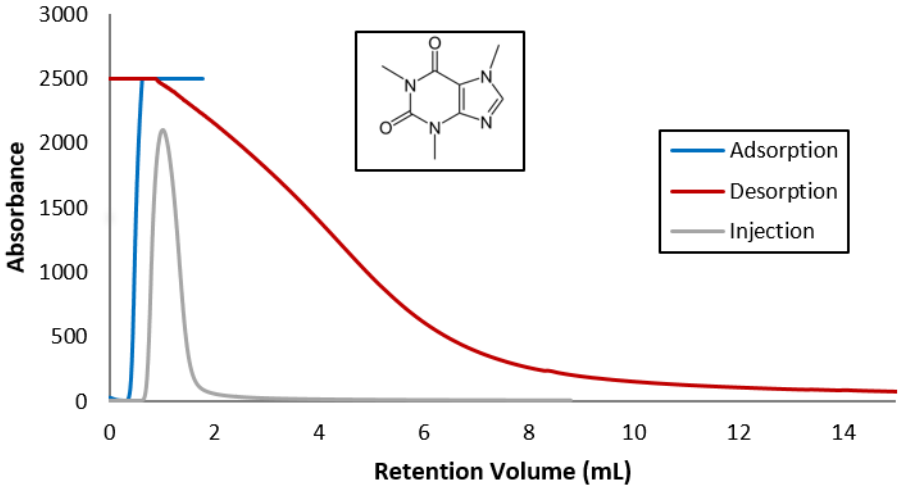

Figure 114. Profiles observed for the adsorption, desorption and injection of CAF (5 mM) in a column packed with a molecularly imprinted polymer synthetized in a micro-reactor (CM10).

In Figure 115 to Figure 119 are presented the results of the adsorption and desorption tests with a solution of CAF (0.1 mM) in a molecularly imprinted polymer synthetized in a batch reactor. In this case the plateau in the saturation (Figure 116) and in the release (Figure 117) processes is well defined. This means that the hydrogel saturates fast with this drug and it doesn't need much time to be completely cleaned. The inflection point presented in Figure 116 and Figure 117 is the point where the area behind and above the curve has the same value. With this point is possible to know the equivalence volume in adsorption and desorption processes.

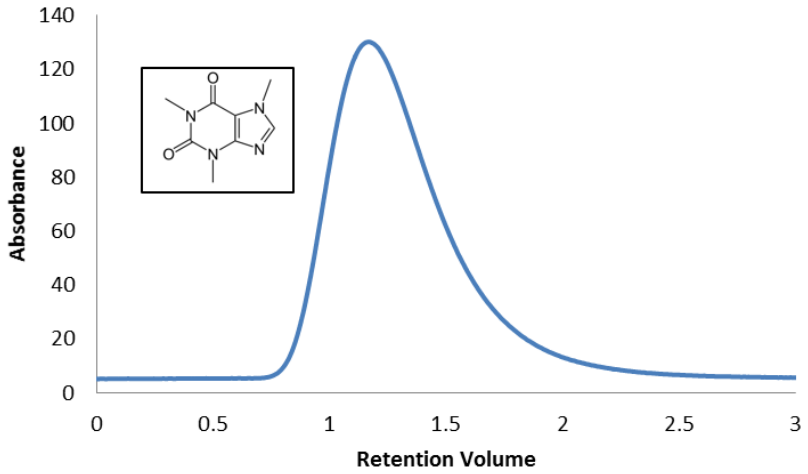

Figure 115. Profile observed for the injection of CAF (0.1 mM) in a column packed with a molecularly imprinted polymer synthetized in a batch reactor (CM05).

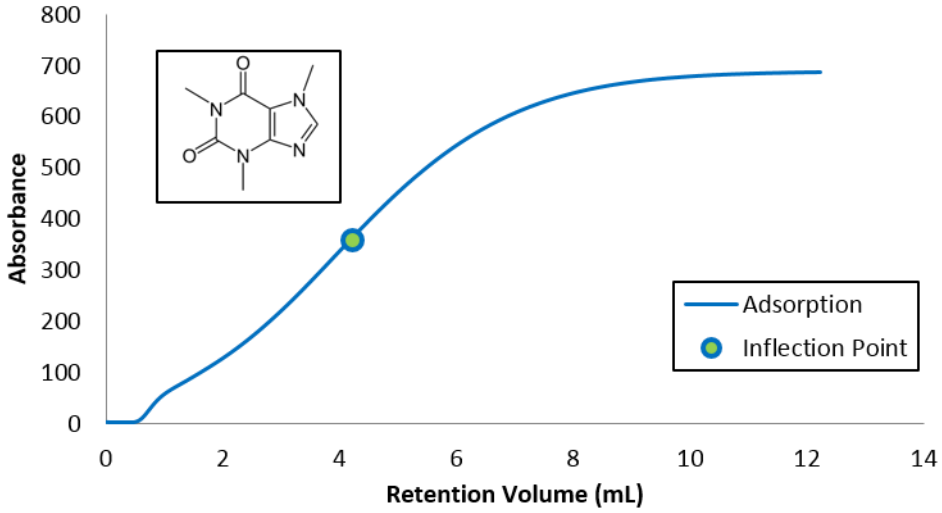

Figure 116. Profile observed for the adsorption of CAF (0.1 mM) in a column packed with a molecularly imprinted polymer synthetized in a batch reactor (CM05).

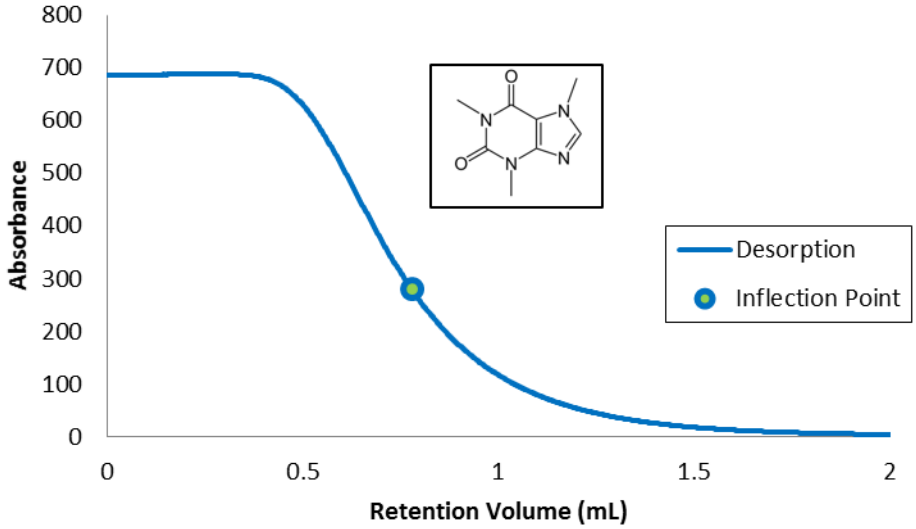

Figure 117. Profile observed for the desorption process of CAF (0.1 mM) in a column packed with a molecularly imprinted polymer synthetized in a batch reactor (CM05).

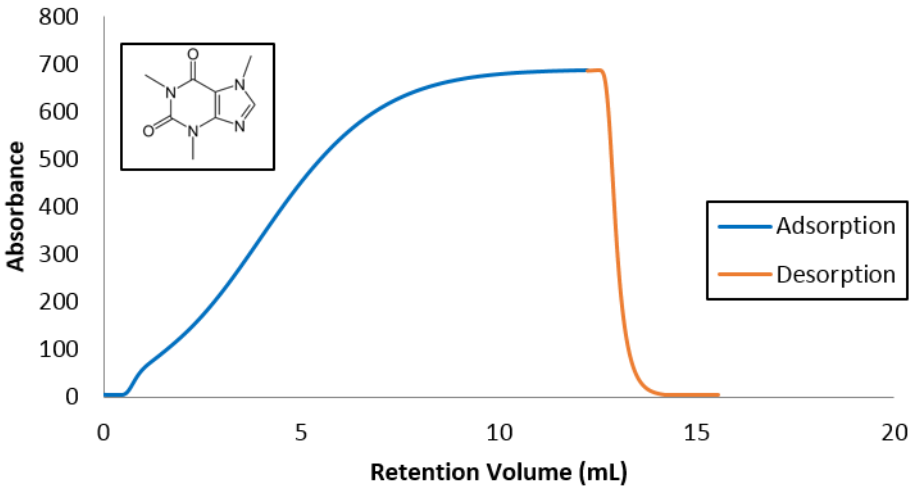

Figure 118. Profile observed for the adsorption and desorption of CAF (0.1 mM) in a column packed with a molecularly imprinted polymer synthetized in a batch reactor (CM05).

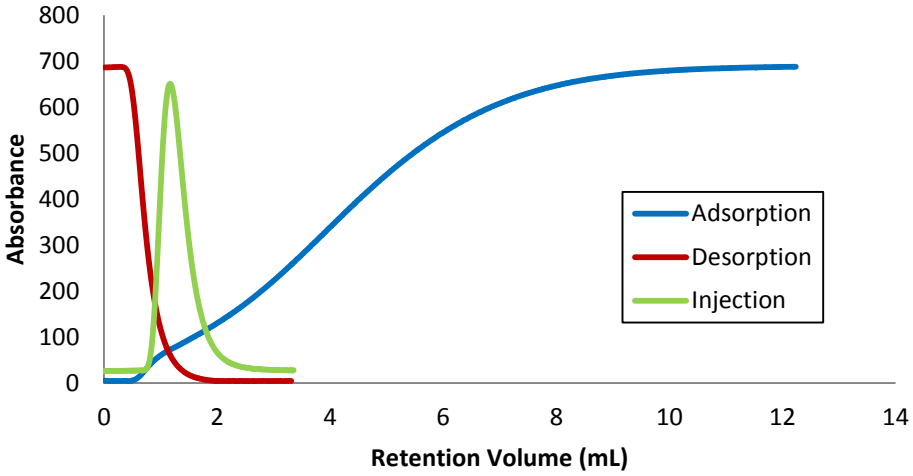

Figure 119. Profiles observed for the adsorption, desorption and injection of CAF (0.1 mM) in a column packed with a molecularly imprinted polymer synthetized in a batch reactor (CM05).

In Figure 120 to Figure 124 are presented the results of the adsorption and desorption tests with a solution of CAF (0.1 mM) in a molecularly imprinted polymer synthetized in a micro-reactor. Comparing with the previous results is visible that this material has less affinity with the drug once it reaches the saturation plateau faster than the last one.

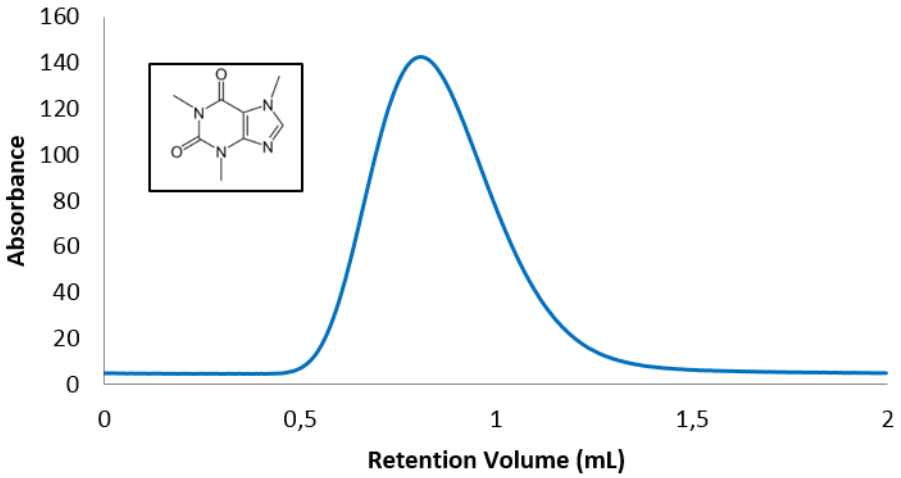

Figure 120. Profile observed for the injection of CAF (0.1 mM) in a column packed with a molecularly imprinted polymer synthetized in a micro-reactor (CM10).

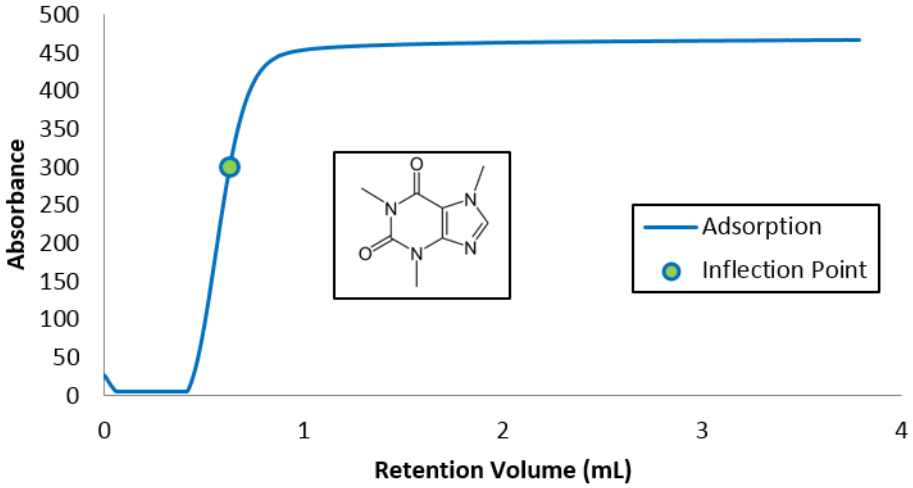

Figure 121. Profile observed for the adsorption of CAF (0.1 mM) in a column packed with a molecularly imprinted polymer synthetized in a micro-reactor (CM10).

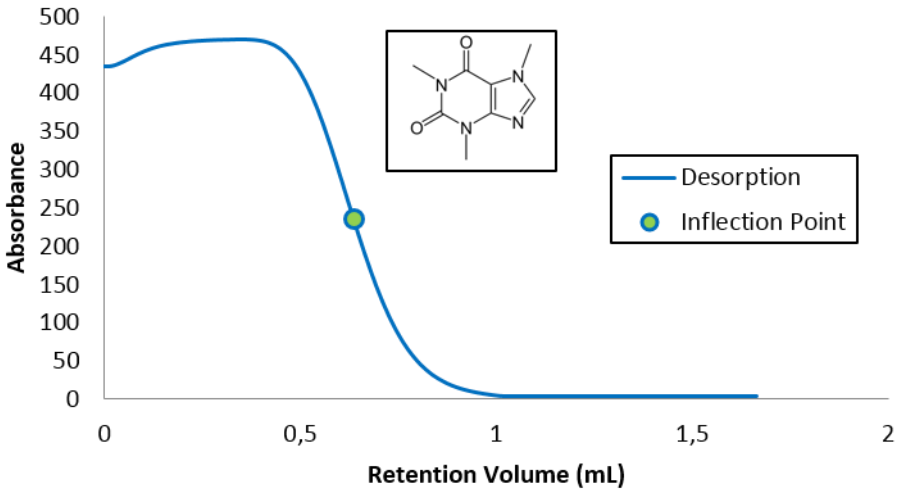

Figure 122. Profile observed for the dsorption of CAF (0.1 mM) in a column packed with a molecularly imprinted polymer synthetized in a micro-reactor (CM10).

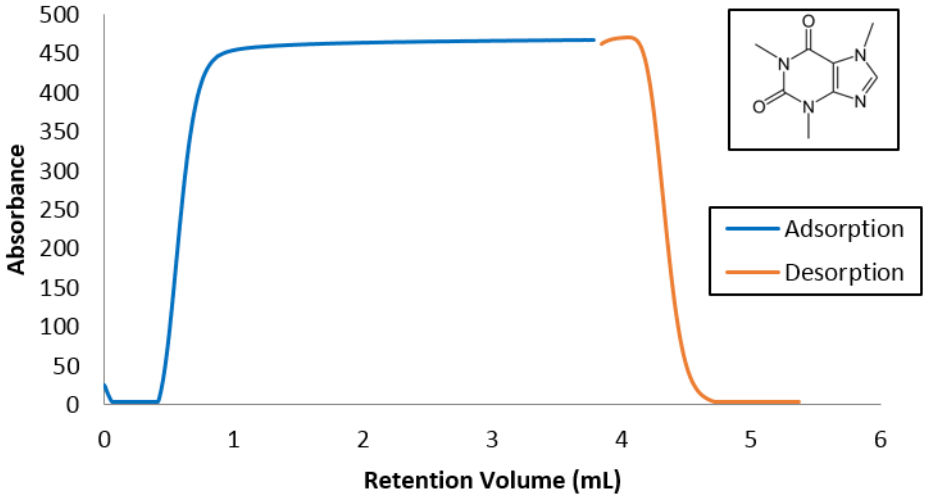

Figure 123. Profile observed for the adsorption and desorption of CAF (0.1 mM) in a column packed with a molecularly imprinted polymer synthetized in a micro-reactor (CM10).

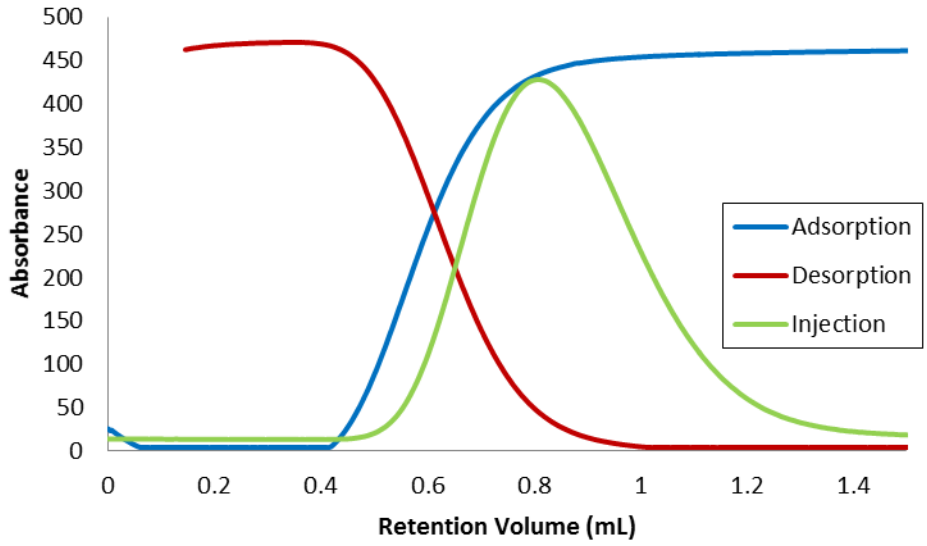

Figure 124. Profiles observed for the adsorption, desorption and injection of CAF (0.1 mM) in a column packed with a molecularly imprinted polymer synthetized in a micro-reactor (CM10).

In Figure 125 to Figure 129 are presented the results of the adsorption and desorption tests with a solution of 4AMP (0.1 mM) in a molecularly imprinted polymer synthetized in a batch reactor. These tests were made in order to compare the affinity of these materials with a drug other than the imprinted one. Although the polymer is molecularly imprinted with caffeine it is visible with these results that it is not going to have affinity with only this target. The linkages between the drug and the monomer can be stronger with other drugs. For example, once 4AMP is a basic molecule, it is going to interact with the acrylic acid (the monomer in these studies) for its acidic factor, i.e. it is not only about the imprinting but also about the compatibility between monomer and drug.

Observing Figure 126 it can be seen that when the retention volume is 120 mL (corresponding to time ~240 min) the curve did not still reach a plateau. It means that the affinity of the hydrogel with 4AMP is really big. The same happens with the desorption test. A saturated 4AMP MIP when synthetized with acrylic acid needs a bigger amount of time to be completely cleaned and saturated.

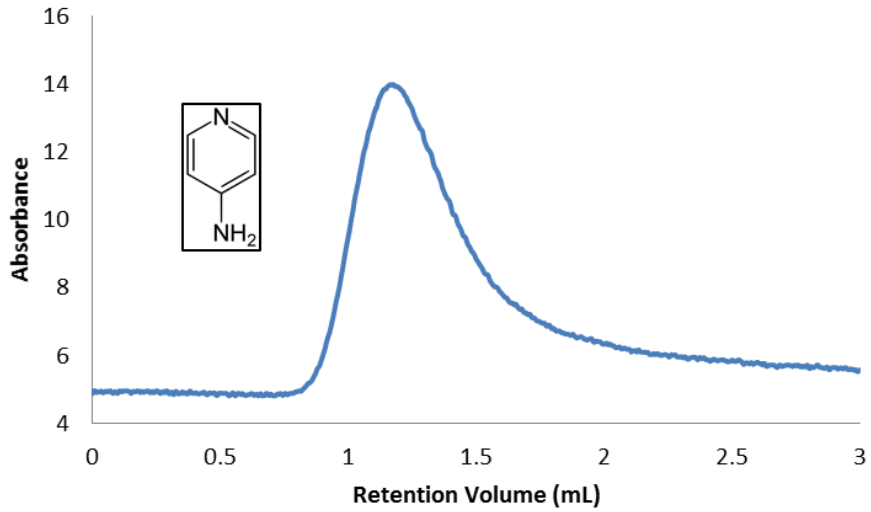

Figure 125. Profile observed for the injection of 4AMP (0.1 mM) in a column packed with a molecularly imprinted polymer synthetized in a batch reactor (CM05).

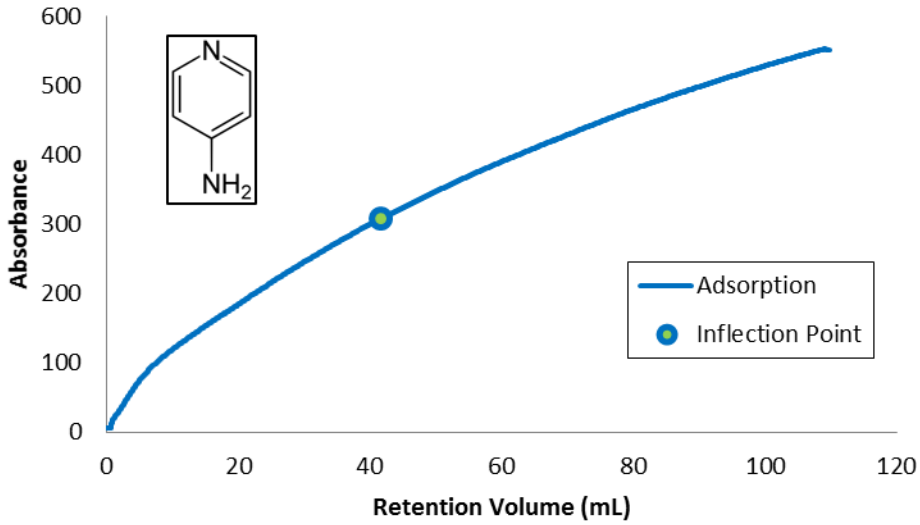

Figure 126. Profile observed for the adsorption of 4AMP (0.1 mM) in a column packed with a molecularly imprinted polymer synthetized in a batch reactor (CM05).

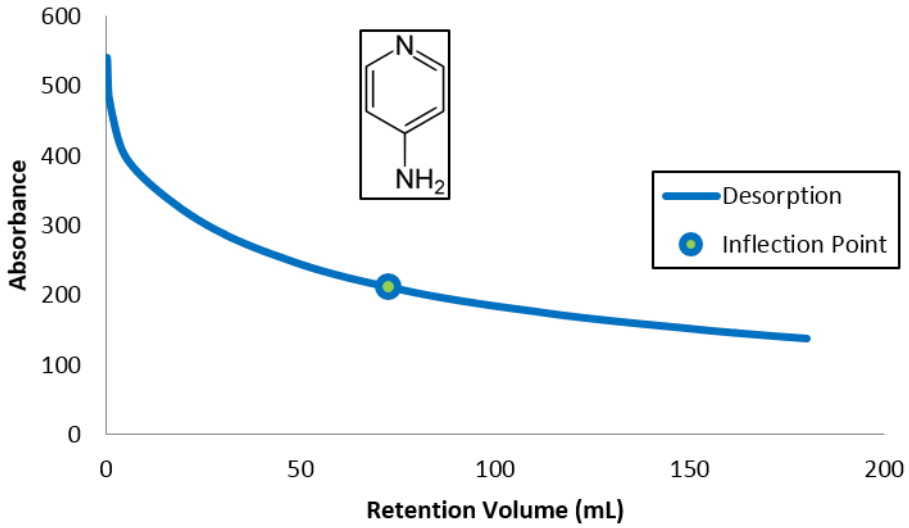

Figure 127. Profile observed for the desorption process of 4AMP (0.1 mM) in a column packed with a molecularly imprinted polymer synthetized in a batch reactor (CM05).

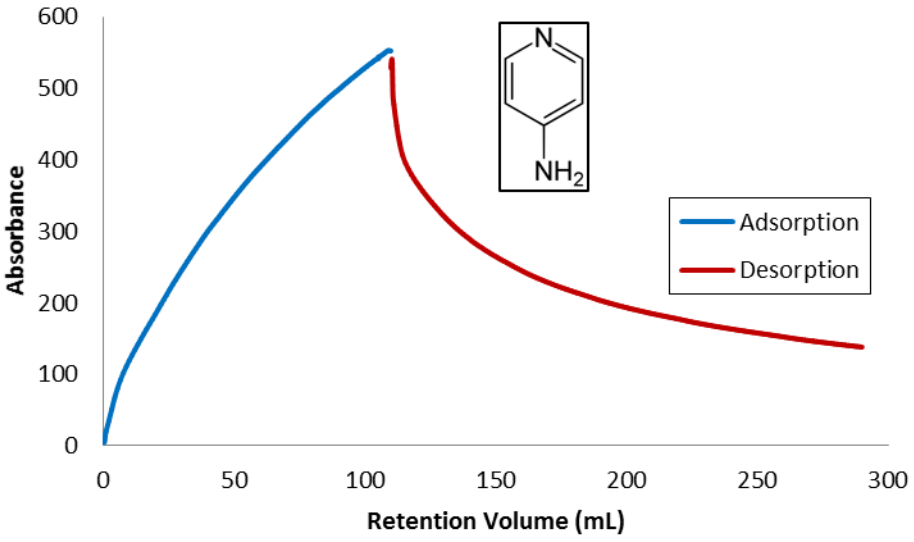

Figure 128. Profile observed for the adsorption and desorption of 4AMP (0.1 mM) in a column packed with a molecularly imprinted polymer synthetized in a batch reactor (CM05).

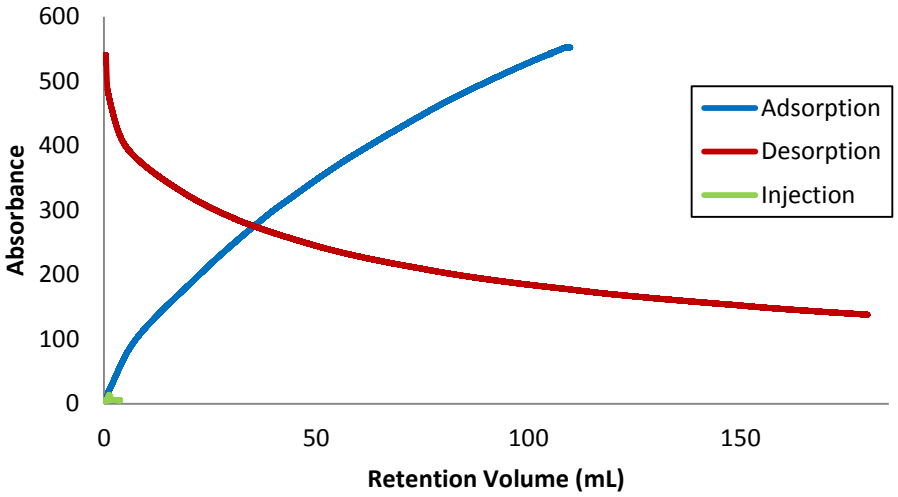

Figure 129. Profiles observed for the adsorption, desorption and injection of 4AMP (0.1 mM) in a column packed with a molecularly imprinted polymer synthetized in a batch reactor (CM05).

In Figure 130 to Figure 134 are presented the results for the adsorption and desorption tests with a solution of 4 AMP (0.1 mM) in a molecularly imprinted polymer synthetized in a micro-reactor. Comparing to the results obtained with a MIP synthetized in a batch reactor (please see Figure 126 and Figure 127) with the same solution it is visible that in this case the affinity is lower. This can be justified because of the plateau presented in the adsorption process is more defined than when using a MIP synthetized in a batch reactor. Note that the curve of the desorption process reached the base line at nearly 60 minutes (retention volume ~30 mL).

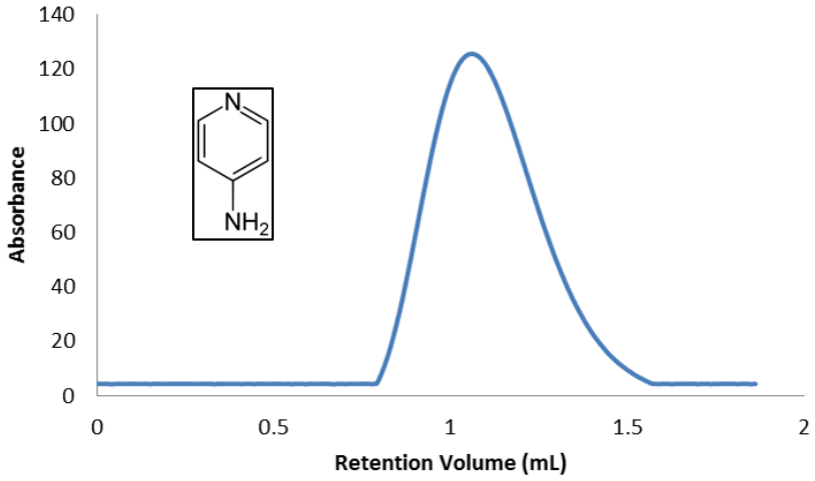

Figure 130. Profile observed for the injection of 4AMP (0.1 mM) in a column packed with a molecularly imprinted polymer synthetized in a micro-reactor (CM10).

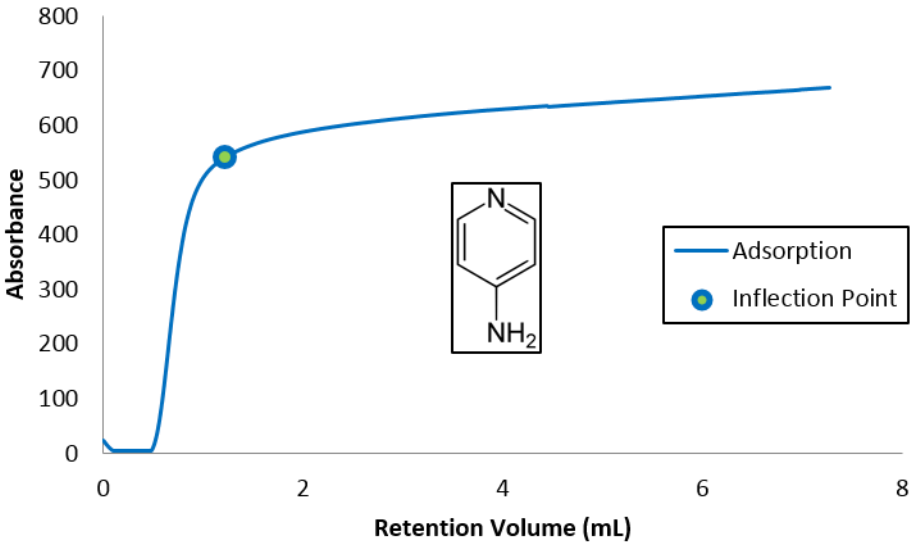

Figure 131. Profile observed for the adsorption of 4AMP (0.1 mM) in a column packed with a molecularly imprinted polymer synthetized in a micro-reactor (CM10).

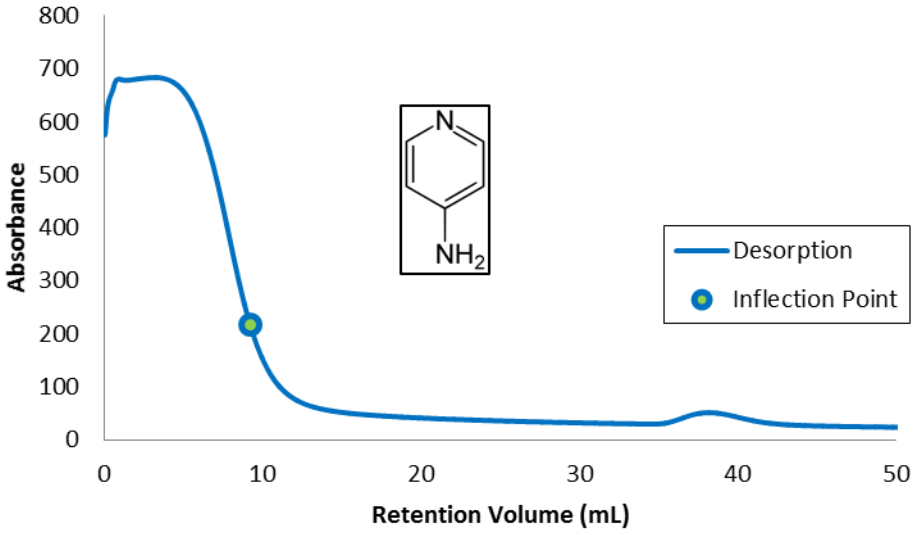

Figure 132. Profile observed for the desorption process of 4AMP (0.1 mM) in a column packed with a molecularly imprinted polymer synthetized in a micro-reactor (CM10).

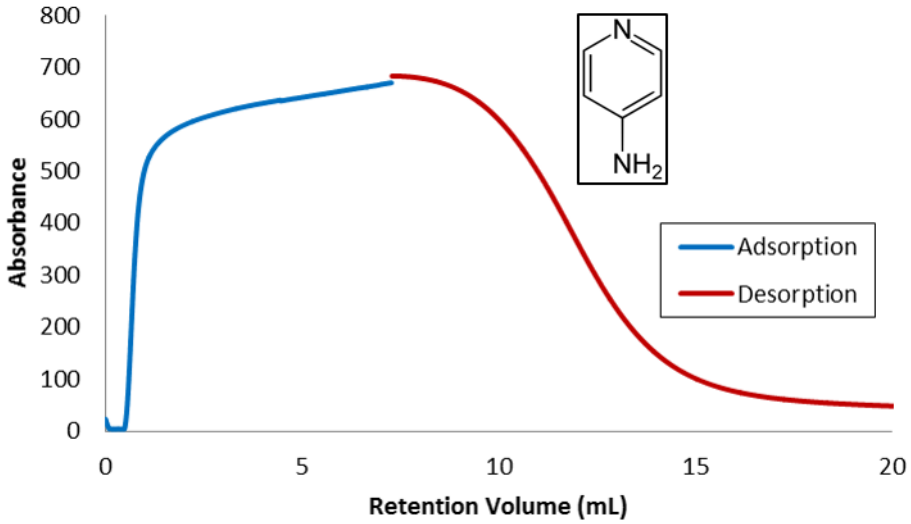

Figure 133. Profile observed for the adsorption and desorption of 4AMP (0.1 mM) in a column packed with a molecularly imprinted polymer synthetized in a micro-reactor (CM10).

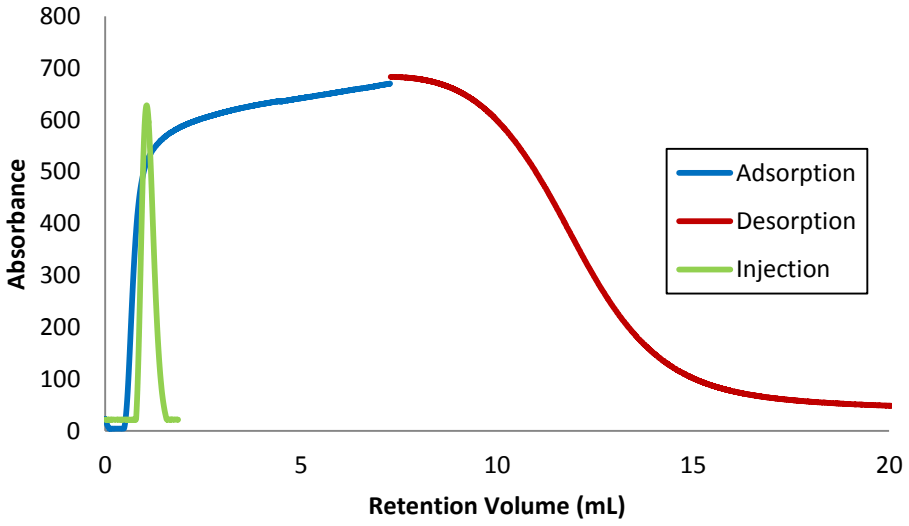

Figure 134. Profiles observed for the adsorption, desorption and injection of 4AMP (0.1 mM) in a column packed with a molecularly imprinted polymer synthetized in a micro-reactor (CM10).

Figure 135 and Figure 136 present the comparison of both saturation and desorption tests considering the combination between different drugs (caffeine and 4-aminopyridine) with different kinds of hydrogels.

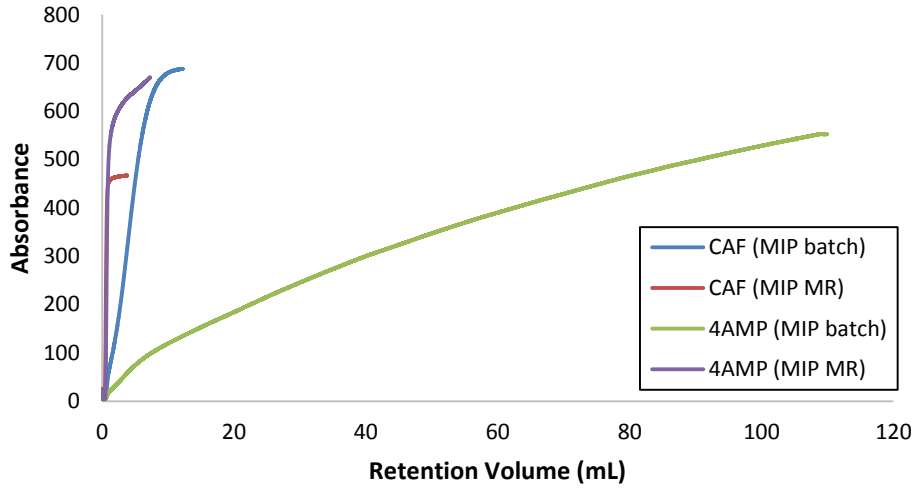

Figure 135. Profiles observed for saturation of CAF and 4AMP in different kinds of smart hydrogels (CM05 and CM10).

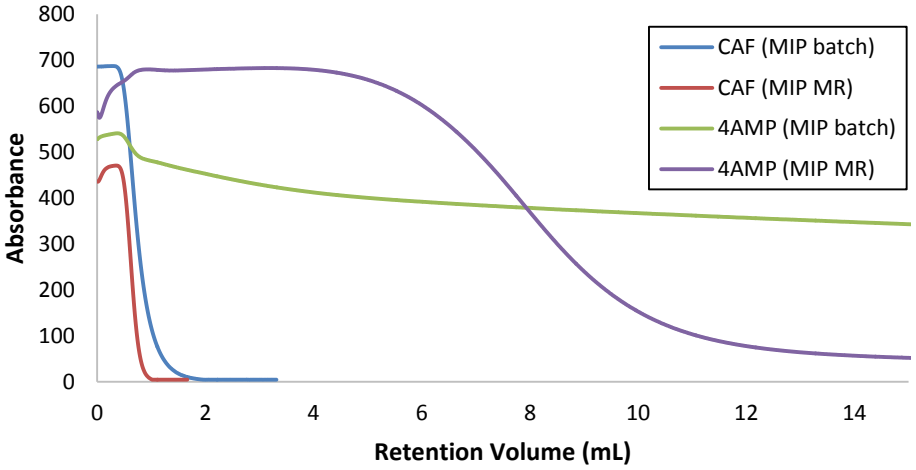

Figure 136. Profiles observed for desorption process of CAF and 4AMP in different kinds of smart hydrogels (CM05 and CM10).

Results above described were obtained when looking for a deeper analysis of the processes concerning the drug adsorption in the smart hydrogels and the subsequent release. Different measurements were performed involving the synthetized materials and template molecules. Batch adsorption (trying adsorption isotherms measurement), solid phase extraction (SPE) and frontal analysis were considered within this purpose. Acrylic acid based smart hydrogels imprinted with caffeine or non-imprinted, with FRP/RAFT synthesis or obtained in batch/micro-reactor were tested. Effect of pH

(stimulation of the acrylic acid based anionic networks) on the swelling of the materials and adsorption/release processes was also assessed. Important difficulties were observed with the measurement of the adsorption isotherms of caffeine in NIP/MIP hydrogels, especially in the higher solute concentration regions (e.g. > 4 mM). These issues can be a consequence of the lack of precision of measurement method (UV readings of batch solutions) with small differences or a slow adsorption process in the batch mode. Effect of pH on caffeine batch adsorption was measured using 5 mM as constant solute starting concentration. Relative small fractions of adsorbed solute were also measured in these conditions (below 10 %) and minor differences were also observed within the different hydrogels tested (MIP/NIP and batch/micro-reactor). In spite of the soxhlet extraction cleaning process used, relative small fractions of adsorbed material observed with MIPs can be a consequence of the presence of impurities in these products. For all the materials, was observed the swelling ratio increase with pH (e.g. SR~5 at pH=2 and SR~20 at pH=10). Nevertheless, smaller values of SR were consistently observed with MIP/RAFT products, which is an important result of this work: it is possible to obtain comparable drug adsorption fractions with materials exhibiting lower swelling ratios if MIP/RAFT products are considered. Note that for several applications (e.g. biological systems, production of materials for packing columns) it is important to control the swelling ratio of the hydrogels because to high values (e.g. 100 or even 1000) are not acceptable. The fast (and cheaper when compared with frontal analysis) SPE technique was also used to quantify the fraction of caffeine (5 mM aqueous solution) adsorbed in different materials. Values obtained are in line with the batch measurements indicating relative small quantities adsorbed (below 10 %).

In order to obtain higher precision with the adsorption/desorption (saturation/release) drug mechanisms, frontal analysis was also considered in the characterization of the different smart hydrogels synthesized. Within this purpose, small GPC empty columns were packed with these materials. In this packing processes was taken advantage of the swelling behavior of the hydrogels in the presence of the GPC eluent (water), promoting the self-packing of the material. Adsorption and desorption where monitored *in-line* through UV absorption. Caffeine and 4-aminopyridine were both adsorbed and desorbed in RAFT/MIP-caffeine hydrogels produced in batch and micro-reactor. It was observed that the adsorption capability of the hydrogels is at least 10 times higher with

4-aminopyridine, in comparison with caffeine (e.g. > 274 mmol/g dried hydrogel with 4-aminopyridine and ~28 mmol/g dried hydrogel with caffeine). This seems to indicate that the high affinity of 4-aminopyridine with acrylic acid based hydrogels is dominant comparatively to the molecular imprinting of the materials with caffeine. It is not clear the effect of the reactor type (batch/micro-reactor) on the retention capabilities of the hydrogels when caffeine is used as template molecule. Comparable values were obtained in three measurements (e.g. around 4 mmol/g dried hydrogel) but a higher adsorbed amount (28 mmol/g dried hydrogel) was observed with the RAFT/MIP/batch product. Lower void volume generated by the bulky material produced in batch can eventually be at the source of these differences (with hydrogel produced in the micro-reactor some void between particles is plausible). In spite of these uncertainties, in both cases, was possible the operation of the GPC packed columns without exceeding the maximum value allowed by the instrument (10 MPa). Maximum pressure observed during these measurements was around 1.2 MPa which confirms and important outcome of this research: it is possible to control the swelling ratio of smart hydrogels (and therefore the pressure generated by the materials when packed) if RAFT/MIP synthesis is used.

Feasibility for the production of smart hydrogels in continuous-flow micro-reactor, combining also RAFT and molecular imprinting, is a major contribution of this work for this research field. It was also shown that RAFT polymerization is an effective tool to modify the network properties, namely to control the swelling ratio of hydrogels. Additional work is needed to clarify the impact of the designing tools developed (RAFT/MIP/micro-reactor) in the end-use properties of these materials, namely the drug adsorption/desorption capabilities. In fact, the imprinting process is affected by several synthesis parameters, namely the amount of crosslinker or even the solvent used in the polymerization. It is suggested the extension of the approach here developed through the synthesis of materials with higher crosslinker content (e.g. more than 10%) and using an organic solvent (e.g. DMF) instead of water (to decrease the hydrogen bonding effect of water). These changes are a hopefully route to increase the affinity and selectivity of the advanced materials here addressed.

Table 8. Summary of results obtained by frontal analysis of molecularly imprinted hydrogel particles (batch synthesis or micro-reactor) also considering different drug tests (saturation tests).

Hydrogel	Swelling Ratio (SR)	Packed dried mass (mg)	Drug	C_0 (mM)	Q (mL/min)	P (MPa)	V_G (mL)	V_0 (mL)	V_a (mL)	V_{eq} (mL)	q* (mmol/mL stationary phase)	q* (mmol/g dried stationary phase)
CM05	21.14	15.2	CAF	0.1	0.5	0.4	0.17	0	0.17	4.21	2.48	27.70
CM05	21.14	15.2	4AMP	0.1	0.5	0.4	0.17	0	0.17	> 41.70	> 42.18	> 274.34
CM10	18.32	15.2	CAF	5.0	0.5	0.7	0.17	0	0.17	NA	NA	NA
CM10	18.32	15.2	CAF	0.1	0.5	0.7	0.17	0	0.17	0.63	0.37	4.14
CM10	18.32	15.2	4AMP	0.1	0.5	1.2	0.17	0	0.17	1.22	0.72	8.03

Table 9. Summary of results obtained by frontal analysis of molecularly imprinted hydrogel particles (batch synthesis or micro-reactor) also considering different drug tests (desorption tests).

Hydrogel	Swelling Ratio (SR)	Packed dried mass (mg)	Drug	C_0 (mM)	Q (mL/min)	P (MPa)	V_G (mL)	V_0 (mL)	V_a (mL)	V_{eq} (mL)	q* (mmol/mL stationary phase)	q* (mmol/g dried stationary phase)
CM05	21.14	15.2	CAF	0.1	0.5	0.4	0.17	0	0.17	0.78	0.46	5.13
CM05	21.14	15.2	4AMP	0.1	0.5	0.4	0.17	0	0.17	> 72.47	> 42.63	> 476.78
CM10	18.32	15.2	CAF	5.0	0.5	0.7	0.17	0	0.17	NA	NA	NA
CM10	18.32	15.2	CAF	0.1	0.5	0.7	0.17	0	0.17	0.64	0.38	4.21
CM10	18.32	15.2	4AMP	0.1	0.5	1.2	0.17	0	0.17	9.23	5.43	60.72

CHAPTER 6 - Conclusions and future work

This work was devoted to the synthesis, characterization and assessment of the end-use performance of smart hydrogels. Different experimental designing tools were combined in a single strategy in order to try the production of advanced materials with tailored properties. Two polymerization mechanisms were alternatively considered, namely the classical Free Radical Polymerization (FRP) and also Reversible Addition-Fragmentation Chain Transfer Polymerization (RAFT) polymerization. The influence of polymerization mechanism on the structure/properties of these kinds of materials was thus sought. Production of smart hydrogels was performed in batch reactor and also in continuous flow micro-reactor. This last device was built-up in this research in order to try the synthesis of particles of smart hydrogels (eventually with different sizes by changing the internal diameter of the tubing used). These particles are easily handled (e.g. for use as packing materials), namely when compared with the bulk materials resulting from batch polymerization. Molecular imprinting was considered as a third vector to try the production of smart hydrogels with tailored properties. Molecularly Imprinted Polymers (MIPs) were synthesized using FRP/RAFT and batch/micro-reactor and the properties of these materials were compared with the analogues Non-Imprinted hydrogels. Research here performed aims to contribute to the finding of linking lines between synthesis conditions, structure and end-use performance of smart hydrogels. Nowadays, these advanced materials find important applications in different fields, such as biotechnology, biomedicine, pharmaceutics or environmental industries. Drug or gene delivery, bio-separations, bio-sensing and tissue engineering are just some examples of these kinds of applications.

In the first stage of this research, was performed the batch controlled release testing in smart hydrogels considering four different drugs used in medicine (isonicotinylhdrazine, ibuprofen, 5-fluoruracil and caffeine). Within this purpose, temperature-sensitive and pH-sensitive hydrogels were used. N-isopropylacrylamide (NIPA) was considered to generate polymer networks with sensitivity to changes in the temperature of the environmental conditions and Acrylic Acid (AA) was used to obtain pH-sensitive materials. Classical FRP and RAFT were alternatively used as

polymerization techniques in order to study the impact of the synthesis conditions on the performance of these kinds of advanced materials.

Hydrogels were loaded with the four targeted drugs through the exploitation of the swelling behavior of these materials in aqueous solutions. Two different batch incubation methods were tested, namely with and without the filtration of the remaining aqueous solution. In the first case (big excess of aqueous media followed by filtration), smaller amounts of drug are incubated in the hydrogel while with the second approach (all the initial aqueous media is taken by the hydrogel) some of the drug is eventually located in the surface of the material.

After loading, the different samples correspondent to different combinations of hydrogels/drugs were submitted to batch drug release tests triggered by different conditions of the surrounding aqueous media. Release studies at T=25 ºC and T=37 ºC were performed with the T-sensitive hydrogels and acid/alkaline conditions were considered with the pH-sensitive materials. In each case, dynamics of drug release was experimentally measured through UV detection in aqueous media of samples collected at different times ($t=0$ is correspondent to the beginning of the drug release process). Results obtained showed the importance of selection of the right combination between hydrogel/drug/surrounding conditions in order to achieve some control on the release process. In fact, physical and chemical interactions between hydrogels, drugs and aqueous solution play a fundamental role in these release mechanisms. For instance, results here obtained showed a huge difference in the release of ibuprofen in acidic or alkaline conditions due to the higher solubility of this molecule in the latter conditions.

The results above described with batch controlled release drive to the search for routes with potential improvement of the affinity between drugs and hydrogels. The use of the molecular imprinting technique was selected within this purpose because, in principle, is the best way to increase the affinity and selectivity of a template molecule (e.g. a drug) with a polymer network. Thus, was performed the synthesis of conventional (non-imprinted) and MIP hydrogels in batch reactor using FRP and RAFT techniques. Besides the expected improvement of the affinity between hydrogels and specific drugs considering MIP materials, these synthesis were also a contribution to the assessment of the influence of the kinetic mechanisms involved (FRP/RAFT) on network performance. Moreover, it was also showed the feasibility of a new experimental

approach, using a continuous microfluidic reactor, and allowing the synthesis of smart hydrogel micro-particles. Imprinted/non-imprinted and FRP/RAFT products were obtained within this task [26, 27]. Expecting for particular interactions between caffeine and acrylic acid molecules, this combination was selected in the molecular imprinting studies here performed.

Size exclusion chromatography with tetra-detection (refractive index + ultraviolet + light – scattering + intrinsic viscosity) was used to measure the molecular architecture of the products synthetized, namely the primary structure of the linear (soluble) analogues of the polymer networks obtained. These measurements were performed using directly water as eluent, avoiding the use of organic solvents with water compatible polymers. Nevertheless, working directly with water as eluent is hampered by the low quality of the light – scattering signal that is observed in these conditions. Presence of salts in the water (e.g. sodium azide to prevent the growth of bacteria in the GPC columns) is probably the source of these issues. In spite if these difficulties, SEC measurements lead to important results because the difference between the molecular architecture of FRP and RAFT products was highlighted. In fact, was shown the strong impact of the RAFT mechanism on the size of the primary chains of the polymers which confirms the possibility for using this mechanism to obtain tailored products (increasing the initial ratio RAFT/monomer is possible to decrease the size of the primary chains). Moreover, SEC measurements also showed that, with the synthesis conditions used, the difference between the molecular architecture of batch/micro-reactor products is small when compared with FRP/RAFT materials.

Looking for a deeper analysis of the processes concerning the drug adsorption in the smart hydrogels and the subsequent release, different measurements were performed involving the synthetized materials and template molecules. Batch adsorption (trying adsorption isotherms measurement), solid phase extraction (SPE) and frontal analysis were considered within this purpose. Acrylic acid based smart hydrogels imprinted with caffeine or non-imprinted, with FRP/RAFT synthesis or obtained in batch/micro-reactor were tested. Effect of pH (stimulation of the acrylic acid based anionic networks) on the swelling of the materials and adsorption/release processes was also assessed. Important difficulties were observed with the measurement of the adsorption isotherms of caffeine in NIP/MIP hydrogels, especially in the higher solute concentration regions (e.g. > 4

mM). These issues can be a consequence of the lack of precision of measurement method (UV readings of batch solutions) with small differences or a slow adsorption process in the batch mode. Effect of pH on caffeine batch adsorption was measured using 5 mM as constant solute starting concentration. Relative small fractions of adsorbed solute were also measured in these conditions (below 10 %) and minor differences were also observed within the different hydrogels tested (MIP/NIP and batch/micro-reactor). In spite of the soxhlet extraction cleaning process used, relative small fractions of adsorbed material observed with MIPs can be a consequence of the presence of impurities in these products. For all the materials, was observed the swelling ratio increase with pH (e.g. SR~5 at pH=2 and SR~20 at pH=10). Nevertheless, smaller values of SR were consistently observed with MIP/RAFT products, which is an important result of this work: it is possible to obtain comparable drug adsorption fractions with materials exhibiting lower swelling ratios if MIP/RAFT products are considered. Note that for several applications (e.g. biological systems, production of materials for packing columns) it is important to control the swelling ratio of the hydrogels because to high values (e.g. 100 or even 1000) are not acceptable. The fast (and cheaper when compared with frontal analysis) SPE technique was also used to quantify the fraction of caffeine (5 mM aqueous solution) adsorbed in different materials. Values obtained are in line with the batch measurements indicating relative small quantities adsorbed (below 10 %).

In order to obtain higher precision with the adsorption/desorption (saturation/release) drug mechanisms, frontal analysis was also considered in the characterization of the different smart hydrogels synthesized. Within this purpose, small GPC empty columns were packed with these materials. In this packing processes was taken advantage of the swelling behavior of the hydrogels in the presence of the GPC eluent (water), promoting the self-packing of the material. Adsorption and desorption where *in-line* monitored through UV absorption. Caffeine and 4-aminopyridine were both adsorbed and desorbed in RAFT/MIP-caffeine hydrogels produced in batch and micro-reactor. It was observed that the adsorption capability of the hydrogels is at least 10 times higher with 4-aminopyridine, in comparison with caffeine (e.g. > 274 mmol/g dried hydrogel with 4-aminopyridine and ~28 mmol/g dried hydrogel with caffeine). This seems to indicate that the high affinity of 4-aminopyridine with acrylic acid based hydrogels is dominant

comparatively to the molecular imprinting of the materials with caffeine. It is not clear the effect of the reactor type (batch/micro-reactor) on the retention capabilities of the hydrogels when caffeine is used as template molecule. Comparable values were obtained in three measurements (e.g. around 4 mmol/g dried hydrogel) but a higher adsorbed amount (28 mmol/g dried hydrogel) was observed with the RAFT/MIP/batch product. Lower void volume generated by the bulky material produced in batch can eventually be at the source of these differences (with hydrogel produced in the micro-reactor some void between particles is plausible). In spite of these uncertainties, in both cases, was possible the operation of the GPC packed columns without exceeding the maximum value allowed by the instrument (10 MPa). Maximum pressure observed during these measurements was around 1.2 MPa which confirms and important outcome of this research: it is possible to control the swelling ratio of smart hydrogels (and therefore the pressure generated by the materials when packed) if RAFT/MIP synthesis is used.

Feasibility for the production of smart hydrogels in continuous-flow micro-reactor, combining also RAFT and molecular imprinting, is a major contribution of this work for this research field. It was also shown that RAFT polymerization is an effective tool to modify the network properties, namely to control the swelling ratio of hydrogels. Additional work is needed to clarify the impact of the designing tools developed (RAFT/MIP/micro-reactor) in the end-use properties of these materials, namely the drug adsorption/desorption capabilities. In fact, the imprinting process is affected by several synthesis parameters, namely the amount of crosslinker or even the solvent used in the polymerization. It is suggested the extension of the approach here developed through the synthesis of materials with higher crosslinker content (e.g. more than 10%) and using an organic solvent (e.g. DMF) instead of water (to decrease the hydrogen bonding effect of water). These changes are a hopefully route to increase the affinity and selectivity of the advanced materials here addressed.

Bibliography

[1] Kryscio DR, P.N., *Mimicking biological delivery through feedback-controlled drug release systems based on molecular imprinting.* AIChE Journal, 2009. 55: p. 1311-1324.

[2] Herrero EP, D.V.E., Peppas NA,, *Protein Imprinting by Means of Alginate-Based Polymer Microcapsules.* Ind. Eng. Chem. Res., 2010. 49: p. 9811–9814.

[3] Nuttelman CR, R.M., Rydholm AE, Salinas CN, Shah DN, Anseth KS, *Macromolecular monomers for the synthesis of hydrogel niches and their application in cell encapsulation and tissue engineering.* Progress in Polymer Science, 2008. 33: p. 167-179.

[4] Pan G, Z.B., Guo X, Zhang Y, Li C, Zhang H, *Preparation of molecularly imprinted polymer microspheres via reversible addition–fragmentation chain transfer precipitation polymerization.* Polymer 2009. 50: p. 2819-2825.

[5] Pan G, Z.Y., Guo X, Li C, Zhang H, *An efficient approach to obtaining water-compatible and stimuli-responsive molecularly imprinted polymers by the facile surface-grafting of functional polymer brushes via RAFT polymerization.* Biosensors and Bioelectronics, 2010. 26: p. 976–982.

[6] Boyer C, S.M., Davis TP, *Building Nanostructures Using RAFT Polymerization.* Journal of Polymer Science Part A: Polymer Chemistry, 2011. 49: p. 551-595.

[7] Russum JP, J.C., Schork FJ, *Continuous Living Polymerization in Miniemulsion Using Reversible Addition Fragmentation Chain Transfer (RAFT) in a Tubular Reactor.* Ind. Eng. Chem. Res., 2005. 44: p. 2484–2493.

[8] Diehl C, L.P., Azzouz N, Seeberger PH, *Accelerated Continuous Flow RAFT Polymerization.* Macromolecules, 2010. 43: p. 10311–10314.

[9] Zhang, J. and N.A. Peppas, *Synthesis and characterization of pH- and temperature-sensitive poly(methacrylic acid)/poly(N-isopropylacrylamide) interpenetrating polymeric networks.* Macromolecules, 2000. 33(1): p. 102-107.

[10] Bajpai, A., et al., *Stimuli Responsive Drug Delivery Systems: From Introduction to Application*. 2010, Shropshire, UK: iSmithers.

[11] Galaev, I. and B. Mattiasson, *Smart Polymers*. Second ed. 2007, United States of America: CRC Press.

[12] Gupta, P., K. Vermani, and S. Garg, *Hydrogels: from controlled release to pH-responsive drug delivery.* Drug Discovery Today, 2002. 7(10): p. 569-579.

[13] Uhrich, K.E., et al., *Polymeric systems for controlled drug release.* Chemical Reviews, 1999. 99(11): p. 3181-3198.

[14] Gonçalves, M.A.D., et al., *Polymer Reaction Engineering Studies on Smart Hydrogels Formation.* Journal of Nanostructured Polymers and Nanocomposites, 2012. 9(2): p. 40-45.

[15] Gonçalves, M.A.D., et al., *Stimuli-Responsive Hydrogels Synthesis using Free Radical and RAFT Polymerization.* Macromolecular Symposia, 2013: p. 41-54.

[16] Costa, R.A.S., *Síntese e Teste de Hidrogéis Inteligentes para a Libertação Controlada de Fármacos*, in *Técnologia Biomédica*. 2013, Escola Superior de Tecnologia e Gestão de Bragança.

[17] Shukla, S., A.K. Bajpai, and J. Bajpai, *Swelling controlled delivery of antibiotic from a hydrophilic macromolecular matrix with hydrophobic moieties.* Macromolecular Research, 2003. 11(4): p. 273-282.

[18] Deus, J.F.d., *Síntese e propriedades físicas de poli(metacrilato de metila-co-metacrilato de 9-metil antracenila)*. 2003, Universidade Federal do Paraná.

[19] Odian, G., *Principles of Polymerization*. 2nd. ed. 1981: New York: John Wiley & Sons.

[20] Florenzano, F.H., *Perspectivas Atuais para a Obtenção Controlada de Polímeros e sua Caracterização.* Polímeros: Ciência e Tecnologia, 2008. 18: p. 100-105.

[21] Garcia, A., *Estudo Comparativo entre as Técnicas de Polimerização Radical Livre Convencional e Radical Livre "Viva" via RAFT para Produção de Poli(Dimetilaminoetilmetacrilato) -PDMAEMA*. 2005, Faculdade de Engenharia Química de Lorena - FAENQUIL.

[22] Graeme Moad, D.H.S., *The Chemistry of Radical Polymerization*. Second Edition ed. 2006: Elsevier.

[23] Renkecz, T., *Novel Molecularly Imprinted Polymers - Membranes, microspheres, photoswitchable particles.*, in *Inorganic and Analytical Chemistry*. 2013, Budapest University of Technology and Economics.

[24] Mark E. Byrne, V.S., *Molecular imprinting within hydrogels II: Progress and analysis of the field.* International Journal of Pharmaceutics, 2008. 364: p. 188-212.

[25] Jantarat, C., *Application of Molecularly Imprinted Polymer for Drug Delivery and Membrane Separation of Chiral Drugs*. 2009, Prince of Songkla.

[26] C. Machado (a), A.F., P. Kadhirvel, R.C.S. Dias, M.R.P.F.N. Costa, *Production of RAFT Imprinted Smart Hydrogel Particles in a Continuous Flow Micro-reactor*. 2014(Accepted to be presented in the 12th International Chemical and Biological Engineering Conference (CHEMPOR 2014), 10-12, September, Porto, Portugal).

[27] C. Machado (b), T.O., P. Reitor, D. Oliveira, A. Freitas, P. Kadhirvel, R.C.S. Dias, M.R.P.F.N. Costa, *Development of Tailored Hydrogels using RAFT Polymerization in Continuous Flow Microreactor.* 2014(Accepted to be presented in the 8TH ECNP INTERNATIONAL CONFERENCE ON NANOSTRUCTURED POLYMERS AND NANOCOMPOSITES, 16-19, September, Dresden, Germany).

[28] Sadao Mori, H.G.B., *Size Exclusion Chromatography*. 1999: Springer Science & Business Media.

[29] Malvern. *Complete Guide for GPC/SEC/GFC Instrumentation and Detection Technolgies*. 2014; Available from: http://www.malvern.com/en/products/product-range/viscotek-range/default.aspx.

[30] F. Gritti, W.P., G. Guiochon, Journal of Chromatography A, 2002. 978: p. 81-107.

[31] H. Kim, F.G., G. Guiochon, Journal of Chromatography A, 2004. 1049: p. 25-36.

[32] P. Sajonz, G.Z., G. Guiochon, Journal of Chromatography A, 1996. 731: p. 1-25.

[33] Simpson, N.J.K., *Solid-Phase Extraction: Properties, Techniques and Applications.* 2000: CRC Press.

Annexes

Annex 1. Calibration curves for the different drugs used in this work.

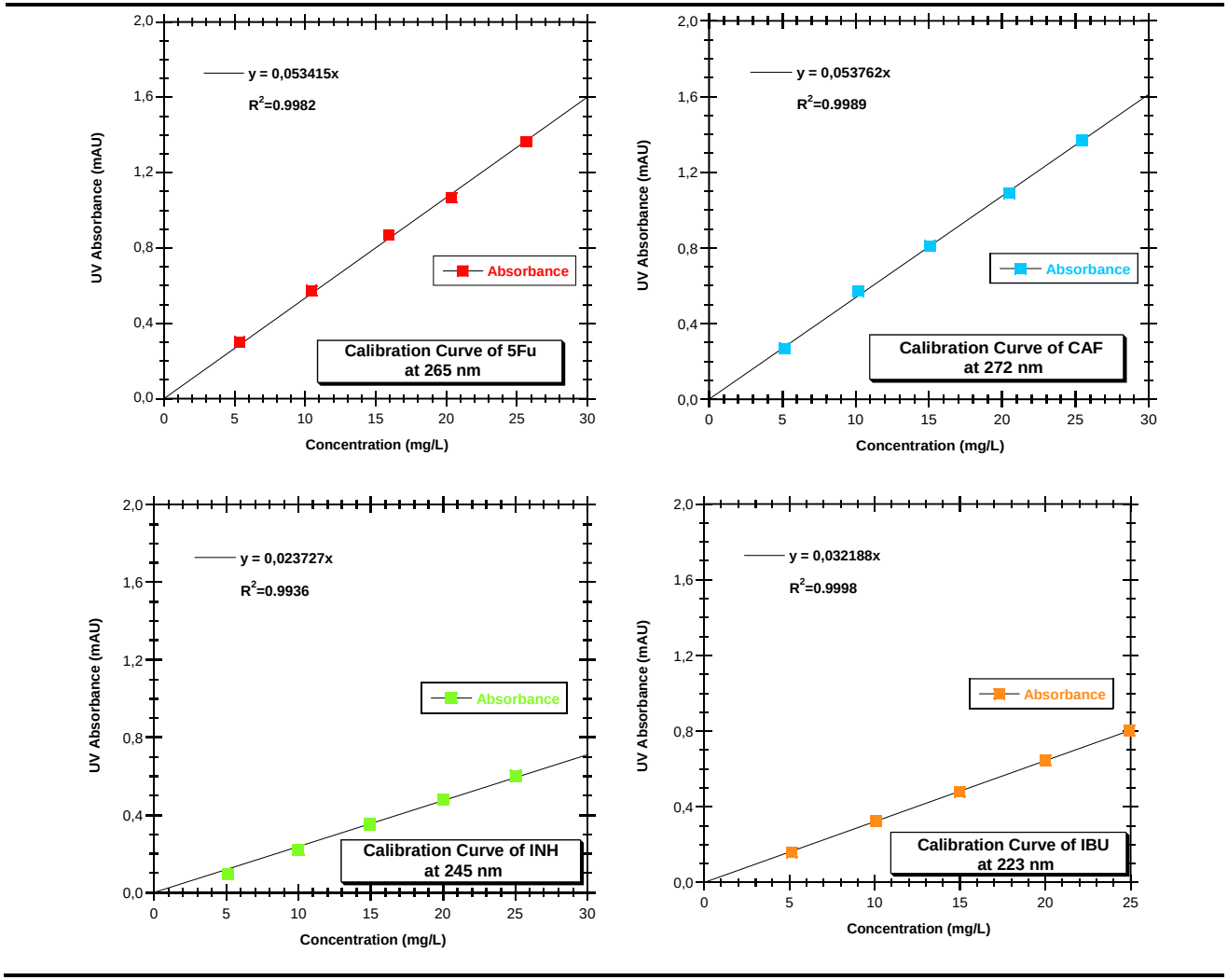

Annex 2. Results of the release test performed at 25 ºC with a 5-FU incubated NIPA hydrogel (HG1).

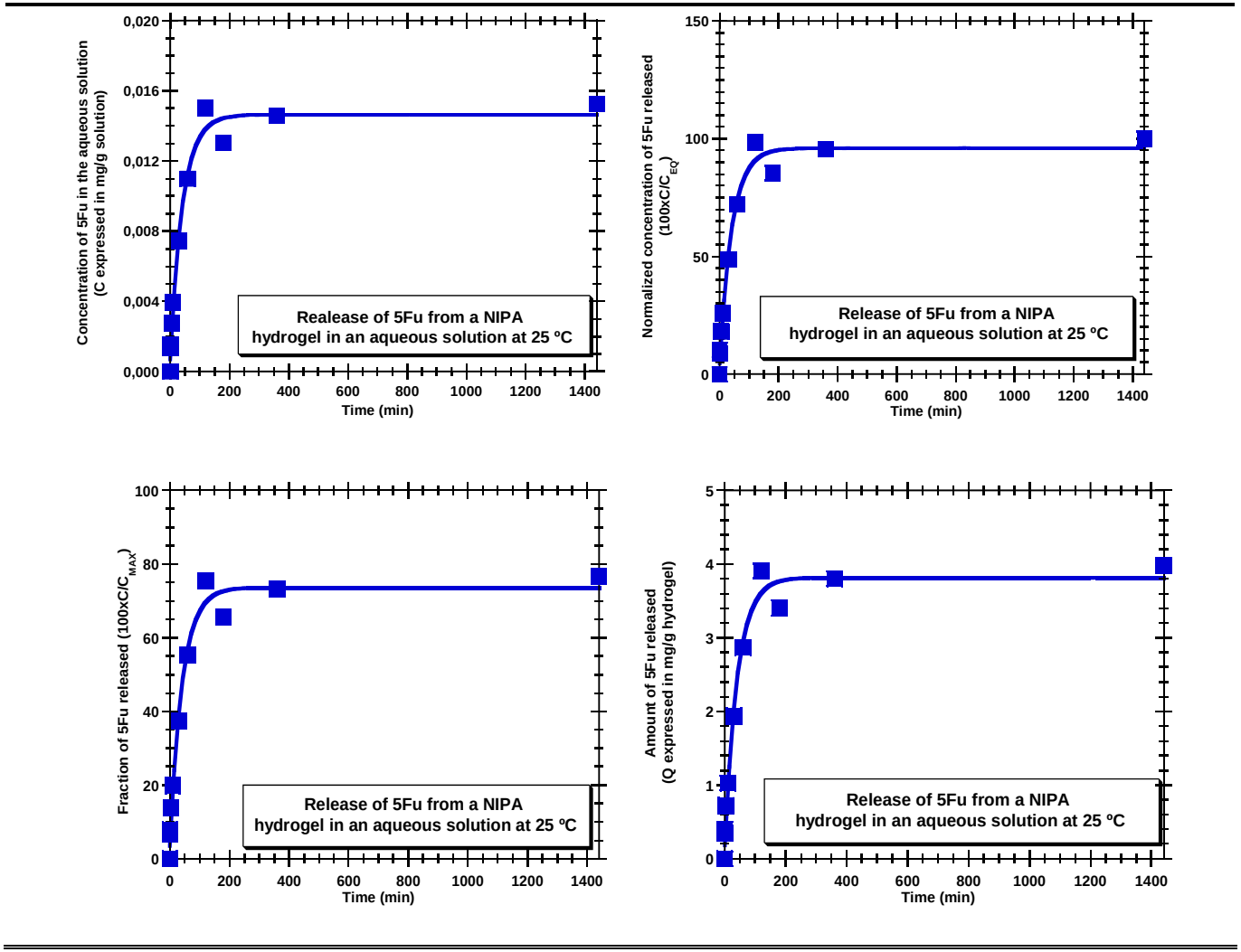

Annex 3. Results of the release test performed at 37 ºC with a 5-FU incubated NIPA hydrogel (HG1).

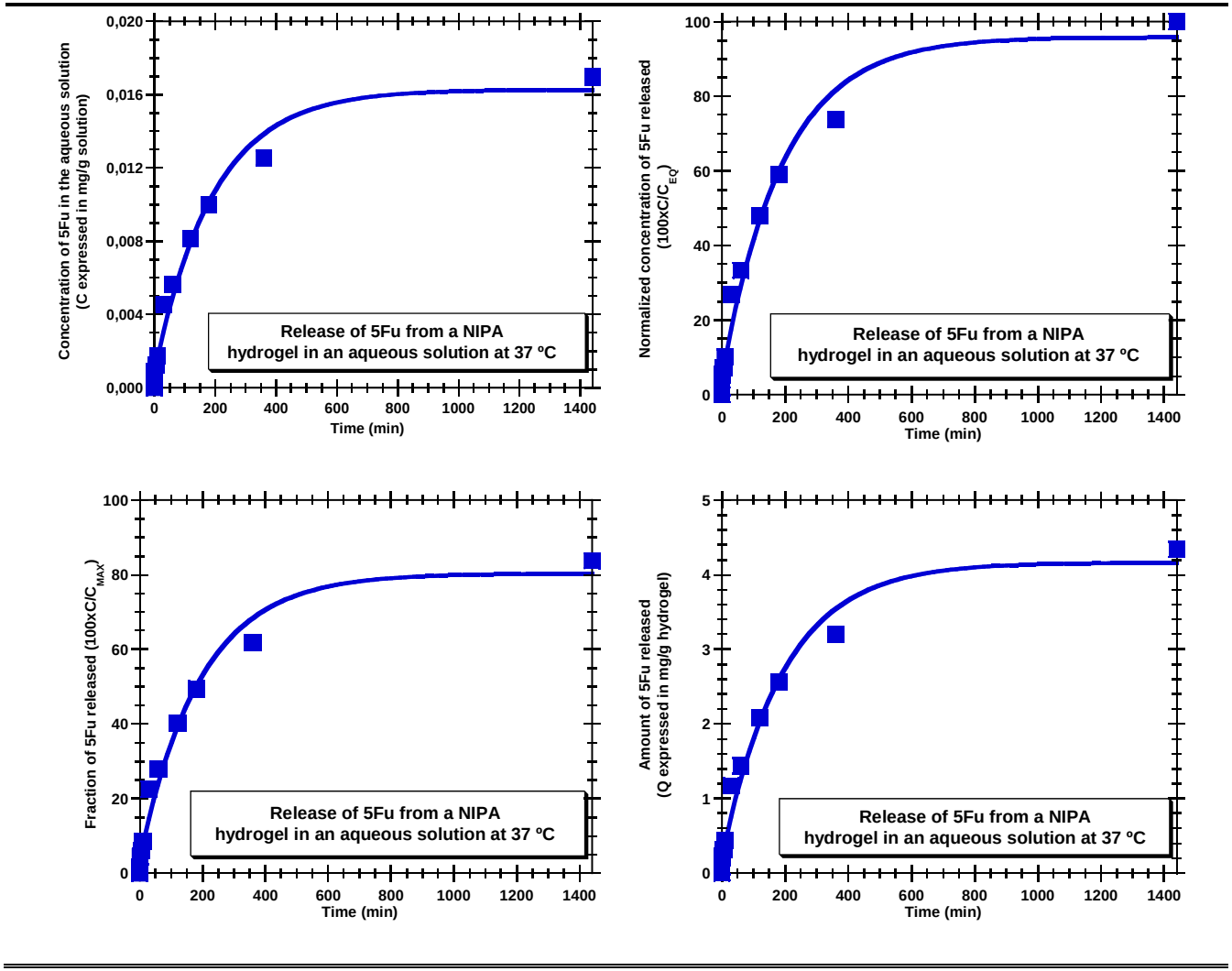

Annex 4. Comparison of the results, at different temperatures, of the release tests with a 5-FU incubated NIPA hydrogel (HG1).

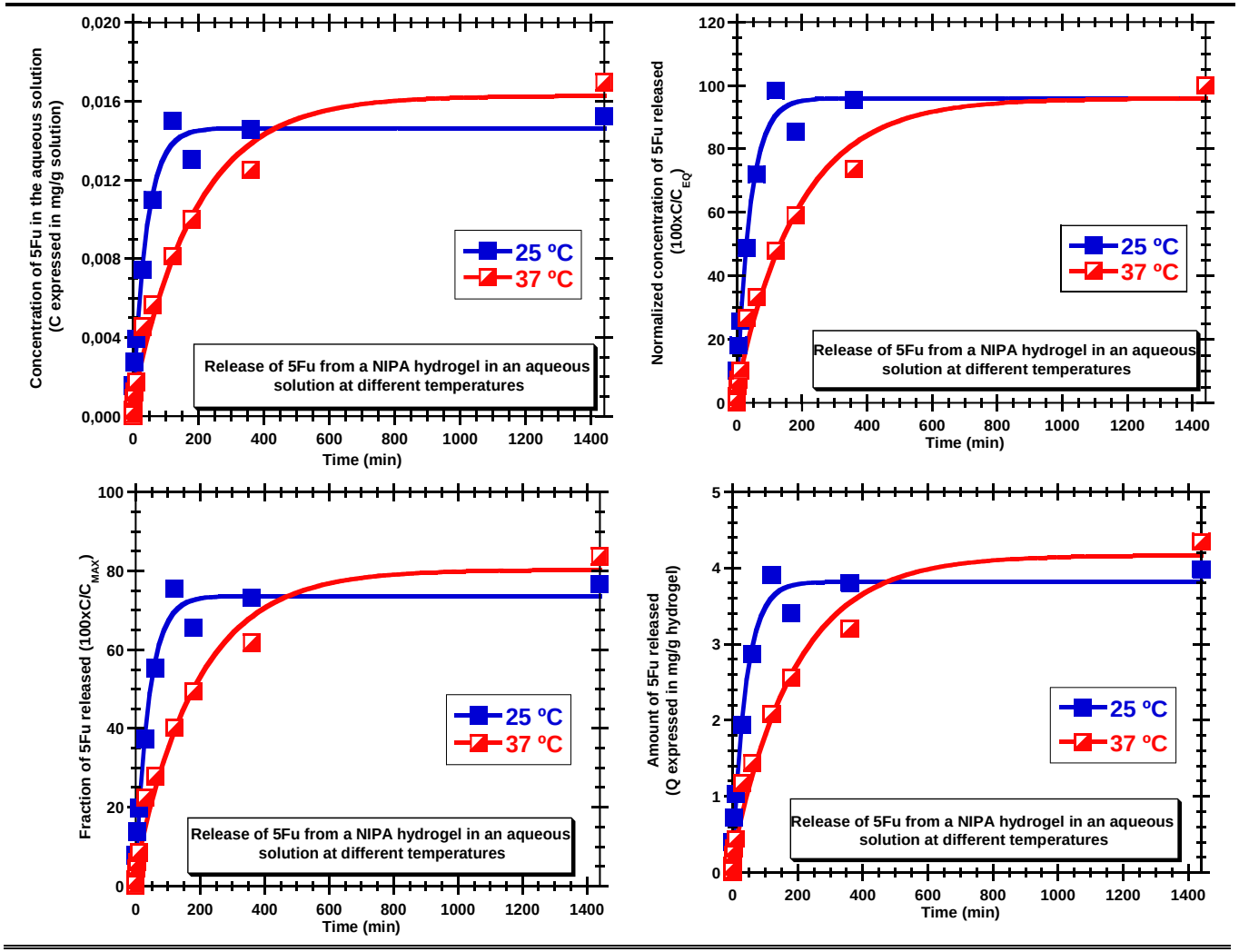

Annex 5. Results of the release test performed at 25 ºC with a caffeine incubated NIPA hydrogel (HG1).

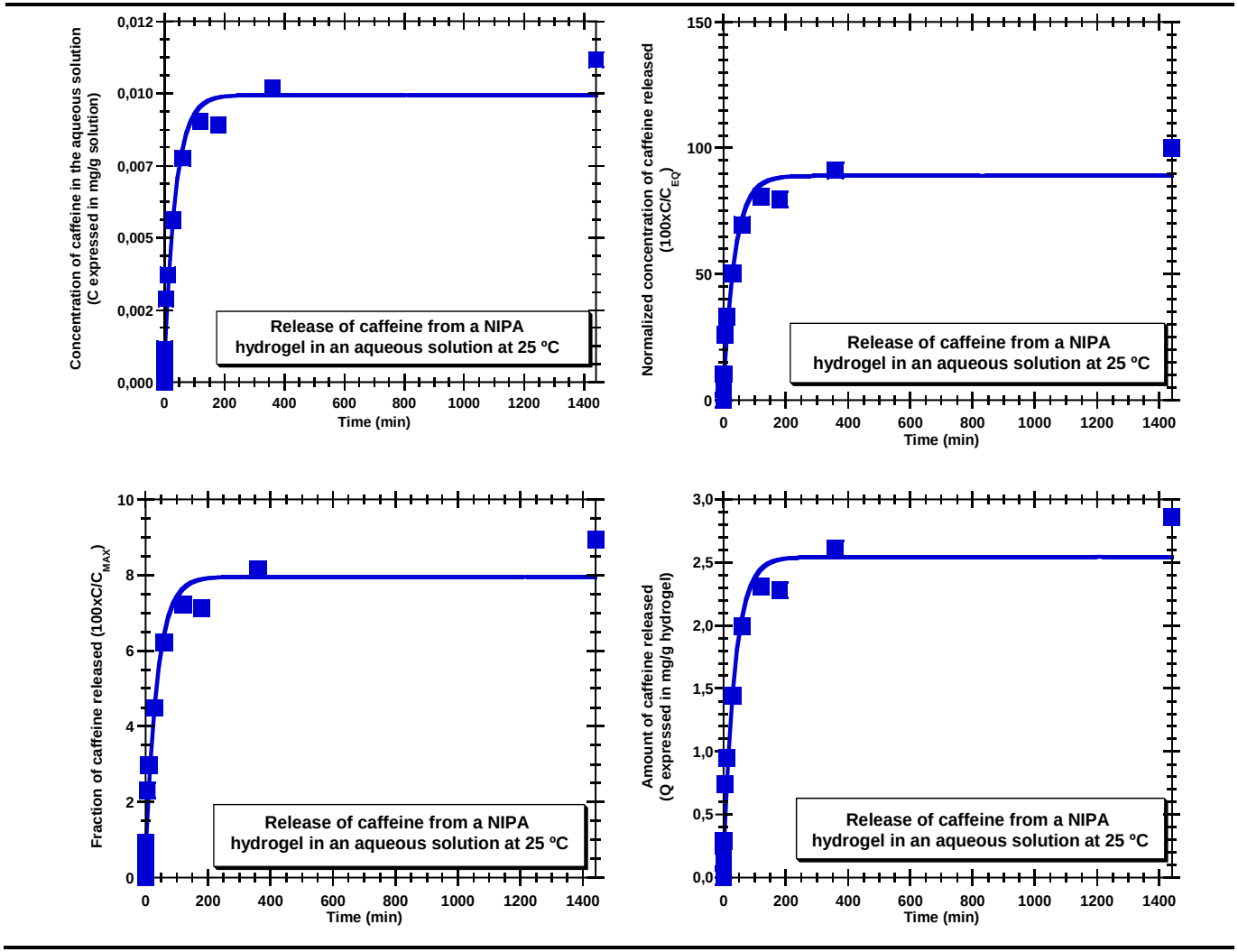

Annex 6. Results of the release test performed at 37 ºC with a caffeine incubated NIPA hydrogel (HG1).

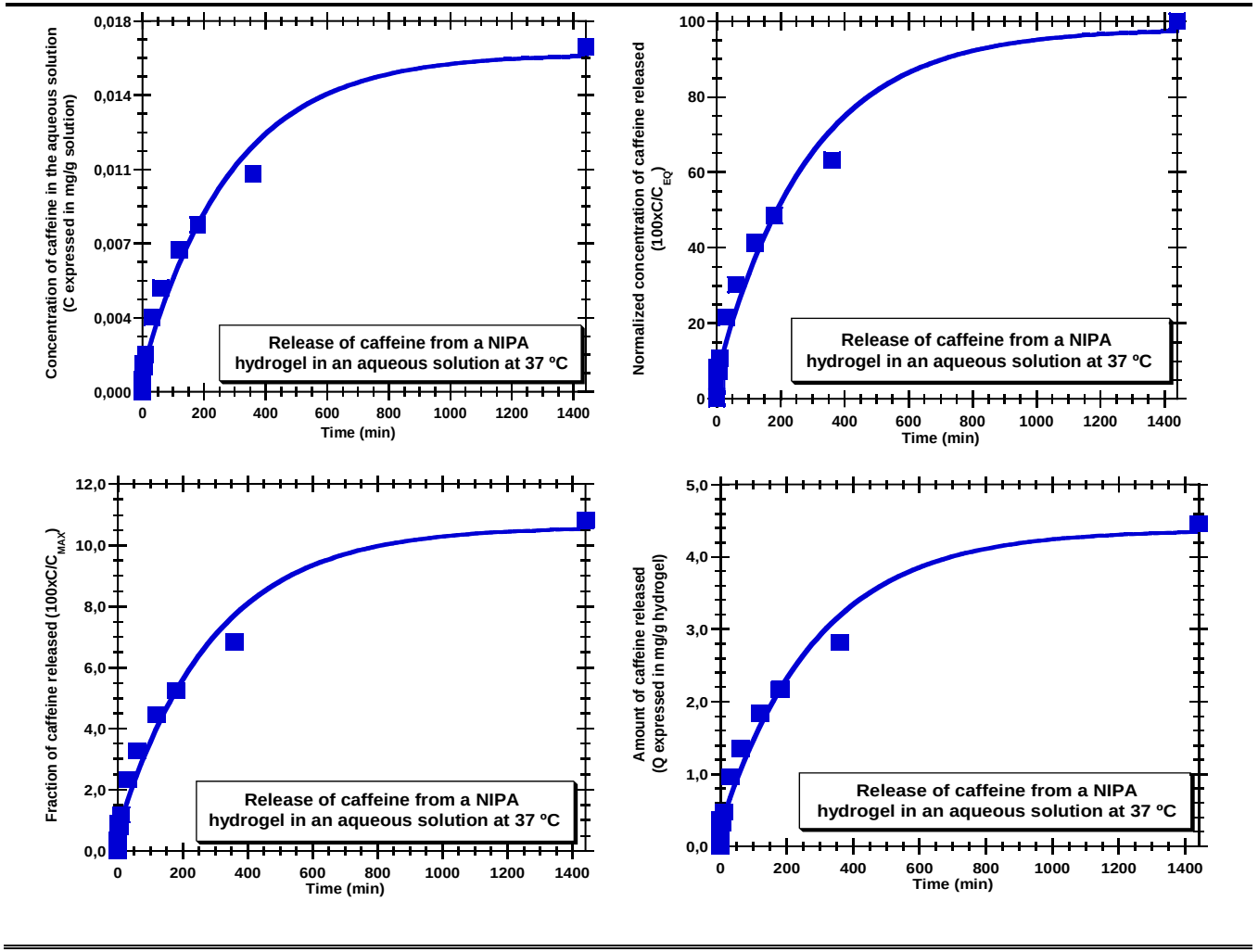

Annex 7. Comparison of the results, at different temperatures, of the release tests with a caffeine incubated NIPA hydrogel (HG1).

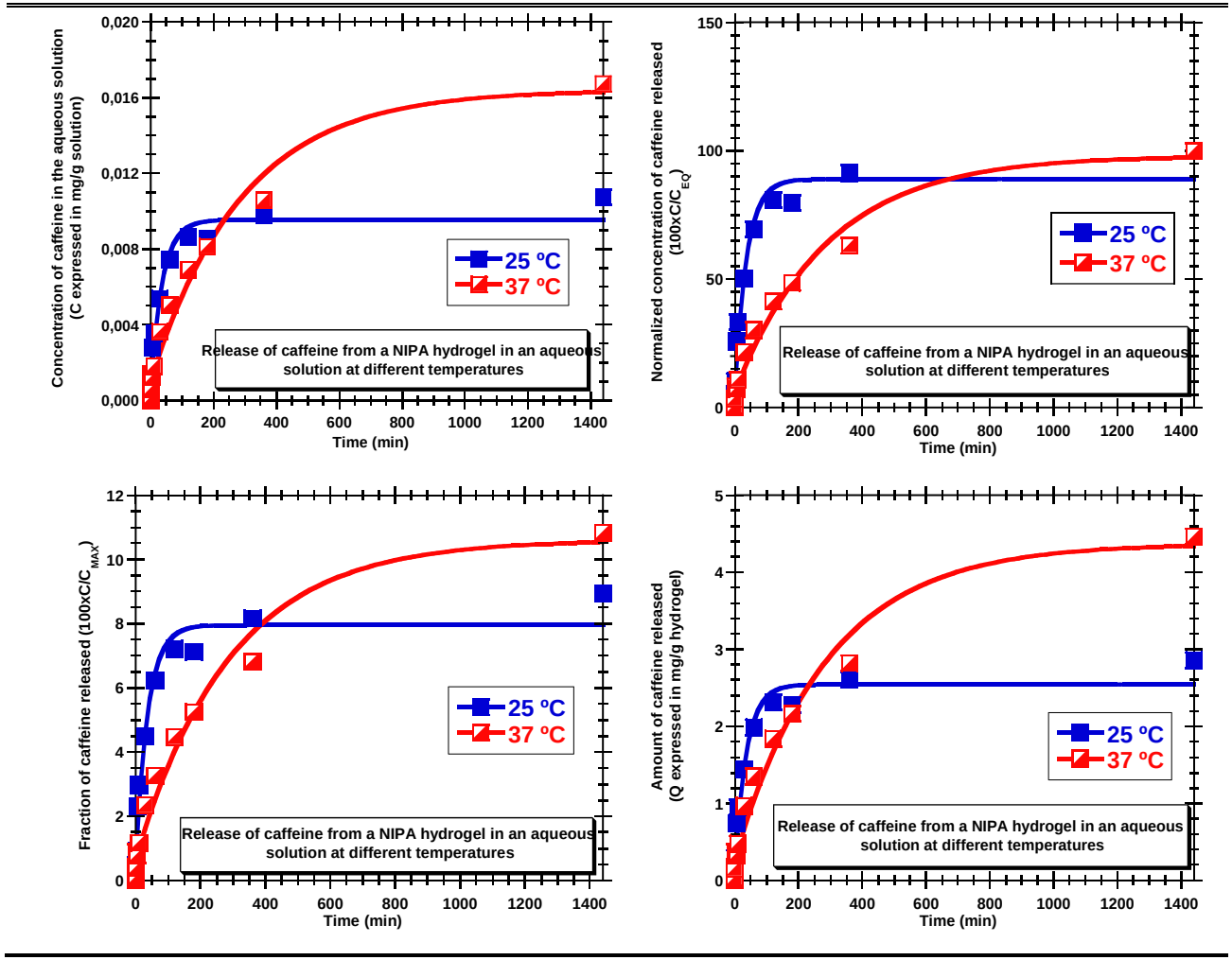

Annex 8. Results of the release test performed at 25 ºC with an INH incubated NIPA hydrogel (HG1).

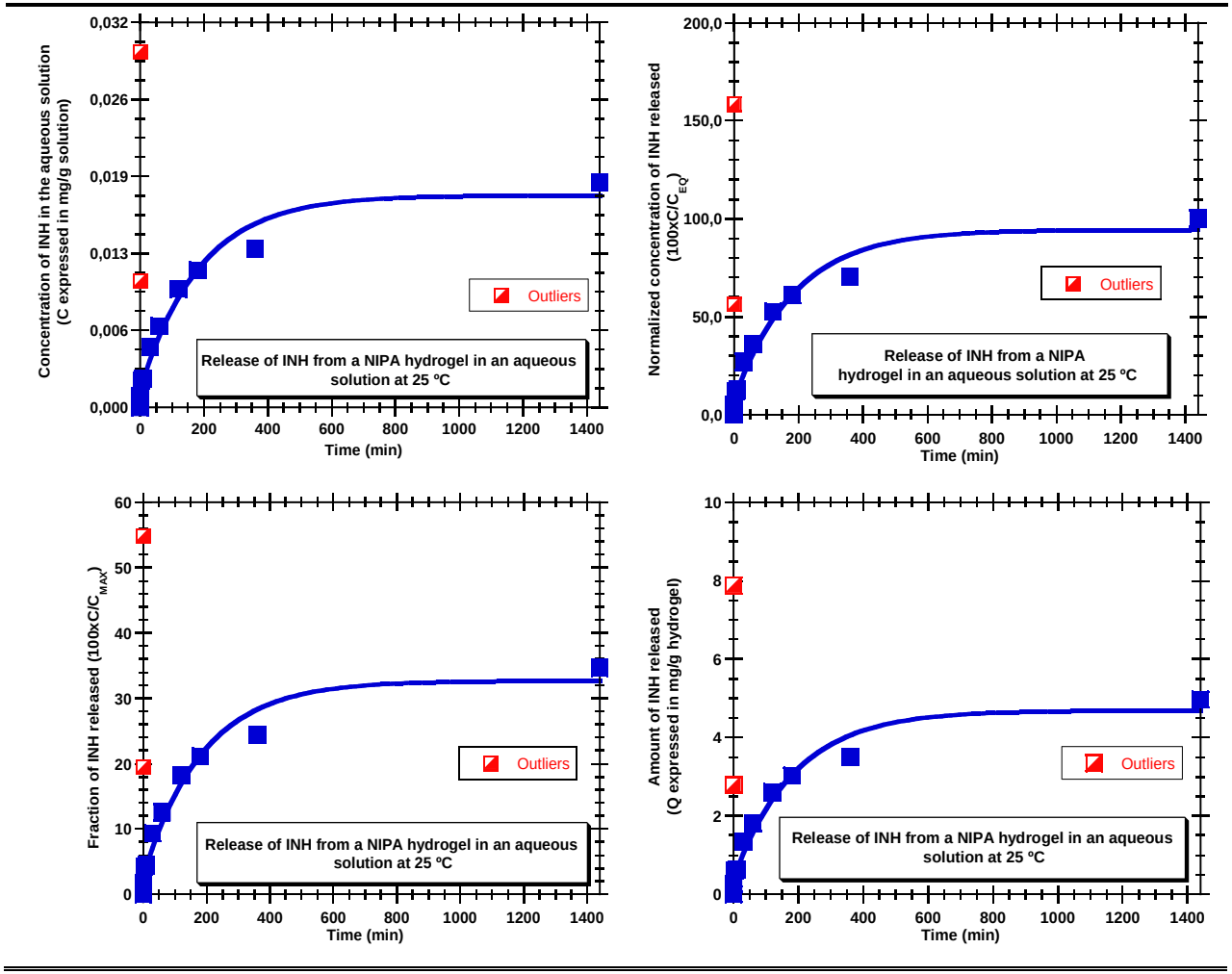

Annex 9. Results of the release test performed at 37 ºC with an INH incubated NIPA hydrogel (HG1).

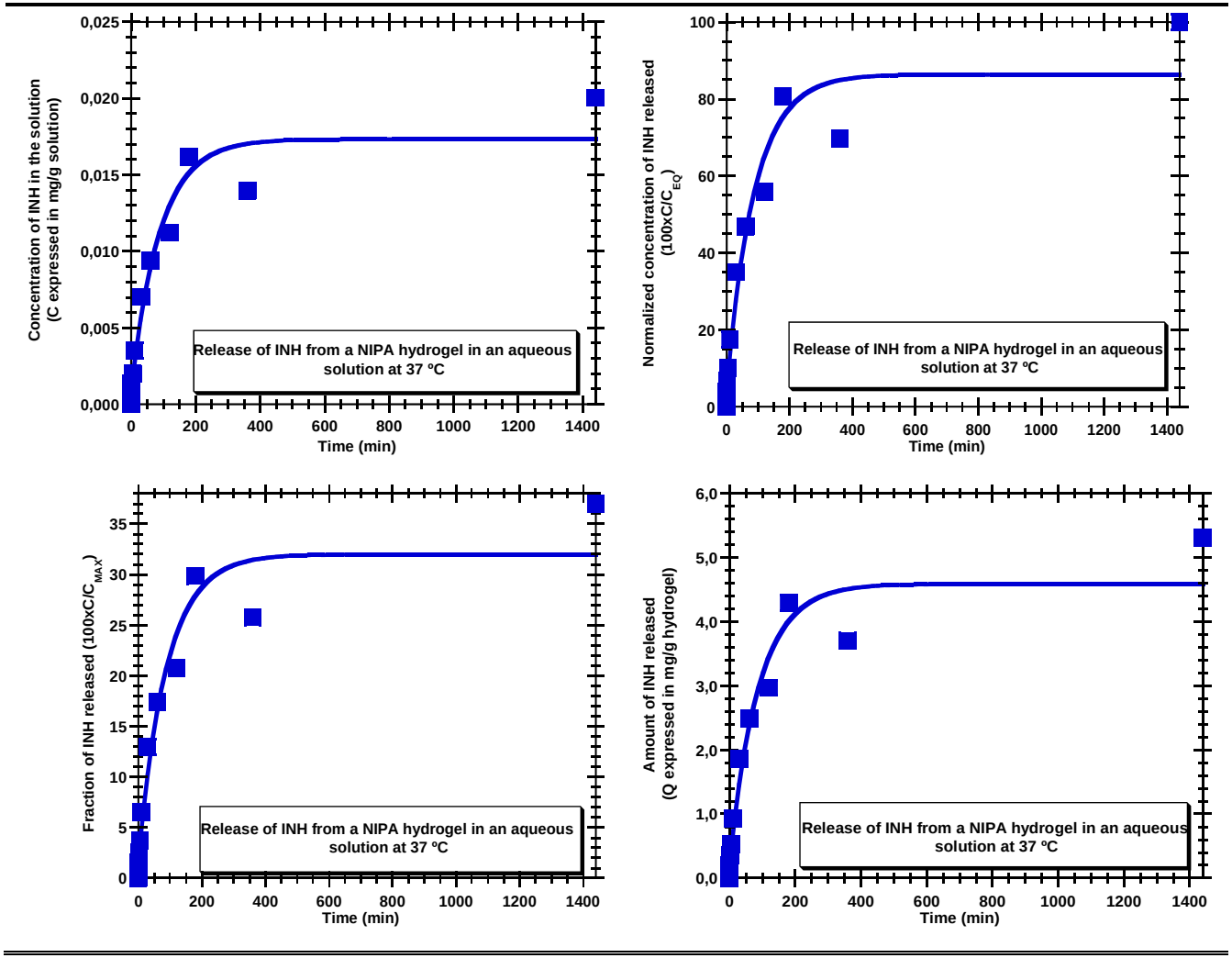

Annex 10. Comparison of the results, at different temperatures, of the release tests with an INH incubated NIPA hydrogel (HG1).

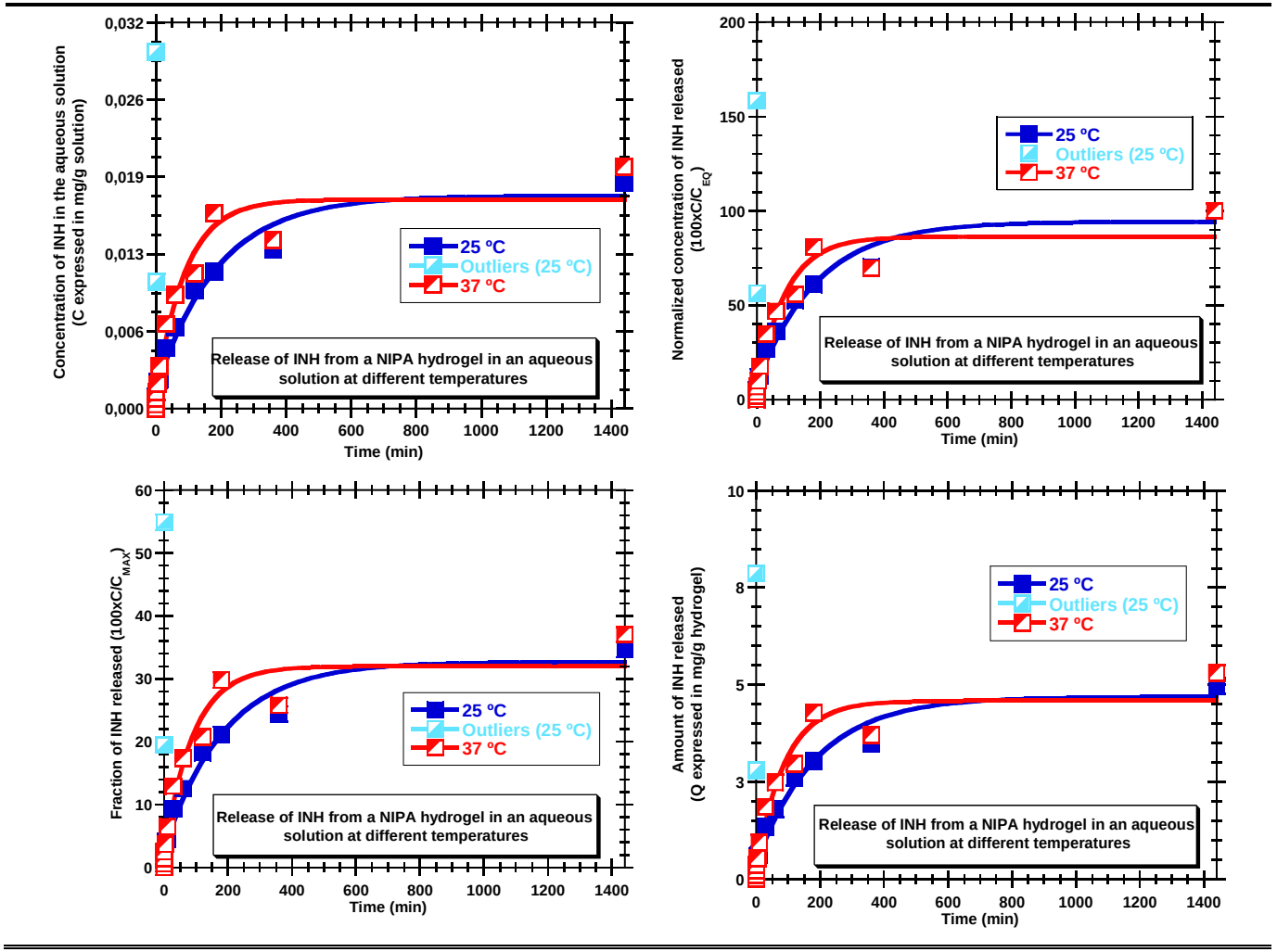

Annex 11. Results of the release test performed at 25 ºC with an IBU incubated NIPA hydrogel (HG1).

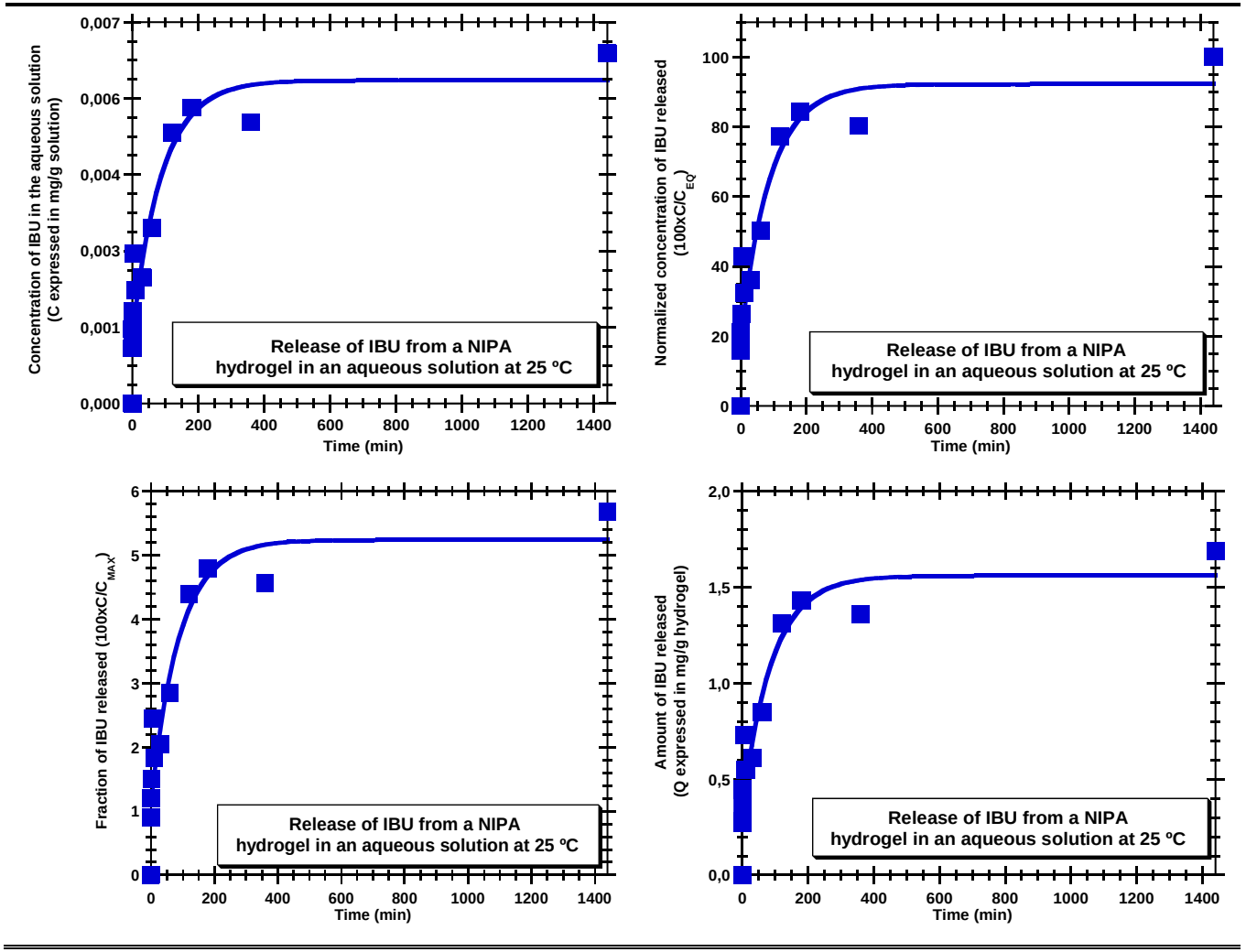

Annex 12. Results of the release test performed at 37 ºC with an IBU incubated NIPA hydrogel (HG1).

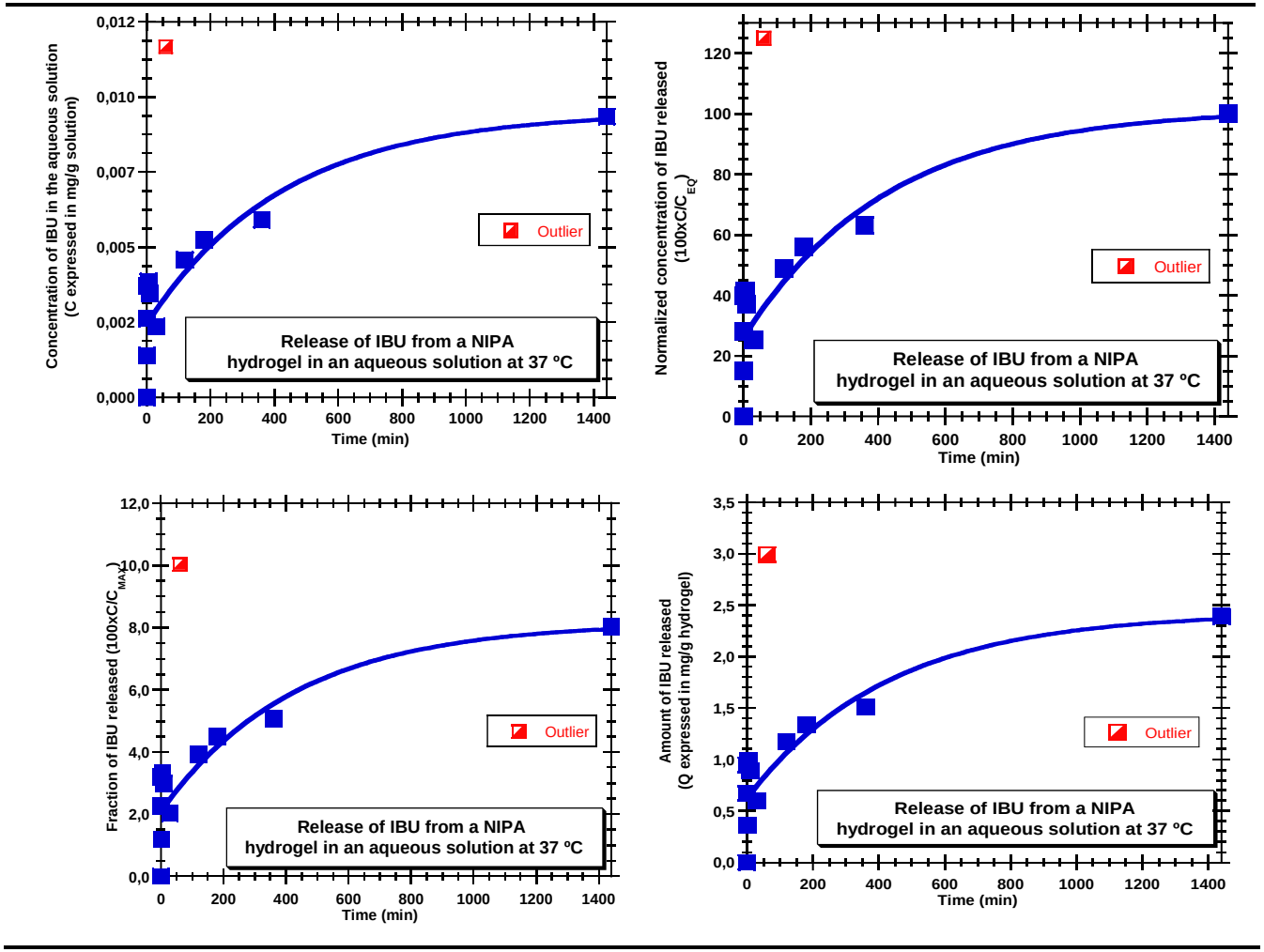

Annex 13. Comparison of the results, at different temperatures, of the release tests with an IBU incubated NIPA hydrogel (HG1).

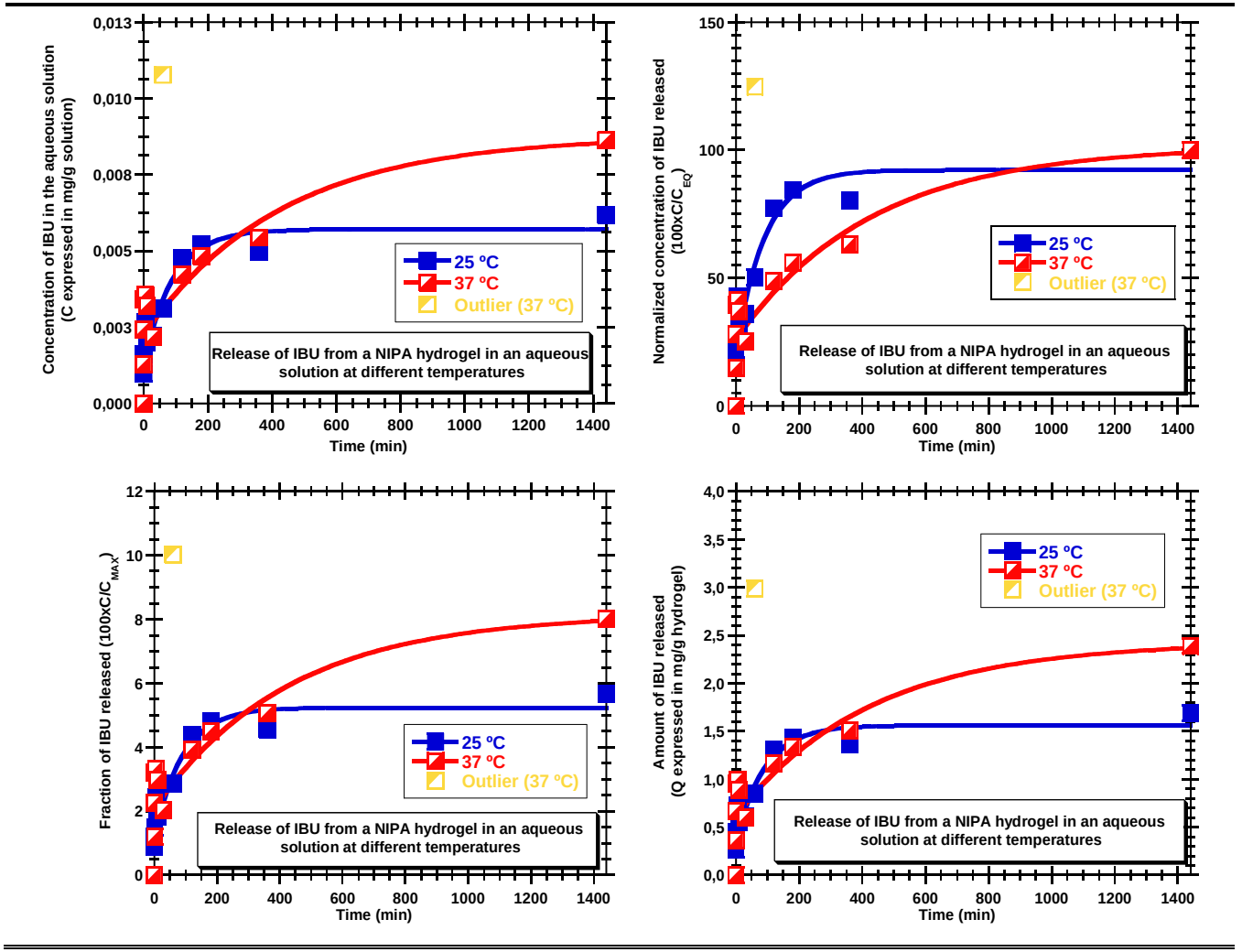

Annex 14. Results of the release test performed at pH 2 with a 5-FU incubated RAFT hydrogel (HG2).

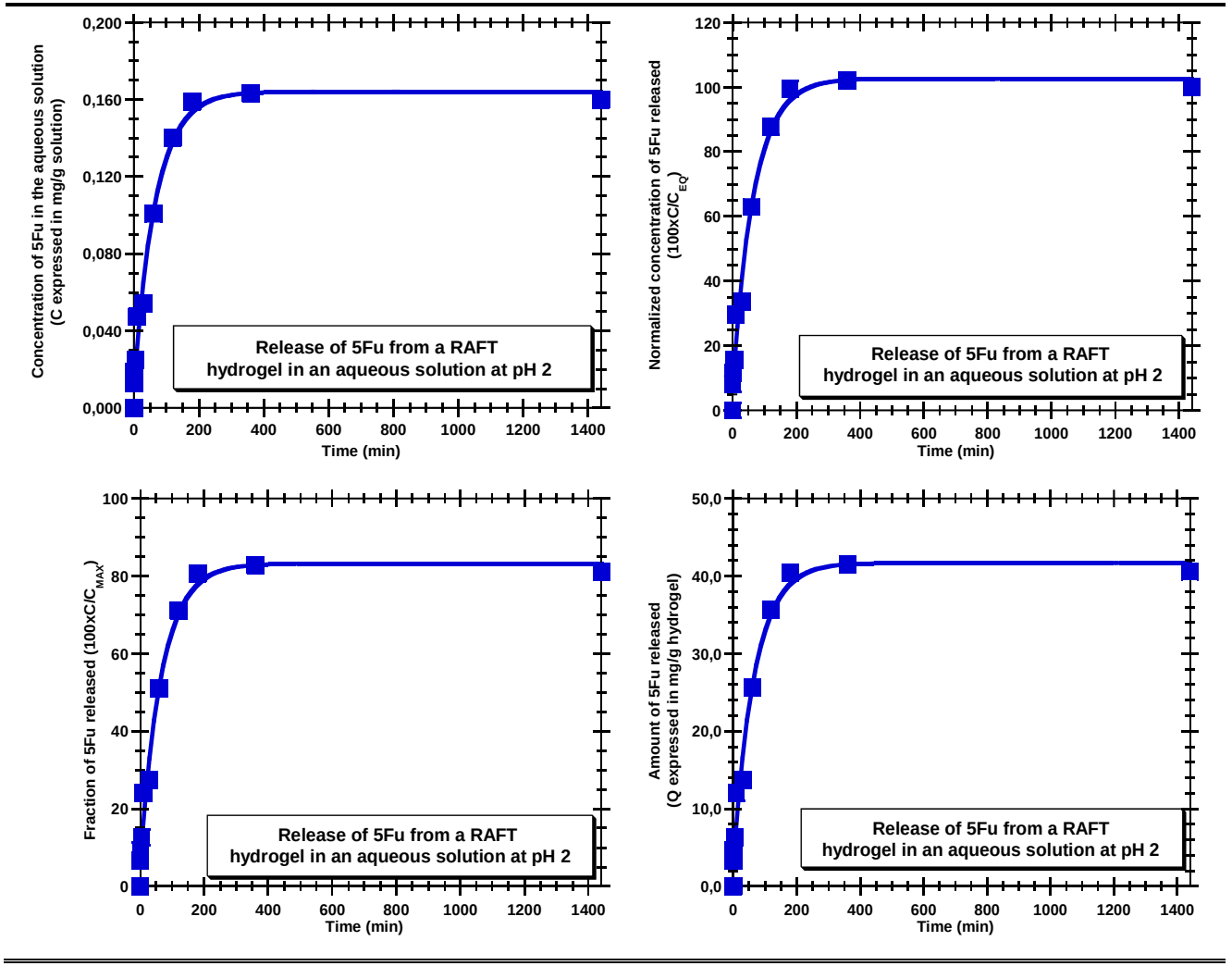

Annex 15. Results of the release test performed at pH 10 with a 5-FU incubated RAFT hydrogel (HG2).

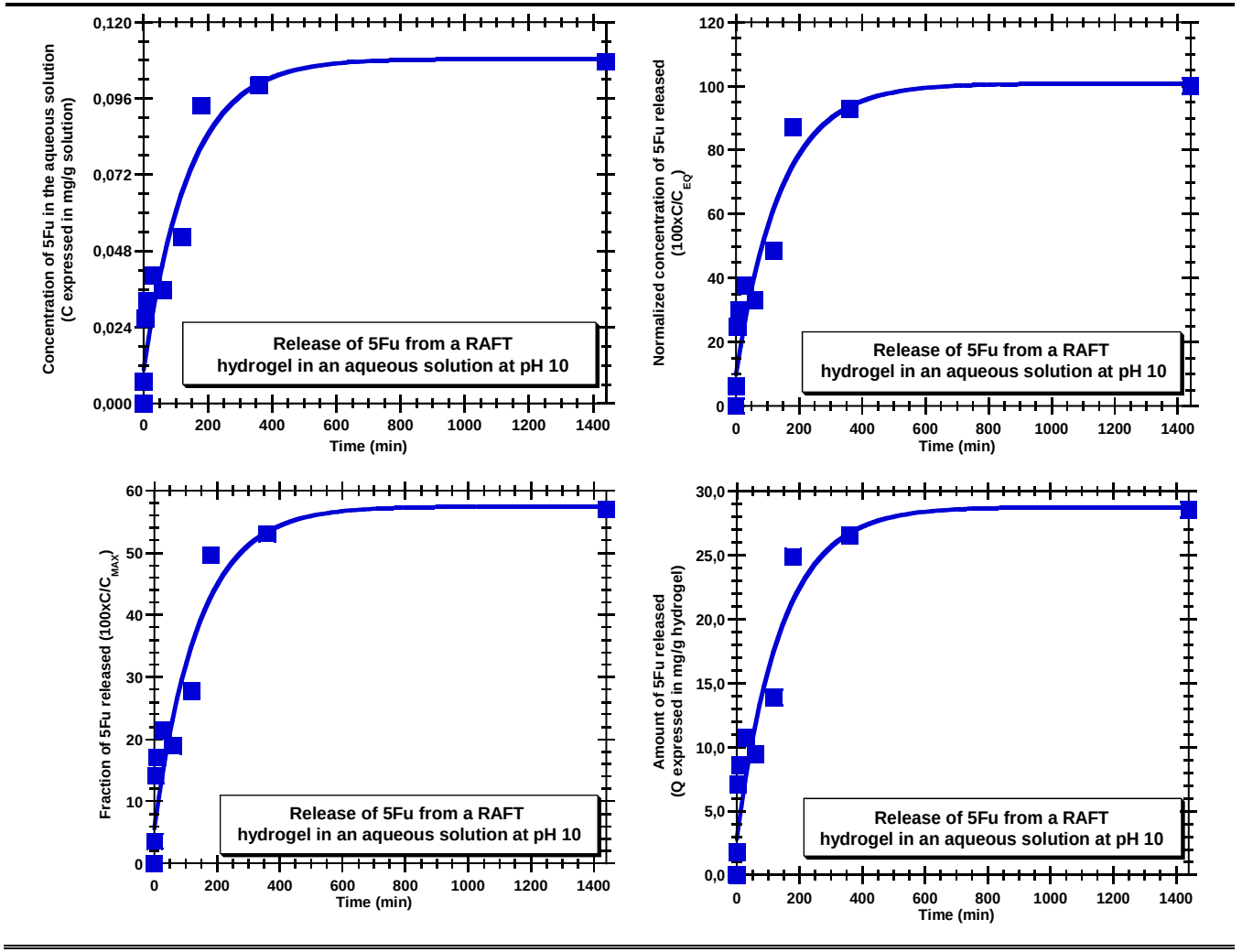

Annex 16. Comparison of the results, at different pH, of the release tests with a 5-FU incubated RAFT hydrogel (HG2).

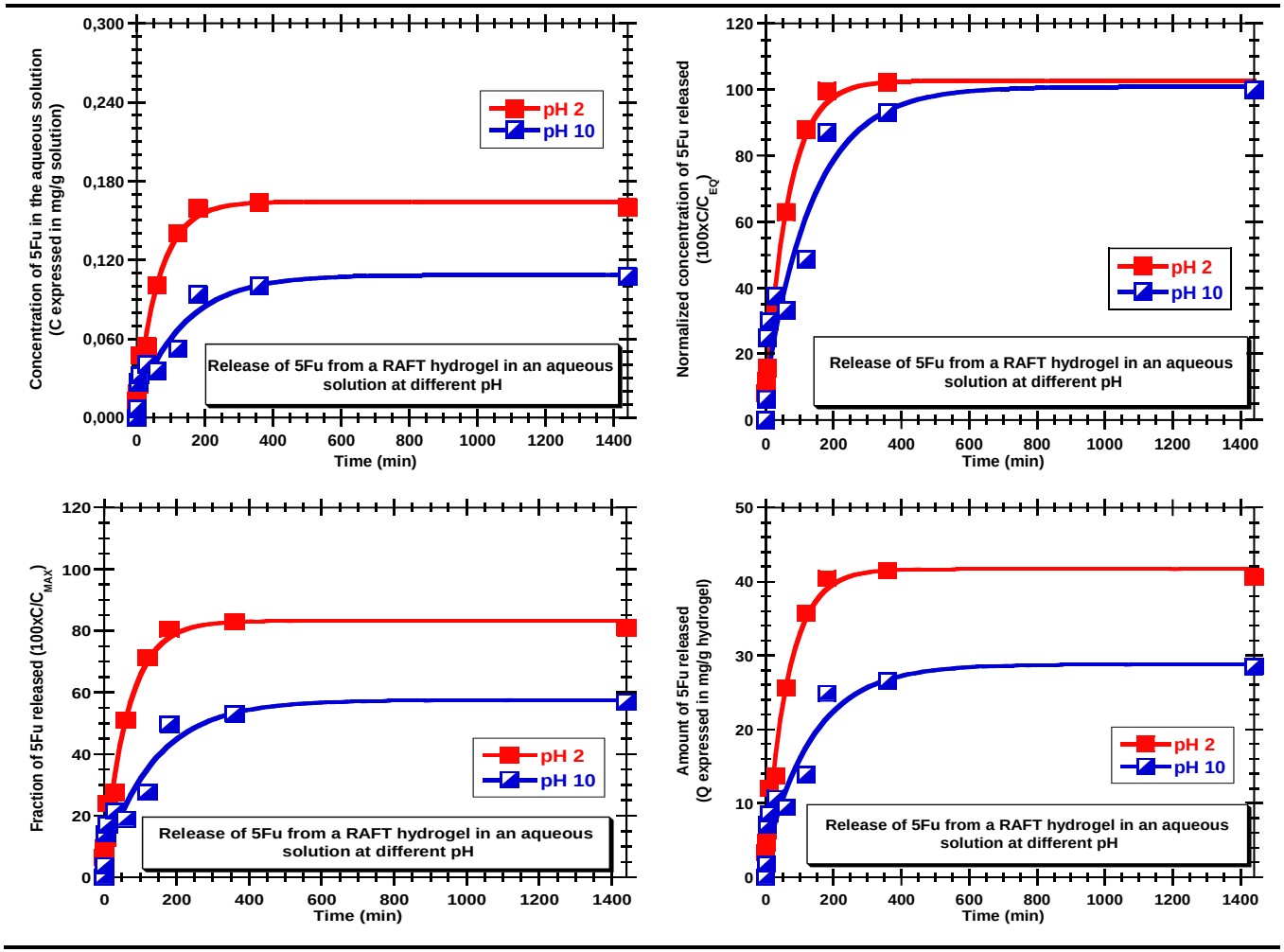

Annex 17. Results of the release test performed at pH 2 with a caffeine incubated RAFT hydrogel (HG2).

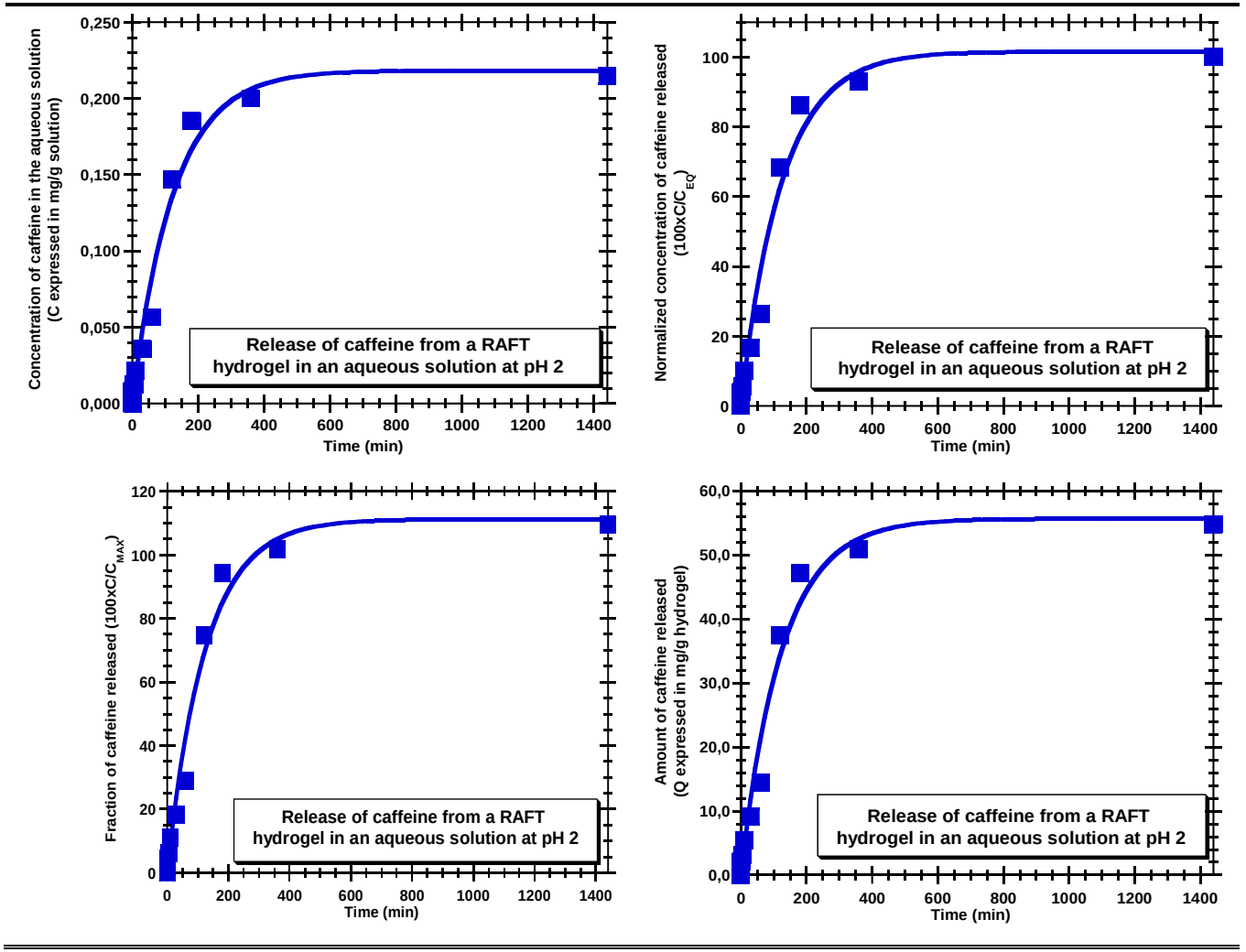

Annex 18. Results of the release test performed at pH 10 with a caffeine incubated RAFT hydrogel (HG2).

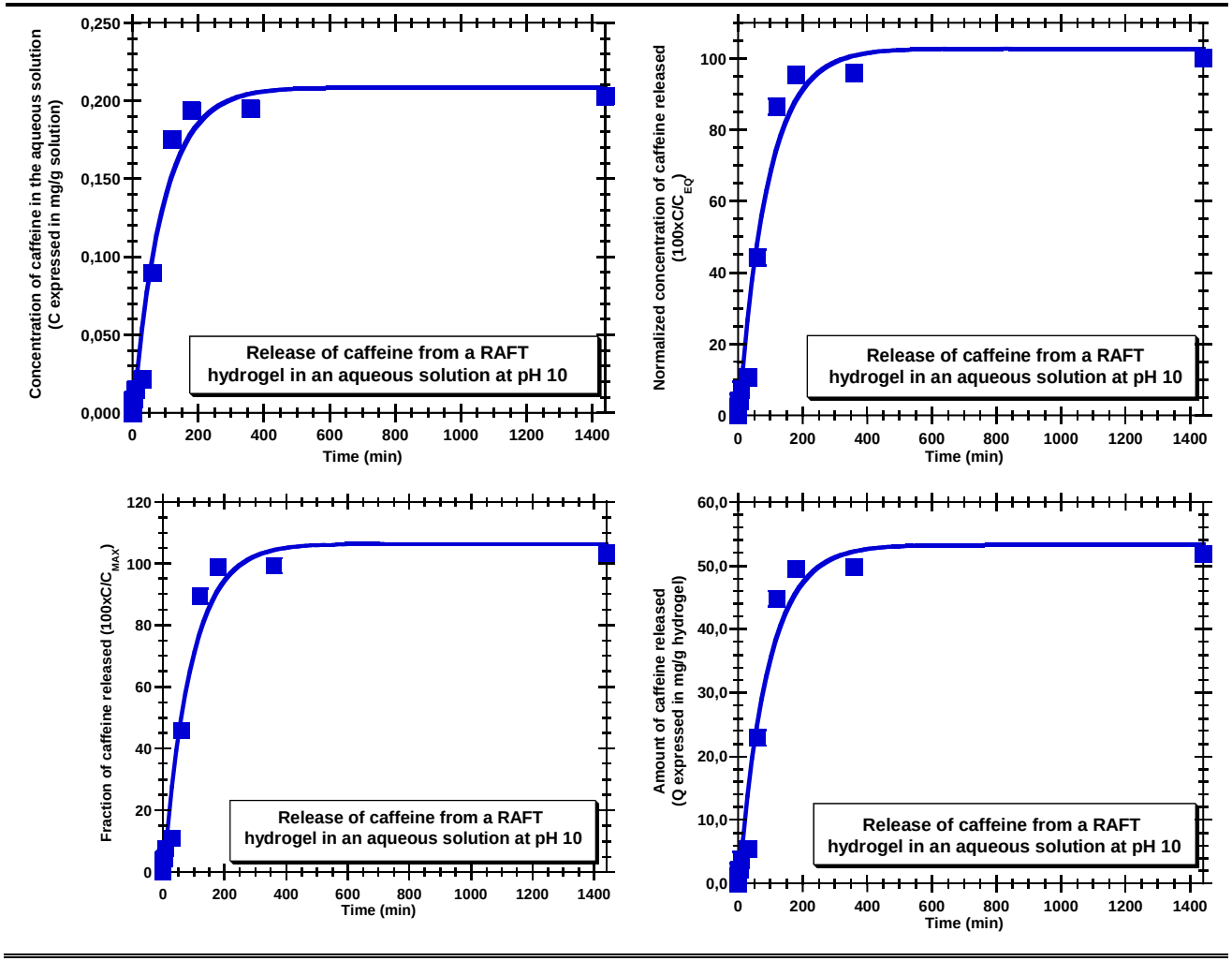

Annex 19. Comparison of the results, at different pH, of the release tests with a caffeine incubated RAFT hydrogel (HG2).

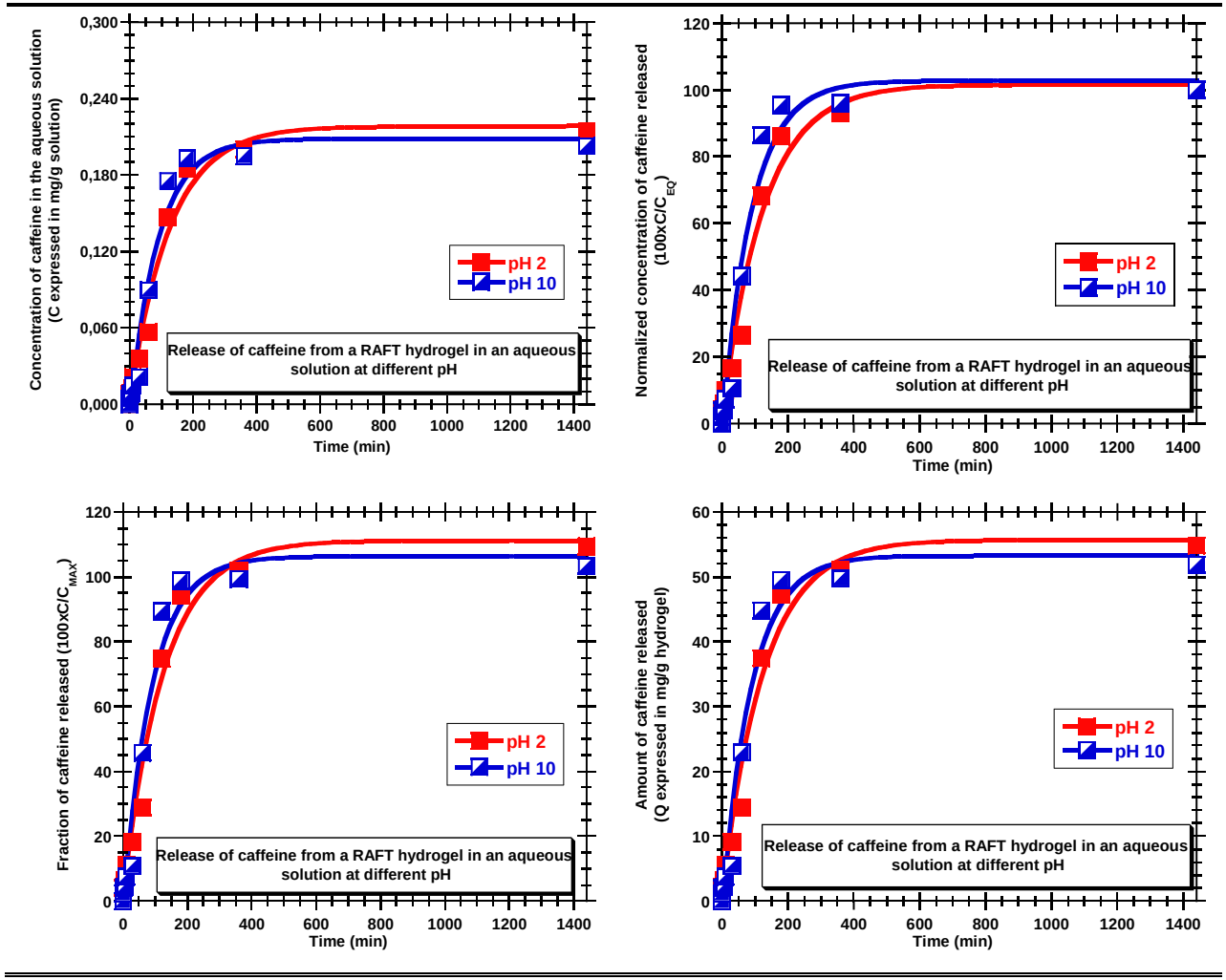

Annex 20. Results of the release test performed at pH 2 with an INH incubated RAFT hydrogel (HG2).

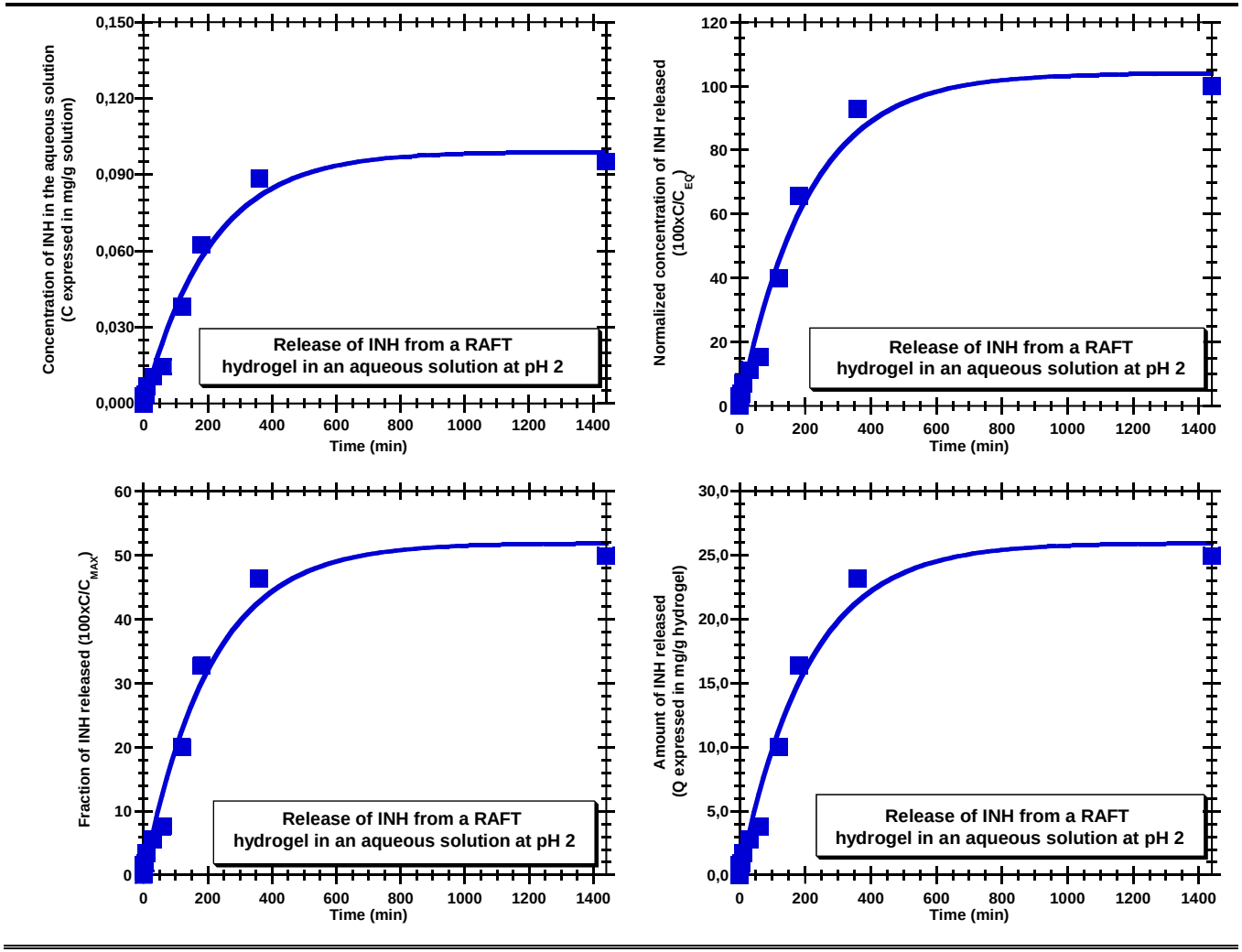

Annex 21. Results of the release test performed at pH 10 with an INH incubated RAFT hydrogel (HG2).

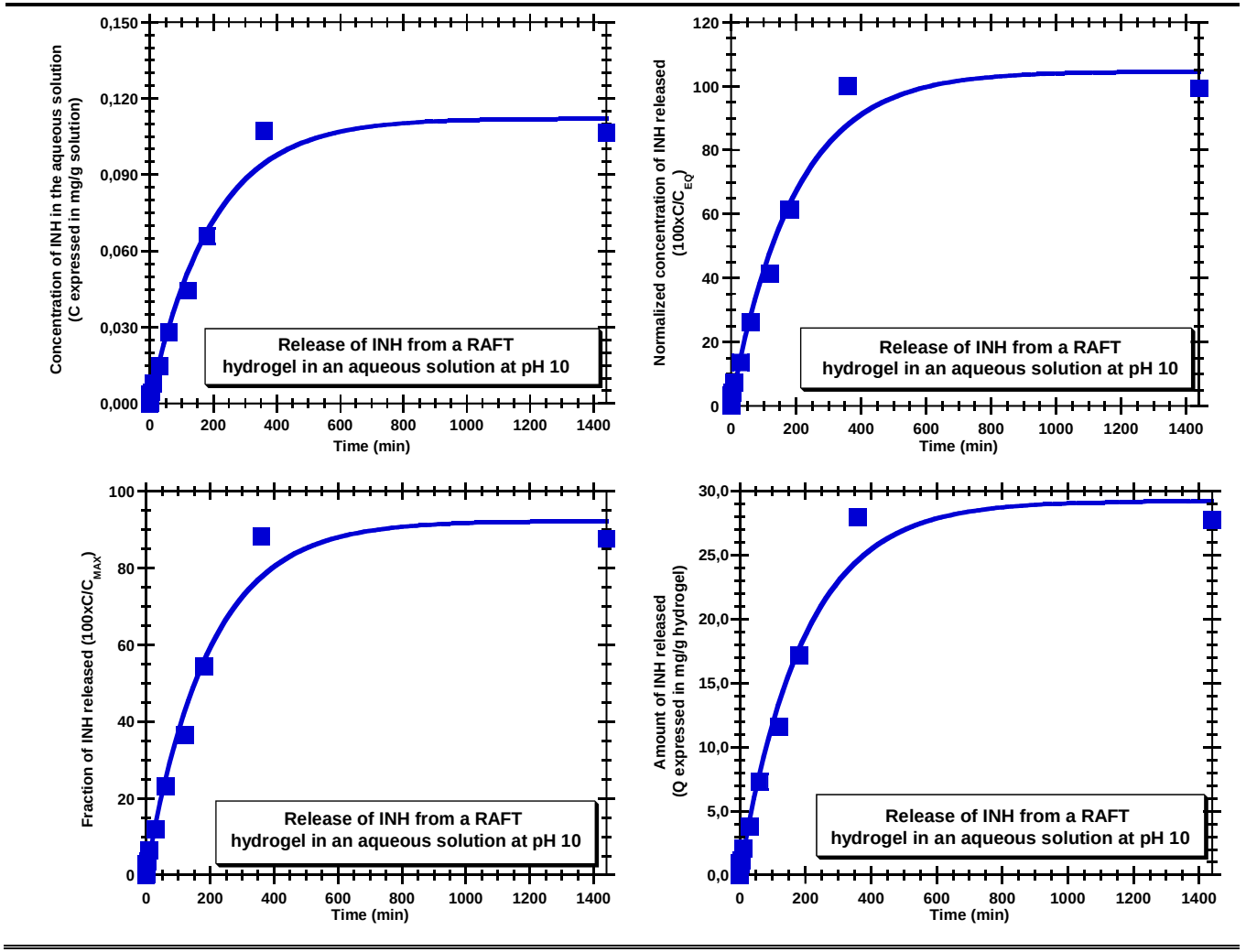

Annex 22. Comparison of the results, at different pH, of the release tests with an INH incubated RAFT hydrogel (HG2).

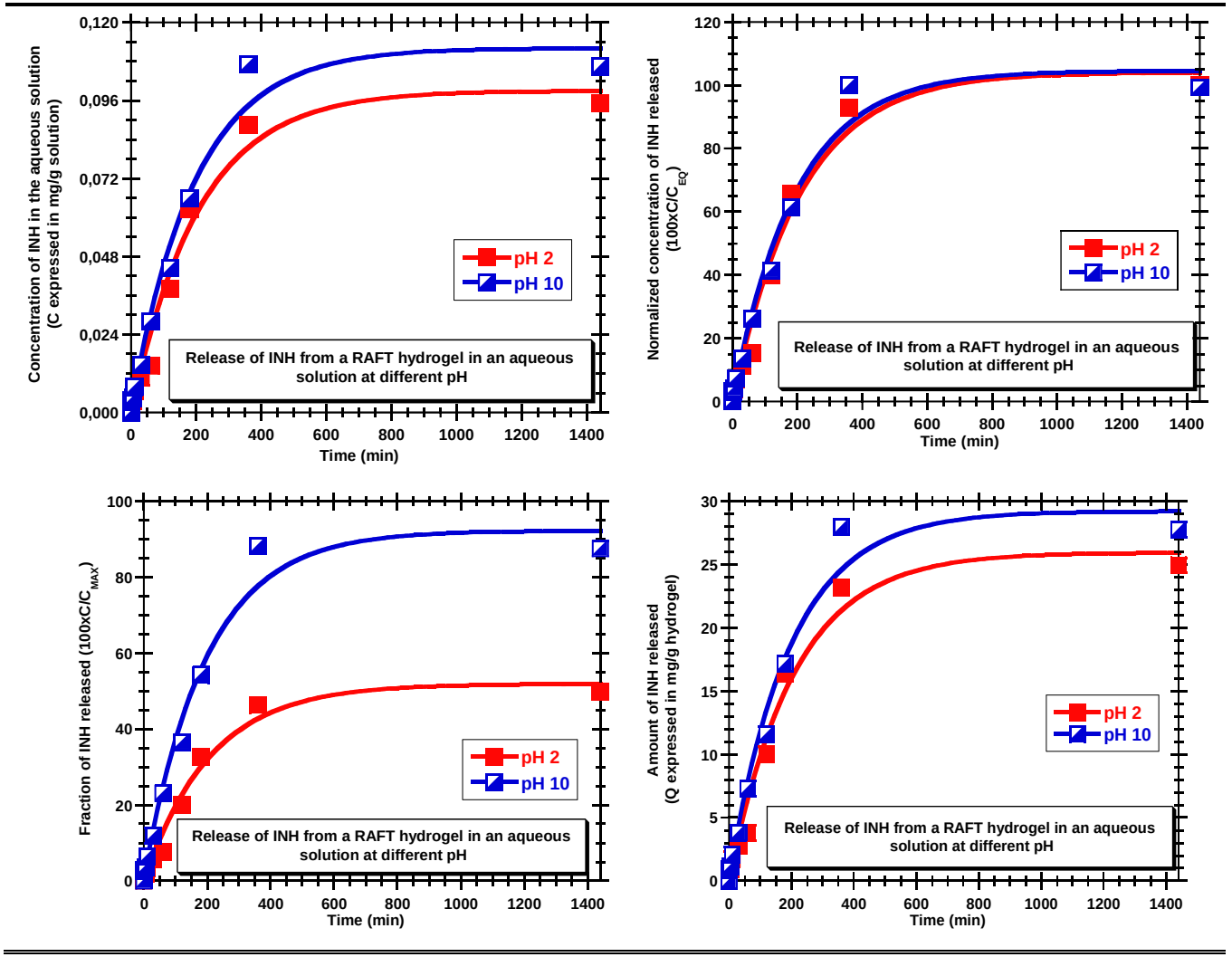

Annex 23. Results of the release test performed at pH 2 with an IBU incubated RAFT hydrogel (HG2).

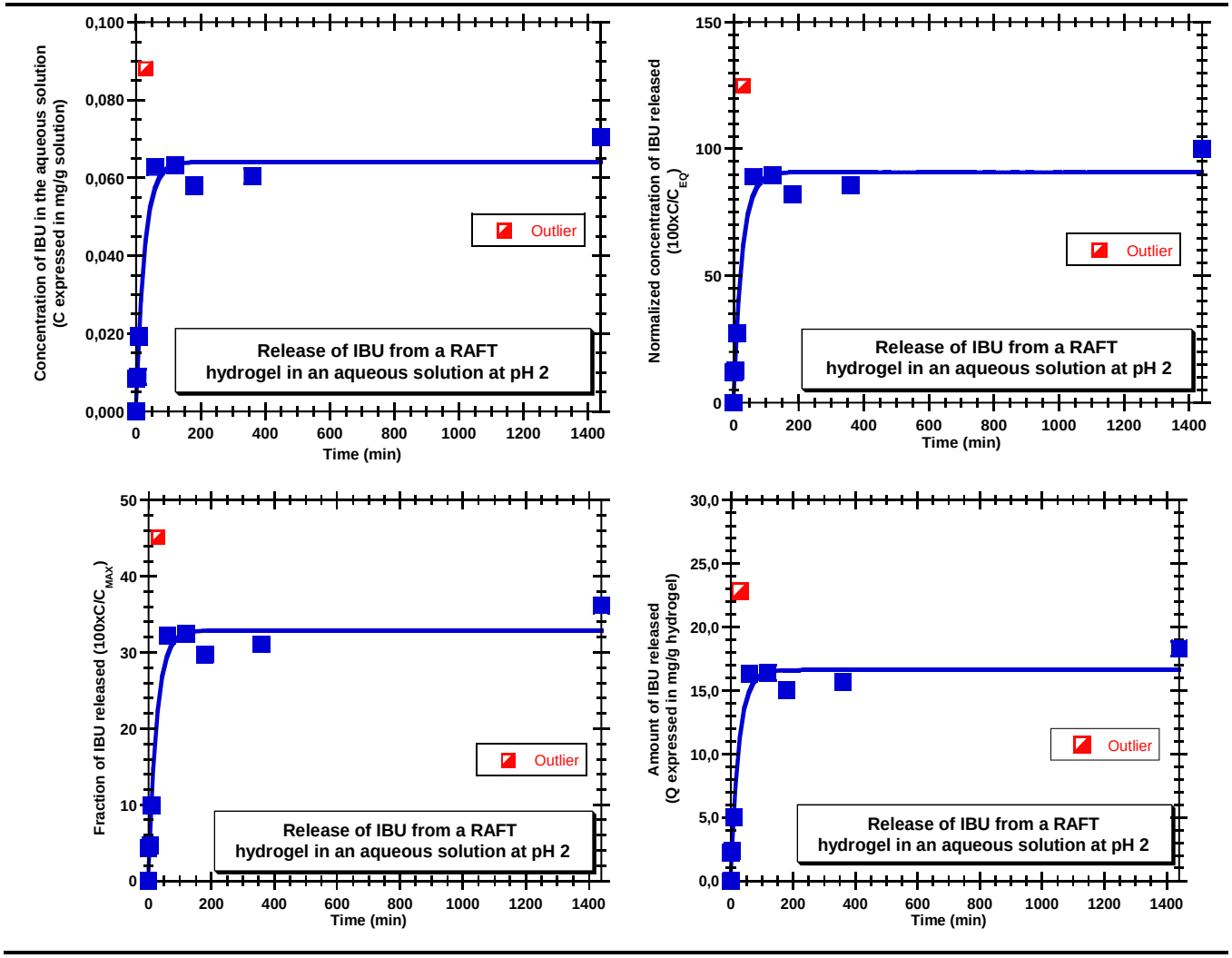

Annex 24. Results of the release test performed at pH 10 with an IBU incubated RAFT hydrogel (HG2).

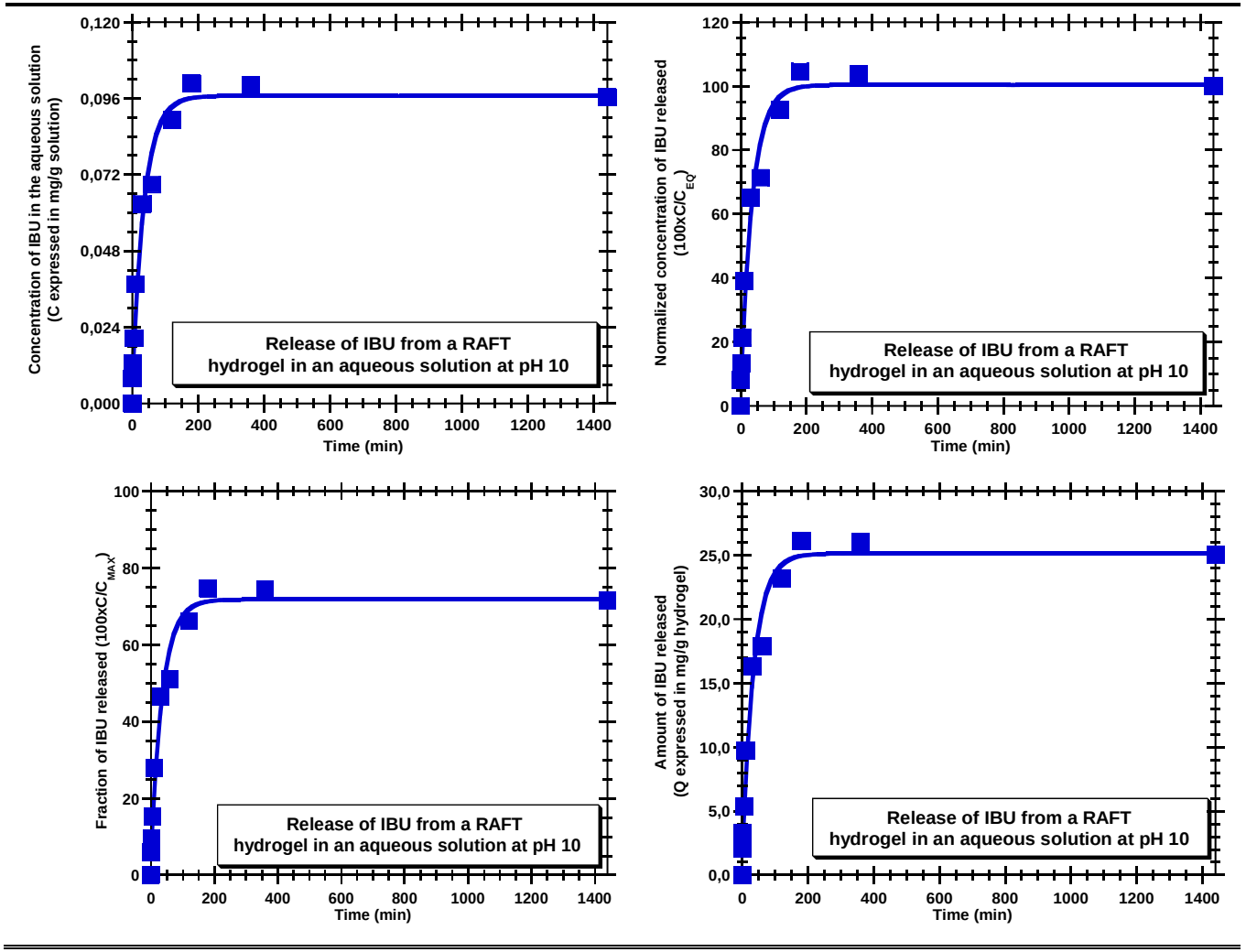

Annex 25. Comparison of the results, at different pH, of the release tests with an IBU incubated RAFT hydrogel (HG2).

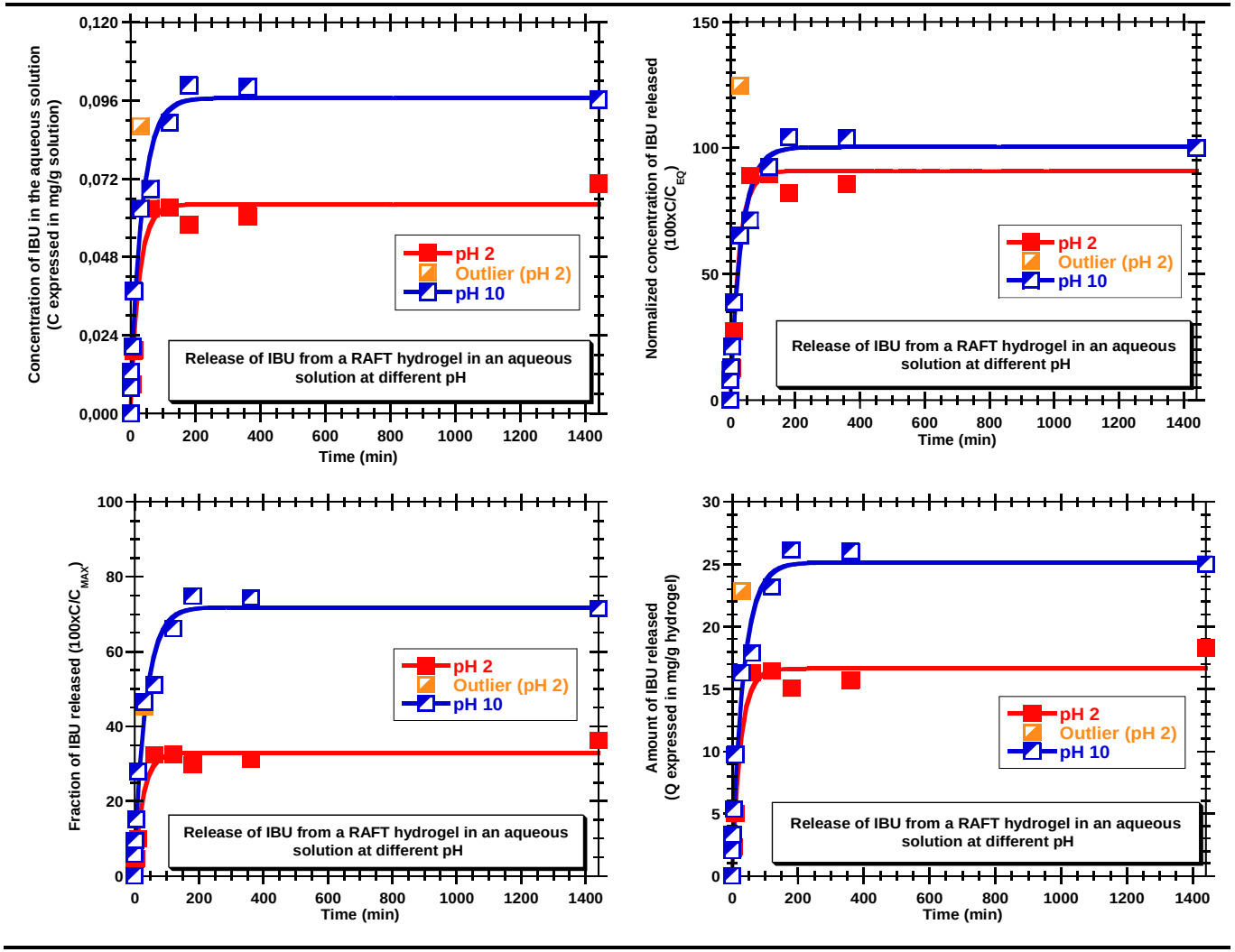

Annex 26. Results of the release test performed at pH 1 with a 5-FU incubated AA hydrogel (HG3).

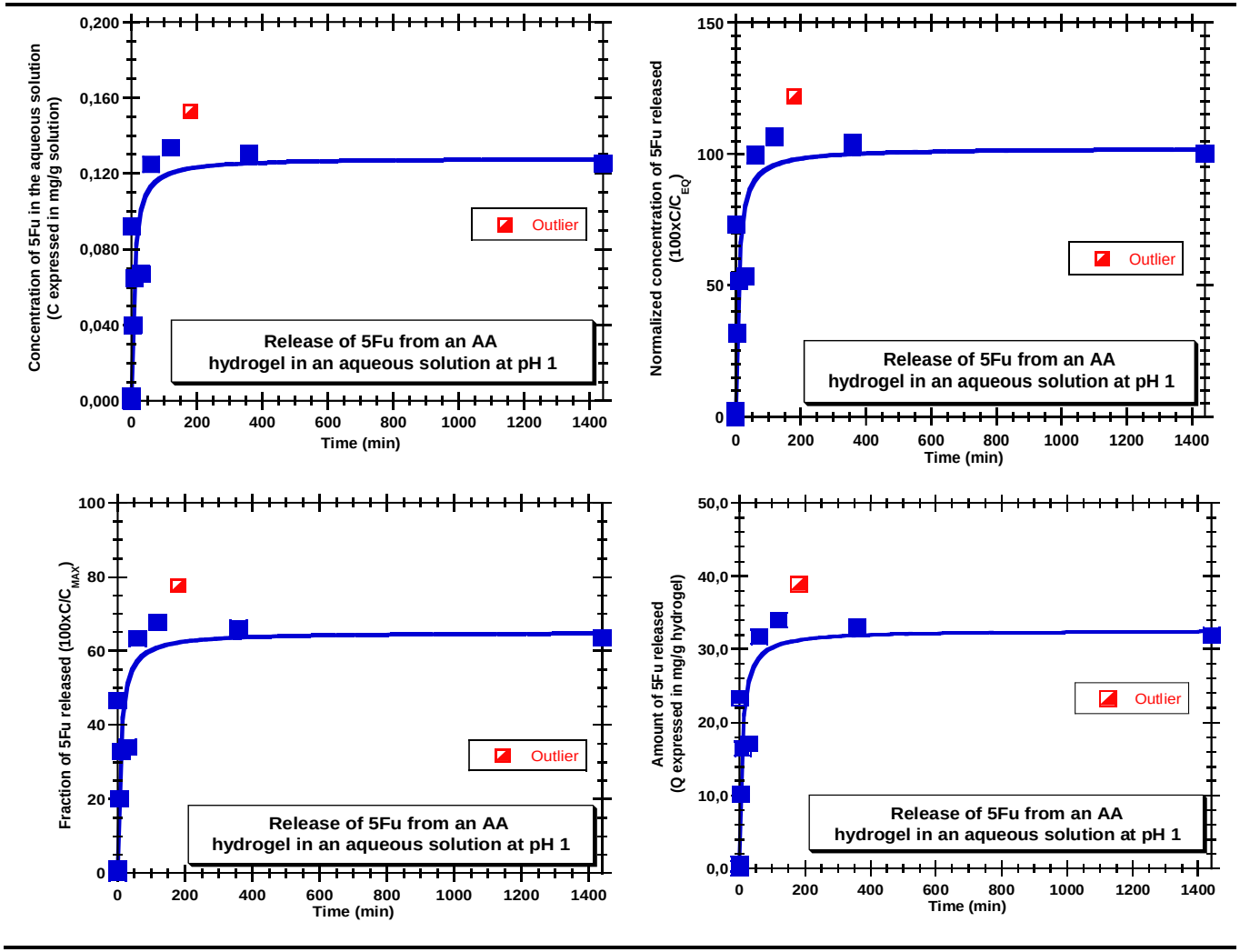

Annex 27. Results of the release test performed at pH 8 with a 5-FU incubated AA hydrogel (HG3).

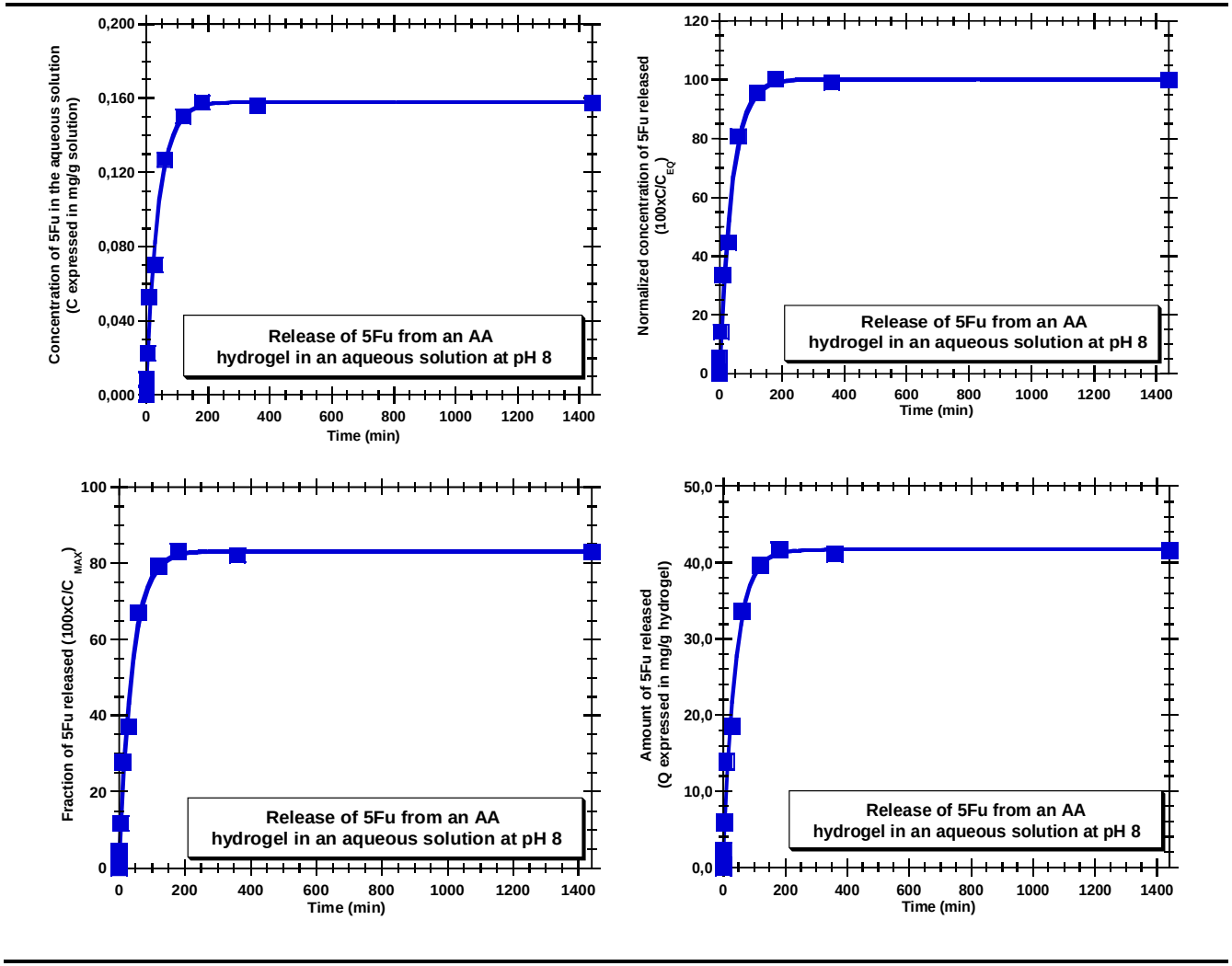

Annex 28. Comparison of the results, at different pH, of the release tests with a 5-FU incubated AA hydrogel (HG3).

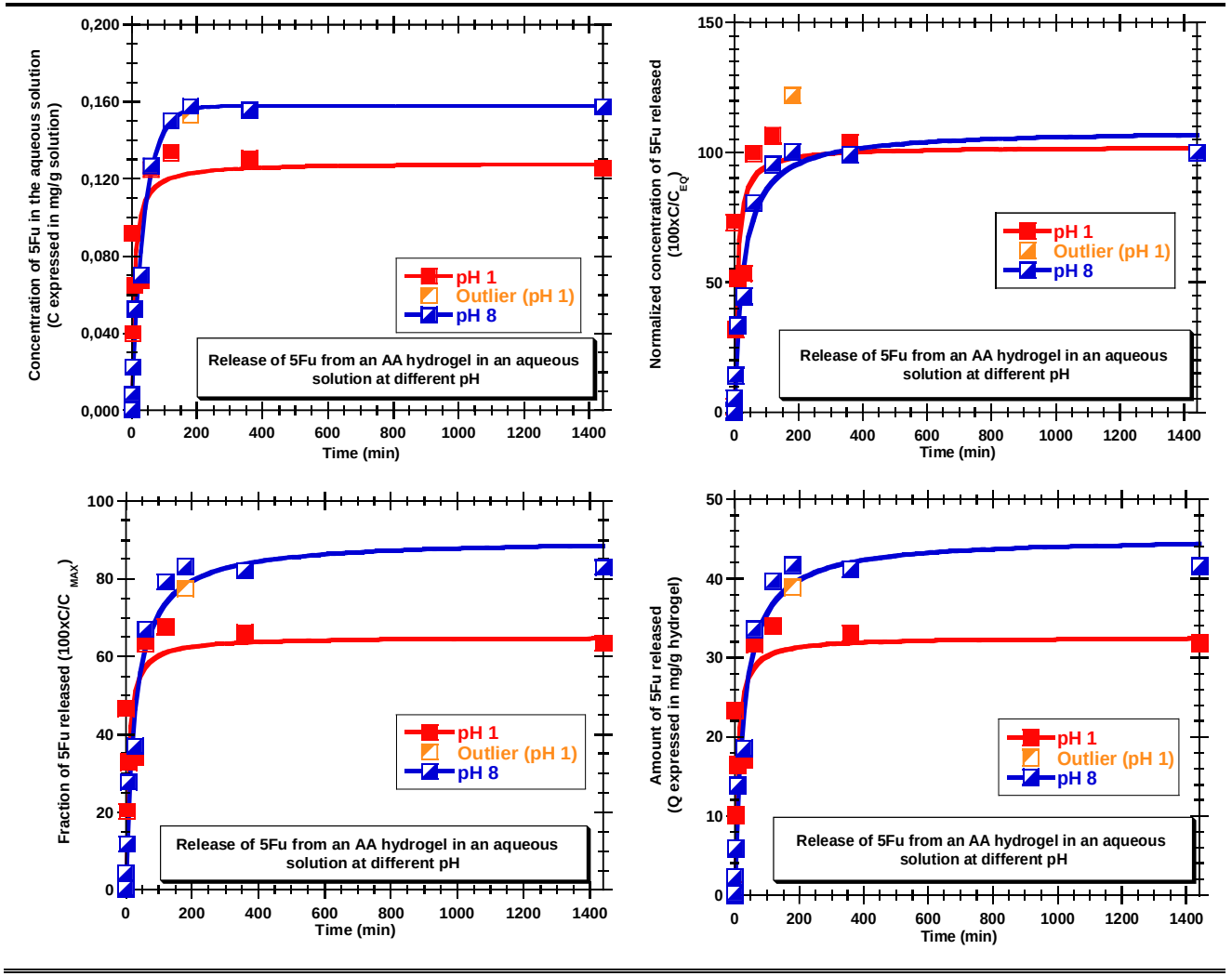

Annex 29. Results of the release test performed at pH 1 with a caffeine incubated AA hydrogel (HG3).

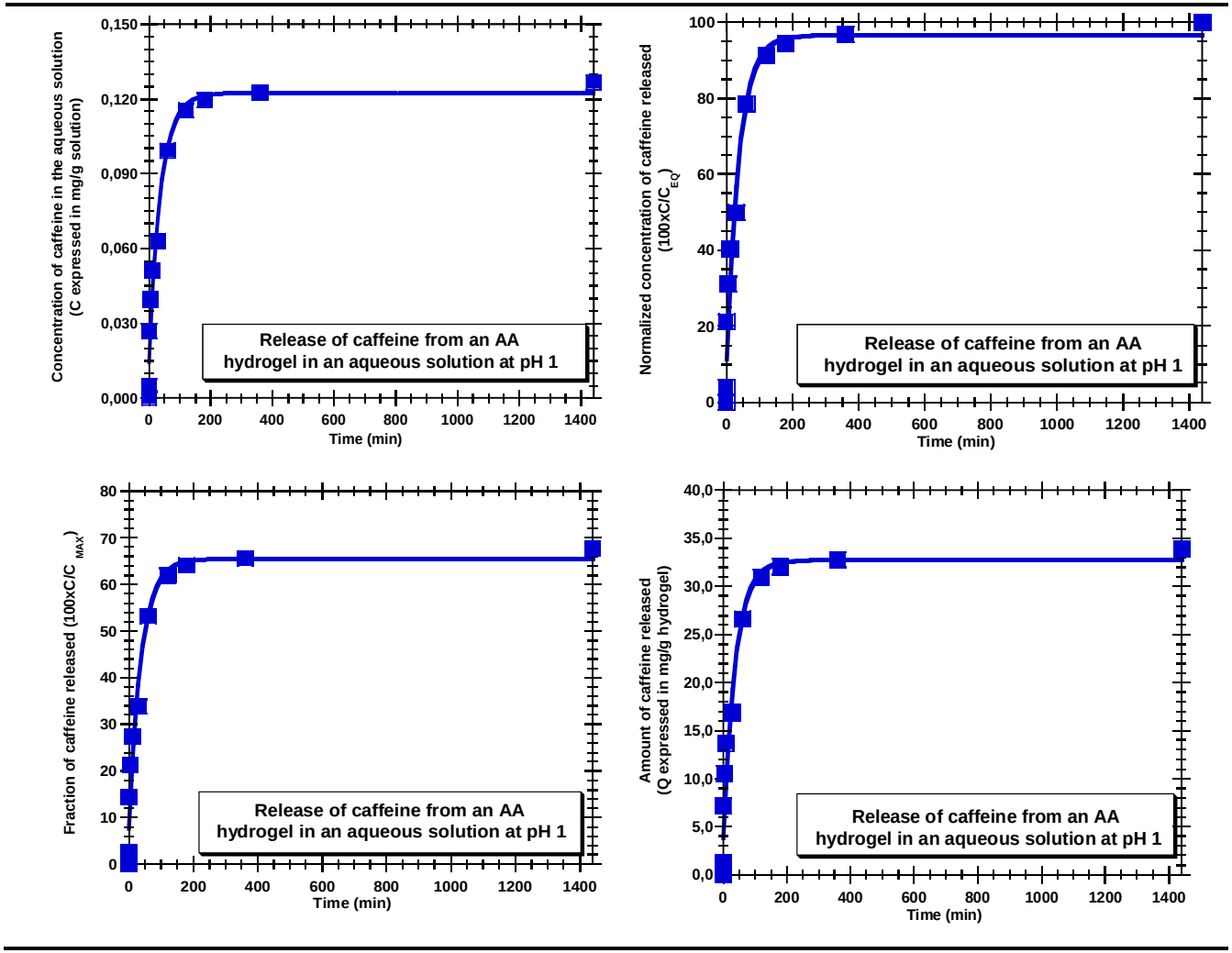

Annex 30. Results of the release test performed at pH 8 with a caffeine incubated AA hydrogel (HG3).

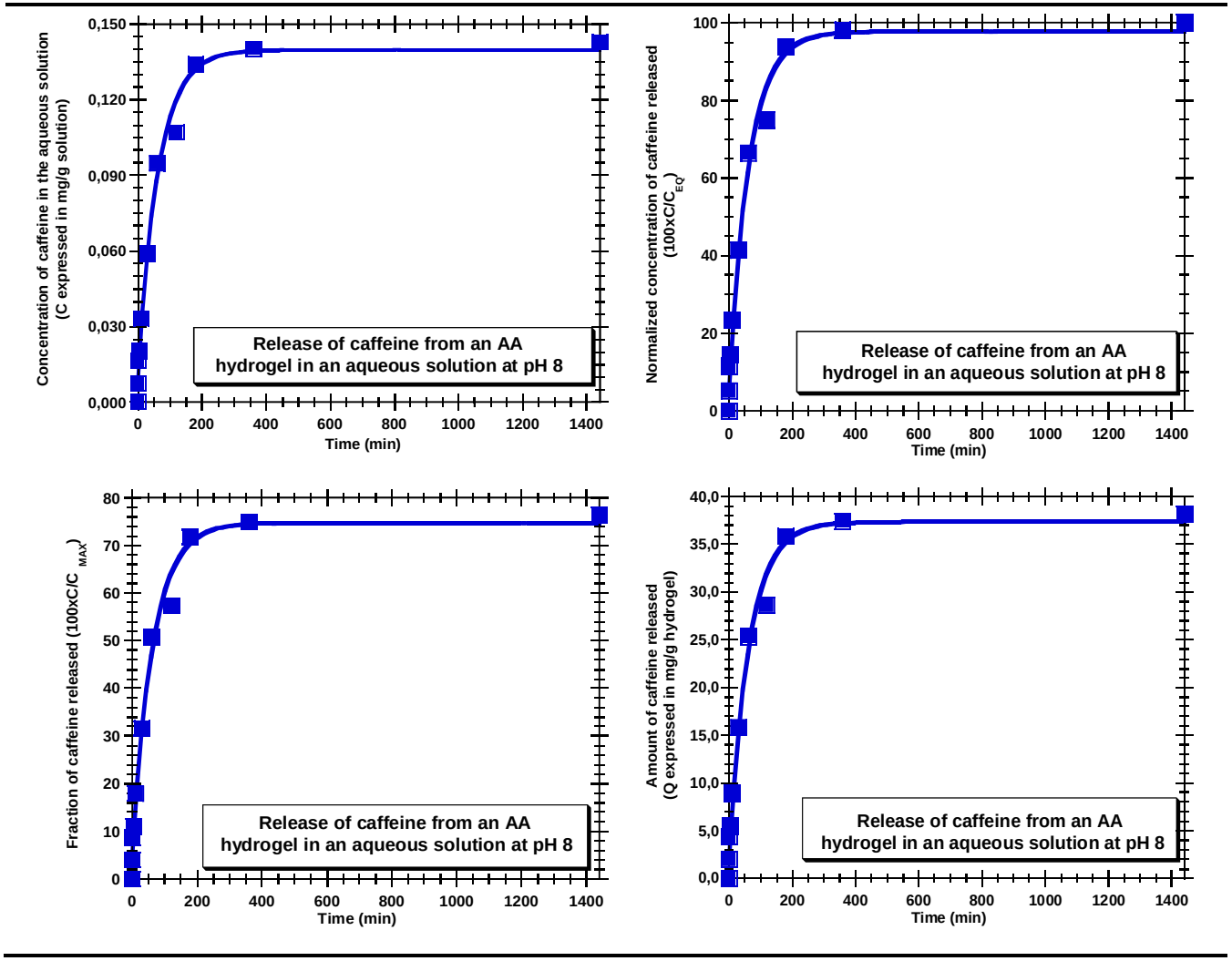

Annex 31. Comparison of the results, at different pH, of the release tests with a caffeine incubated AA hydrogel (HG3).

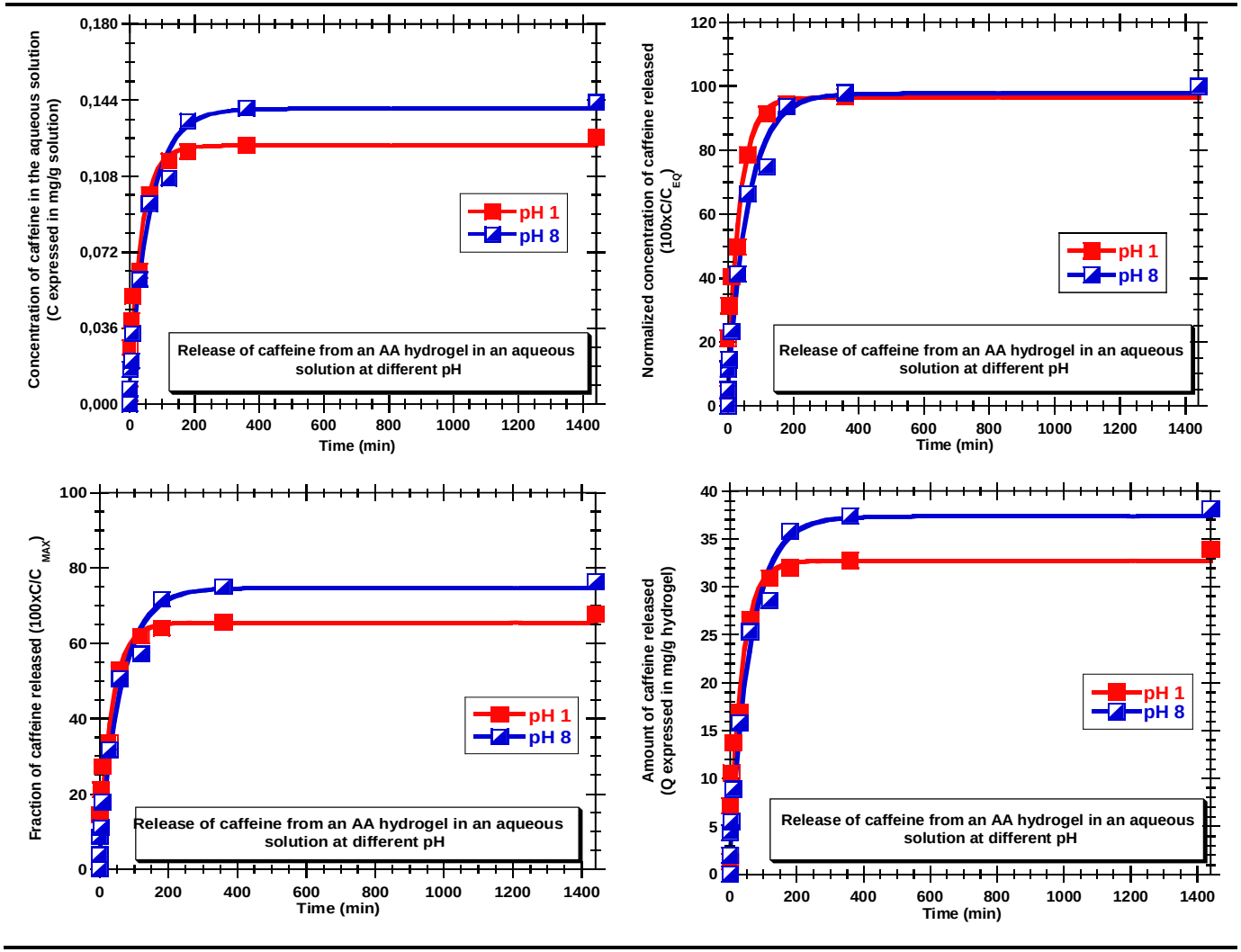

Annex 32. Results of the release test performed at pH 1 with an INH incubated AA hydrogel (HG3).

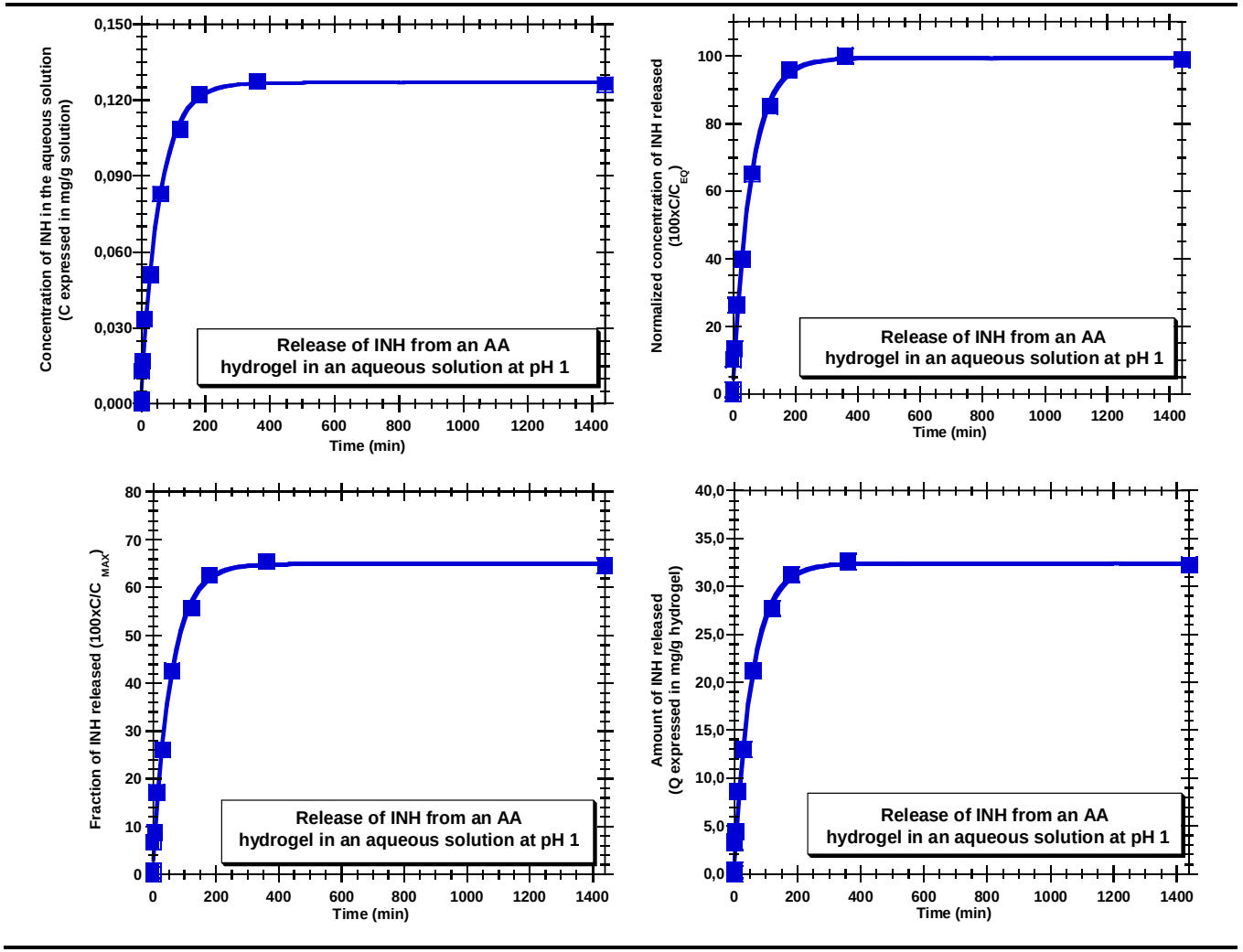

Annex 33. Results of the release test performed at pH 8 with an INH incubated AA hydrogel (HG3).

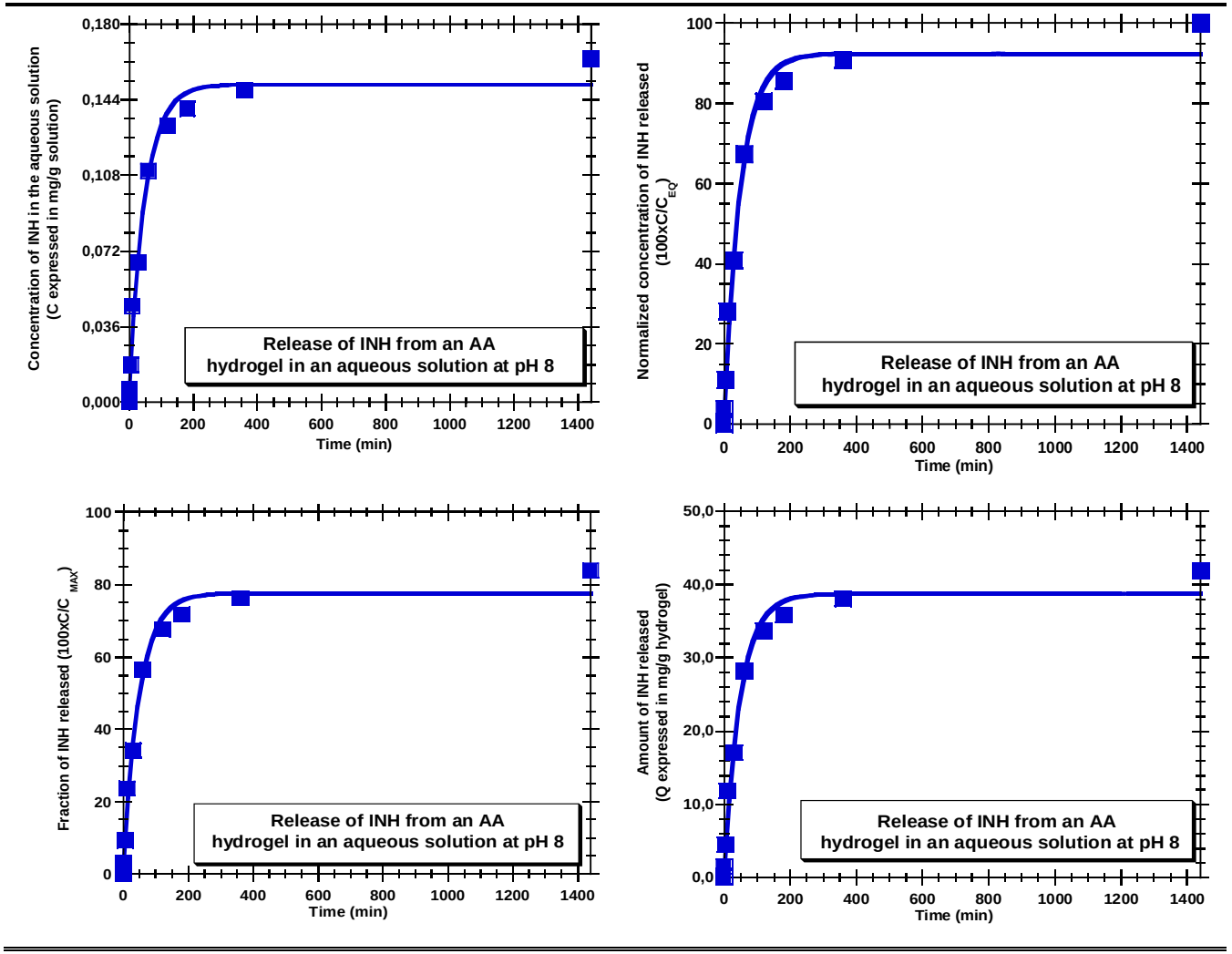

Annex 34. Comparison of the results, at different pH, of the release tests with an INH incubated AA hydrogel (HG3).

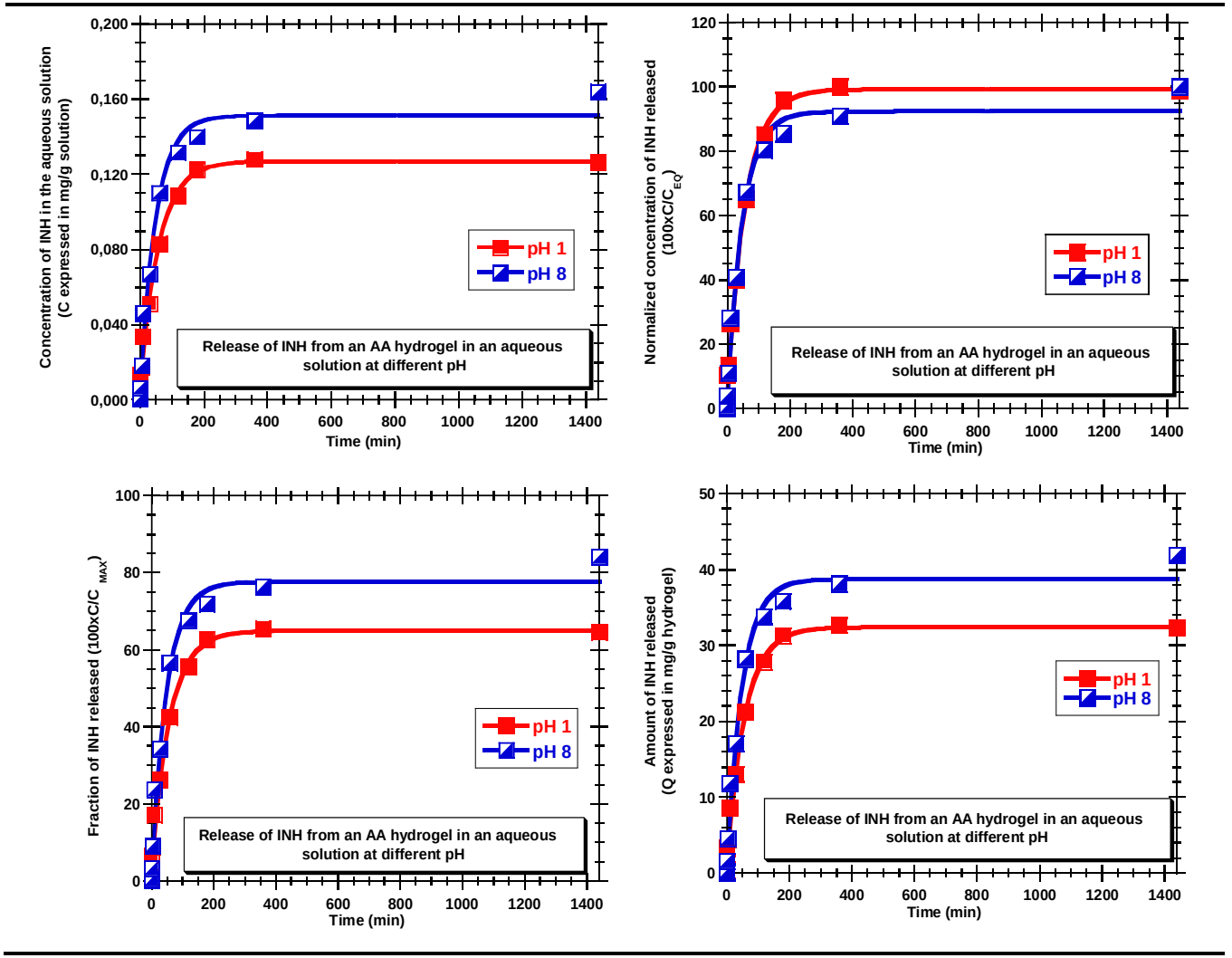

Annex 35. Results of the release test performed at pH 1 with an IBU incubated AA hydrogel (HG3).

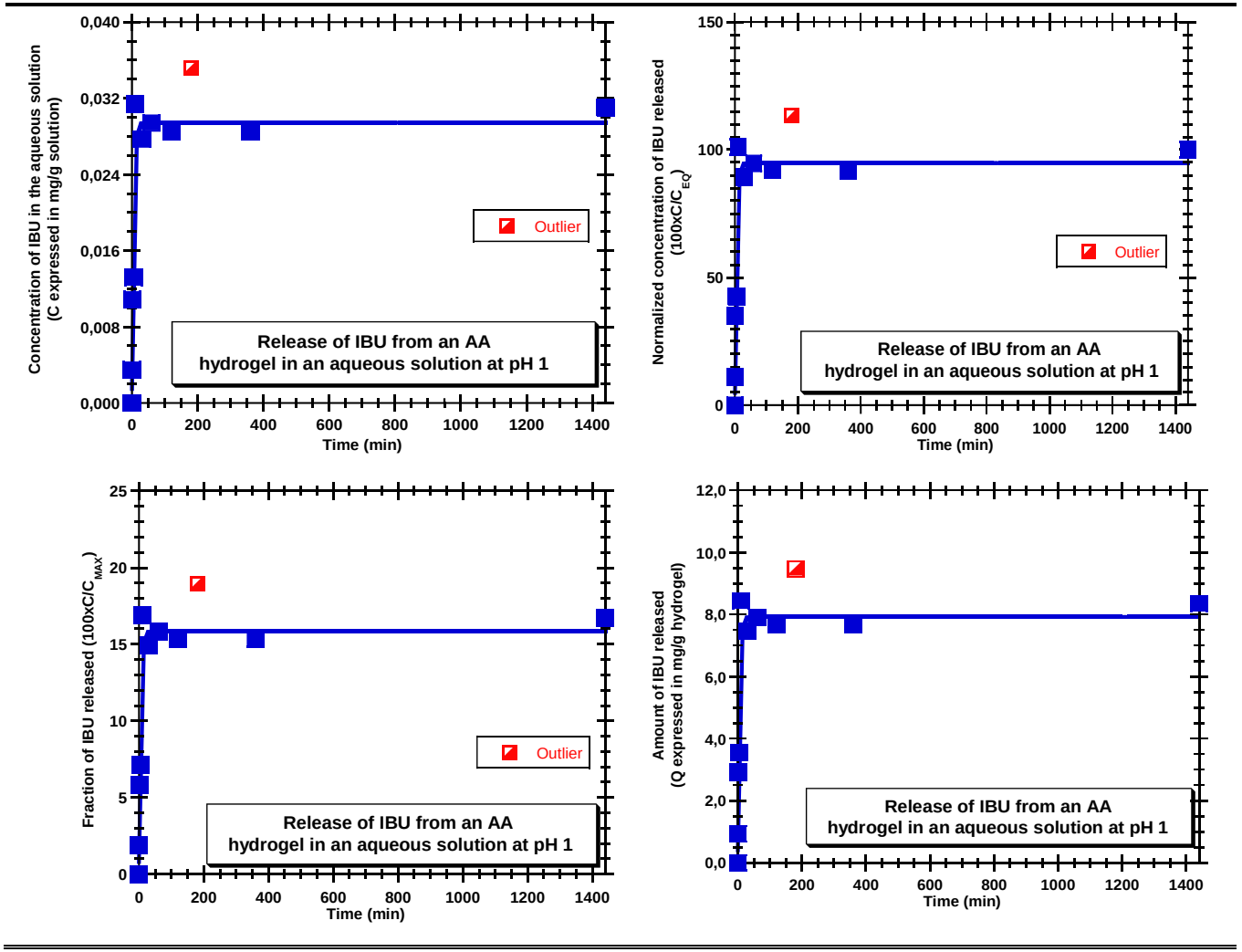

Annex 36. Results of the release test performed at pH 8 with an IBU incubated AA hydrogel (HG3).

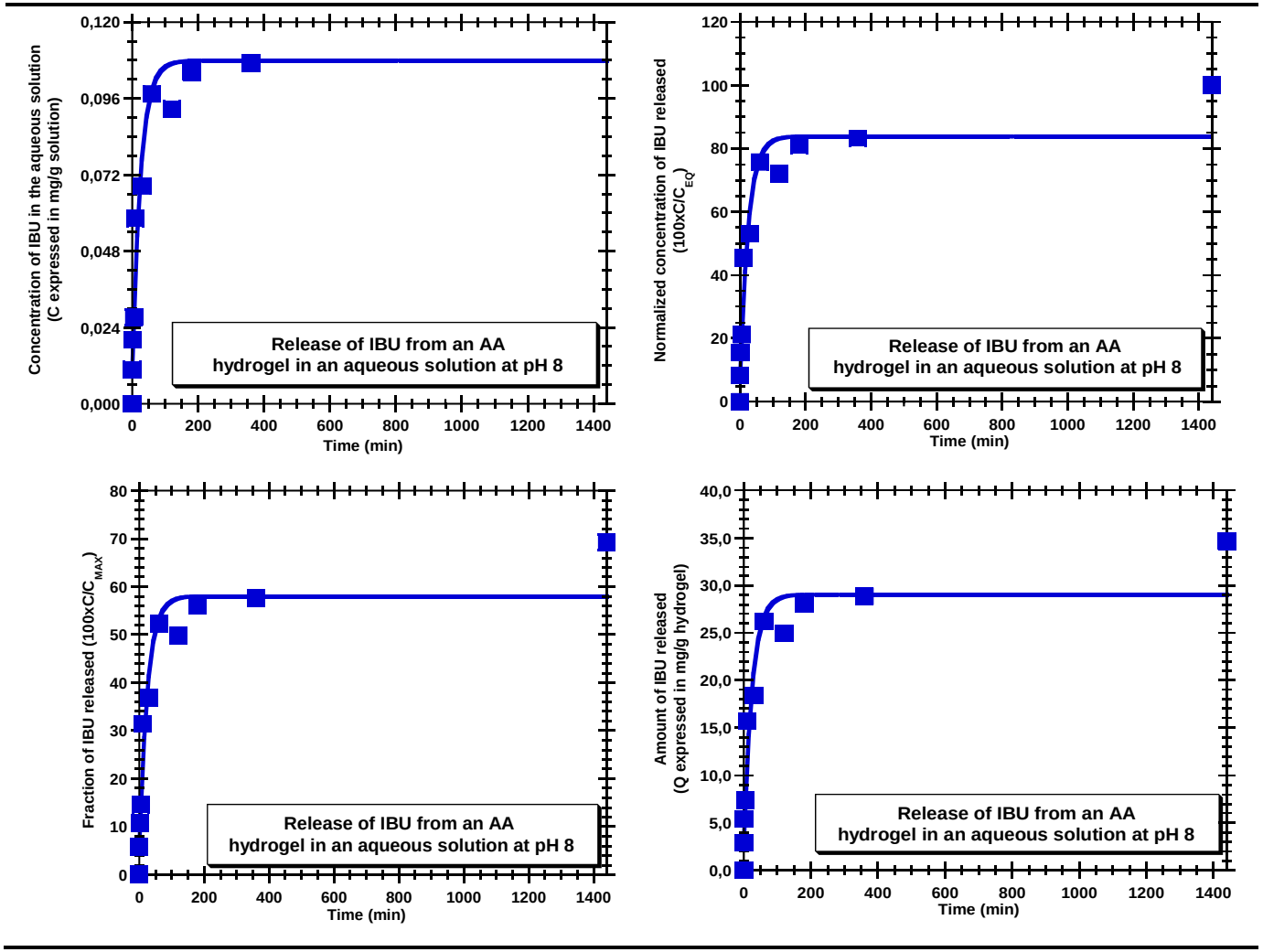

Annex 37. Comparison of the results, at different pH, of the release tests with an IBU incubated AA hydrogel (HG3).

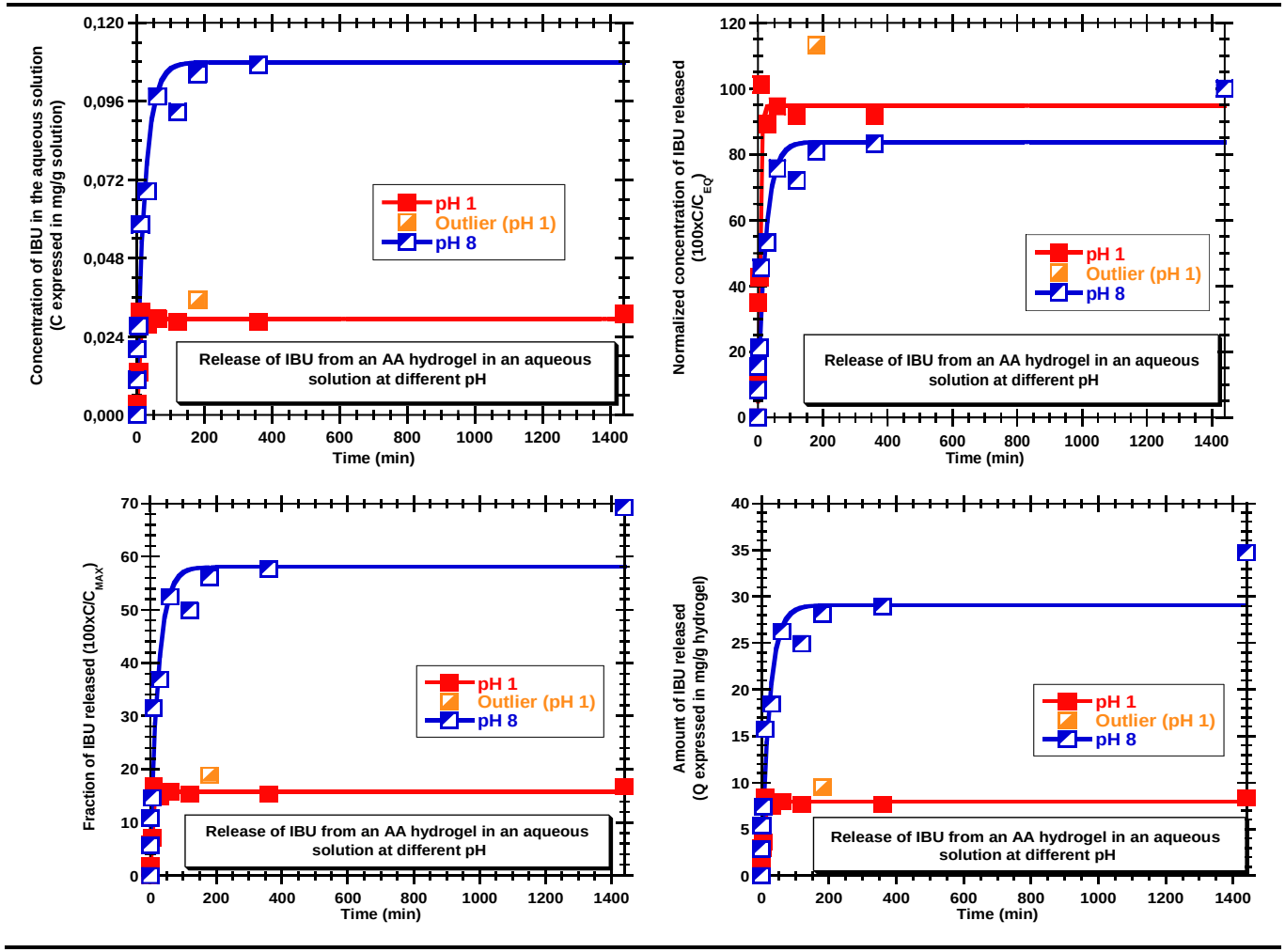

Annex 38. Results of the release test performed at 25 ºC with a 5-FU incubated NIPA hydrogel (HG1) with incubation method 2.

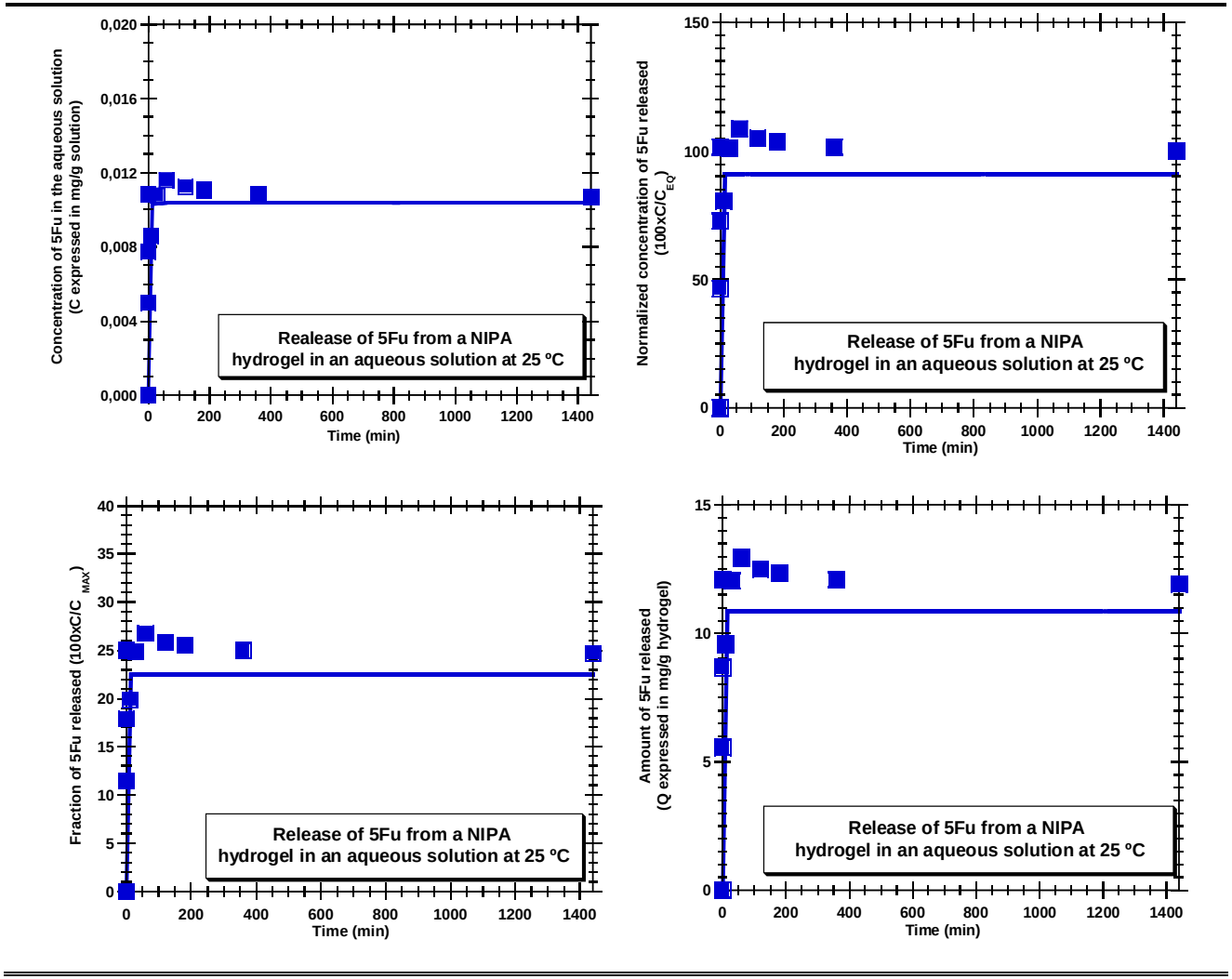

Annex 39. Results of the release test performed at 37 ºC with a 5-FU incubated NIPA hydrogel (HG1) with incubation method 2.

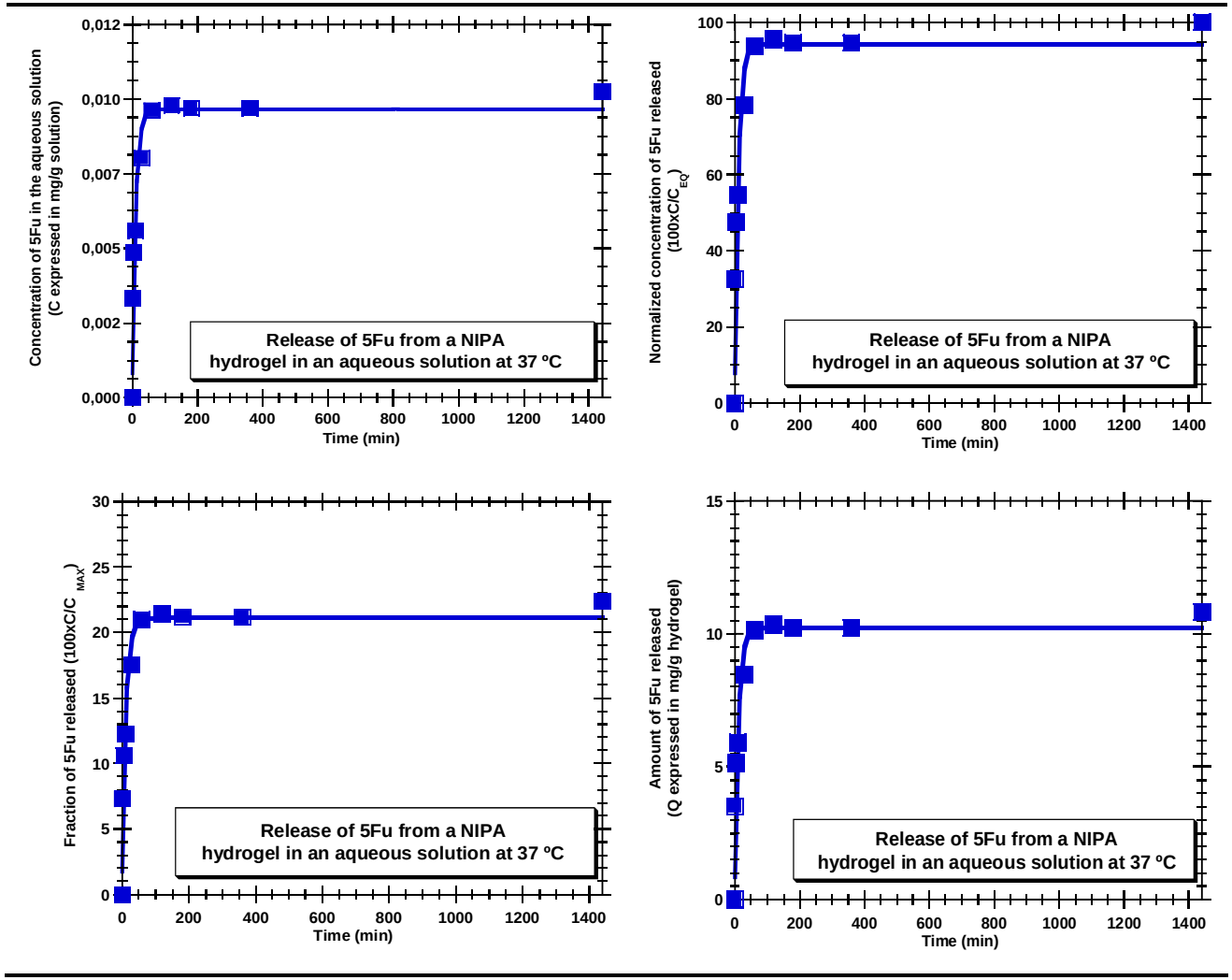

Annex 40. Comparison of the results, at different temperatures, of the release tests with a 5-FU incubated NIPA hydrogel (HG1) with incubation method 2.

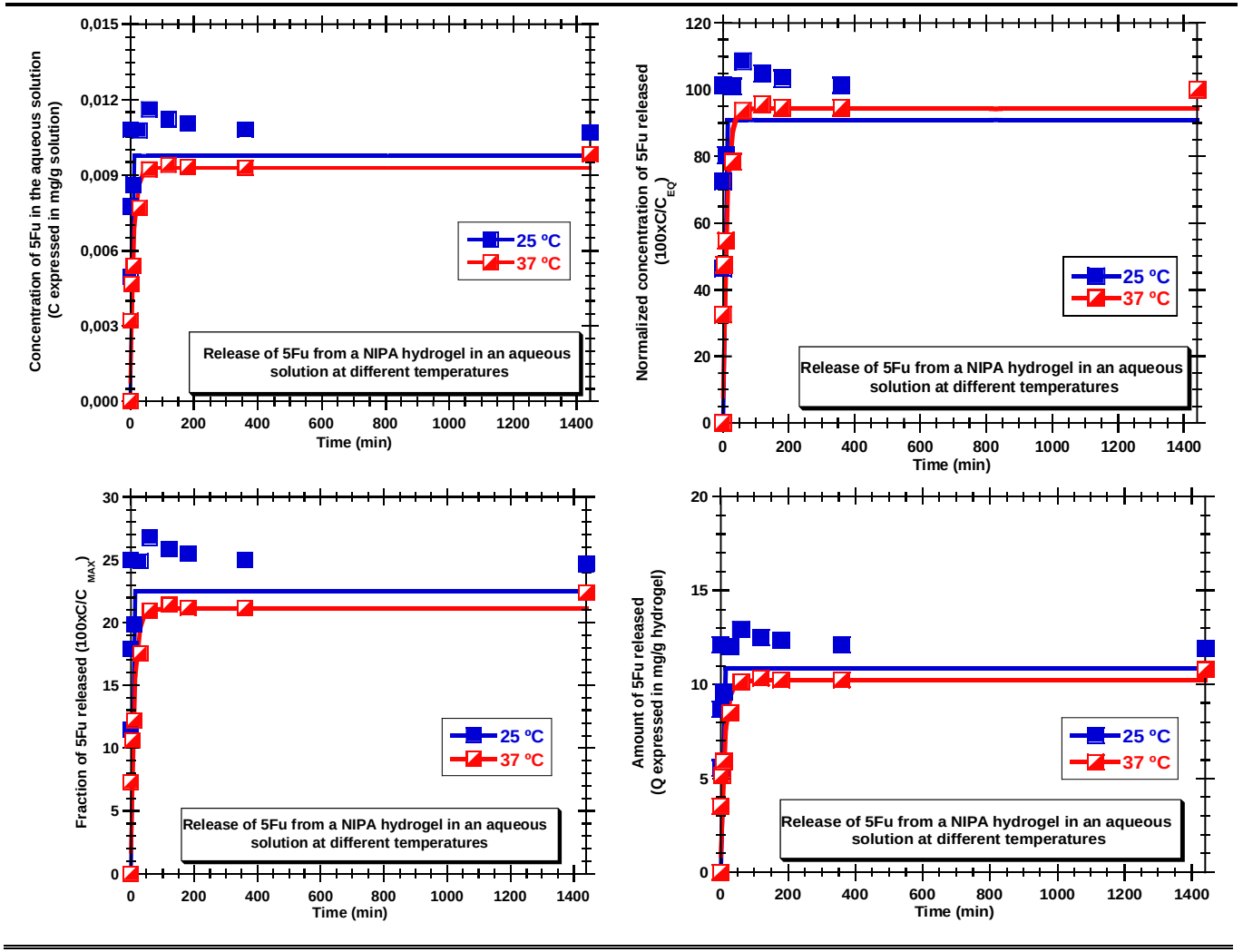

Annex 41. Results of the release test performed at 25 ºC with a caffeine incubated NIPA hydrogel (HG1) with incubation method 2.

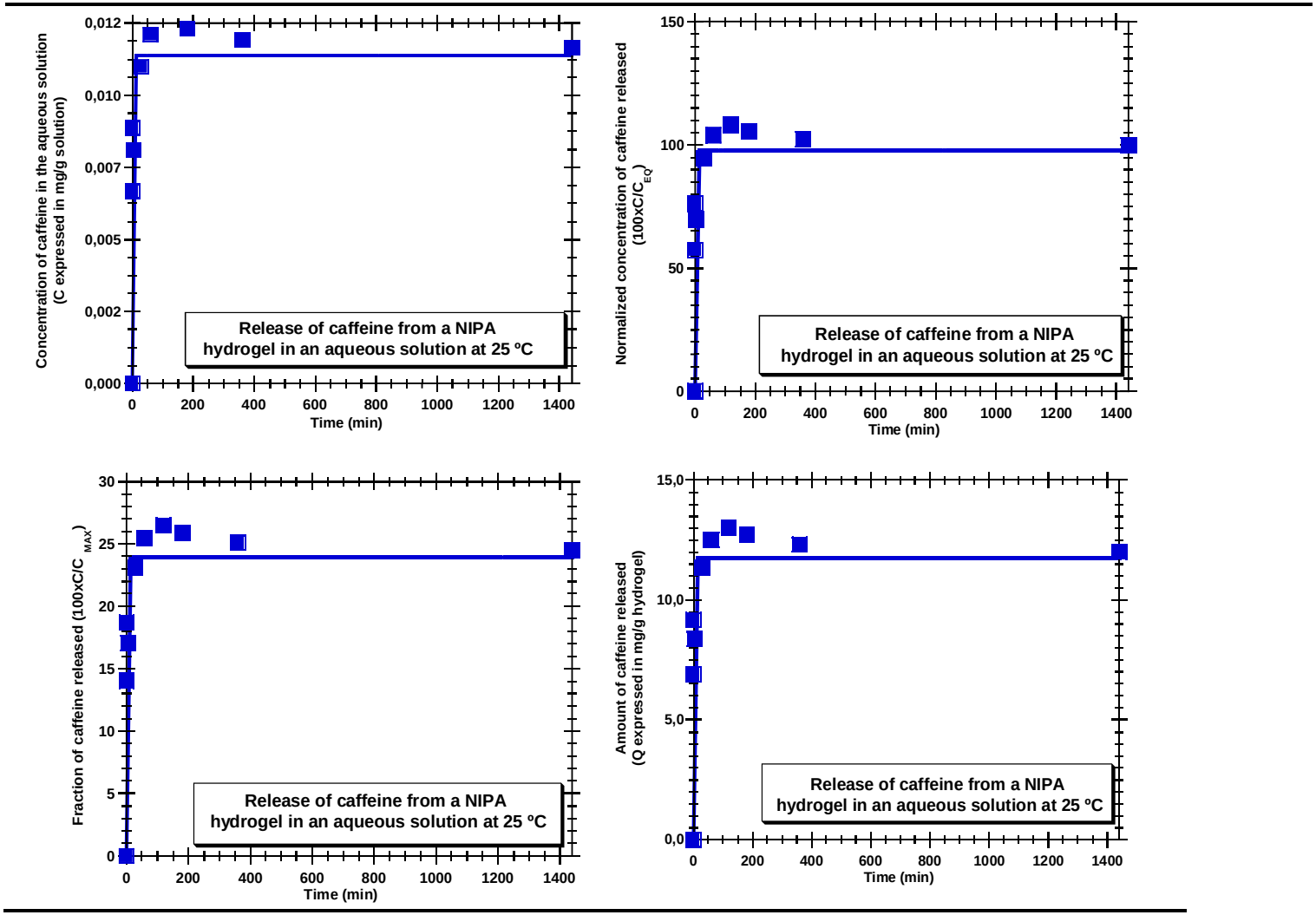

Annex 42. Results of the release test performed at 37 ºC with a caffeine incubated NIPA hydrogel (HG1) with incubation method 2.

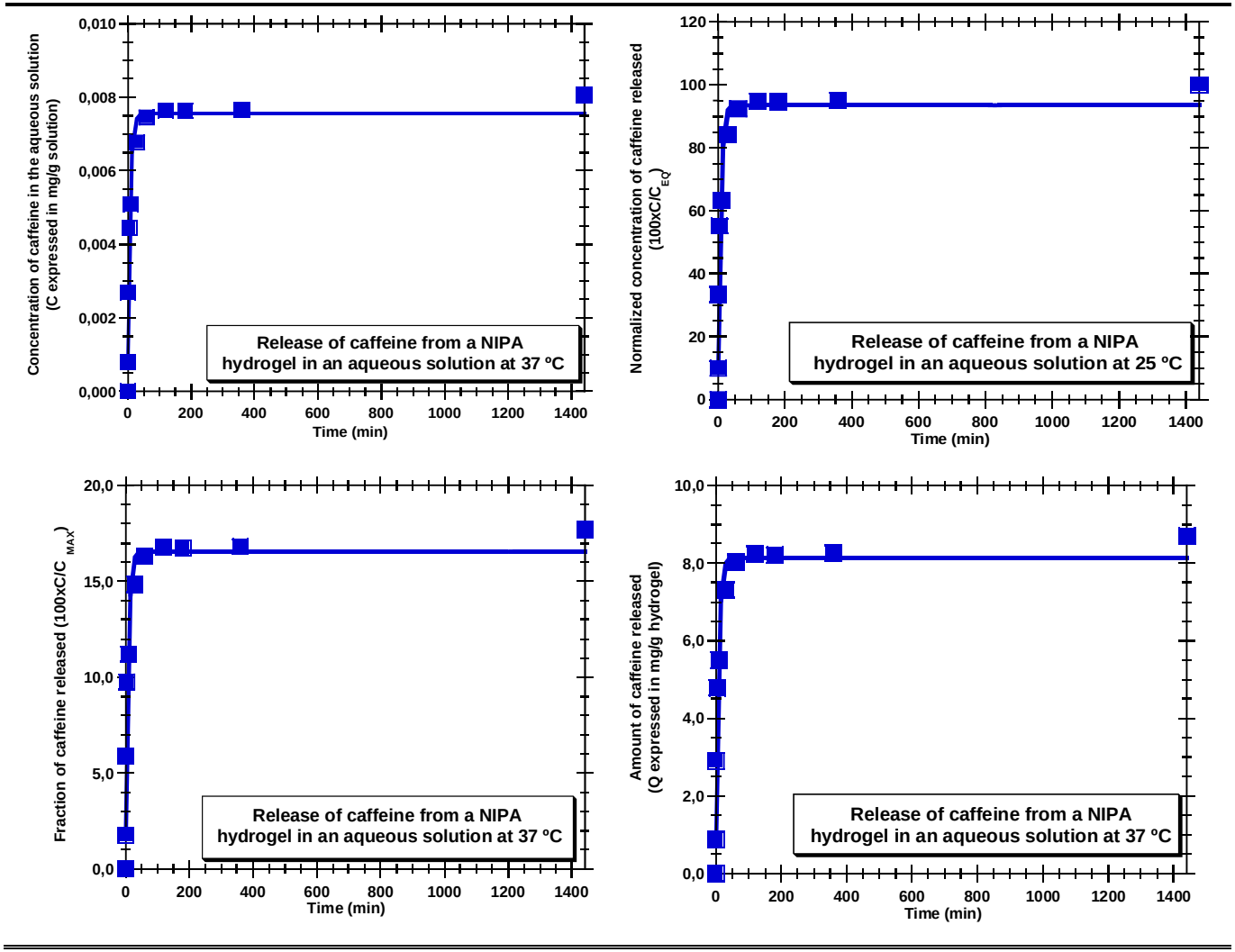

Annex 43. Comparison of the results, at different temperatures, of the release tests with a caffeine incubated NIPA hydrogel (HG1) with incubation method 2.

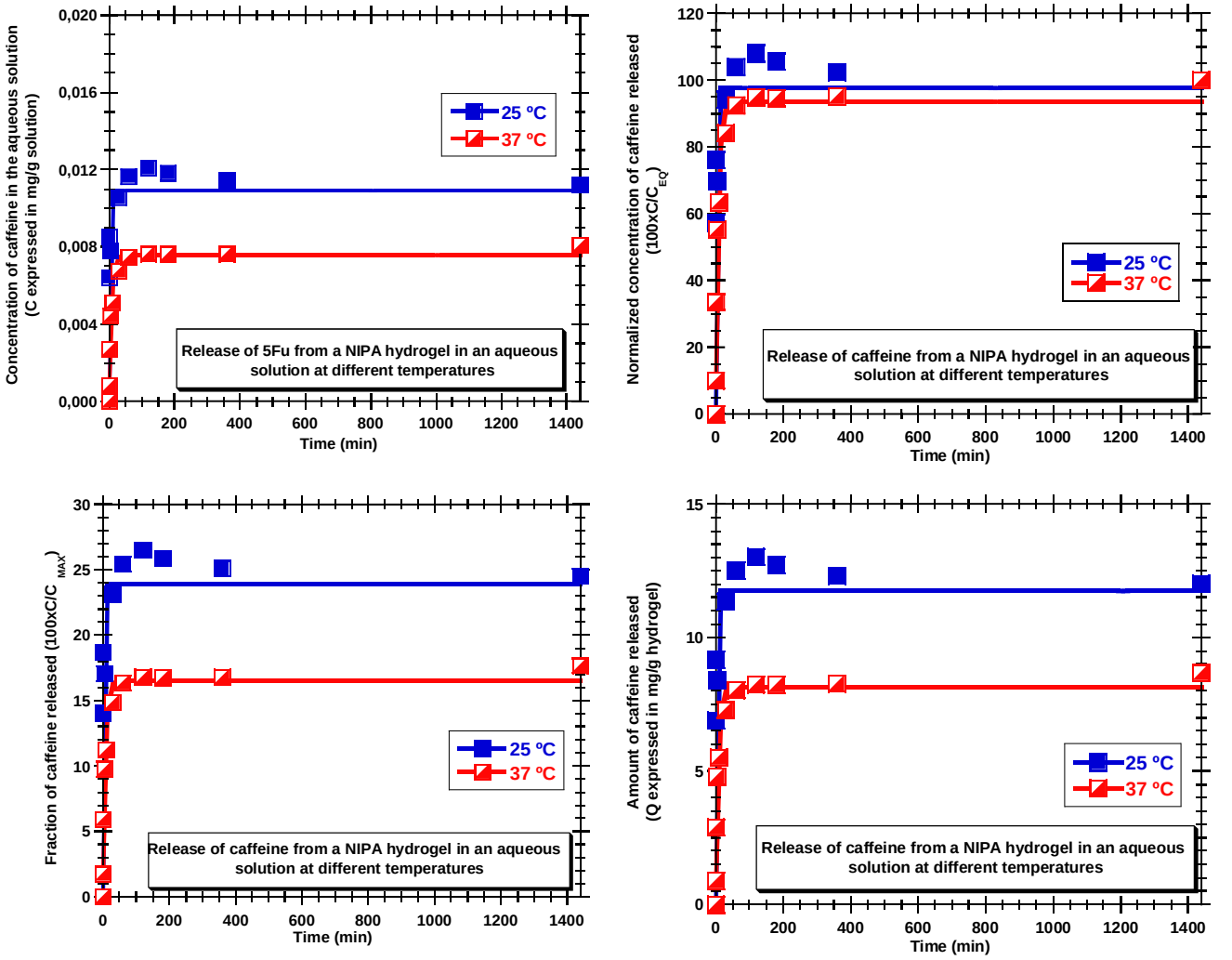

Annex 44. Results of the release test performed at 25 ºC with an INH incubated NIPA hydrogel (HG1) with incubation method 2.

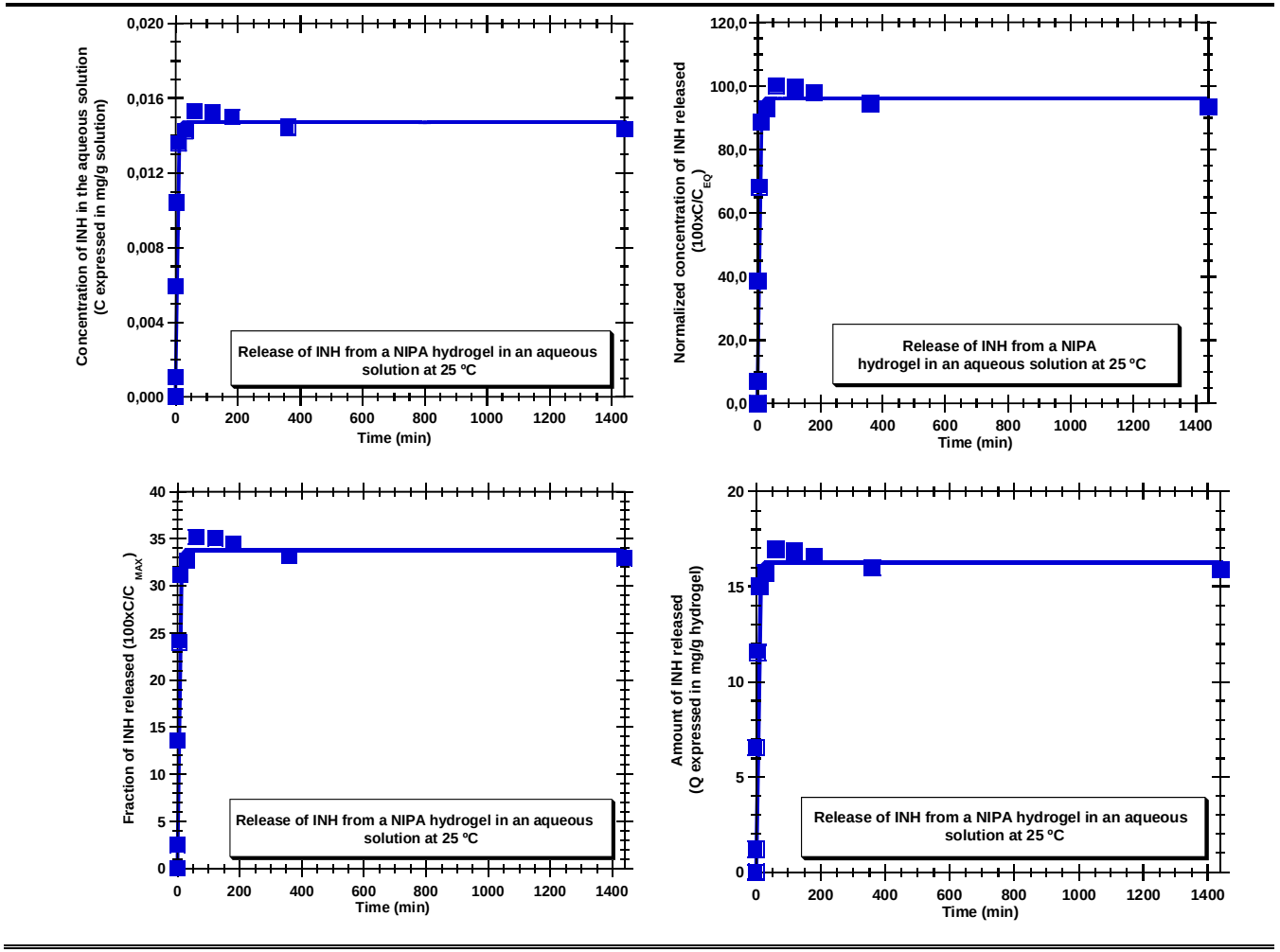

Annex 45. Results of the release test performed at 37 ºC with an INH incubated NIPA hydrogel (HG1) with incubation method 2.

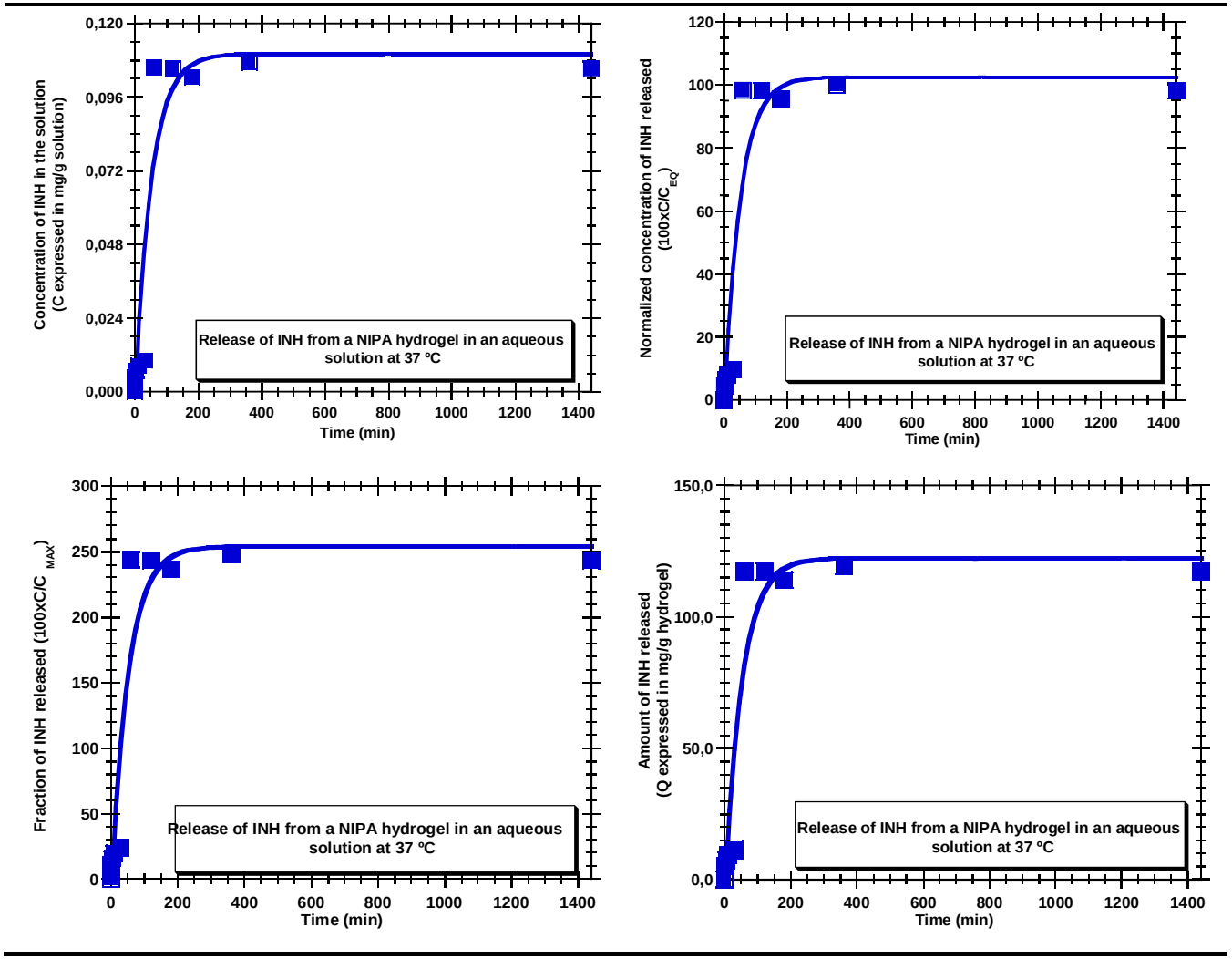

Annex 46. Comparison of the results, at different temperatures, of the release tests with an INH incubated NIPA hydrogel (HG1) with incubation method 2.

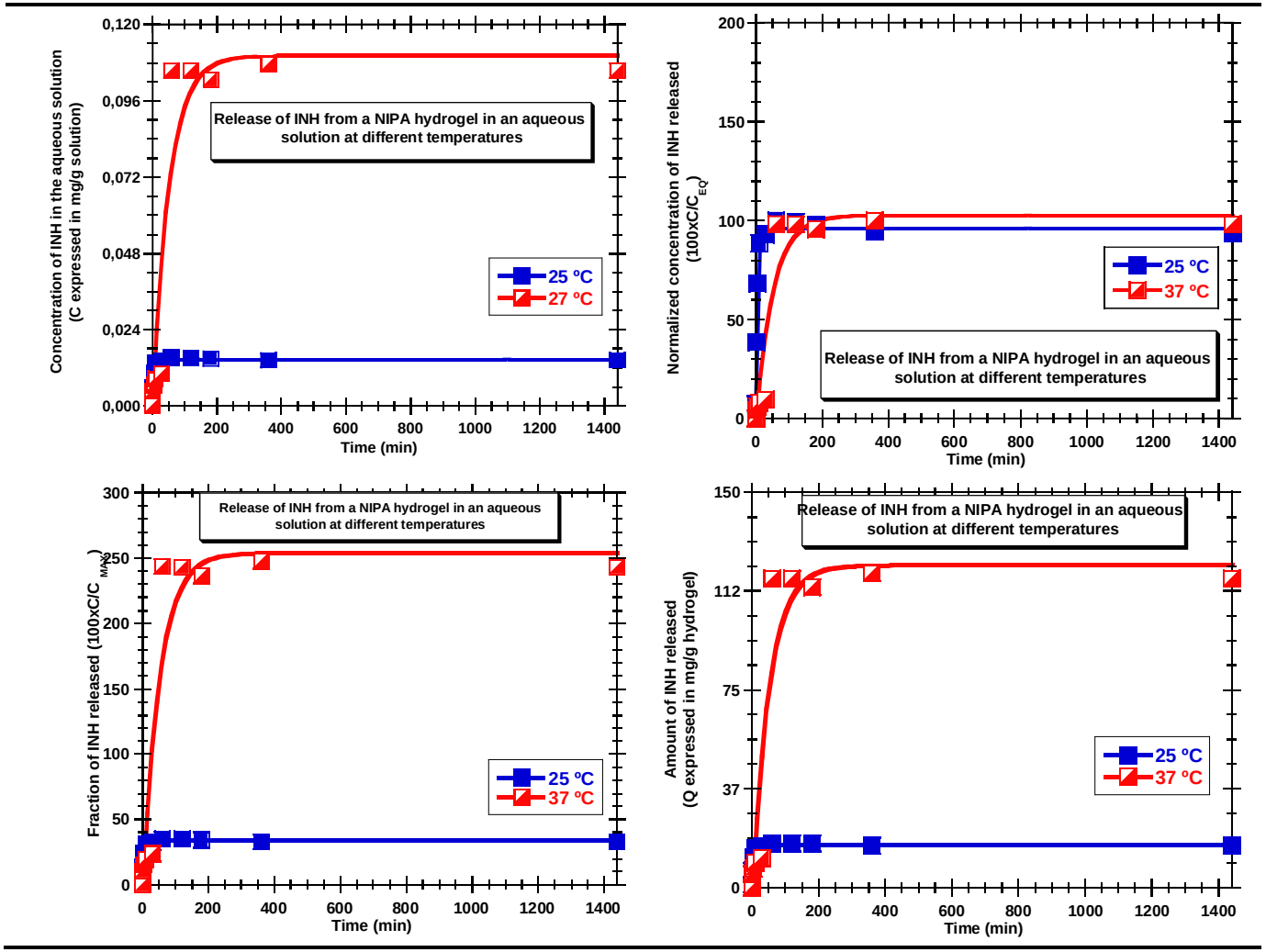

Annex 47. Results of the release test performed at 25 ºC with an IBU incubated NIPA hydrogel (HG1) with incubation method 2.

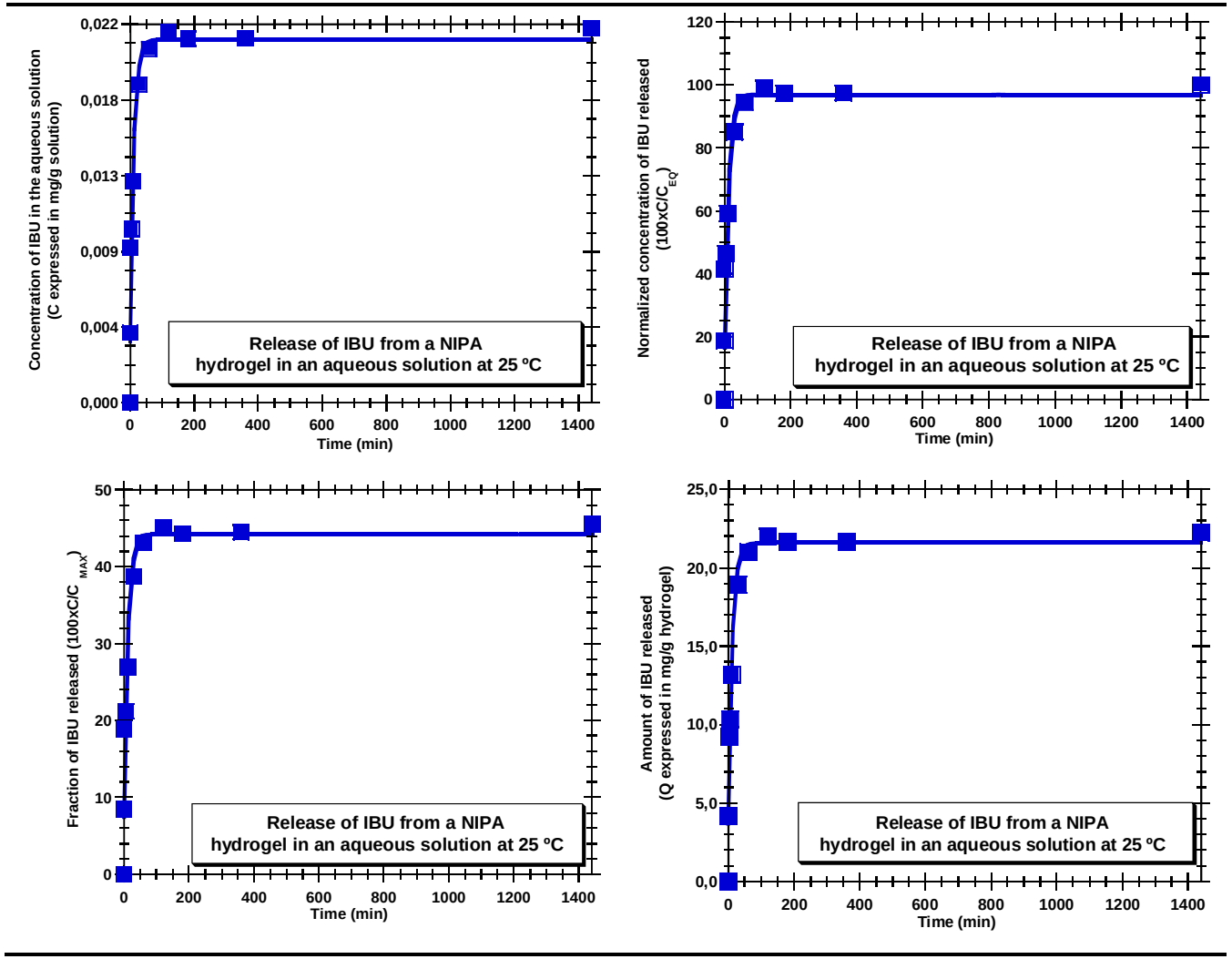

Annex 48. Results of the release test performed at 37 ºC with an IBU incubated NIPA hydrogel (HG1) with incubation method 2.

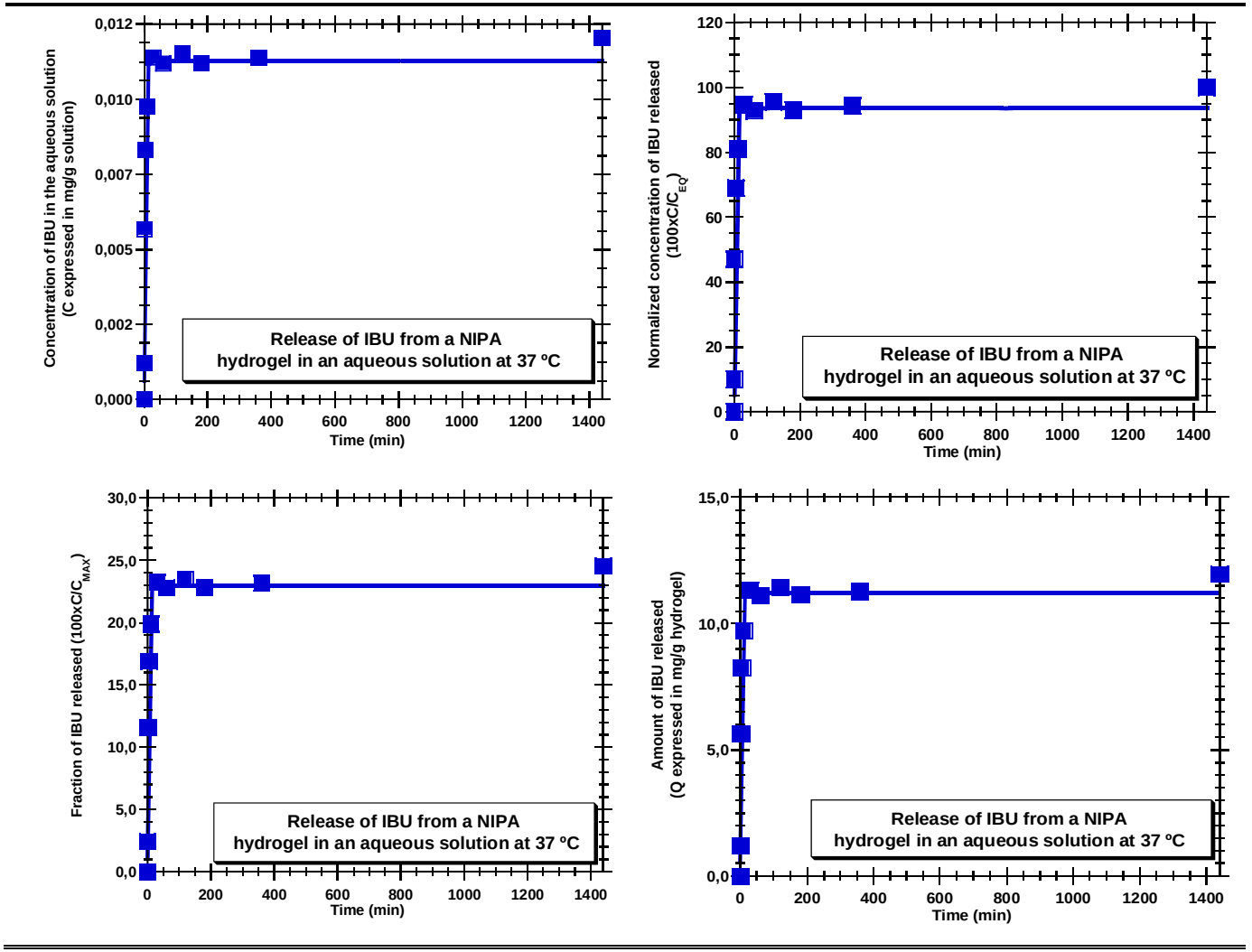

Annex 49. Comparison of the results, at different temperatures, of the release tests with an IBU incubated NIPA hydrogel (HG1) with incubation method 2.

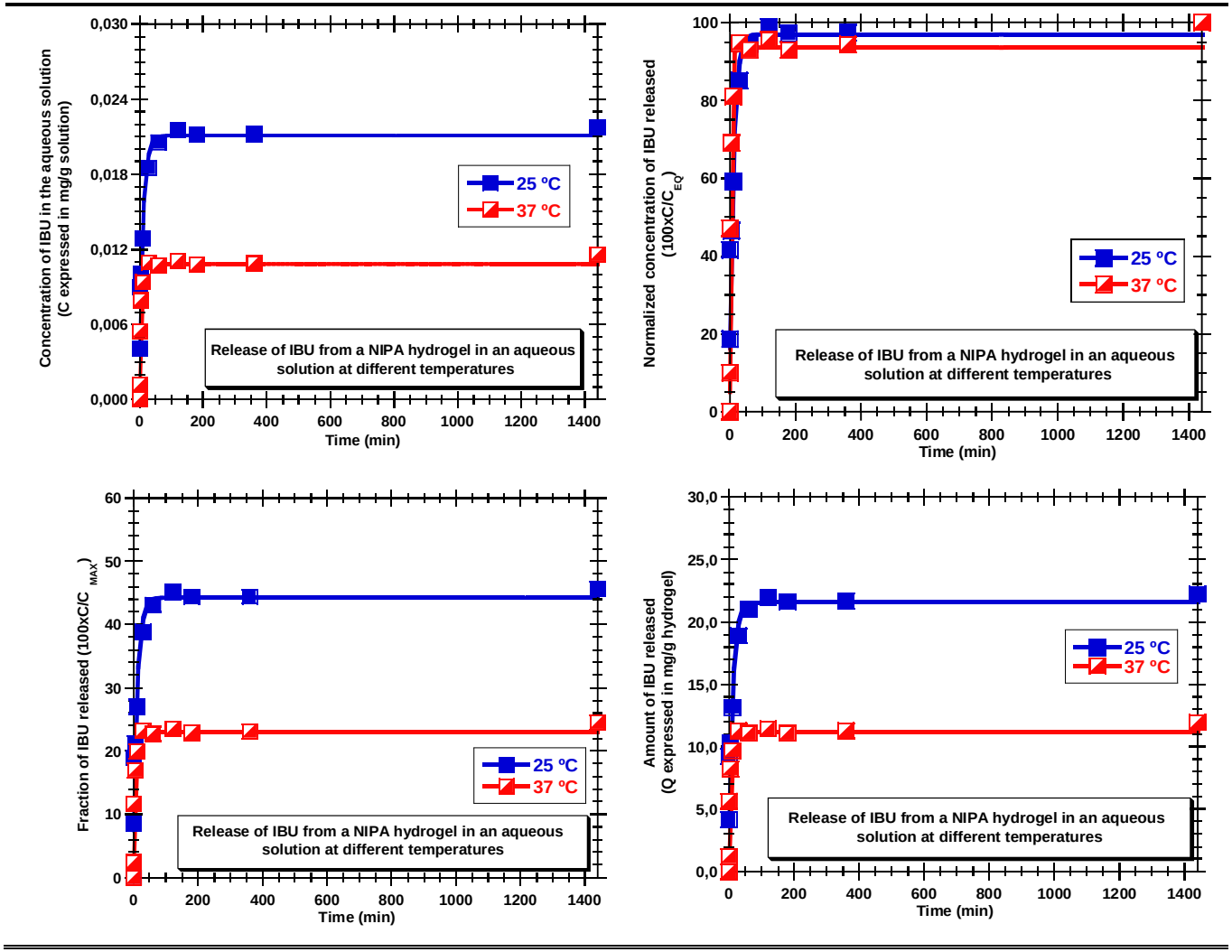

Annex 50. Characterization by SEC with tetra-detection of linear AA polymer synthetized using FRP in a micro-reactor (CM06).

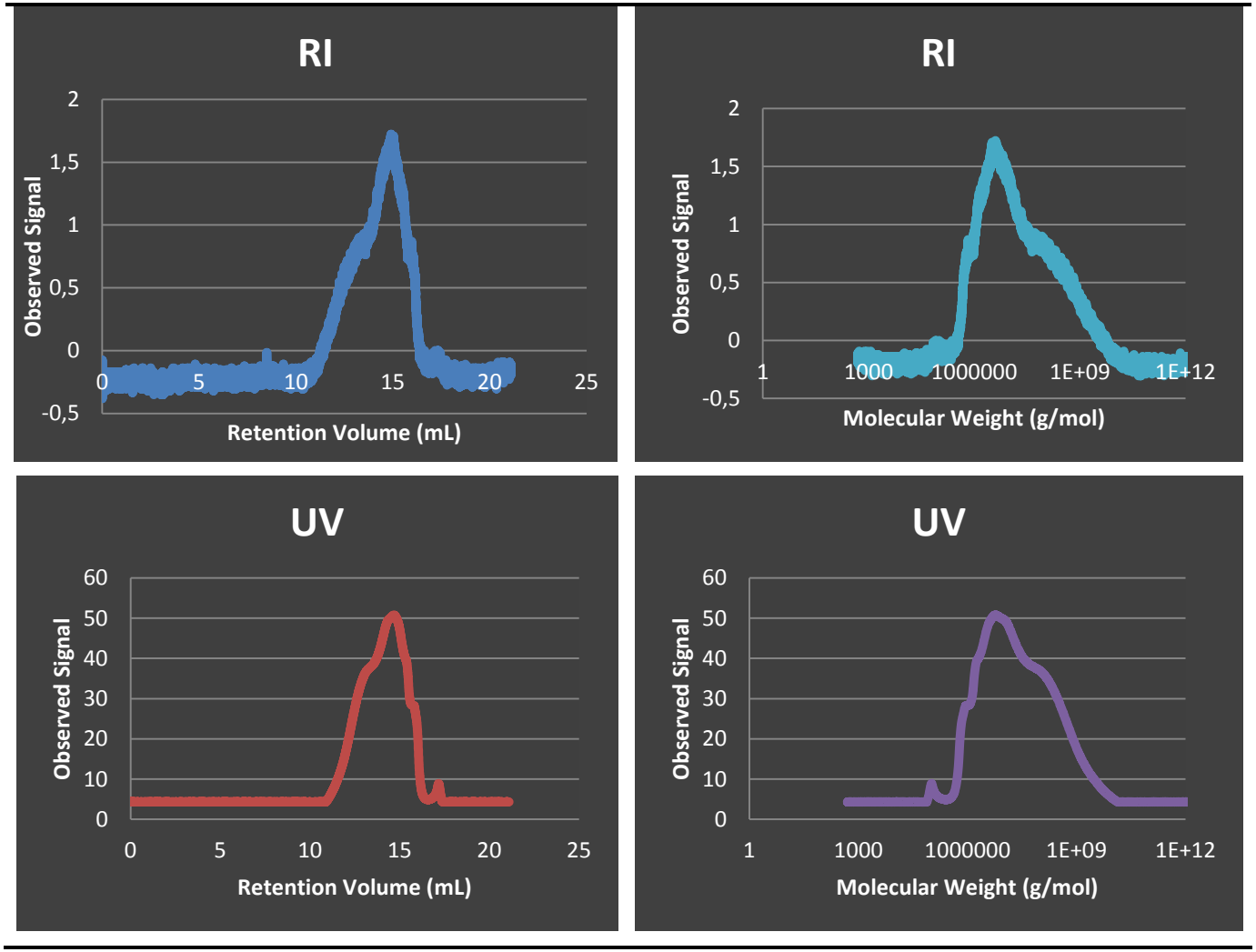

l

Annex 51. Characterization by SEC with tetra-detection of linear AA polymer synthetized using FRP in a micro-reactor (CM06).

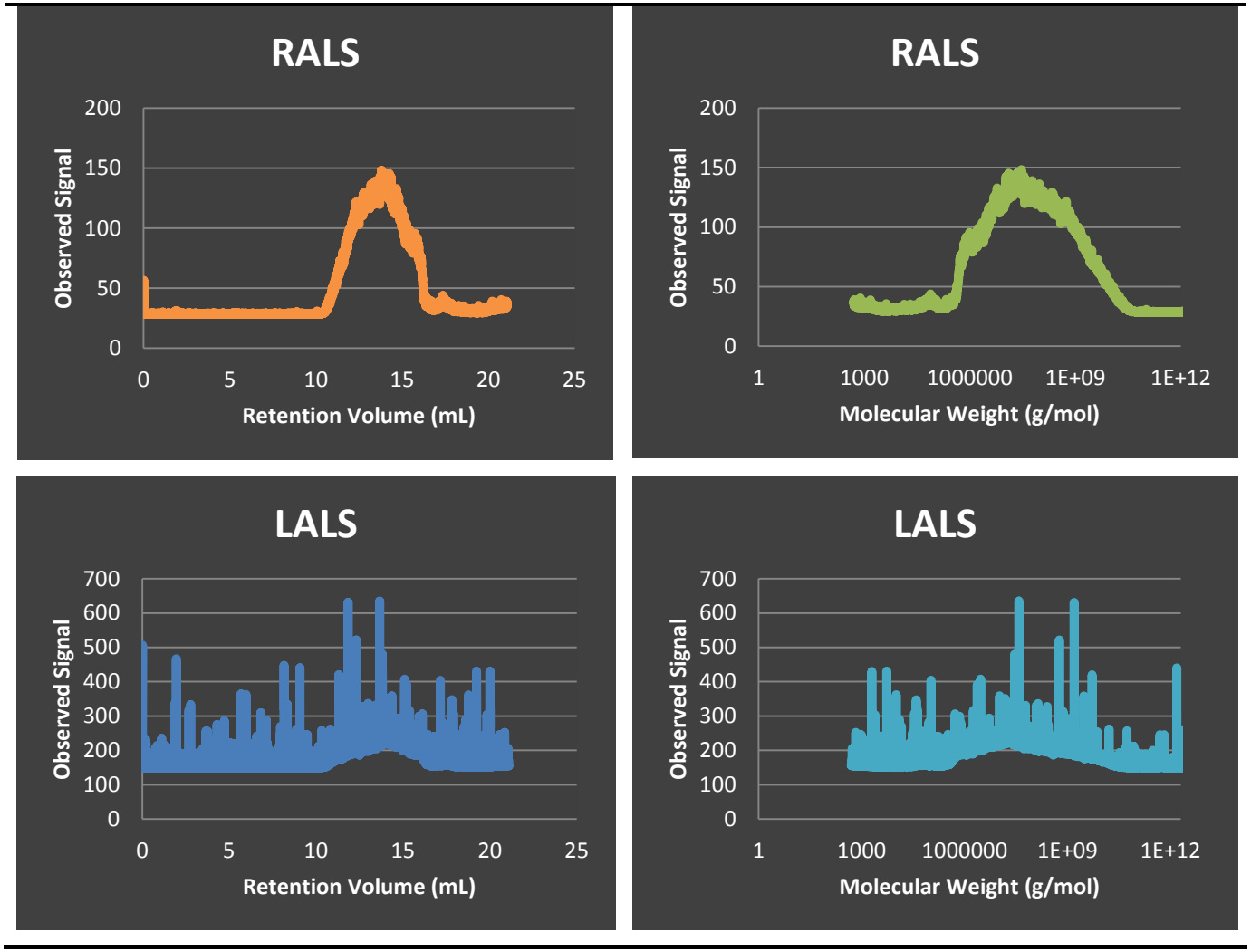

Annex 52. Characterization by SEC with tetra-detection of linear AA polymer synthetized using FRP in a micro-reactor (CM06).

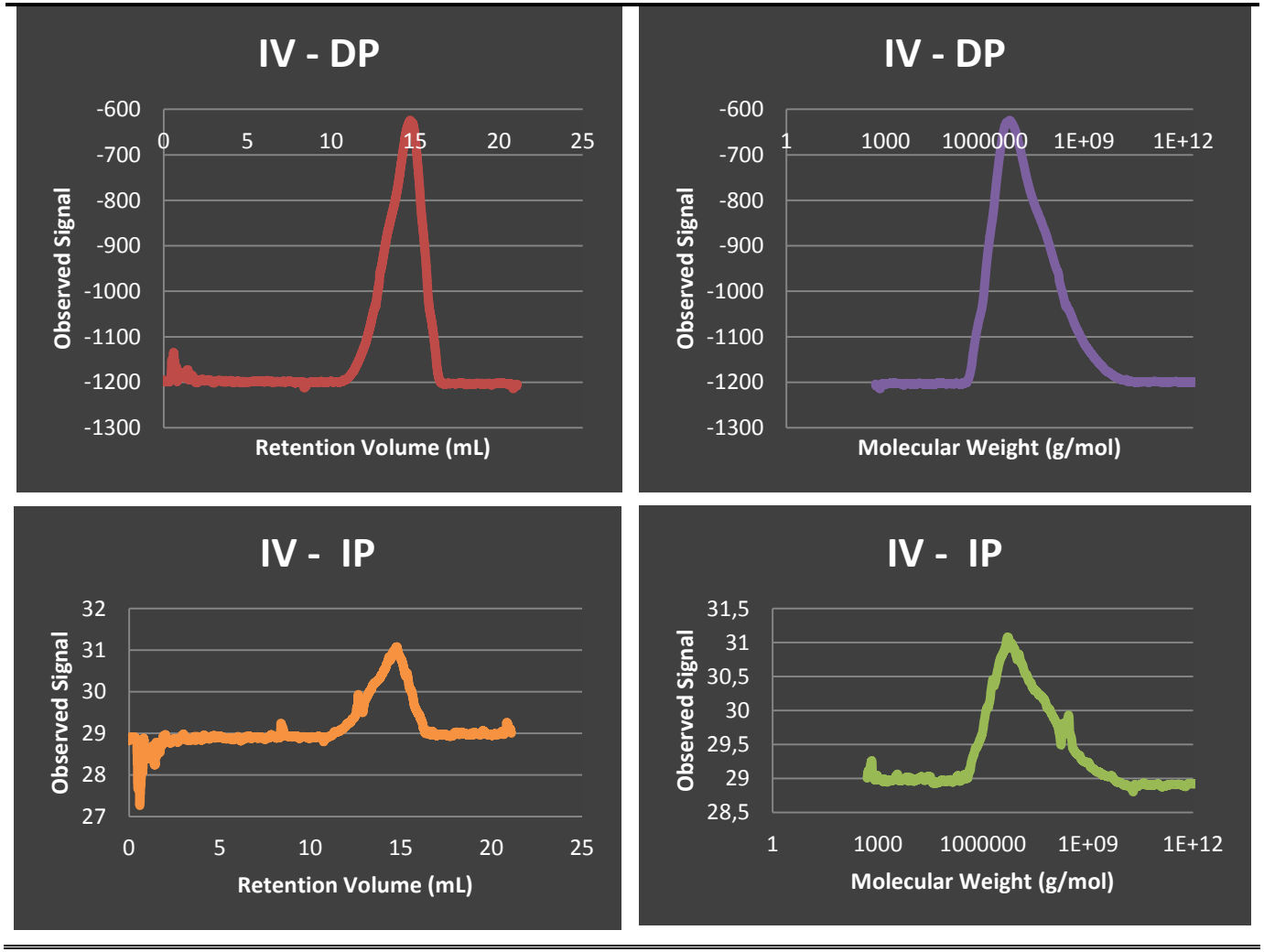

Annex 53. Characterization by SEC with tetra-detection of linear AA polymer synthetized using FRP in a batch reactor (CM07).

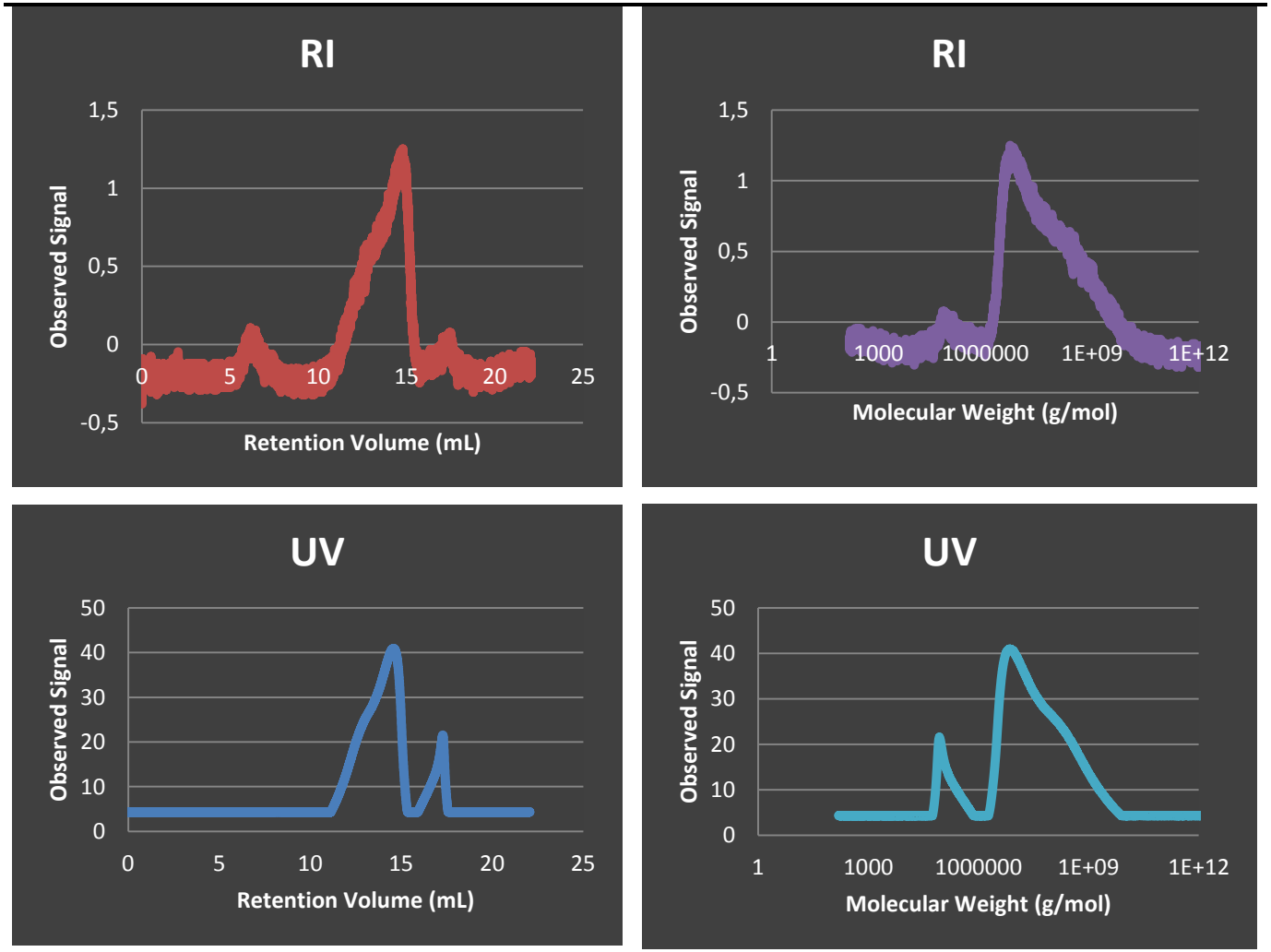

Annex 54. Characterization by SEC with tetra-detection of linear AA polymer synthetized using FRP in a batch reactor (CM07).

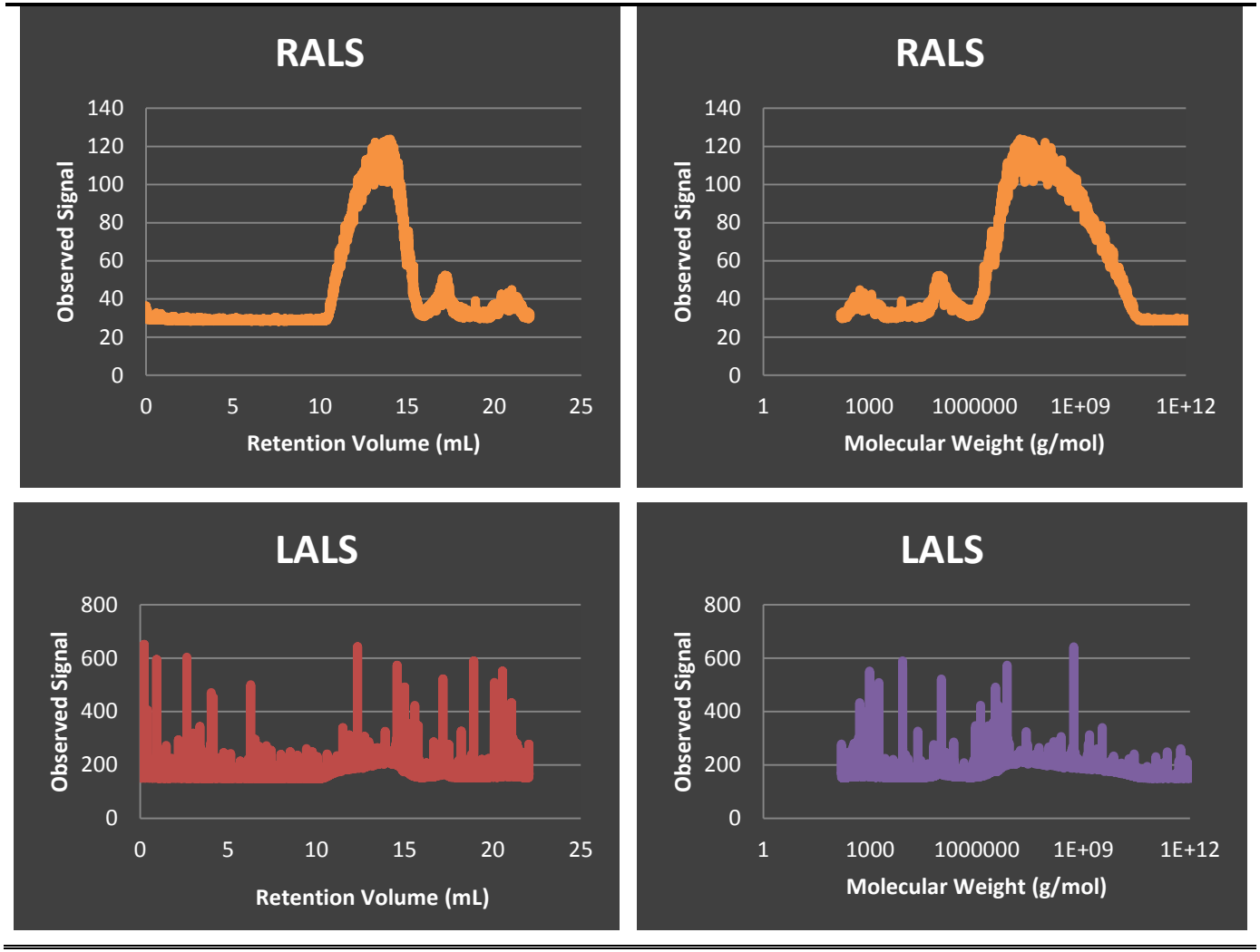

Annex 55. Characterization by SEC with tetra-detection of linear AA polymer synthetized using FRP in a batch reactor (CM07).

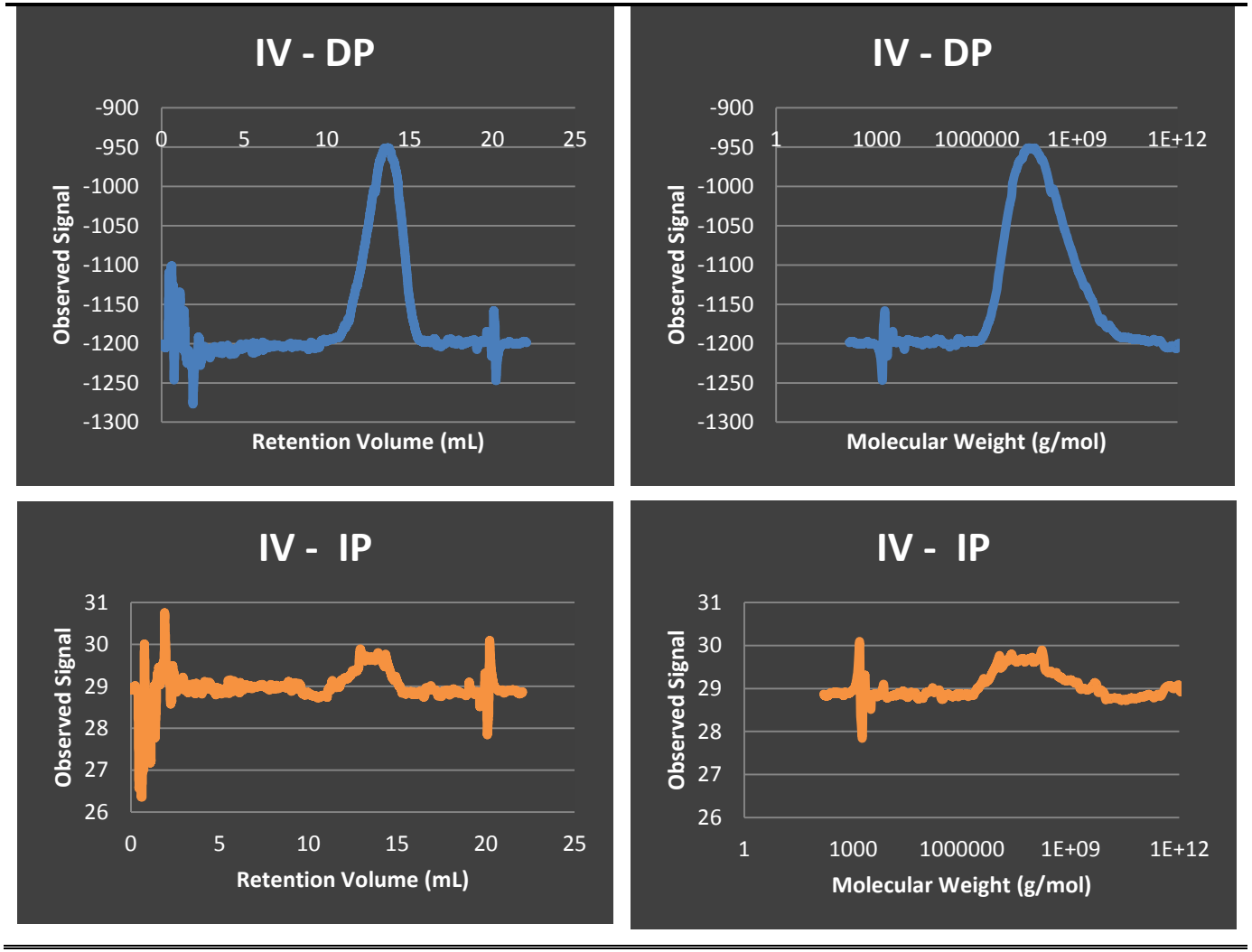

Annex 56. Characterization by SEC with tetra-detection of linear AA polymer synthetized using RAFT in a micro-reactor (CM08).

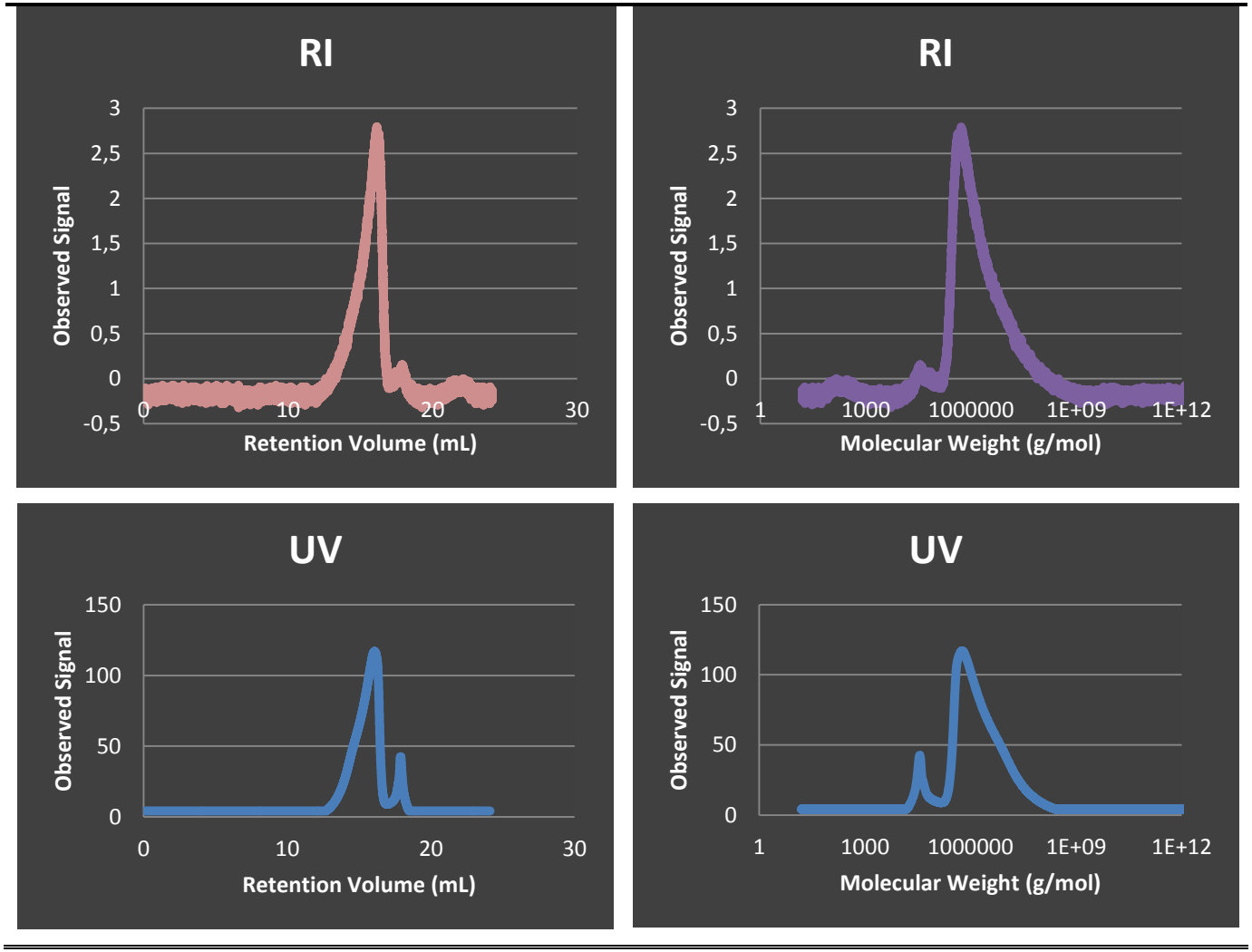

Annex 57. Characterization by SEC with tetra-detection of linear AA polymer synthetized using RAFT in a micro-reactor (CM08).

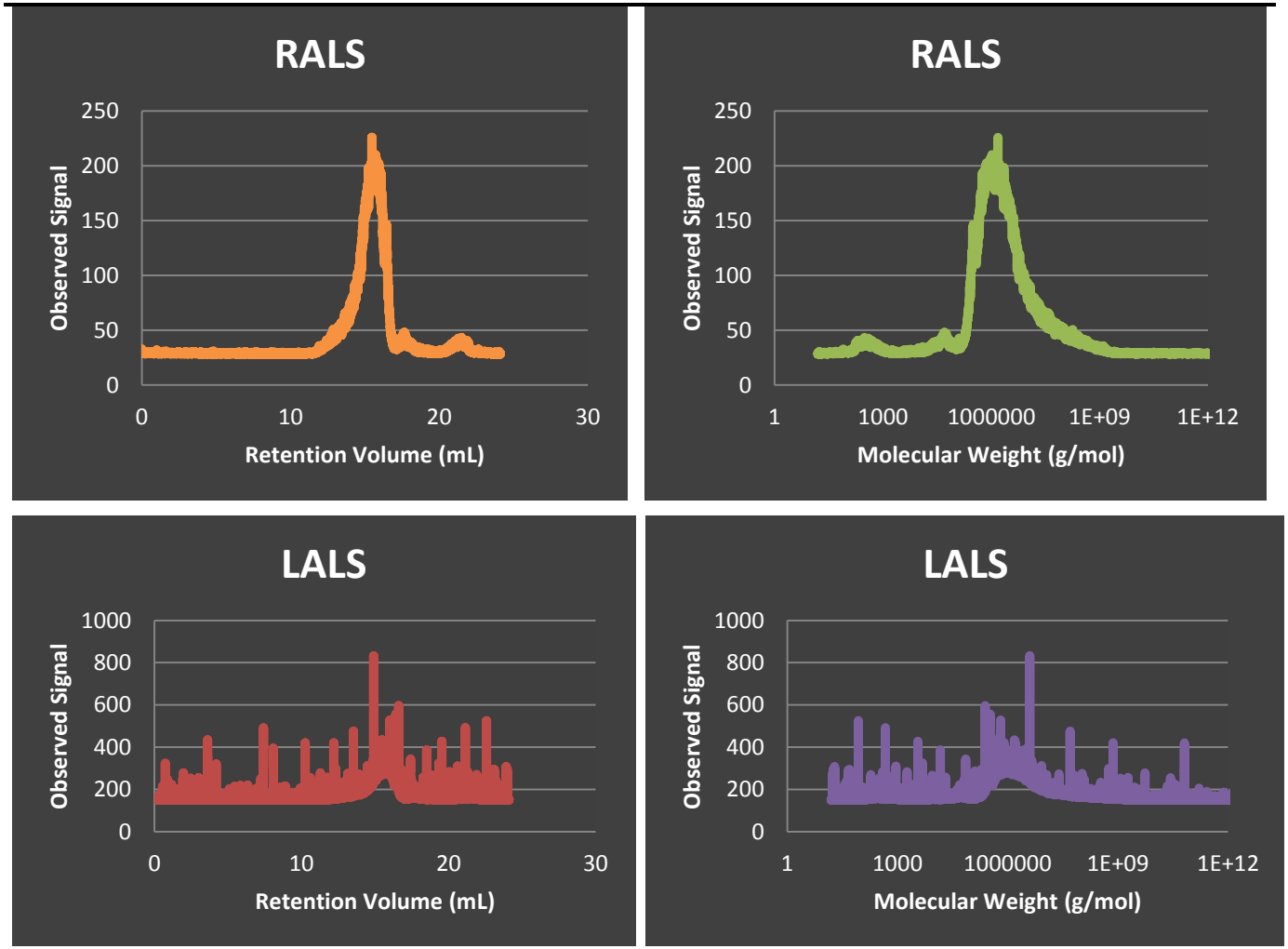

Annex 58. Characterization by SEC with tetra-detection of linear AA polymer synthetized using RAFT in a micro-reactor (CM08).

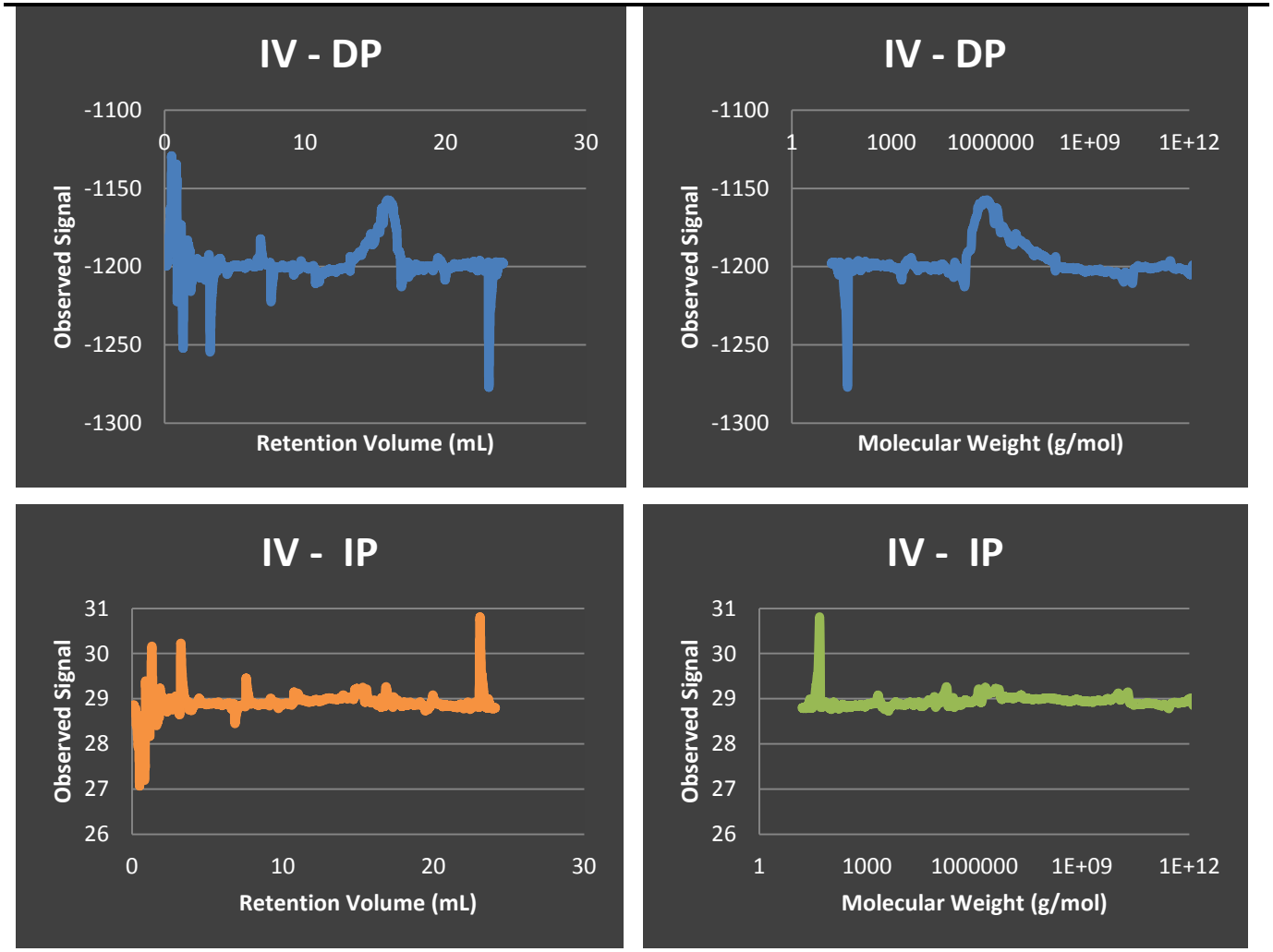

Annex 59. Characterization by SEC with tetra-detection of linear AA polymer synthetized using RAFT in a batch reactor (CM09).

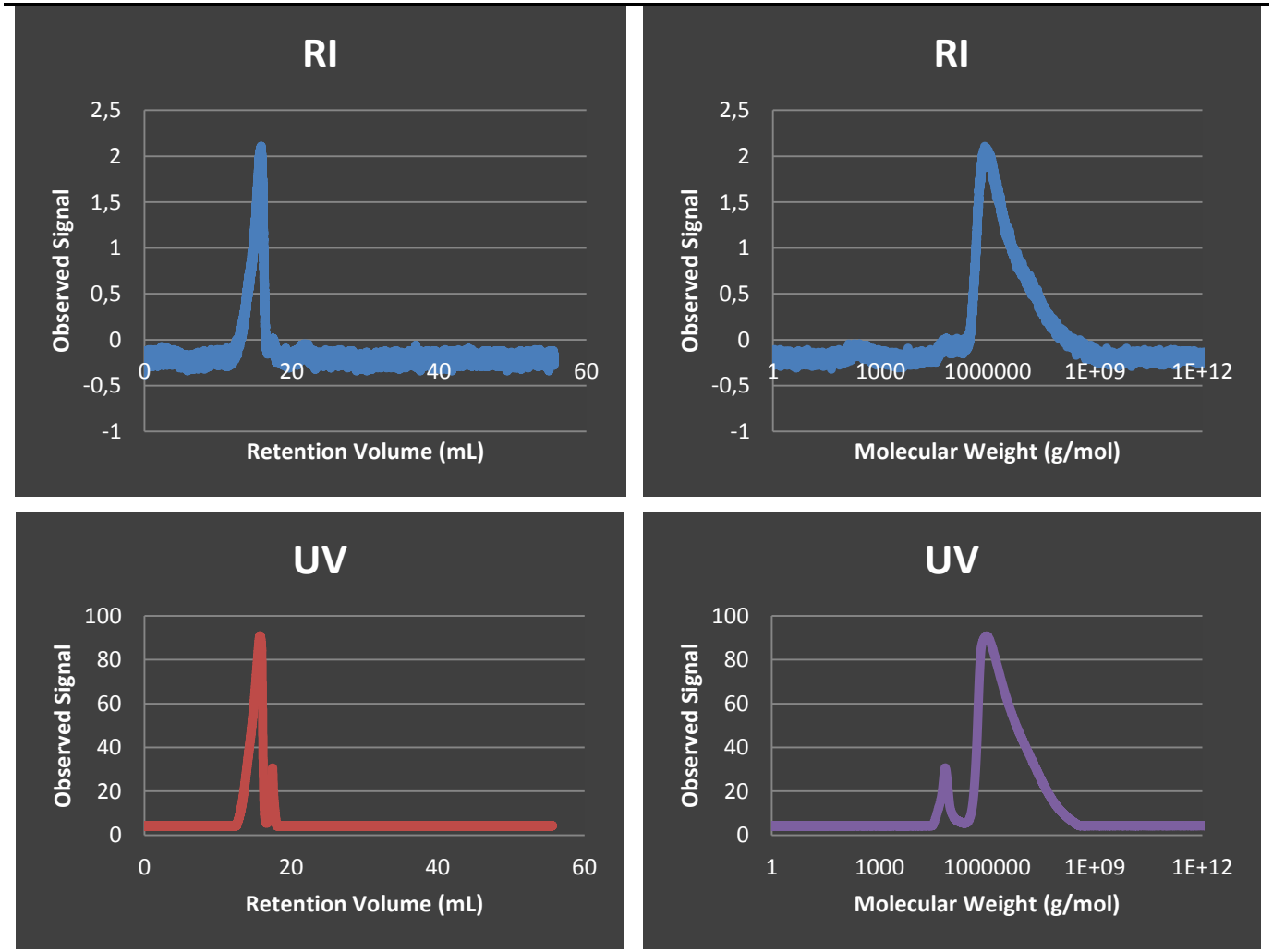

Annex 60. Characterization by SEC with tetra-detection of linear AA polymer synthetized using RAFT in a batch reactor (CM09).

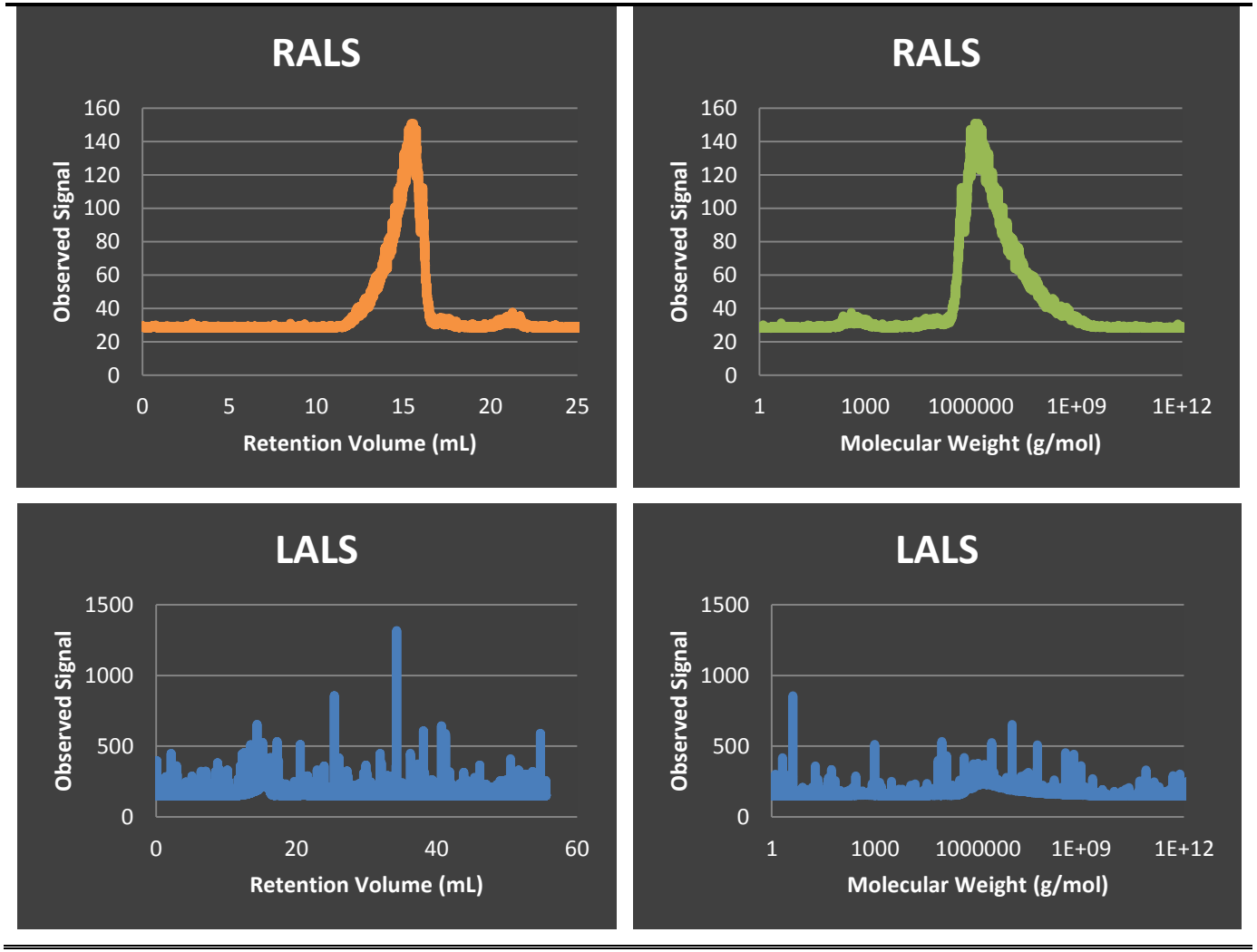

Annex 61. Characterization by SEC with tetra-detection of linear AA polymer synthetized using RAFT in a batch reactor (CM09).

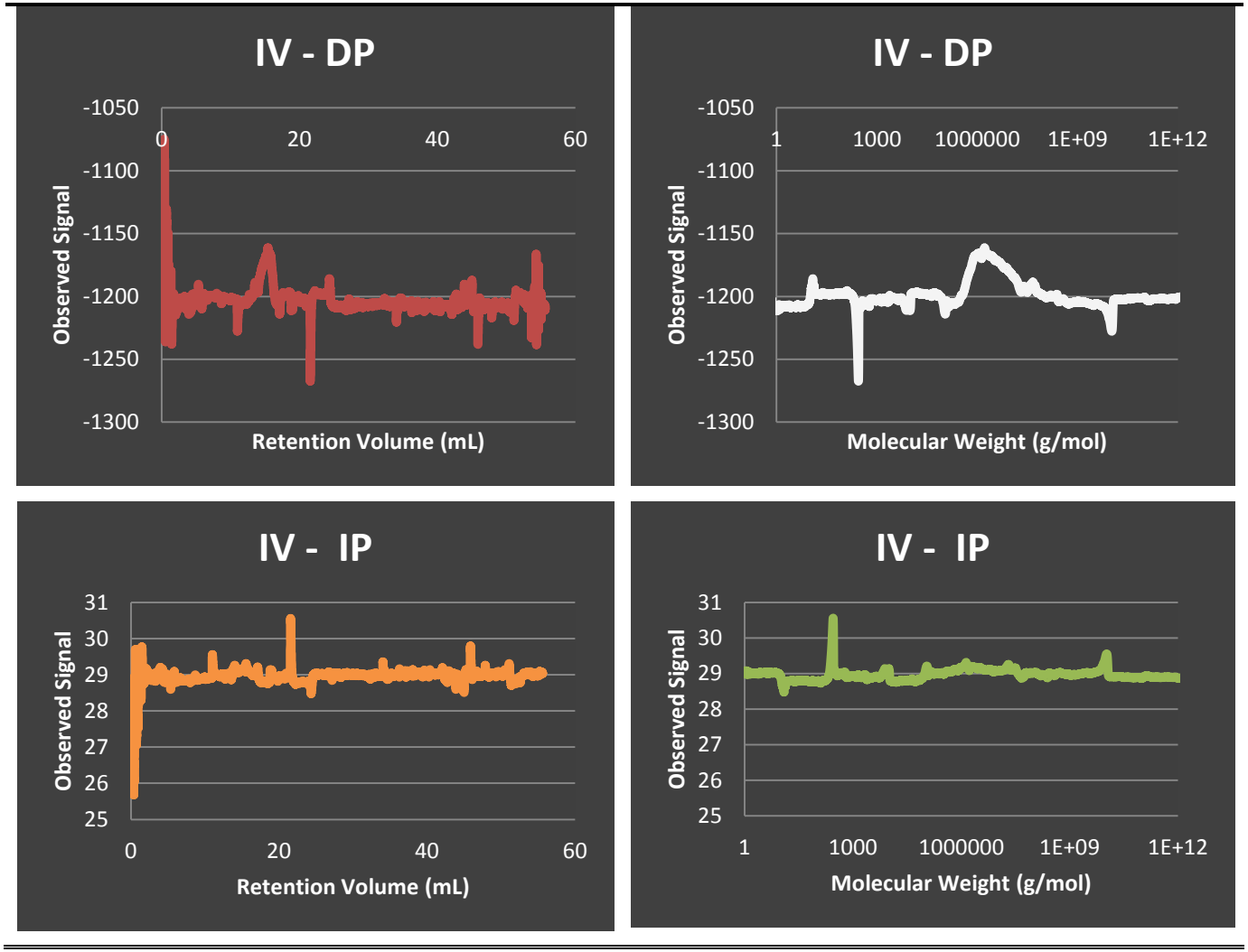

Annex 62. Characterization by SEC with tetra-detection of linear AA polymer synthetized using FRP in a micro-reactor (second concentration) (CM06).

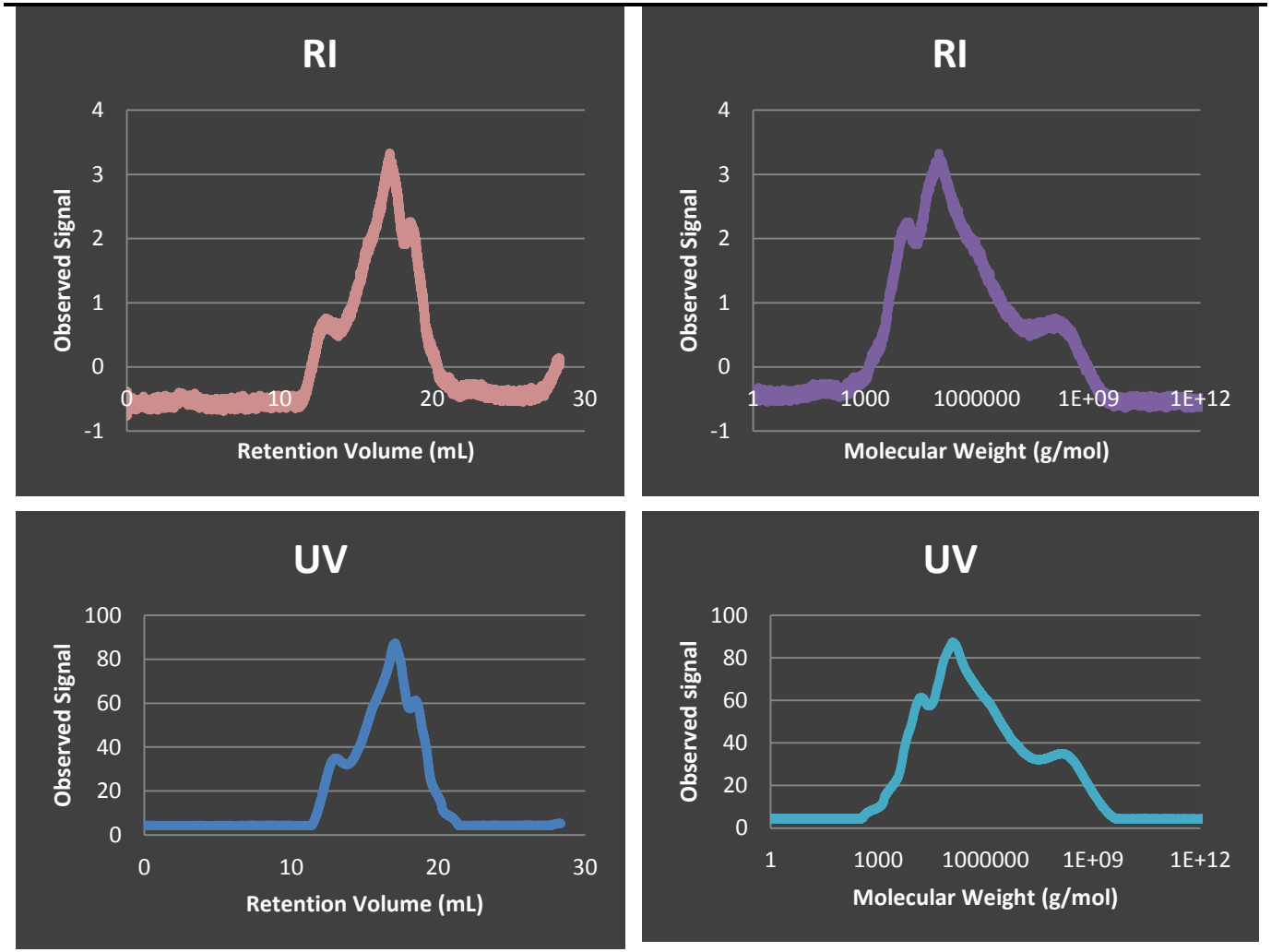

Annex 63. Characterization by SEC with tetra-detection of linear AA polymer synthetized using FRP in a micro-reactor (second concentration) (CM06).

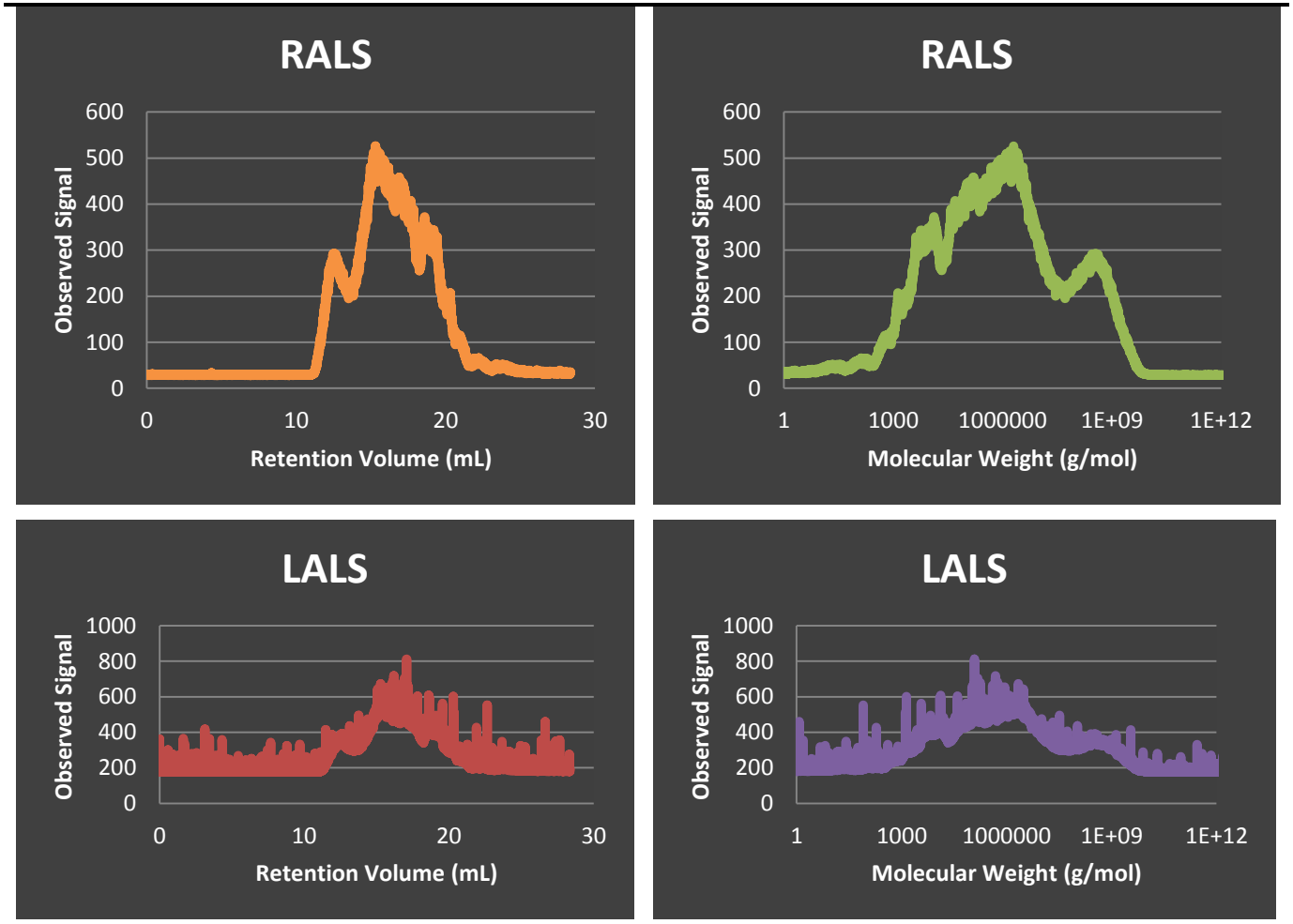

Annex 64. Characterization by SEC with tetra-detection of linear AA polymer synthetized using FRP in a micro-reactor (second concentration) (CM06).

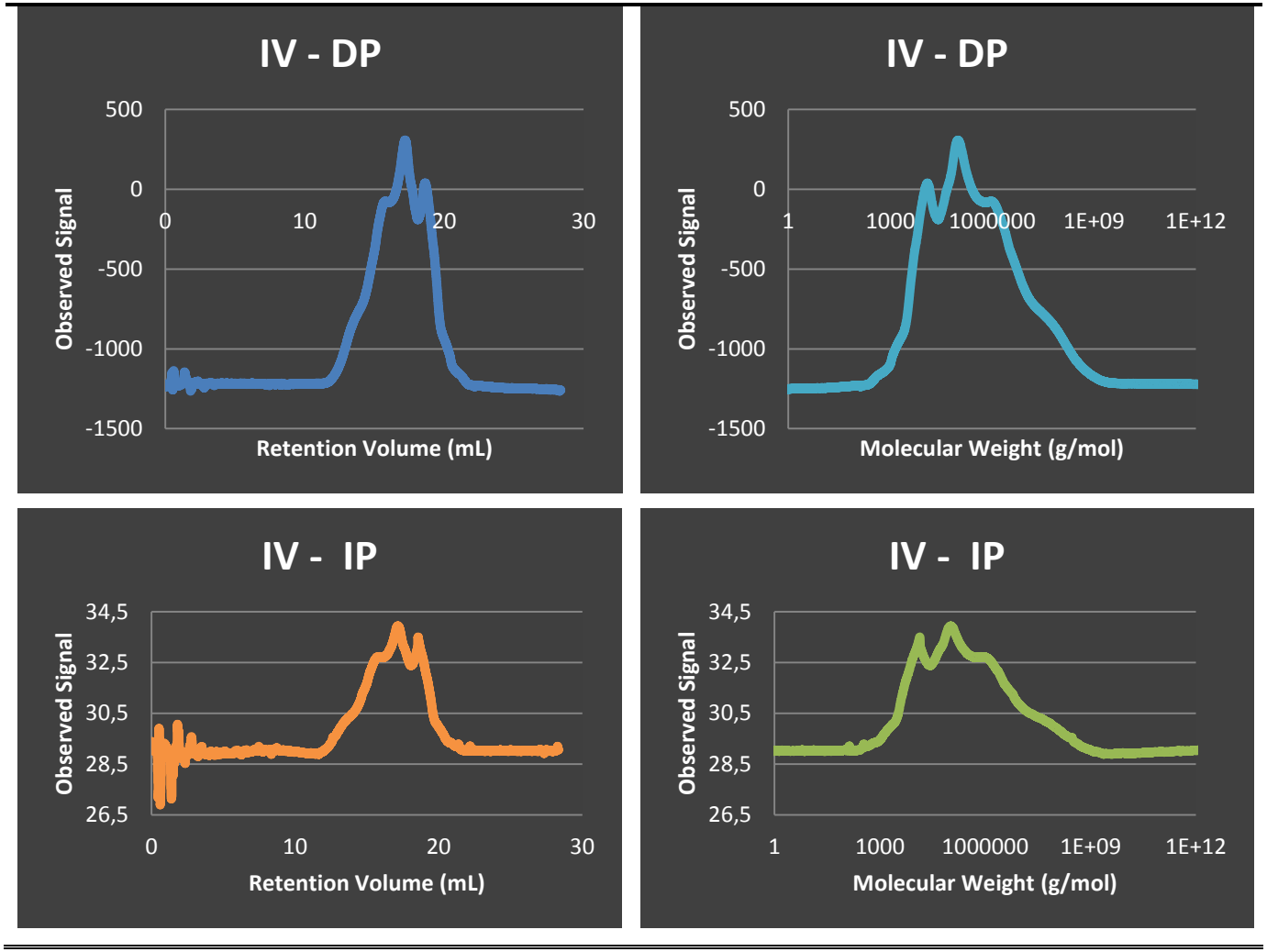

Annex 65. Characterization by SEC with tetra-detection of linear AA polymer synthetized using RAFT in a batch reactor (second concentration) (CM09).

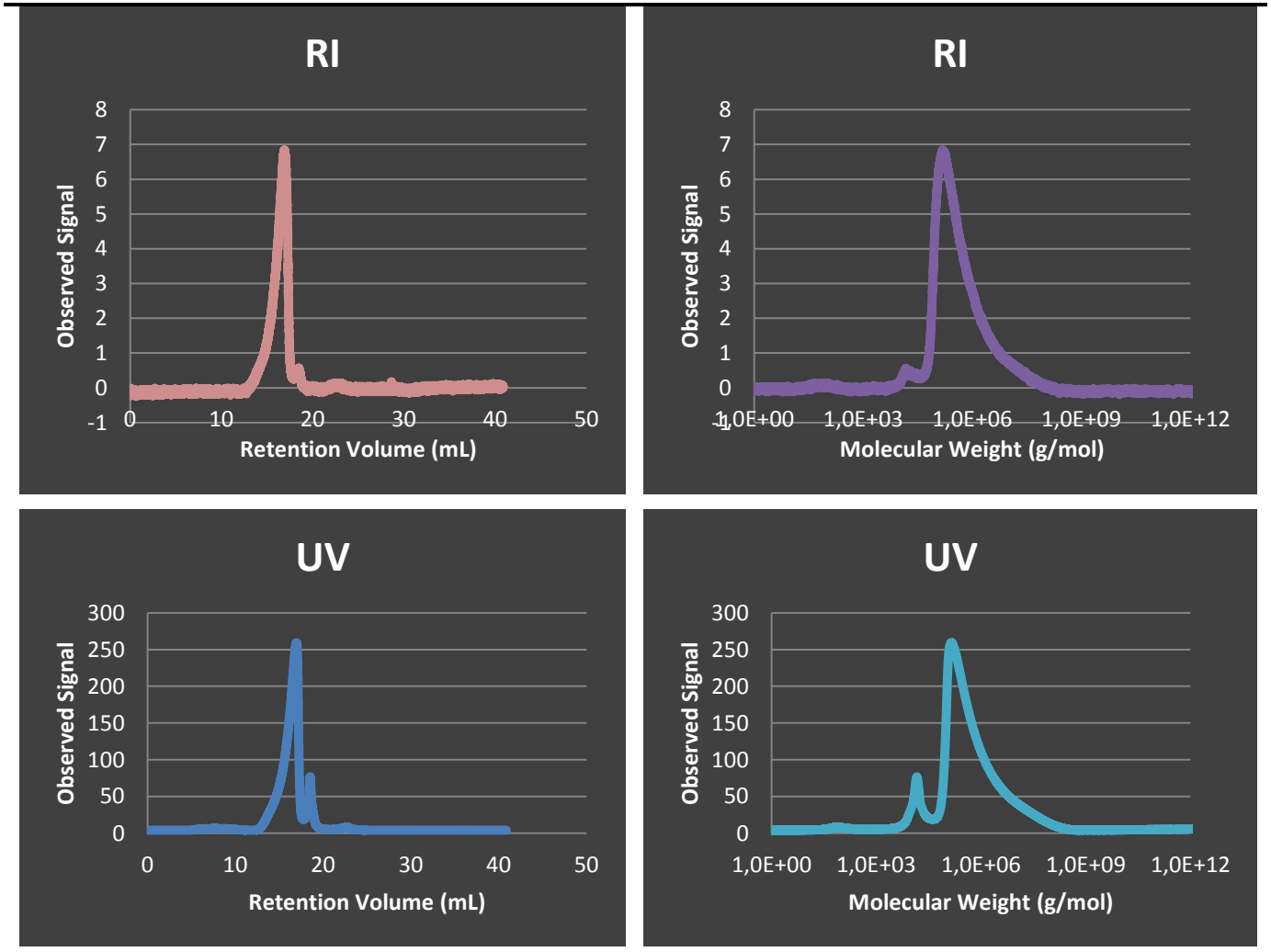

Annex 66. Characterization by SEC with tetra-detection of linear AA polymer synthetized using RAFT in a batch reactor (second concentration) (CM09).

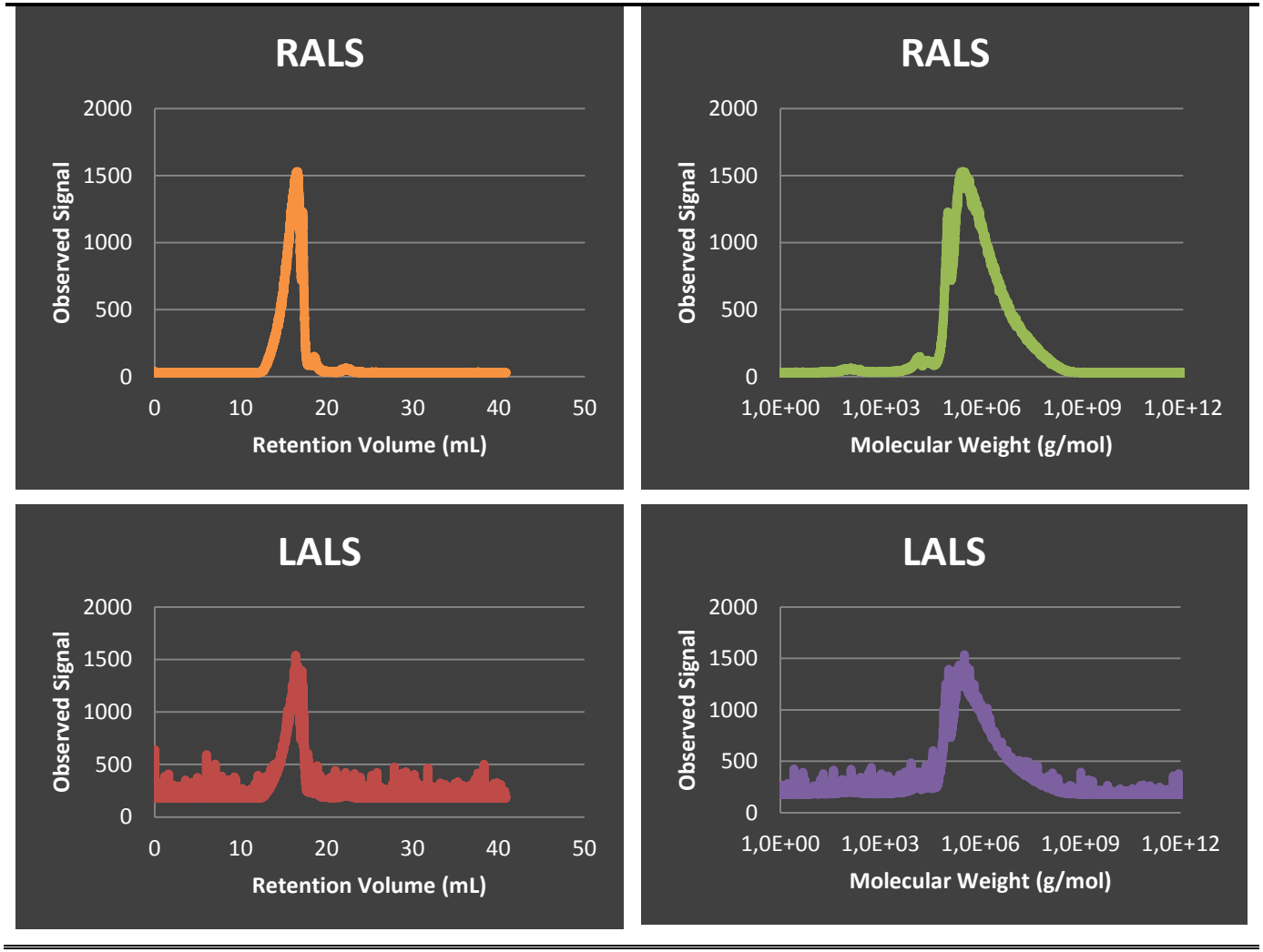

Annex 67. Characterization by SEC with tetra-detection of linear AA polymer synthetized using RAFT in a batch reactor (second concentration) (CM09).

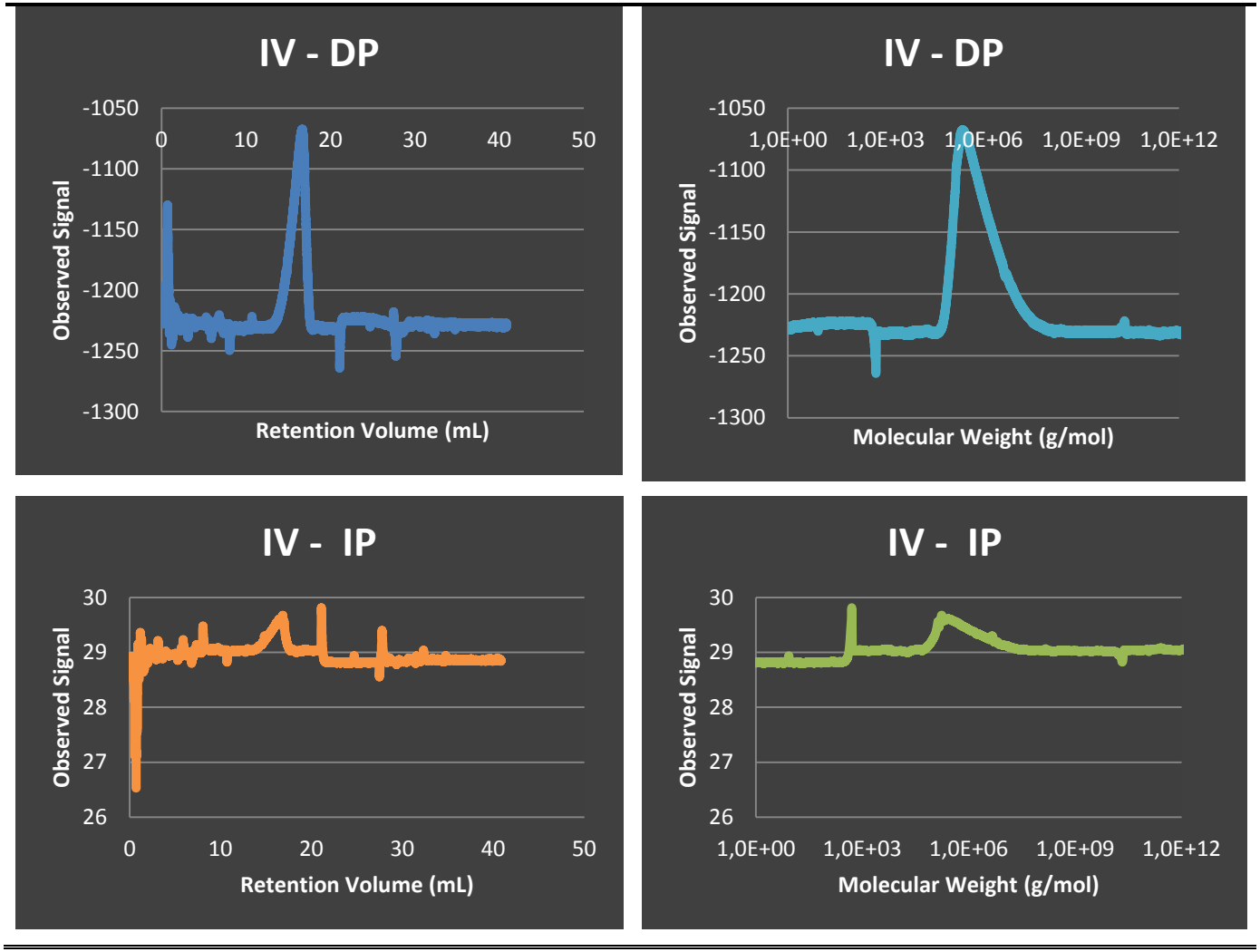

Annex 68. Characterization by SEC with tetra-detection of the PEO standard with MW=5300 g/mol.

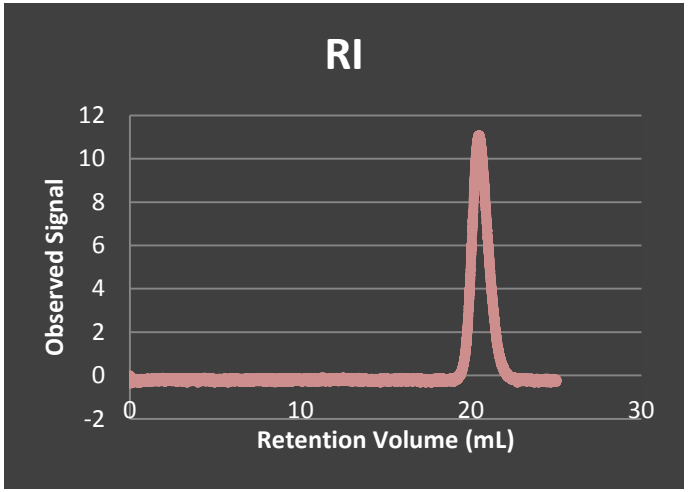

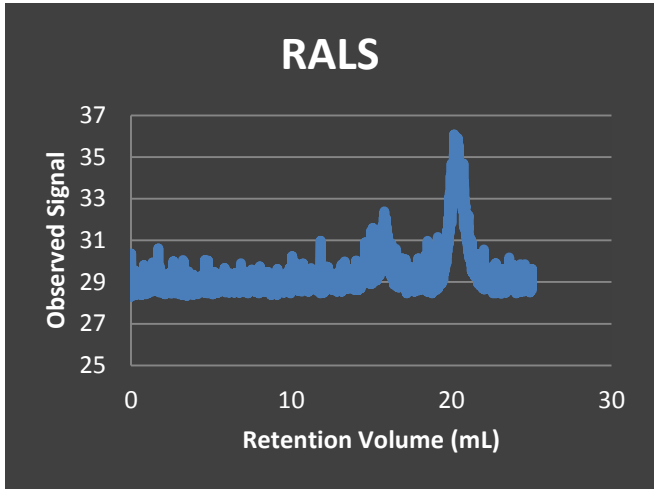

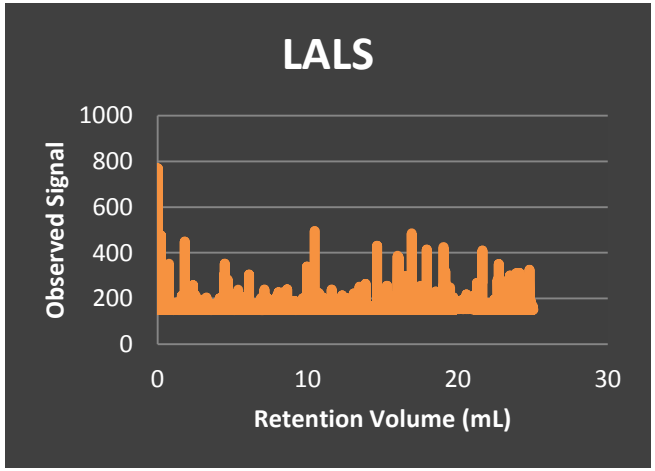

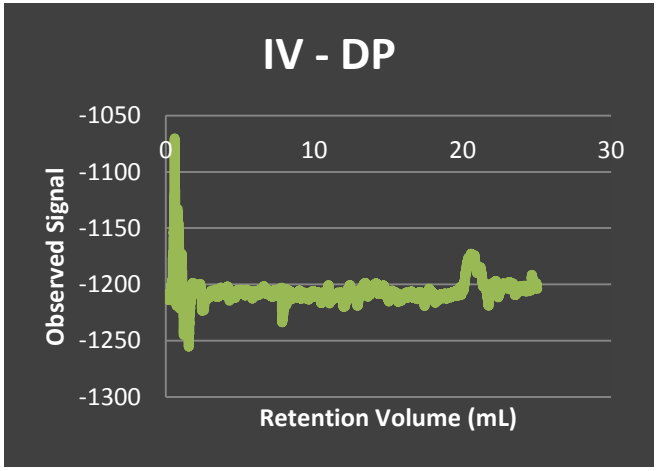

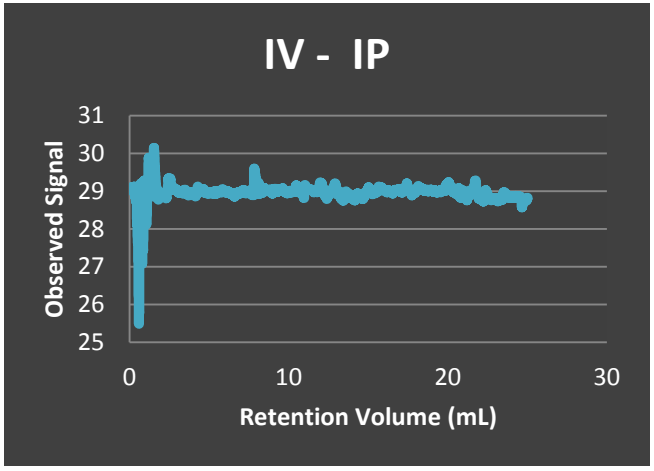

Annex 69. Characterization by SEC with tetra-detection of the PEO standard with MW=19000 g/mol.

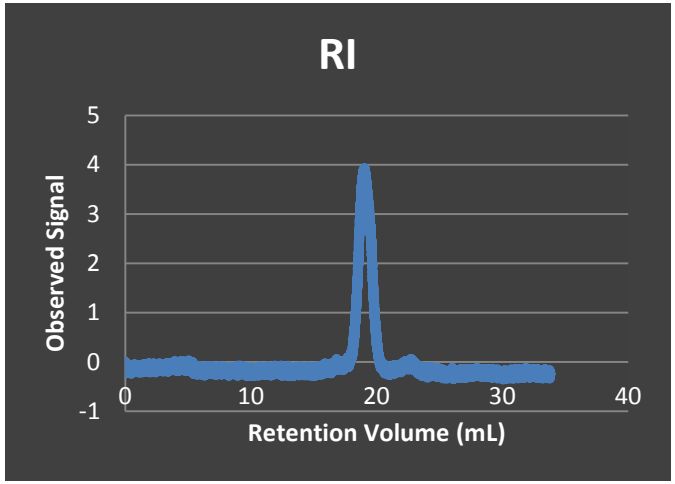

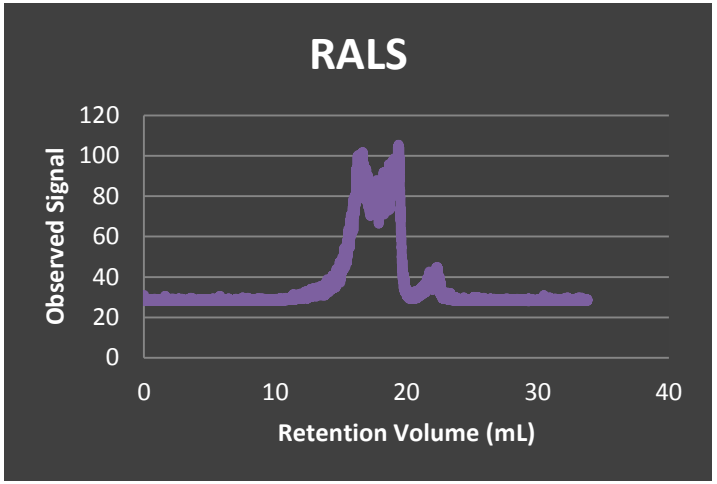

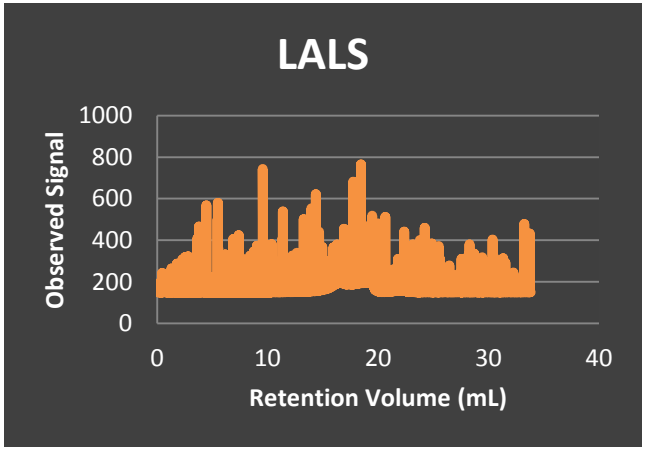

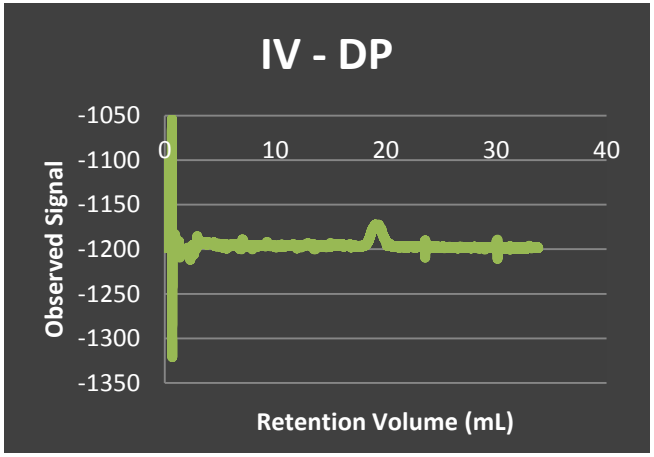

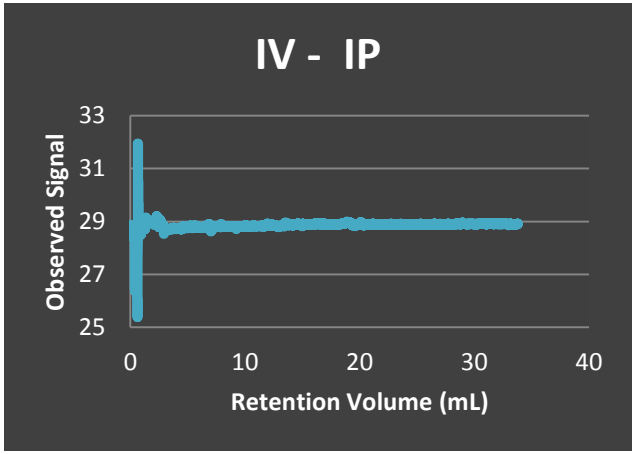

Annex 70. Characterization by SEC with tetra-detection of the PEO standard with MW=66600 g/mol.

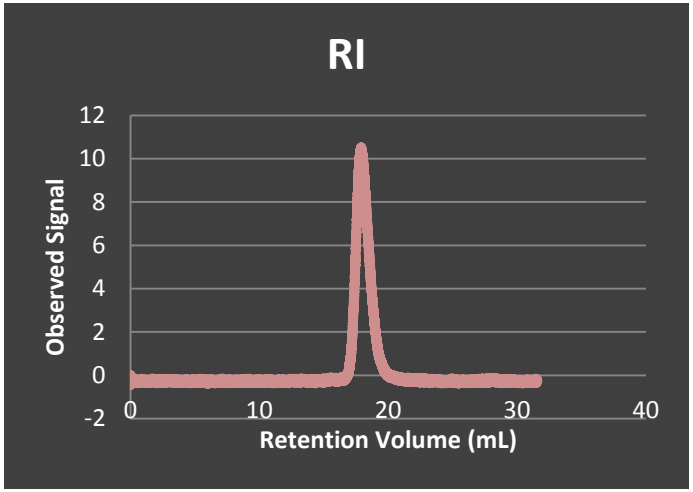

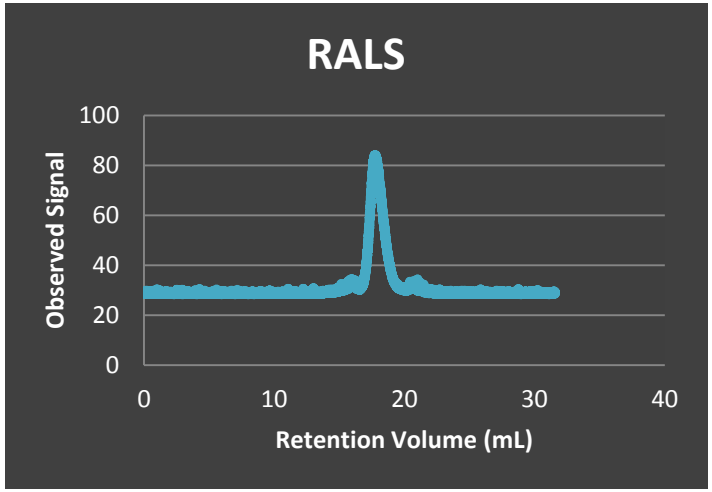

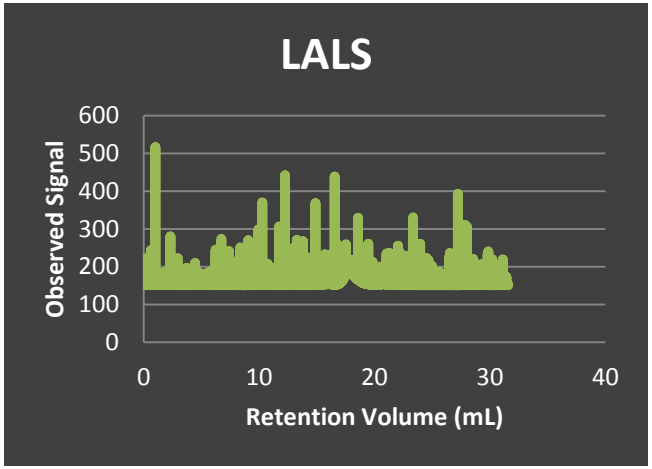

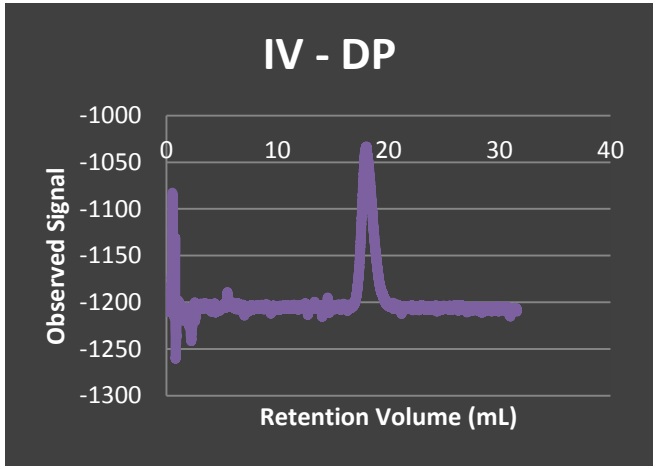

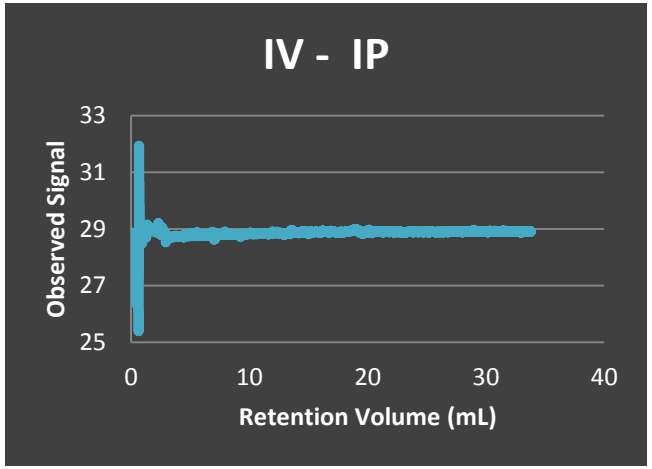

Annex 71. Characterization by SEC with tetra-detection of the PEO standard with MW=920000 g/mol.

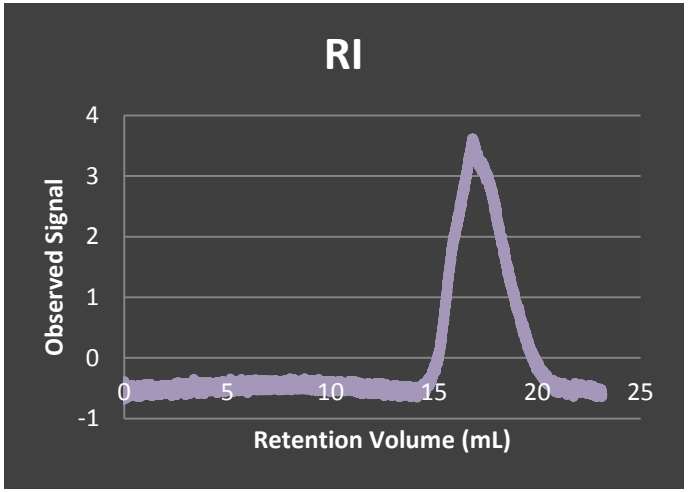

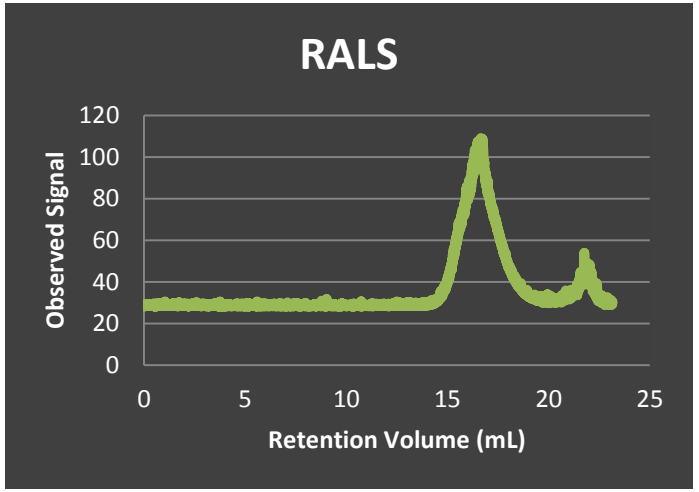

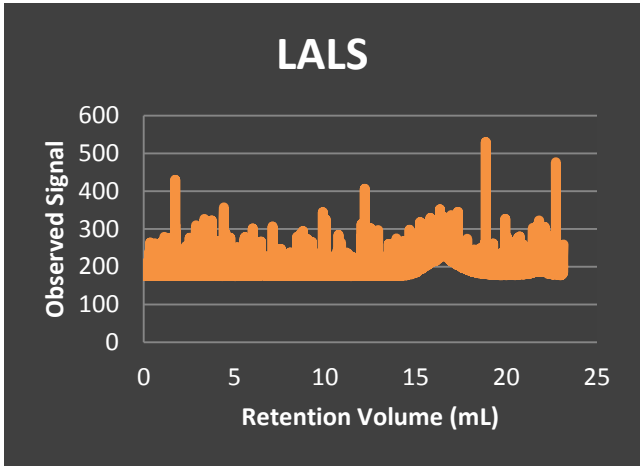

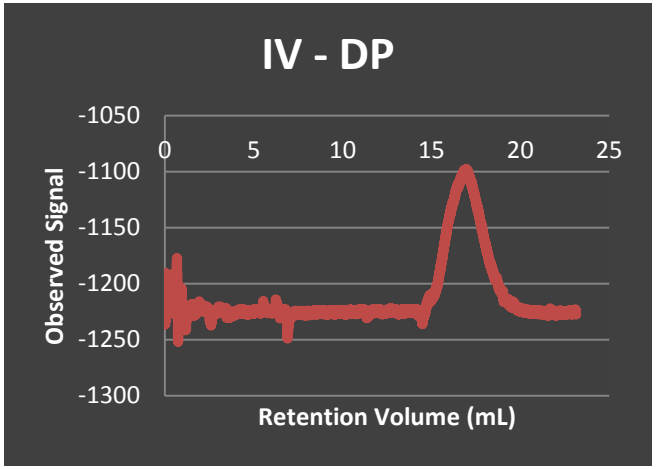

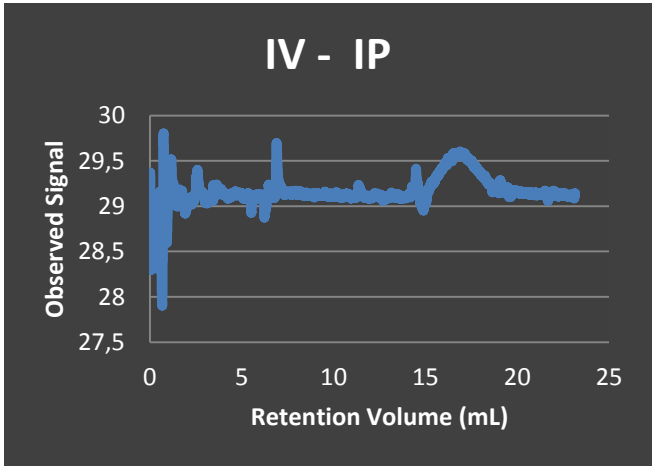

Annex 72. Quantities of MIP(CM05) and NIP (CM06) used in the adsorption tests in batch process at neutral pH and the concentrations of each solution.

	AA Hydrogel (mg) MIP	AA Hydrogel (mg) NIP	20 mM of CAF (µL)	H_20 (µl)	C0 (mM)	C0 (ppm)	V (ml)
1	15.3	15.3	0	20000	0	0	20
2	15.3	15.0	65	25935	0.05	9.7095	26
3	15.2	15.3	97.5	25903	0.075	14.56425	26
4	15.4	15.2	130	25870	0.1	19.419	26
5	15.2	15.0	260	25740	0.2	38.838	26
6	15.3	15.5	390	25610	0.3	58.257	26
7	15.1	15.0	520	25480	0.4	77.676	26
8	15.2	15.3	650	25350	0.5	97.095	26
9	15.2	15.4	1300	24700	1.0	194.19	26
10	15.3	15.2	2600	23400	2.0	388.38	26
11	15.0	15.5	3900	22100	3.0	582.57	26
12	15.5	15.1	5200	20800	4.0	776.76	26
13	15.4	15.5	6500	19500	5.0	970.95	26
14	15.1	15.0	7800	18200	6.0	1165.14	26
15	15.2	15.5	9100	16900	7.0	1359.33	26
16	15.2	15.2	10400	15600	8.0	1553.52	26
17	15.4	15.2	11700	14300	9.0	1747.71	26
18	15.4	15.4	13000	13000	10.0	1941.9	26
19	15.3	15.3	19500	6500	15.0	2912.85	26
20	15.0	15.3	26000	0	20.0	3883.8	26